# The role of septin 9 in lipid droplet accumulation and liver pathogenesis through intracellular trafficking regulation

Peixuan Song

université PARIS-SACLAY

# Le rôle de la septine 9 dans l'accumulation des gouttelettes lipidiques et la pathogenèse du foie par la régulation du trafic intracellulaire

*The role of septin 9 in lipid droplet accumulation and liver pathogenesis through intracellular trafficking regulation*

**Thèse de doctorat de l'université Paris-Saclay**

École doctorale n° CBMS – 582
Cancérologie : biologie, médecine, santé
Spécialité de doctorat : aspects moléculaires et cellulaires de la biologie
Unité de recherche : INSERM U1193
Référent : Faculté de médecine

**Thèse présentée et soutenue à Paris-Saclay, le 27/10/2021, par**

**Peixuan SONG**

## Composition du Jury

| | |
|---|---|
| **Didier Samuel**<br>PUPH, Inserm UMR 1193, Hôpital Paul-Brousse | Président |
| **Bruno Goud**<br>Directeur de recherche, Institut Curie, (Paris) | Rapporteur |
| **Alenka Copic**<br>Chef d'équipe, CRBM - Montpellier Cell Biology Research Center | Rapporteur |
| **Anne Corlu**<br>Directrice de recherche, Institut NuMeCan(Rennes) | Examinatrice |
| **Abdou-Rachid Thiam**<br>Directeur de recherche, Ecole Normale Supérieure | Examinateur |

## Direction de la thèse

| | |
|---|---|
| **Ama Gassama-Diagne**<br>Directrice de recherche, Inserm UMR 1193, Hôpital Paul- Brousse | Directrice de thèse |

Thèse de doctorat

NNT : 2021UPASL080

# ACKNOWLEDGEMENT

First of all, I would like to express my deep gratitude to **Dr. Ama Gassama-Diagne**, my thesis director who trusted me and welcomed me in her team to do my Ph.D. I thank you for your patience, your availability and your precious help in the reflections and scientific experiments. I thank you for having always encouraged me and given me the means to realize this research work. I have learned a lot on the scientific level. These years in your team have given me, I am sure, all the elements to become a good scientist.

Furthermore, I would like to sincerely thank the members of my thesis jury for having accepted to evaluate this work in a short time. First of all, I would like to thank **Dr. Alenka Copic** and **Pr. Bruno Goud** for having accepted to be the rapporteur of my thesis work. I would also like to thank **Pr. Anne Corlu** and **Pr. Abdou-Rachid Thiam**, for having accepted to be examiner of the work presented in this thesis. I would like to thank **Pr. Didier Samuel**, director of the research unit 1193, who allowed me to join his laboratory.

Many thanks to all the people of the Research Unit 1193 who give a special atmosphere to the laboratory. I would like to give a special thanks to **Dr. Nassima Benzoubir** for your help with the training in the laboratory. I sincerely thank **Alice Deshayes** for the managing of all the materials and **Dr. Nicolas Moniaux** who teach me how to use the ultracentrifuge, excuse me for always bother you and allow me to use your instruments. Thank you, **Dr. Jean Agnetti, Dr. Juan Peng Wang, Vanessa Bou Malhamand** and **TingTing Cai** for your friendships, kindness and the nice moments I spent with you during these years. I am so happy and proud to work and share success with you. I wish you all the best for the future. You were there for me whenever I needed it. I would also like to thank our biostatistician, **Dr. Christophe Desterke** for his help for the bigdata analysis. I would like to thank **Dr. Alexandre Dos Santos**, who sits in the same office as me, gave me a lot of advice on learning R and gave me a book on the basics of the language. Even now I am still not familiar with R. Although I can't understand your jokes very well due to the language barrier, I can still feel your wit and love for life.

A huge thank you to my Chinese friends who always accompanied me, for their presence, their good mood, their advice and their support. Thank you, **Dr. Hong Wang, Dr. YiFan Sun** and **All friends** who have lived at the Orsay Fleming Residence. All our parties and trips are my precious memories.

I would never have reached this major step in my personal and professional development, the submission of my doctoral thesis, without the support of my family and friends. I would like to thank with all my heart my dear parents, **AnQi Wang** without whom I would not have been able to go to the end of this work. You have accompanied me with all their love.

# TABLE OF CONTENTS

# LIST OF ABREVIATIONS

| | |
|---|---|
| **ABHD5** | 1-acylglycerol-3-phosphate O-acyltransferase |
| **ACAT** | Acetyl-CoA acetyltransferase |
| **ACTA1** | Cholesterol O-acyltransferases |
| **ADAMs** | A Disintegrin and Metalloproteinase-domain proteins |
| **ADH** | Alcohol dehydrogenase |
| **ADRB2** | β-adrenergic receptor |
| **ADRP** | Adipocyte differentiation related protein |
| **AGPAT** | Acylglycerolphosphate acyltransferase |
| **AMPK** | 5' AMP-activated protein kinase |
| **ApoB** | Apolipoprotein B |
| **Aps** | Clathrin adaptor proteins |
| **AT** | Adipose tissue |
| **ATF6** | Activating transcription factor 6 |
| **ATF6** | Activating transcription factor 6 |
| **ATGs** | Ubiquitin-like-conjugating enzymes |
| **ATP/ADP** | Adenosine triphosphate/diphosphate |
| **ATP/ADP** | Adenosine triphosphate |
| **CDC** | Cell-division cycle |
| **CDC** | Cell division cycle |
| **CD-M6PR** | Cation-dependent M6PR |
| **CGI-58** | Comparative gene identification 58 |
| **CIDE** | Cell death activator |
| **CI-M6PR** | Cation-independent M6PR |
| **CMA** | Chaperone-mediated autophagy |
| **CMA** | Chaperone-mediated autophagy |
| **COPI** | Coat protein complex I |
| **CYP2E1** | Cytochrome P450 2E1 |
| **DAG** | Diacylglycerol |
| **DGAT** | Diacylglycerol O-acyltransferase |
| **EEA1** | Early endosome antigen 1 |
| **EGF** | Epidermal growth factor |
| **EGFR** | Epidermal growth factor receptor |
| **ER** | Endoplasmic reticulum |
| **ERK** | Extracellular signal-regulated kinase |
| **ESCRT** | Endosomal sorting complexes required for transport |
| **FA** | Focal adhesion |
| **FFA** | Free fatty acid |
| **FIT** | Fat-storage-induced transmembrane protein |
| **FYCO1** | FYVE and coiled-coil domain containing protein 1 |
| **G3P** | Glycerol-3-phosphate |
| **GAGs** | Glycosaminoglycans |
| **GAPDH** | Glyceraldehyde 3-phosphate dehydrogenase |
| **GAPs** | GTPase-activating proteins |

| | |
|---|---|
| **GDP** | Guanosine diphosphate |
| **GEFs** | Guanine nucleotide exchange factors |
| **GPAT** | Glycerol-3 phosphate acyltransferase |
| **GTP** | Guanosine-5'-triphosphate |
| **HCV** | Hepatitis C virus |
| **HIF1α** | Hypoxia-inducible factor-1α |
| **HOPS** | Homotypic fusion and vacuole protein sorting |
| **HSCs** | Hepatic stellate cells |
| **HSL** | Hormone-sensitive lipase |
| **IRE1** | Inositol-requiring protein 1 |
| **KIF1** | kinesin 3 |
| **KIF5** | kinesin 1 |
| **LAL** | Lysosomal acid lipase |
| **LAMP** | Lysosomal-associated membrane protein |
| **LDLR** | Low-density lipoprotein receptor |
| **LPA** | Lysophosphatidic acid |
| **LSD** | Lysosomal storage disorders |
| **LSECs** | Liver sinusoidal endothelial cells |
| **M6P** | Mannose-6 phosphate |
| **M6PR** | Mannose-6 phosphate receptors |
| **MCAD** | Medium-chain acyl-CoA dehydrogenase |
| **MGL** | Monoglyceride lipase |
| **MLL** | Mixed lineage leukemia |
| **MMPs** | Matrix metalloproteinases |
| **MT** | Microtubule |
| **mTOR** | Mammalian target of rapamycin |
| **mTORC1** | Nutrient-regulated mechanistic target of rapamycin complex 1 |
| **MTP** | Microsomal triglyceride transfer protein |
| **MVB** | multivesicular bodies |
| **NAFLD** | Nonalcoholic fatty liver disease |
| **PA** | Phosphatidic acid |
| **PAP** | Phosphatidic acid phosphatase |
| **PBR** | Polybasic region |
| **PC** | Phosphatidylcholine |
| **PE** | Phosphatidylethanolamine |
| **PERK** | Protein kinase RNA-like ER kinase |
| **PI** | phosphatidylinositol |
| **PI3KC2β** | Phosphatidylinositol 3-kinase, class 2 beta |
| **PI4K2A** | Phosphatidylinositol 4-kinase type 2-alpha |
| **PKA** | cAMP-dependent protein kinase (Protein kinase A) |
| **PLIN** | Perilipin |
| **PNPLA2** | Patatin-like phospholipase domain-containing protein 2 |
| **PPARα** | Peroxisome proliferator-activated receptor alpha |
| **PPARγ** | Peroxisome proliferator-activated receptor gamma |
| **PS** | Phosphatidylserine |
| **PtdIns** | Phospholipids |

| | |
|---|---|
| **PTMs** | Post-translational modifications |
| **RAB** | Ras-related protein |
| **RILP** | Rab-interacting lysosomal protein |
| **ROS** | Reactive oxygen species |
| **SCAD** | Short-chain acyl-CoA dehydrogenase |
| **SIRT1** | NAD-dependent deacetylase sirtuin-1 |
| **SM** | Sphingomyelin |
| **SREBP-1** | Sterol regulatory element-binding transcription factor 1 |
| **TFEB** | Transcription factor EB |
| **TfR** | Transferrin receptor |
| **TG** | Triglycerides |
| **TGF-β** | Transforming growth factor beta |
| **TGN** | Trans Golgi network |
| **TIMPs** | Tissue inhibitors of metalloproteinases |
| **TLR** | Toll-like receptor |
| **UPR** | Unfolded protein response |
| **VLDL** | Very-low-density lipoprotein |
| **VPS34** | Phosphatidylinositol 3-kinase catalytic subunit type 3 |

# LIST OF FIGURES

# INTRODUCTION

# Chapter I

# The liver

## I. Macroscopic structure and functional organization

The liver is the largest full organ in the human body, accounting for almost 2% of body weight in adults. It performs a very large number of tasks that support the functionality of other organs and impact all physiological systems. The essential functions of the liver are the synthesis, metabolism, and storage of proteins, including the metabolism of amino acids, carbohydrates, fats, and vitamins. The liver is also responsible for removing exogenous agents from the systemic circulation. It participates in the maintenance of the organism's homeostasis as an active, bidirectional biofilter because it rapidly metabolizes most nutritional compounds and neutralizes and prepares for the removal toxic exogenous and endogenous materials. While essential, this exceptional purification capacity puts the liver at risk by making it highly susceptible to damage from excessive exposure to fat, alcohol, drugs, and other toxins as well as a host of several pathogens such as hepatitis viruses. Given the importance of this organ, it is not surprising that liver diseases, including fibrosis, cirrhosis, hepatitis and hepatocarcinoma, contribute significantly to morbidity and mortality throughout the world (Trefts et al., 2017; Vekemans and Braet, 2005).

The key position of the liver, in the upper right part of the abdomen, just under the rib cage and the diaphragm (Figure1 a) and its unique vascular system allow it to degrade toxins and waste products. This organ consists of two parts, the left lobe (1/3 of the volume) and the right lobe (2/3 of the volume), delineated only by being supplied and drained by separate first- and second-order branches of the portal and hepatic veins. The right and left lobes are separated by the remnants of the embryonic umbilical vein called the falciform ligament. It is supplied by two major blood vessels: the portal vein and the hepatic artery. The blood brought by the portal vein is poor in oxygen but rich in nutrients coming from the digestive tract. Whereas the hepatic artery originates from the heart supplies the liver with oxygen-rich blood. These two vessels, entering the liver, are divided into several branches to supply its different parts, thus making the liver a highly vascularized organ. After irrigating all the liver cells, the blood is evacuated through the hepatic vein, which then flows into the inferior vena cava which returns to the heart (Abdel-Misih and Bloomston, 2010; Sibulesky, 2013) (Figure 1b).

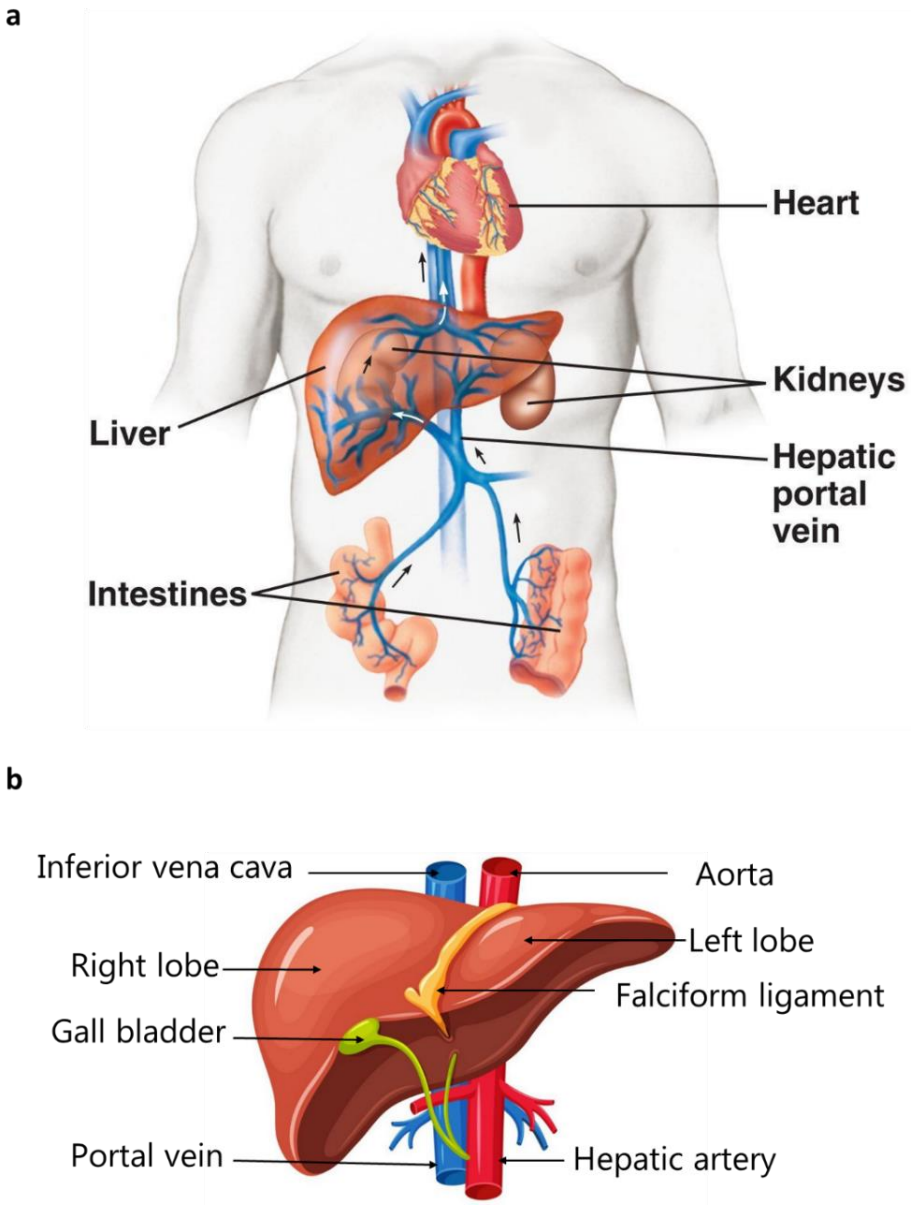


*Figure 1 Liver position in human body*

*a) The liver is located in the right part of the abdomen, under the diaphragm. It is richly vascularized and allows the purification of blood from the portal vein.*

*b) The liver is specific by its double vascularization, arterial (hepatic artery dividing into right and left hepatic arteries) and venous (portal vein). The hepatic arteries and the portal vein enter the liver through the hilum, the portal vein behind, the hepatic arteries in front and to the left. Liver blood flow is around 1.5 liters per minute. The portal vein provides 70 to 80% of hepatic blood flow and supplies blood from the entire sub-diaphragmatic digestive tract, pancreas, and spleen. The hepatic arteries supply oxygenated blood representing 20 to 30% of the total flow and ensure the exclusive vascularization of the bile ducts. Part of the hepatic venous blood flows directly into the inferior vena cava via accessory hepatic veins from the adjacent hepatic segments.*

# II. Microscopic structure and the liver cells

The liver is divided into thousands of small units with hexagonal shape called lobules which represent the microstructural unit of the liver and consists of plates of hepatocytes radiating from a central vein. A distinctive component of a lobule is the portal triad, which can be found at each corner of the lobules. The portal triad consists of a branch of the hepatic artery, a branch of the hepatic portal vein, and a bile duct, which run in parallel, with lymphatic vessels and a branch of the vague nerve (Krishna, 2013) (Figure 2a). Between the hepatocyte plates are hepatic sinusoids, which are enlarged capillaries facilitating the exchange between the blood and hepatocytes (Figure 2a)

The liver is constituted of five major cell types including the two epithelial cells including hepatocytes which represent 60% of the hepatic cells and cholangiocytes which line the biliary duct, the sinusoidal endothelial cells, the Kupffer cells which are the resident macrophages of the liver, and the stellate cells, also called Ito cells. The spatiotemporal cooperation of these cells to shape and maintain liver structure and functions (Figure 2b).

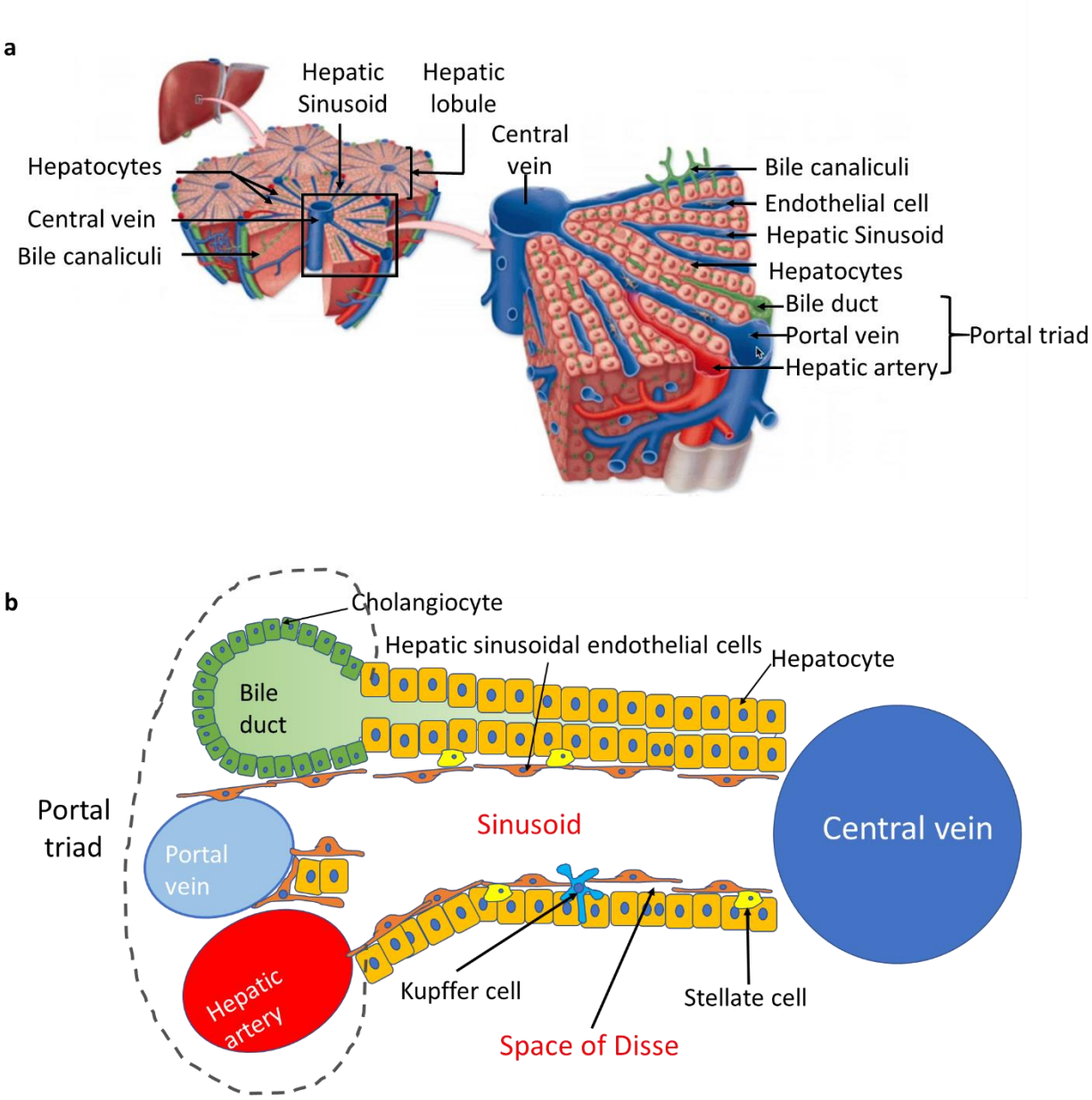


*Figure 2 Sturcture of a hepatic lobule and the different cell types for liver*

*a) The hepatic lobules are hexagonal with a branch of the central vein in the center and at each corner the portal triad, formed by a bile duct, a branch of the portal vein and the hepatic artery. Between these two entities, the liver cells are organized into spans.*

*b) Representation of a hepatic lobe located between the central lobular vein and the portal triad. The spatial relationship among the different cell types of the liver. Sinusoidal plasma comes in direct contact with hepatocytes in the space of Disse. The endothelial cells are fenestrated and lack a basement membrane. Kupffer cells are located in the lumen of the sinusoid, where they are in direct contact with the sinusoidal endothelial cells and portal blood. Stellate cells are situated between the endothelial cells and hepatocytes and come in direct contact with both cell types.*

### II.1.1 Liver sinusoidal endothelial cells (LSECs)

LSECs are highly specialized endothelial cells representing the interface between blood cells on one side and hepatocytes and hepatic stellate cells on the other side. In physiological conditions, LSECs regulate hepatic vascular tone contributing to the maintenance of a low portal pressure despite the major changes in hepatic blood flow occurring during digestion. In pathological conditions, it play a key role in the initiation and progression of chronic liver diseases (Poisson et al., 2017).

### II.1.2 Kuppfer cells

The Kuppfer cells are the resident macrophages of the liver. They capture and eliminate tissue or cell debris and bacterial endotoxins. These cells play a very important role in immune surveillance and are involved in the modulation of systemic responses to severe infections, as well as in the control of immune responses by presenting antigens and suppressing proliferation of T cells. They are also involved in the modulation of metabolic activities of hepatocytes via the production of cytokines which negatively regulate several genes involved in the metabolism and elimination of xenobiotics (Higuchi et al., 2007; Sunman et al., 2004; Wu et al., 2006).

### II.1.3 Hepatic stellate cells (HSE)

The stellate cells have varied functions in normal liver homeostasis ranging from liver regeneration and development, retinoid metabolism, extracellular matrix homeostasis, secretion of mediators, drug metabolism to detoxification of noxious substances and metabolites. HSCs in the space of Disse produce ECM components like collagen 1, laminin, collagen III and IV (Puche et al., 2013).

### II.1.4 Cholangiocytes

Cholangiocytes are the epithelial cells that line the bile ducts. They represent about 5% of the population of liver cells. Cholangiocytes contribute to the composition of bile via the secretion of bicarbonate in the canaliculi and the bile ducts (Celli et al., 1998). Bile is a secretory fluid product of the hepatobiliary system containing a variety of components, including bile acids, electrolytes, lipids, proteins and endobiotic and xenobiotic compounds. These factors contribute to health by aiding digestion of nutrients, maintaining the enterohepatic circulation, and helping to eliminate unwanted compounds from the body. They are actively involved in the absorption and secretion of water, lipids, electrolytes and in the regulation of bile secretion (Banales et al., 2019;

Tabibian et al., 2013).

## II.1.5 Hepatocytes

Hepatocytes comprise up to 80% of the total cell population and volume of the human liver and are intimately associated with both arterial and venous blood (Blouin et al., 1977). Remarkably, >12% of our blood volume resides within the liver, flowing past and over long rows of hepatocytes. Thus, each hepatocyte is literally 'bathed in blood' along multiple surfaces via a system of highly fenestrated vessels that course through the liver to enable the bidirectional, cell-to-plasma exchange of components. The hepatocytes constitute the liver parenchyma and they do accommodate a huge macromolecules flow linked to both endocrine and exocrine functions through managing lipids, glycogen and amino acids metabolism and bile production (Schulze et al., 2019). For example, the hepatocytes also synthesis and secrete proteins such as α-fetoprotein, transferrin, plasminogen, fibrinogen, and albumin into circulation. Hepatocytes are also responsible for the synthesis of bile, which aids in the emulsification, digestion, and adsorption of dietary fats within the intestinal lumen, as well as the removal of foreign biological substances (xenobiotics) and endogenous waste products (Schulze et al., 2019). In addition, hepatocytes also contribute to maintain the systemic homeostasis of iron which is an essential cofactor for many cellular functions, including mitochondrial respiration, gene transcription, and DNA replication and repair (Bogdan et al., 2016; Ganz, 2013). They could absorb and store iron and govern the release of iron into the bloodstream by signaling to Kupffer cells and other circulating macrophages that are rich in stored iron (Schulze et al., 2019). Indeed, if any of these functions become compromised, the liver can quickly succumb to advanced disease, including hepatitis, cirrhosis, or even hepatocellular carcinoma (Schulze et al., 2019).

# III. LIVER DISEASES

The Liver disease refers to a gradual decline in the health and condition of the liver. The liver disease progresses through the same stages across different patients, such as the hepatic steatosis, fibrosis, cirrhosis, and liver cancer (Figure 3).

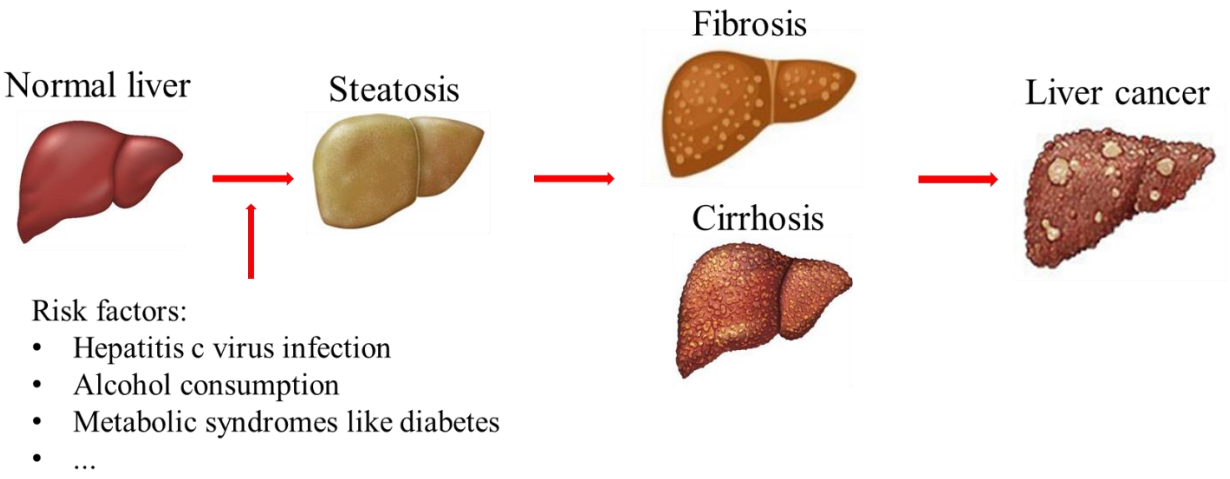


*Figure 3 The different stages of liver diseases*

## III.1 Hepatic steatosis

Hepatic steatosis or fatty liver is defined as intrahepatic triacylglycerol (TG) accumulation which could represent at least 5% of hepatocytes containing lipid. Liver steatosis is graded based on the percentage of TG within the hepatocytes: grade 0 (healthy, <5%), grade 1 (mild, 5%-33%), grade 2 (moderate, 34%-66%), and grade 3 (severe, >66%)(Qayyum et al., 2012). Hepatic steatosis is triggered by multiple metabolic, environmental, and pathogenesis factors such as the alcohol consumption, viral infection, hepatic and peripheral insulin resistance, Type 2 Diabetes Mellitus, obesity, and unhealthy dietary habits.

The hepatic steatosis always arises from the excessive importation, diminished exportation, and/or diminished breakdown of free fatty acid in the liver. Excessive FFAs delivered to the liver from the Adipose tissue(AT) or the intestine form fatty acyl-CoAs that are either oxidized by mitochondrial fatty acid β-oxidation or stored inside cytoplasmic lipid droplets in the form of TGs and DGs, or other lipid metabolites such as ceramides (Ferramosca and Zara, 2014; Jacome-Sosa and Parks, 2014). Insulin resistance correlates strongly with the development of hepatic steatosis and causes profound changes to normal systemic lipid metabolism. Systemic insulin resistance leads to excessive lipolysis in the adipose tissue causing the release of high amounts of FFAs that are then delivered to the liver (Bugianesi et al., 2010). In addition, hepatic insulin resistance contributes to

hyperinsulinemia and increased hepatic LD accumulation through increased de novo lipogenesis and inhibition of FFAs β-oxidation, thereby exacerbating steatosis (Postic and Girard, 2008). Hepatic *de novo* lipogenesis was found to be elevated in hepatic steatosis patients compared to controls and is not decreased by fasting (Lambert et al., 2014). In addition, the consumption of diets rich in fats and sugars increases hepatic fat delivery and accumulation as well as hepatic de novo lipogenesis, respectively (Boden, 2006; Cusi, 2009).

## III. 2 Fibrosis and cirrhosis

Liver fibrosis is a chronic liver condition that develops as a result of a chronic wound healing response following long-standing liver injury. During hepatic fibrogenesis, the liver parenchyma undergoes fundamental remodeling characterized by progressive accumulation of fibrillar extracellular matrix (ECM) associated with nodular regeneration of the liver parenchyma (Böttcher and Pinzani, 2017). Liver cirrhosis is defined as an advanced stage of liver fibrosis with distortion of the hepatic vasculature and architecture which causes hemodynamic instability and portal hypertension and leads to global liver dysfunction (Noor and Manoria, 2017; Reungoat et al., 2021). The development of liver fibrosis and subsequent cirrhosis is driven by ongoing liver injury through multiple mechanisms and can be considered as an excessive wound healing response fueled by a pathogenic vicious circle of hepatocyte necrosis, inflammation, and excessive ECM deposition (Böttcher and Pinzani, 2017; Pinzani, 2015).

HSCs are the predominant cell type primarily responsible for liver fibrosis. In normal liver, HSCs are quiescent and play a major role in liver development and regeneration by expressing and secreting hepatocyte mitogens such as hepatocyte growth factor (HGF) or epidermal growth factor (EGF) (Gupta et al., 2019). In the injured liver, HSCs become activated, with a continuum of changes in gene expression during activation. Activated HSCs migrate and accumulate at the sites of tissue repair, secreting large amounts of ECM (Khomich et al., 2020). Activation of HSCs is stimulated by damaged and apoptotic hepatocytes. This activation is performed through two main routes: release of damage-associated reactive oxygen species (ROS) (Tao et al., 2021) and recruitment of immune cells, which in turn mediate HSC activation and stimulate collagen secretion through the release of cytokines and chemokines (Luedde et al., 2014). In addition, recent findings from human study and animal models have shown that the impaired communication among different cell types of the liver could contribute to the development of fibrosis and cirrhosis. The involved mechanisms include Toll-like receptor, TGFβ and hedgehog mediated hepatocytes damage (Kumar et al., 2021).

## III. 3 Liver cancer

Primary liver cancer is the sixth most commonly diagnosed cancer and the third leading cause of cancer death worldwide in 2020, with approximately 906,000 new cases and 830,000 deaths (Sung et al., 2021). The two major primary liver cancers are hepatocellular carcinoma (HCC) (comprising 75%-85% of cases) and intrahepatic cholangiocarcinoma (10%-15%).

### III.3.1 HCC

Excess body weight and diabetes are linked to an increased risk of cancer in multiple organs (Stone et al., 2018). Excess body weight and diabetes can induce systemic changes, including altered immune function and systemic endocrine changes, which are hallmarks of multiple types of cancer (Avgerinos et al., 2019). Excess body weight and diabetes are always shown associated with fatty liver disease. Current evidence shows that fatty liver disease is rapidly becoming the leading cause of HCC (Orabi et al., 2021). Studies have demonstrated that liver-specific mechanisms through which Non-Alcoholic Fatty Liver Disease (NAFLD) or Nonalcoholic Steatohepatitis (NASH) promote HCC involve metabolic and oxidative stress, altered immune function, pathological inflammatory responses, and altered endocrine or adipokine signaling (Anstee et al., 2019; Sutti and Albano, 2020). In the past decade, there have been improvements in non-drug therapies and drug therapies for HCC treatment. Non-drug therapies include hepatic resection, liver transplantation, trans-arterial chemoembolization (TACE), and ablation. Meanwhile, drugs including small-molecule targeted drugs like sorafenib and monoclonal antibodies such as nivolumab are mainly used for the systematic treatment of advanced HCC (Chen et al., 2020).

Pathological inflammation and cell damage induced by oxidative stress and endoplasmic reticulum (ER) stress seem to have a key role in promoting HCC. The deranged fatty acid metabolism in hepatocytes can cause DNA damage owing to increased ROS, produced as a result of mitochondrial dysfunction (Nishida et al., 2016). The altered expression of specific metabolic enzymes can affect hepatocytes by decreasing their ability to repair DNA damage (Tummala et al., 2014). Thus, the ER stress, increased ROS production could cause oncogenic genetic alterations in hepatocytes and promote the expansion of malignant cells.

### III.3.2 CCA

CCAs are usually asymptomatic in early stages and, therefore, often diagnosed when the disease is already in advanced stages, which highly compromises therapeutic options, resulting in a dismal prognosis (Andersen et al., 2012; Banales et al., 2016). CCAs are a heterogeneous group of tumors that arise from the cholangiocytes that line the biliary tree. Based on their anatomic location, CCAs are classified as intrahepatic CCA (iCCA), perihilar CCA (pCCA), or distal CCA (dCCA)

(Razumilava and Gores, 2013). In addition, the high heterogeneity of CCAs at the genomic, epigenetic, and molecular levels severely compromises the efficacy of the available therapies (Banales et al., 2020).

CCA often arises in the setting of chronic biliary inflammation and/or cholestasis (Andersen, 2015). For instance, in the western world, primary sclerosing cholangitis (PSC) is associated with 10% of CCA cases (Clements et al., 2020). Uncommon defects of biliary anatomies, such as choledochal cysts (bile duct cyst), Caroli's syndrome (intrahepatic biliary cysts), biliary papillomatosis or adenoma, are linked with a high risk (6-30%) of CCA development (Clements et al., 2020; Tyson and El-Serag, 2011).

Chronic inflammation and/or cholestasis can provide a unified pathway for the molecular pathogenesis of CCA by acting on a series of intercellular pathways that encourage carcinogenesis (Labib et al., 2019). For example, the inflammatory cytokine Interleukin-6 (IL-6) affects multiple intracellular pathways that contribute to cholangiocarcinogenesis, such as, increasing Akt pathway activation which mediates cell survival, mitosis, migration, and angiogenesis (Frampton et al., 2012; Zabron et al., 2013). Inflammatory cytokine Tumor necrosis factor α (TNFα) causes upregulation of Activation-Induced cytidine Deaminase (AID) resulting in multiple somatic gene mutations including in tumor suppressor gene p53 and the MYC proto-oncogene (Komori et al., 2008).

Just as shown above, the progression from steatosis to fibrosis/cirrhosis and even liver cancers is an extremely complex process. But the initiation of liver disease is clearer which is always associated with hepatocyte metabolism dysfunction and/or death induced by multiple factors. Since one of the hallmark features for liver disease occurrence is excessive lipid droplet accumulation. Therefore, understanding the molecular mechanisms of how those risk factors affect hepatocyte's LD metabolism is essential to prevent the development of liver disease.

## III. 4 Hepatitis C virus (HCV)

The HCV is an enveloped, single-stranded RNA virus of the genus *Hepacivirus*, and the family *Flaviviridae*. The HCV genome encodes a large polyprotein precursor subject to proteolytic cleavage by viral and host proteases to generate both structural (core, E1 and E2) and non-structural (p7, NS2, NS3, NS4A, NS4B, NS5A, and NS5B) proteins. The single-stranded RNA genome is encapsulated in an icosahedral protein coat, within a lipid envelope in which the highly glycosylated E1 and E2 glycoproteins are embedded (Beeck and Dubuisson, 2003; Kato, 2000).

A hallmark of HCV infection is the presence of steatosis in the liver, which is thought to be linked to liver disease and can be detected in up to 70% of infected individuals (Leandro et al., 2006). In chronic hepatitis C patients, the prevalence of steatosis ranges from 40% to 86% (mean,

55%) (Mihm et al., 1997; Rubbia-Brandt et al., 2000). Steatosis occurs more frequently in patients with chronic hepatitis C (55%) than in the general population (20%-30%) of adults in the Western world (Clark et al., 2002). It seems that HCV genotype can play a role in inducing steatosis. As, genotype 3 has the highest association with steatosis, which is present in 73% of patients with genotype 3 and in 50% of patients infected with other genotypes (Asselah et al., 2006).

Although the mechanisms underlying the development of steatosis in HCV infection are not exactly known, there are some findings to describe the mechanism of TG accumulation. For example, HCV proteins core and NS5A are suspected to interact with the cell machinery involved in lipid metabolism. They inhibit microsomal triglyceride transfer protein (MTP) activity, which is a rate-limiting enzyme with a key role in the assembly of very-low-density lipoprotein (VLDL). The direct and likely consequence of this is the accumulation of TG in the cells causing steatosis (Asselah et al., 2006; Koike, 2009). HCV core proteins are also capable of impairing the mitochondrial lipid oxidation by decreasing expression of medium-chain acyl-CoA dehydrogenase (MCAD) and short-chain acyl-CoA dehydrogenase (SCAD), both of which are involved in regulating β-oxidation of fatty acids in a process controlled by Forkhead box protein A2 (FoxA2), which also inducing overproduction of reactive oxygen species (ROS) (Hino et al., 2014; Saad et al., 2014).

# Chapter II

# The lipid droplet

## I. Generalities

The lipid droplets (LDs) were first described by Richard Altmann and E. B. Wilson in 1890 and 1896, respectively, as fat droplets inside cells. Because LDs were assumed to be inert forms of fat storage, investigation of their biology was limited for much of the next century. This aspect changed, however, in 1991 when Dean Londos and his laboratory discovered that LDs contained proteins, the most abundant of which he named perilipin (Greenberg et al., 1991). Across different cell types, the size and number of LDs differ considerably. Small droplets (300–800 nm diameter) that are designated initial LDs form in nearly all cells. Later in LD formation, most cells convert some initial LDs to larger so-called expanding LDs (>1 μm diameter), giving rise to two distinct LD types within cells (Wilfling et al., 2013). The LDs have several functions which are all crucial for the maintenance of body homeostasis (Olzmann and Carvalho, 2019; Thiam and Dugail, 2019).

# II. LD structure

The LDs have a unique structure with a hydrophobic core of neutral lipids surrounded by a monolayer of phospholipids in contrast to other organelles enclosed in a bilayer membrane, the monolayer surface contains a number of proteins (Figure 4).

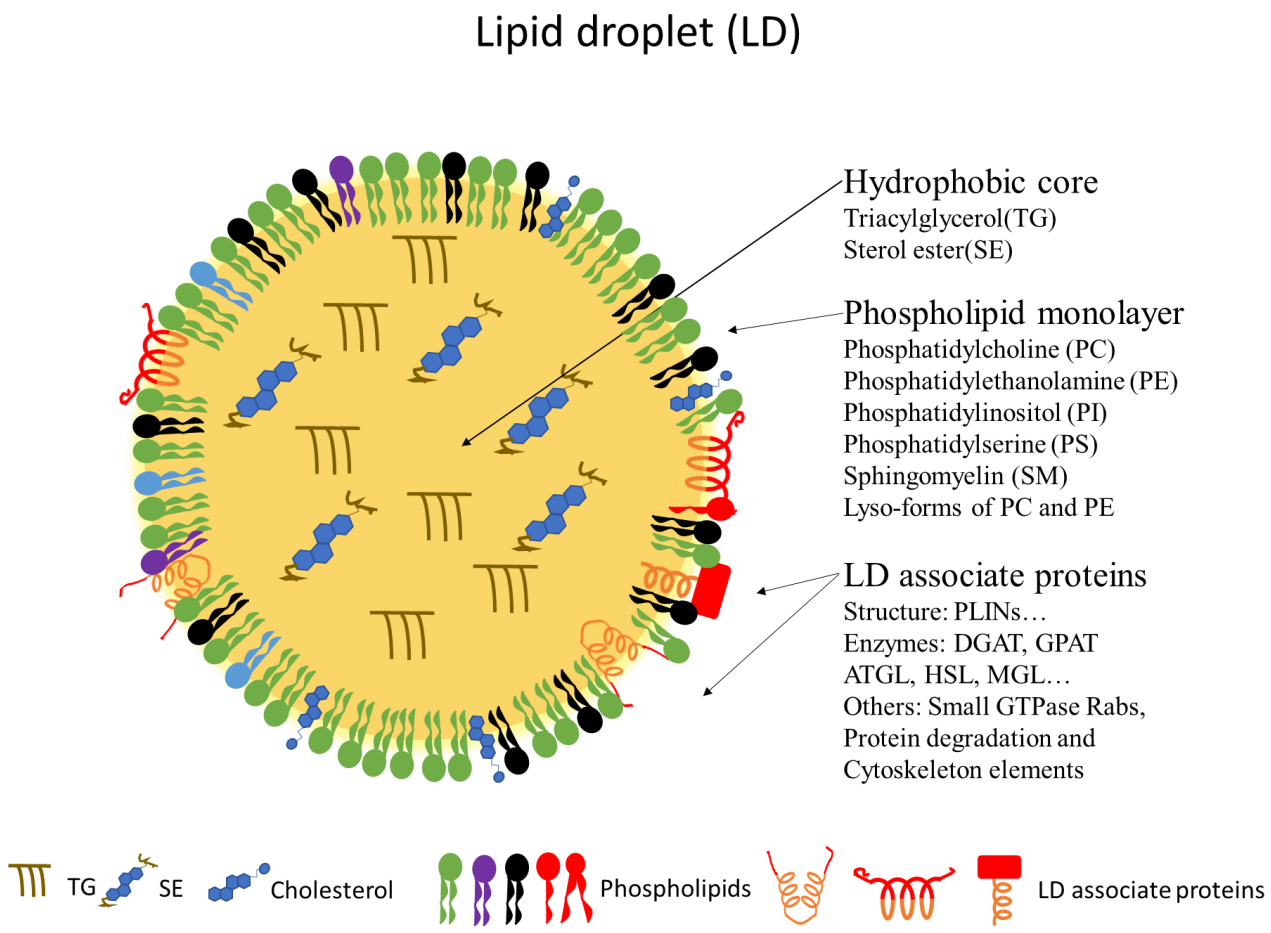


*Figure 4 Lipid droplet structure*

*LDs are surrounded by a phospholipid monolayer enclosing a core filled by neutral lipids, most commonly TGs and SEs, on the surface, different proteins have been identified, such as perilipin and enzymes involved in LD metabolism and proteins for trafficking.*

## II.1. The hydrophobic core

The hydrophobic core of LDs contains predominantly neutral lipids such as triacylglycerol (TG) and sterol esters (SE) (Figure 4). Depending on the cell type, the ratio between the neutral lipids is different. For example, in white adipocytes, TGs are primarily stored in LDs, whereas in steroidogenic cells, SEs are the main component (Fujimoto et al., 2008). Although, many other lipids such as retinyl esters, ether lipids are stored in the LD core (Blaner et al., 2009; Wilfling et al., 2014a).

## II.2. Phospholipid monolayer

To prevent the coalescence of droplets, cells coat the hydrophobic core of LDs with a surface monolayer of phospholipids (Walther and Farese, 2012), which act as surfactants and stabilize the dispersed particles. The main constituent of LD monolayer membranes is phosphatidylcholine (PC) that is followed by phosphatidylethanolamine (PE), phosphatidylinositol (PI), phosphatidylserine (PS), sphingomyelin (SM), and lyso-forms of PC and PE (Chitraju et al., 2012; McIntosh et al., 2010; Penno et al., 2013) (Figure 5). Phosphatidic acid (PA) and free cholesterol are also present in LD surfaces in small amounts (Fei et al., 2011; Tauchi-Sato et al., 2002) (Figure 4). Many studies have shown that changes in the composition of phospholipids can affect LD in a variety of ways, and therefore the phospholipid composition of LDs plays an important role in their homeostasis.

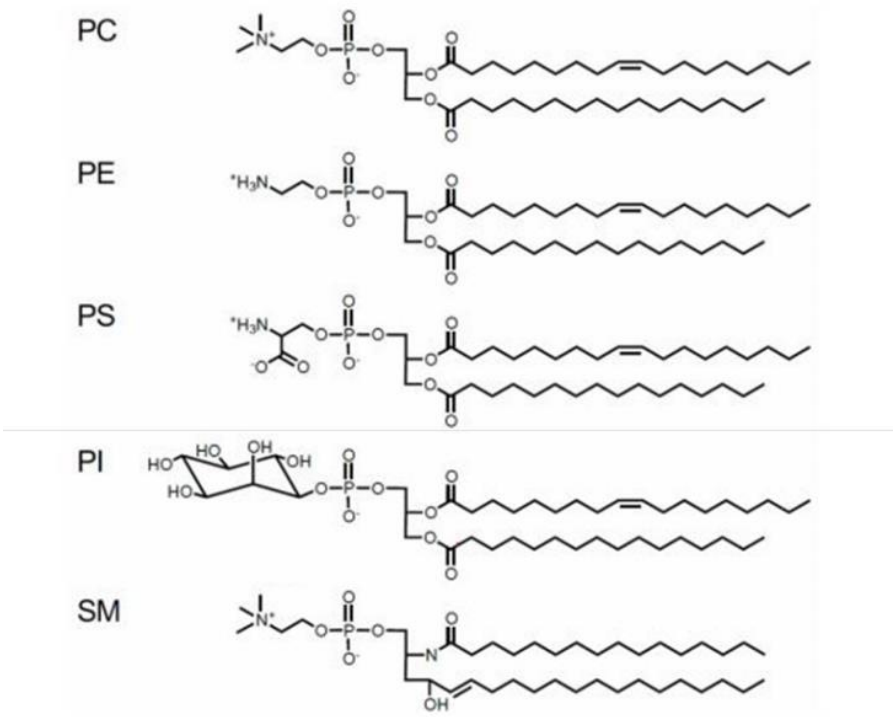


*Figure 5 Structures of the phospholipid classes*

*Diagram for different phospholipids in membranes. These phospholipid molecules contain various acyl chains.*

## II.3. LD associate proteins

Besides the phospholipids, the proteins associated with the monolayer of LDs are also important factors in the regulation of the homeostasis of LDs and various proteomics-based approaches have determined their complete repertoire (Bersuker et al., 2018; Brasaemle et al., 2004; Krahmer et al., 2013a). Those studies revealed that over two hundred proteins are localized to the surface of LDs. Irrespective of the cell types, LD proteomes are dominated by enzymes involved in lipid metabolism and members of the perilipin family. Nevertheless, proteins with other functions such as membrane trafficking and protein degradation are also represented (Figure 4) (Olzmann and Carvalho, 2019).

### II.3.1 Protein motifs for LD targeting

The most common motifs that target a protein to LD surface are amphipathic helices (AH) and hydrophobic domains such as hydrophobic helices (HH) and hydrophobic hairpin (HP) (Thiam and Dugail, 2019) (Figure 6).

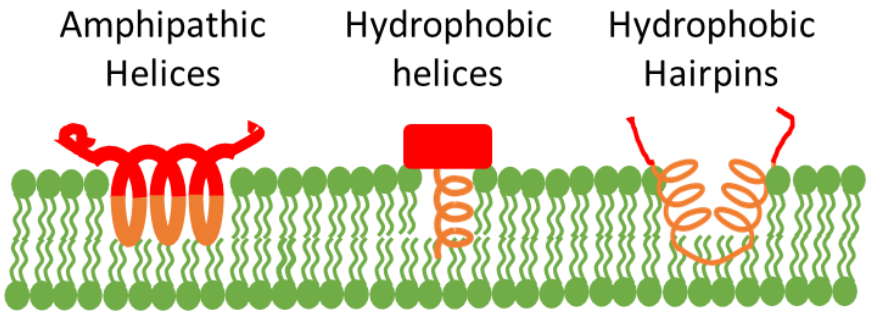


*Figure 6 The main protein motifs for LD targeting*

*Schematic representation of interactions of specific protein motifs such as AH, HH, and HP with LDs. The orange parts are hydrophobic and the red parts are hydrophilic or the domains towards the cytosol.*

#### II.3.1.1 Amphipathic helices

Amphipathic helices (AHs) are protein sequences that fold into a helical structure upon contact with a polar/non-polar interface (Figure 6). The AH motifs are well presented in, perilipins (PLINs) which all use an 11-mer AH repeat in their N-terminus for localization to LDs (Rowe et al., 2016). While it is noteworthy that although AH motif provides membrane binding capacity, how proteins were able to specific binding to LDs is still a fascinating question. For this problem, some possible mechanisms have been proposed. For example, the LD surface can accommodate a lower phospholipid density compared to bilayers, which may easily detect and bind by the AHs (Prévost et

al., 2018; Thiam et al., 2013a). A tuned balance of the hydrophobic level of an AH may also be required for the specific reorganization. This hydrophobic balance depends on several parameters such as the hydrophobicity of the amino acids in the AH, the proportion of hydrophobic amino acids in the AH sequence, and AH length (Thiam and Dugail, 2019). Increasing the number of bulky hydrophobic residues on the hydrophobic face of AH, such as tryptophan or phenylalanine, will impair its binding specificity to LDs (Giménez-Andrés et al., 2018; Prévost et al., 2018). Further in proteins with long AH sequences such as PLIN4, which has a weak hydrophobic face but the overall hydrophobic level equal to shorter AHs with more hydrophobic resides may gain specificity to LDs by having an optimal length (Čopič et al., 2018).

### II.3.1.2 Hydrophobic domains

The hydrophobic domains are another motif that is always present in LD associate proteins (Figure 6). Indeed, the lipid synthesis enzymes, such as GPAT4 (Wilfling et al., 2013), DGAT2 (Stone et al., 2006) possess hydrophobic domains. Interestingly, a peroxisomal membrane protein fatty acyl-CoA reductase 1 (Far1) may use a similar motif to attach LD (Exner et al., 2019). These proteins are generally thought to adopt a hairpin conformation in which a hydrophobic domain embedded in the monolayer is flanked by hydrophilic regions that are exposed to the cytosol, forming a V shape extending from the membrane. And the lack of luminal loops or domains typically found in transmembrane proteins allow them to be accommodated in the outer leaflet of the ER and the monolayer of the LD (Roberts and Olzmann, 2020). Most of the proteins that contain HHs target LDs after their initial incorporation into the ER membrane, Their targeting to LDs is through membrane bridges from the ER (Kory et al., 2016).

It is worth noting that the proteins associated with LD are not invariable and the composition of the proteins can change, under different physiological conditions. Proteins are dynamically recruited to and dissociated from the LD surface to control LD behavior and function. And it has been believed that this dynamic change was achieved by the temporal remodeling of the physical chemistry properties of the LD surface (Thiam and Dugail, 2019). In the following, we present the different stages of the lipid droplet, from lipid droplets synthesis to its catabolism process, to discuss the crucial role of LD proteins and surface phospholipids composition in regulating lipid droplets.

# III. LDs biogenesis

LD biogenesis is processed by three major steps: the synthesis of neutral lipids and lens formation in ER, LD budding from the ER membrane and the cytosolic stages of LD growth, and maturation.

## III.1. The neutral lipids synthesis and lens formation

The first step in LD biogenesis is the synthesis of neutral lipids, most commonly TGs and SEs. This process is mediated by several enzymes which are all localized primarily to the ER. The SEs are made by acyl-CoA: cholesterol O-acyltransferases (ACAT1 and ACAT2). Whereas TGs synthesis in the ER are involving several steps, the first and rate-limiting step is catalyzed by GPAT3 or GPAT4, which convert glycerol 3-phosphate (G3P) and fatty acyl-CoA (Acyl-CoA) to lysophosphatidate (LPA). LPA is then converted to phosphatidic acid (PA) by AGPAT enzymes. PA is subsequently dephosphorylated to diacylglycerol (DG) by lipin PAP enzymes (lipin 1, 2, or 3). The final step is the conversion of DG to TG, which is catalyzed by DGAT1 and DGAT2. (Figure 7). The newly formed neutral lipids are transferred into the intermembrane space of the ER. At low concentrations, neutral lipids are dispersed between the leaflets of the ER bilayer. As long as the neutral lipid concentration reaches a critical level, neutral lipids eventually coalesce, forming a lipid lens (Figure 7).

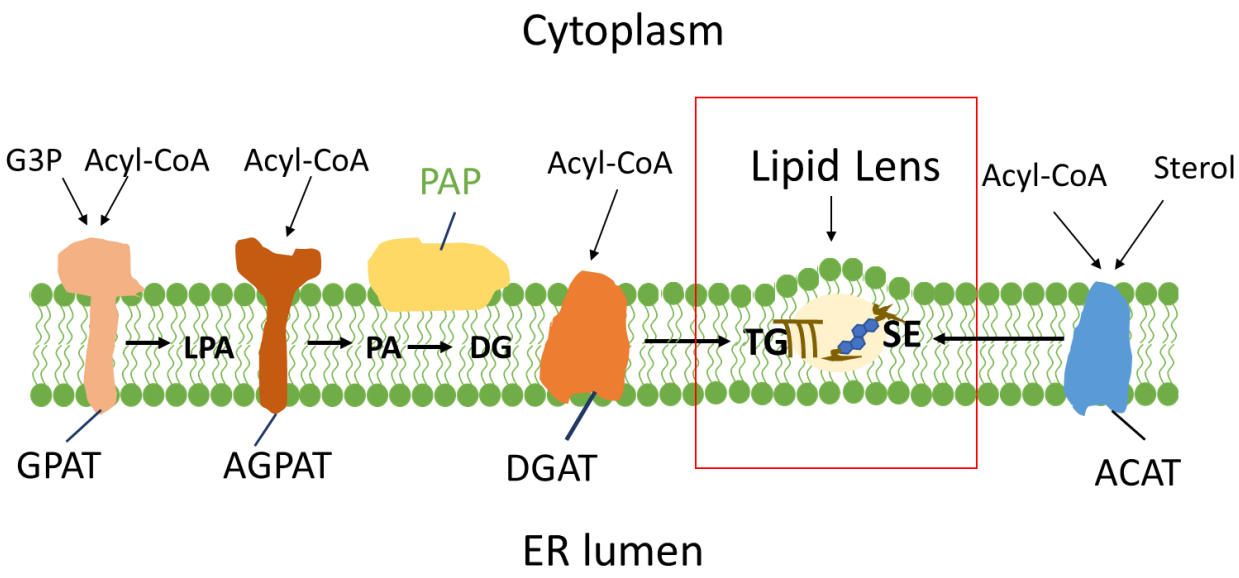


*Figure 7 Neutral lipid synthesis and lens formation in ER*

*Lipid synthesis and lens formation occur within the ER outside membrane, and it takes a few steps: first, triacylglycerol (TAG) synthesis and cholesterol ester synthesis enzymes deposit neutral lipids in between the leaflets of the ER bilayer. Second, the TG and SE reached a critical level and coalesce. AGPAT, acylglycerolphosphate acyltransferase; DG, diacylglycerol; DGAT: diacylglycerol acyltransferase; G3P, glycerol-3-phosphate; GPAT, glycerol-3 phosphate acyltransferase; LPA, lysophosphatidic acid; PA, phosphatidic acid; PAP, phosphatidic acid phosphatase; ACAT, Acetyl-CoA acetyltransferase.*

The formation of lipid lens has been described as a phase de-mixing phenomenon, which is controlled by energetic constraints in response to the increased accumulation of TGs in the intermembrane space of the ER (Thiam and Forêt, 2016), which means the formation of lipid lens needs to overcome an energy barrier. Thus, the region where the lens is formed is likely to have a lower energy barrier as seen in the situation like membrane curvature (Thiam and Beller, 2017). For instance, LDs appear to arise from ER tubules in mammalian cells, which are the highly curved region of the ER (Kassan et al., 2013).

One way to induce membrane curvature is the insertion of proteins into the membrane (McMahon and Boucrot, 2015). Among the several proteins inserted in the ER membrane, the seipin protein, has been shown to play an important role in regulating LD lens formation sites and impacts lipogenesis (Bi et al., 2014; Wang et al., 2016). The fat-storage-induced transmembrane (FIT) proteins are also needed for the budding of lipid droplets from the ER membrane (Choudhary et al., 2015) (Figure 8). The membrane curvature is also essentially controlled by the globe and local

phospholipid composition of the ER (Figure 8). For instance, phospholipase A2 (PLA2) can generate membrane curvature by generating lysophospholipids, and promote LD biogenesis *in vitro* (Ben M'barek et al., 2017). Overexpressing PLA2 in HeLa and Huh7 cells promoted LD formation, and lyso-PC also stimulated LD formation from the ER (Ben M'barek et al., 2017; Choudhary et al., 2018). Interestingly, the change of phospholipid composition in lens formation site seems also to be controlled by proteins. Such as seipin protein which has been reported specifically binding to the PA (Sui et al., 2018; Yan et al., 2018).

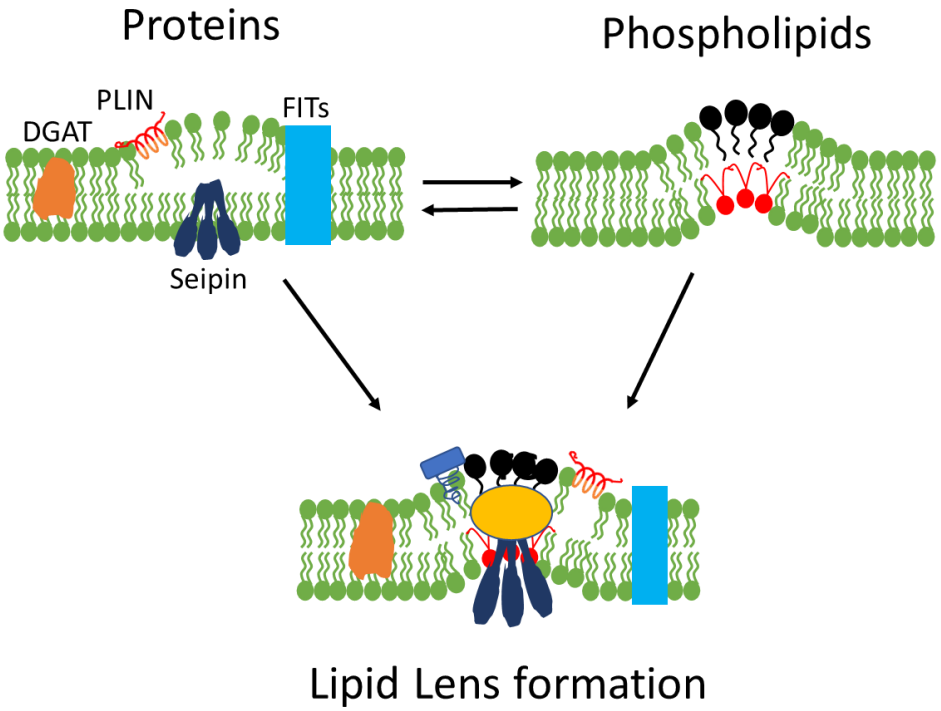


*Figure 8 The lipid lens formation site determines by the proteins inserted in or the phospholipid composition of ER membrane.*

*The favorite site for Lens formation is where a membrane curvature emerged, and the emergency of curvature membrane could be arising from the composition change of Phospholipids and proteins insertion.*

## III.2. LD Budding

The LDs budding from the ER membrane results from the expansion of the neutral lipid lens. Although, during the budding stage, the LD shares its phospholipid monolayer with the ER while the composition of the two membranes is different (Zanghellini et al., 2010). Furthermore, several works, particularly those performed *in vivo*, confirmed that ER membrane phospholipid composition is

critical for LD budding (Adeyo et al., 2011; Skinner et al., 2009). It has been proposed that the ER phospholipid composition affects budding efficiency mostly through geometric effects. For example, the conically shaped molecules, such as DG or PE, disfavor budding, whereas molecules with opposite geometry, such as lysophospholipids, promote budding (Ben M'barek et al., 2017; Choudhary et al., 2018) (Figure 9). It should be noticed that the positive curvature that enriched of inverted cone structure lipid, like LysoPIs, facilitated the initial LD emergence into the cytoplasm, However, the fully emerged LDs are connected to the ER through a neck with a strong negative curvature. Thus, the final scission of LDs from the ER may be promoted by conical/negative curvature generating shaping lipids such as PA and DAG (Gao et al., 2019). The alteration of phospholipid composition also appears to impose directionality on the budding process, at least *in vitro* (Chorlay and Thiam, 2018).

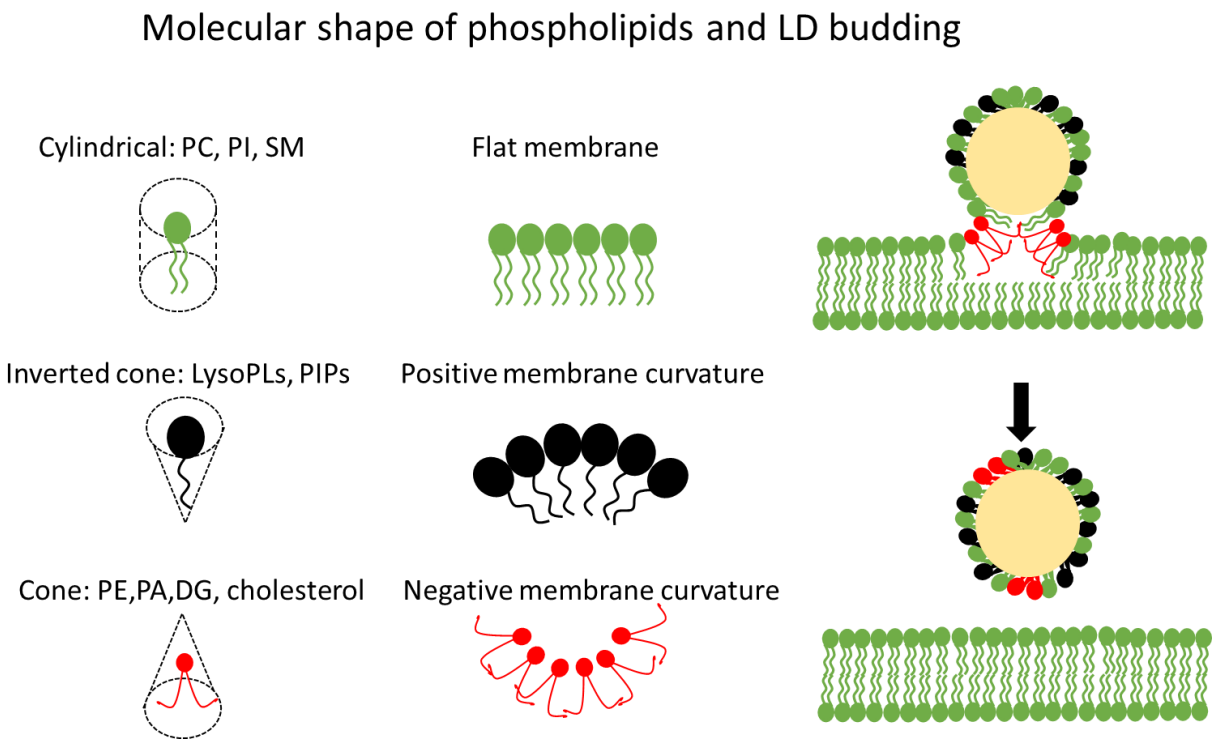


*Figure 9 The molecular shape of Phospholipids affects LD budding.*
*Lipids with different headgroups and acyl chains are inscribed within their corresponding geometrical shapes. Alignment of the same molecular shape lipids will produce different membrane curvatures. In LD budding process, ER phospholipid composition affects budding efficiency.*

## III. 3 LD growth and maturation

The LD growth could occur through their fusion, transfer of TG to LDs via ER membrane bridges, or through TG synthesis directly on the LD surface.

### III.3.1 LDs fusion

Two different pathways of LD fusion have been described. It can occur by Ostwald ripening or coalescence of small LD to form one large LD (Thiam et al., 2013a). Although usually, the surfactant properties of the phospholipid on the LD surface prevent LD fusion, an alteration of the phospholipid composition which reduced the surface tension leads to the spontaneously merge of LDs (Figure 10). For example, the PC deficiency resulting from genetic depletion or culture conditions specifically leads to LD coalescence (Guo et al., 2008; Krahmer et al., 2011).

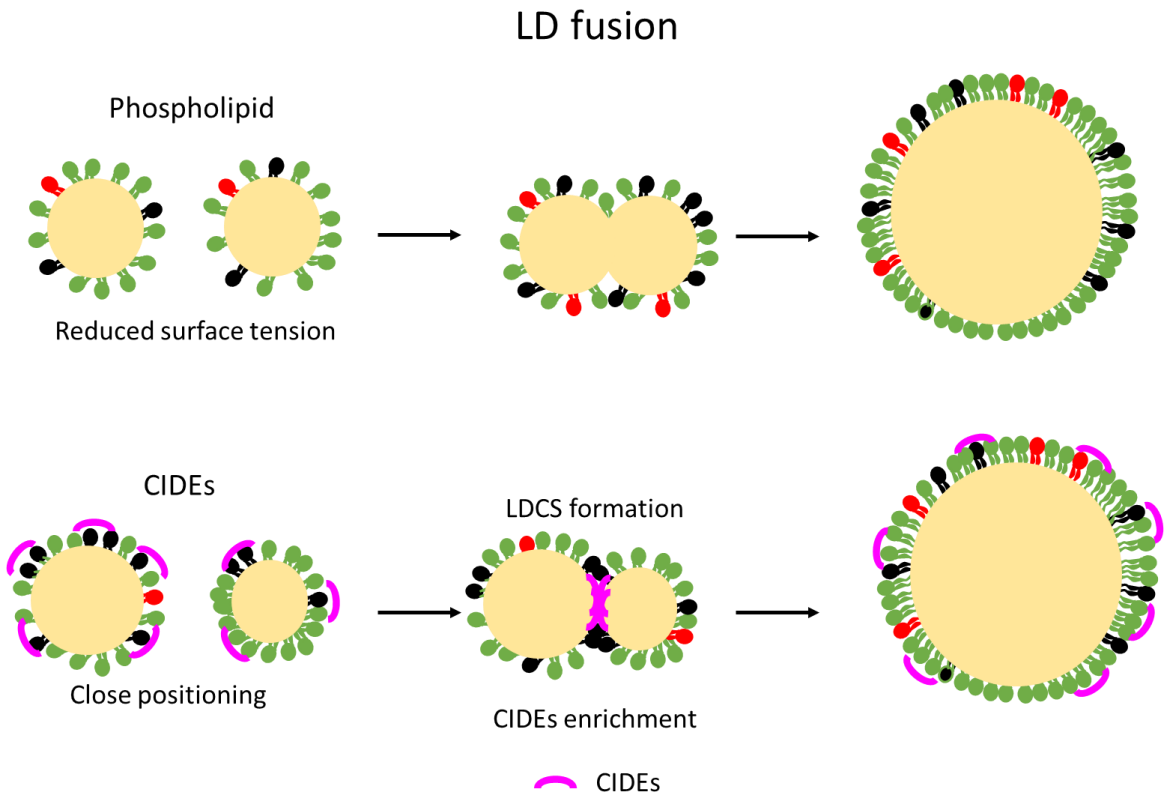


*Figure 10 The LD surface phospholipids and CIDE proteins in LDs fusion*
*Model depicting the mechanism of Phospholipid composition change and CIDEs-mediated LD growth. The alter of the phospholipid composition which reduced the surface tension, lead to the spontaneously merging of LDs. When two LD are closed contacted, the CIDE proteins are re-localized, enriched, and clustered at LDs contact sites and promote LD fusion and growth.*

In addition to the alteration of the phospholipid composition, some specific proteins are

involved in LD fusion, such as the cell death-inducing DFF45-like effector (CIDE) family proteins. When two LD are closed contacted, the CIDE proteins are re-localized, enriched, and clustered at LD-LD contact sites and promotes LD fusion and growth by generating a special pore/channel-like structure allowing lipid transfer from smaller to larger LDs in the contacted pair and the final merging and growth of the LDs (Gong et al., 2011; Sun et al., 2013) (Figure 10). A further study on CIED proteins identified CIDEA protein as a PA interactor (Barneda et al., 2015), thus, they proposed that the CIDEA LD fusion activity needs their interaction with LD surface PA, since they found that CIDEA was inactive in cells defective in phospholipase D (pld1$\Delta$), which catalyzes the production of PA from PC (Rose et al., 1995). In addition, although the author didn't mention it, their results also showed CIEDA interacted with several phosphatidylinositols (Barneda et al., 2015), thus, the PIs may also involve in the CIDEA dependent LD fusion.

### III.3.2 Local synthesis by enzymes

The localized synthesis of TGs is enabled through the re-localization of several enzymes from the ER to the LD surface, with newly made TG accumulating in LD hydrophobic core (Figure 11).

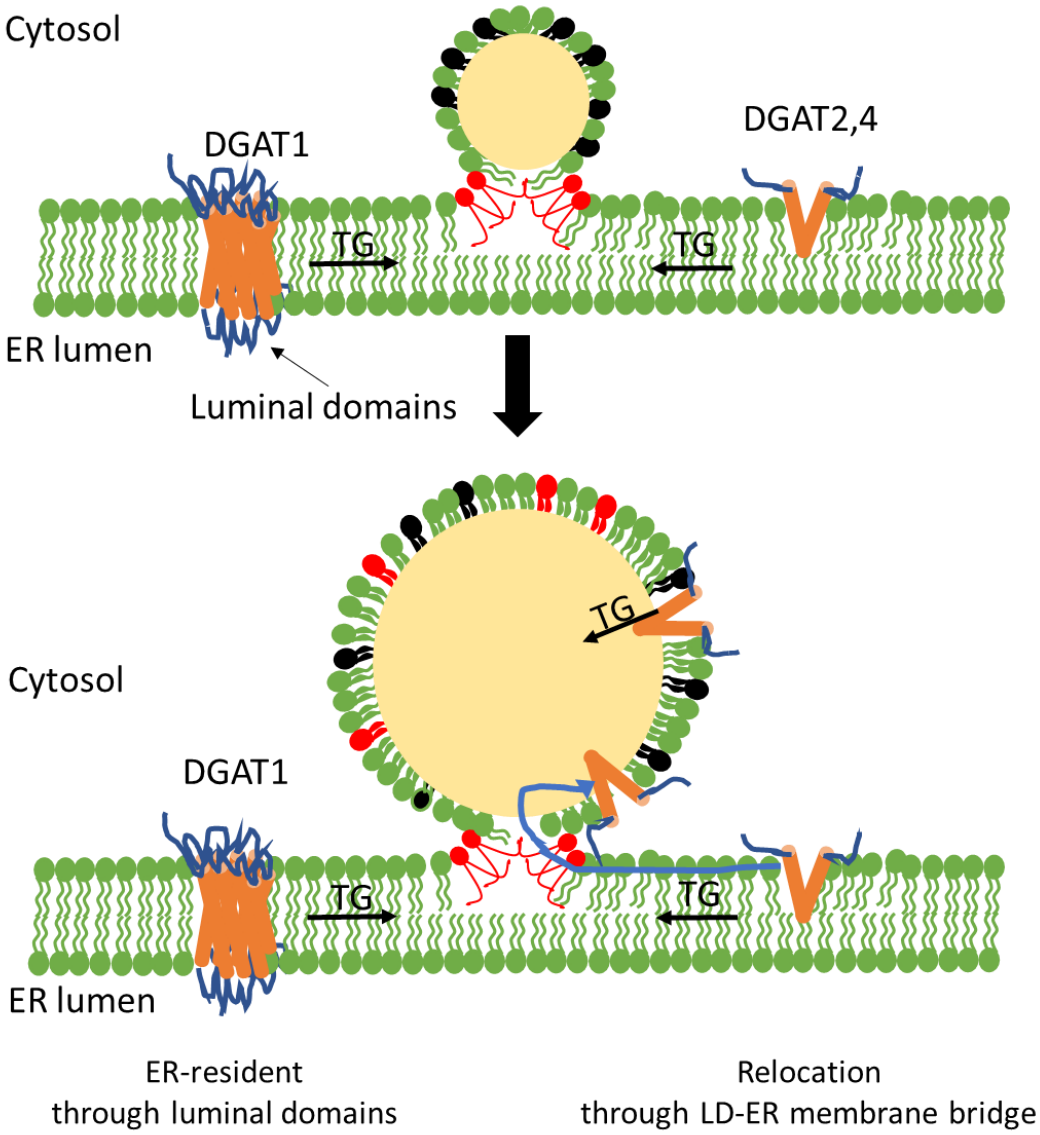


*Figure 11 The re-localization of several enzymes from the ER to the LD surface promotes the LD growth.*

*The enzymes that re-localize from the ER to the surfaces of LD are GPAT 4 and DGAT2. DGAT1 remain localized in ER duo to its ER luminal domains.*

The enzymes that re-localize from the ER to the surfaces of LD are GPAT 4 and DGAT2 which catalyze the first and last steps of TG synthesis, respectively. While, some TG synthesis enzymes, such as DGAT1, always remain in the ER. This retention may raise from the structure of the protein, indeed, DGAT1 contains multiple membranes spanning domains with large ER luminal domains that anchor the protein in the ER (McFie et al., 2010). By contrast, GPAT4 and DGAT2 are mostly in the cytoplasm and are anchored by a membrane-embedded segment that does not seem to

span the entire bilayer and might adopt a hairpin conformation (Wilfling et al., 2013). These ER luminal domains may determine whether the enzymes are localized to the LD surface or not.

### III.3.3 COPI for LD growth

In addition, to these two pathways, proteins involved in membrane trafficking could play a role in this modification of LD composition and growth. The coat protein complex I (COPI), which is known for its function in the trafficking of proteins and lipids from the Golgi back to the ER (Beck et al., 2009) and small cargo between Golgi stacks (Pellett et al., 2013), has been shown to control several proteins targeting to LDs surface, such as the GPAT4, DGAT2 (Wilfling et al., 2014b). This is also achieved through modifying the LDs surface composition by budding nano-LDs, which in turn altered the phospholipid composition of LDs and increase LD surface tension (Thiam et al., 2013b), and promoting the formation of bridges between matured LD and the ER (Wilfling et al., 2014b).

### III.3.4 The protein composition changes during LD growth and maturation

The composition of the binding proteins is changing during LD growth and maturation (Figure 12). For example, in adipocytes, small LDs stained positive for PLIN3, while medium LDs had PLIN2 and the largest LDs were enriched with PLIN1 (Wolins et al., 2005). This change of proteins composition on LDs surface at different stages of their expansion has been corroborated by video-microscopy of LD biogenesis (Kassan et al., 2013) and by a proteomics study that identified the proteins present on purified LDs of different sizes (Zhang et al., 2016c). Thus, it was proposed that a unique set of proteins is recruited and subsequently dissociated as LDs grow and mature (Wolins et al., 2006). Although the exact mechanism for this exchange is currently unknown, the different binding affinity of each PLINs to the phospholipid monolayer at the LD surface may have a role in this process (Thiam and Beller, 2017). Furthermore, the sequential recruitment of proteins could also be based on an enzyme-mediated remodeling of the phospholipid monolayer, which would result in altered biophysical properties of lipid droplet surface that are potentially recognized by the given protein (Thiam and Beller, 2017).

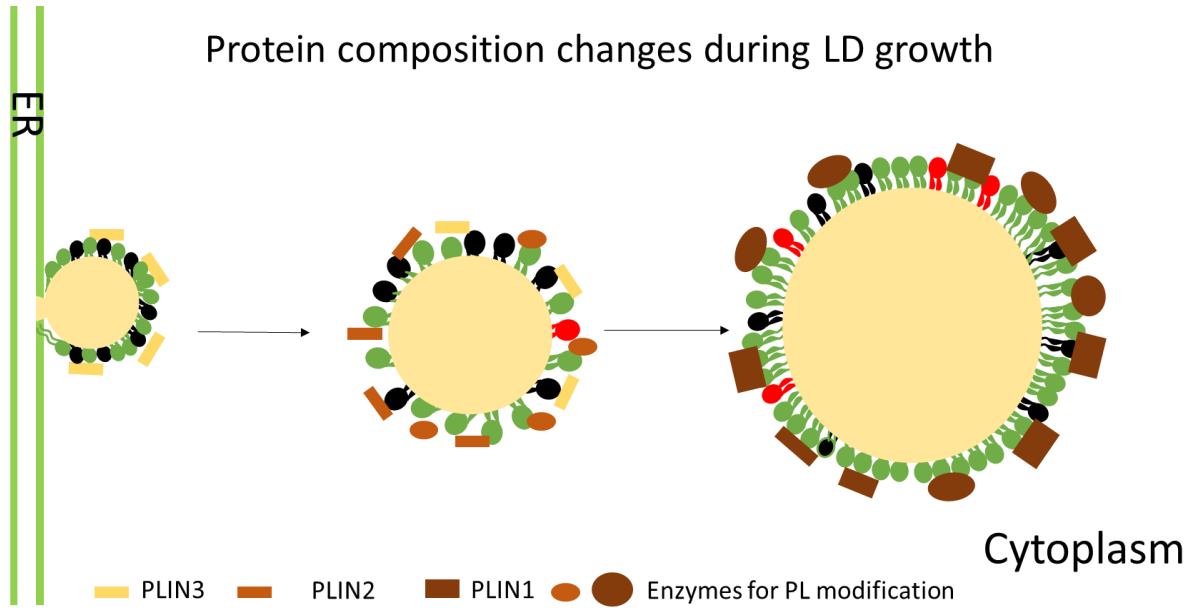


*Figure 12 The PLINs association change during LD growth.*

*During the LD growth, the LD associated PLINs change, small LDs stained positive for PLIN3, while medium LDs had PLIN2 and the largest LDs were enriched with PLIN1, this change may arise from the different membrane affinity among the different PLINs.*

### III.3.5 Phospholipid synthesis

Noticed that the cytoplasmic leaflet of the ER membrane was needed to continually supply additional phospholipids for the monolayer of LD, thus, under very active LD expansion, new phospholipid synthesis is required to maintain phospholipid homeostasis (Olzmann and Carvalho, 2019). And it seems like that the biosynthesis level of phospholipid is also crucial for regulating the LD size. For example, cells lacking the rate-limiting step in phosphatidylcholine (PC) synthesis, CCTα (phosphocholine cytidylyltransferase α), have only very large LDs, lacking a sufficient level of phospholipids to cover the surface of many small LDs (Krahmer et al., 2011).

# IV. LD catabolism

The studies on LD catabolism generally refer to the hydrolysis of TGs to FAs and glycerol. So far, TG hydrolysis occurs through two different processes, the action of lipases that act directly on the LD surface and the delivery of LDs to lysosomes where they will be hydrolyzed by the lysosomal acid lipase.

## IV. 1 Lipases

There are three main lipases implicated in the complete hydrolysis of TG. The patatin-like phospholipase domain-containing protein 2 (PNPLA2), also known as adipocyte triglyceride lipase (ATGL) catalyzes the first step of TG to generate DG and FA. DG is then cleaved into MG and FA by hormone-sensitive lipase (HSL), which is a multifunctional enzyme with broad substrate specificity and could hydrolyze TG, MG, and CE. MG is finally cleaved into glycerol and FA by monoglyceride lipase (MGL) (Figure 13).

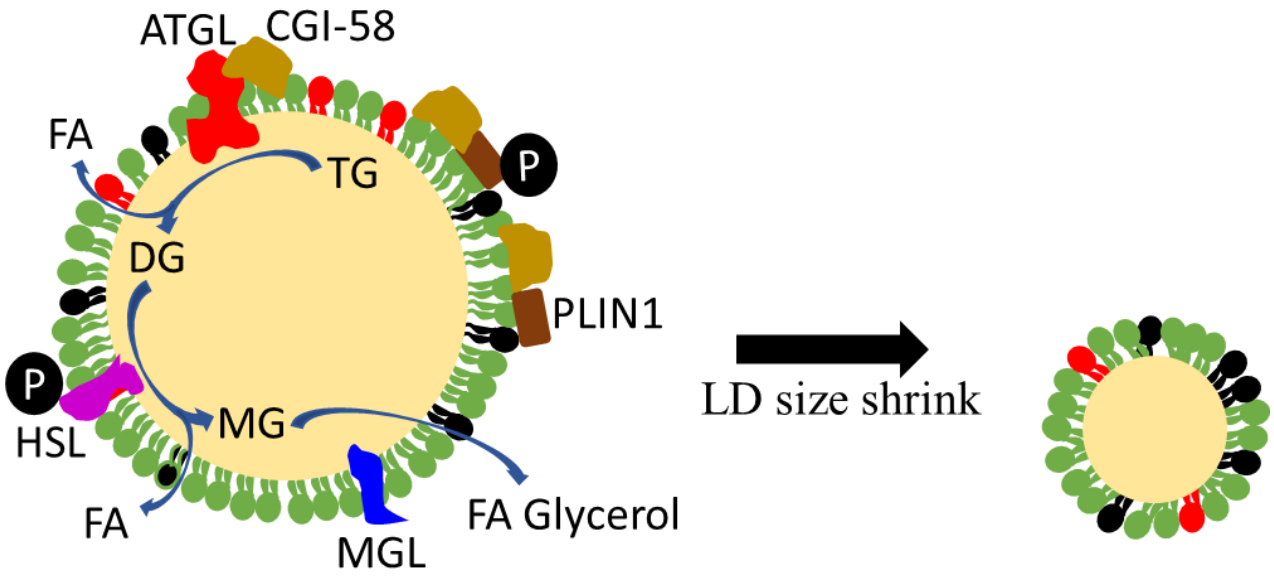


*Figure 13 Lipolysis in LDs catabolism.*
*Schematic representation of lipolysis. ATGL catalyzes the first step of lipolysis. HSL is also bound to LD, hydrolyses DG into FFA and MG. MG is, in turn, hydrolyzed to FFA and glycerol by MGL in the cytosol. The size of the LD decreases over time.*

The physiological activities of ATGL, HSL, and MGL are regulated by their interaction with different proteins and co-activators (Krintel et al., 2008)(Garton et al., 1989). For example, ATGL requires a coactivator protein, comparative gene identification-58 (CGI-58), for full hydrolase activity. Normally, in adipocytes, PLIN1 interacts with CGI-58, preventing its binding to ATGL, when the

lipolysis is stimulated, the protein kinase A (PKA) phosphorylates PLIN1 and causing the release of CGI-58, then the coactivator bins and stimulates ATGL (Granneman et al., 2009; Miyoshi et al., 2007). For HSL, the phosphorylation is important for its enzyme activity and several kinases such as protein kinase A (PKA), AMP-activated protein kinase (AMPK), extracellular signal-regulated kinase (ERK), glycogen synthase kinase-4 (GSK-4), and $Ca^{2+}$/calmodulin-dependent kinase (CAMK) (Lass et al., 2011) have been involved in its modulation. The targeting of ATGL to LDs also depends on COPI (Beller et al., 2008; Soni et al., 2009), thus the proper intercellular trafficking is crucial for LD homeostasis. In addition, the lysosomal acid lipase (LAL) which is localized in the lysosome, exhibits broad substrate specificity, hydrolyzing TGs, DGs SEs (Sheriff et al., 1995; Warner et al., 1981) and REs (Grumet et al., 2016), and contributes to LD catabolism. Thus, the interaction of LDs and lysosomes is also crucial for the regulation of the LD size.

When lipases digest the core of LDs, the LDs shrink in size, and as a consequence, the LD surface also shrinks (Kory et al., 2015). What happens to the proteins on the LD surface under these conditions is not fully understood, but at least two pathways have been suggested: either proteins decreased due to the macromolecular crowding (Kory et al., 2015) or, they could be selectively eliminated by lysosomal degradation.

## IV .2 Autophagy and lysosome

In addition to the lipases described above, cells also utilize autophagy to catabolize LDs. Autophagy is a process in which intracellular components and dysfunctional organelles are delivered to the lysosome for degradation and recycling (Yang and Klionsky, 2020). The Basis on the mechanism of lysosomal cargo delivery and the cargo type delivered to the lysosome, autophagy is classified into three distinct categories: macroautophagy (He and Klionsky, 2009), microautophagy (Sahu et al., 2011), and chaperone-mediated autophagy (CMA) (Cuervo and Wong, 2014). Macroautophagy is the best-characterized and most universal mechanism among the three types of autophagy (Soto-Avellaneda and Morrison, 2020). It is capable of sequestering cytosolic organelles inside double-membrane vesicles known as autophagosomes, which deliver this cargo to lysosomes upon heterotypic fusion with their membrane (Mizushima et al., 2008; Yang and Klionsky, 2010). In this process, a complex interplay of proteins is required, such as ATGs (autophagy-related proteins), LC3 (microtubule-associated proteins 1A and 1B, light chain 3), and P62 (ubiquitin-binding protein p62). In contrast, microautophagy transports cytosolic material into lysosomes through direct invagination or protrusion of the lysosomal membrane (Mijaljica et al., 2011). CMA selectively degrades single proteins with a specific amino acid signature, which is recognized by cytosolic heat shock cognate protein 70 (Hsc70) and then delivered to lysosomes by the CMA receptor lysosomal associated membrane glycoprotein 2A

(LAMP2A).

All three forms of autophagy could be utilized to catabolize LD (Figure 14). For example, the selective degradation of LD by macroautophagy was first described in mouse hepatocytes by electron microscopy data confirming sequestrations of LDs by autophagosomes (Singh et al., 2009). Further studies revealed that the recognition of LD by an autophagosomal membrane is through LC3 (Singh and Cuervo, 2012; Wang, 2016), also LC3 promotes the movement of cytoplasmic ATGL to LD and induces lipophagy (Sathyanarayan et al., 2017). For microautophagy, LD entry into invaginated lysosomes was observed (Tsuji et al., 2017) in yeast. A more recent study also showed microautophagy in hepatocytes, since they observed that LDs appear to be directly injected into or "fuse" with adjacent lysosomal structures (Schulze et al., 2020). In the CMA pathway, PLIN2 and PLIN3 are CMA targets, which are abundant LD-associated proteins that prevent LDs from lipases (Kaushik and Cuervo, 2015). Thus, stimulated CMA leads to the release of PLIN2 and PLIN3 from the LD surface, consequently, enables ATGL to efficiently access the LD surface, thereby increasing lipolytic rates.

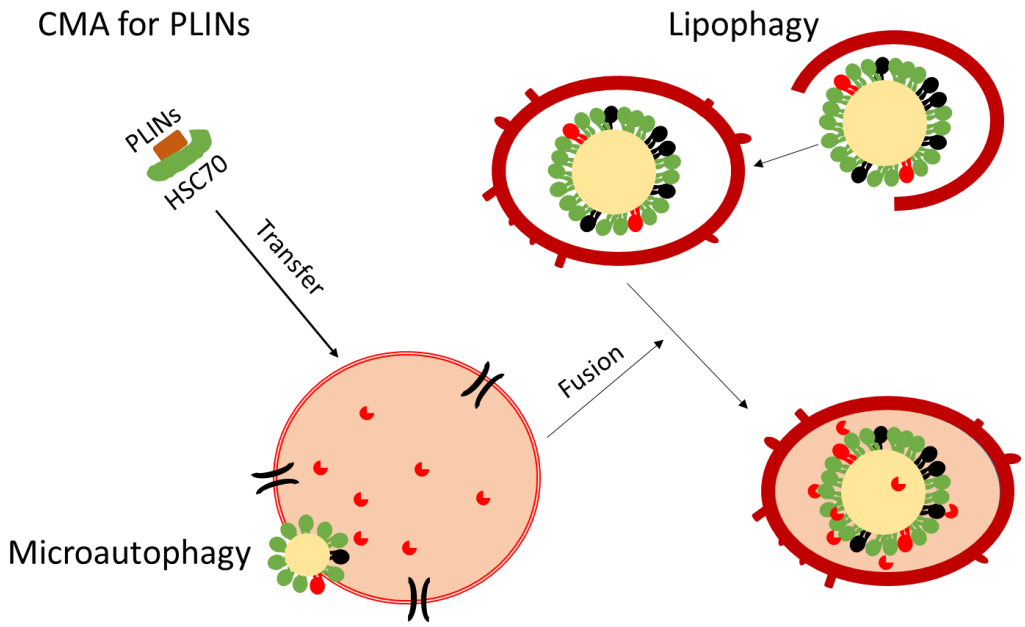


Figure 14 The autophagy for LD catabolism

*Model showing LD autophagy (lipophagy, Microautophagy, and CMA) An autophagosome forms in the cytosol and encapsulates LD, and fuse with lysosomes. LD is directly injected into adjacent lysosomal structures. The PLINs such as PLIN2/3, were shown targeted by HSC70 and be transferred to the lysosome for degradation. Adopted from (Gluchowski et al., 2017)*

It is important to note that to complete the entire degradation process for all forms of autophagy, the interaction with lysosomes is necessary. Meanwhile, the lysosome itself is a very dynamic organelle and its own function needs to be strictly controlled. Therefore, it can be inferred

that the factors that affect lysosomes may also affect LDs.

### IV.3.1 Lysosome structure

Lysosome is an organelle delimited by a bilayer lipid membrane with an acidic internal pH of 4.5-5.0 which is maintained by an adenosine triphosphate (ATP)-dependent proton pump (Figure 15). Morphologically, it is a highly heterogeneous organelle. The lysosome size, shape, and number are variable according to the cell types. The primary cellular function of the lysosome is the degradation and recycling of several macromolecules, including nucleic acids, proteins, glycosaminoglycans (GAGs), oligosaccharides, sphingolipids, and other lipids. Hydrolysis of these macromolecules is achieved by the action of soluble hydrolases present in the lumen of the lysosome that are active at the acidic pH of this organelle (Ballabio and Bonifacino, 2019; Saftig and Klumperman, 2009).

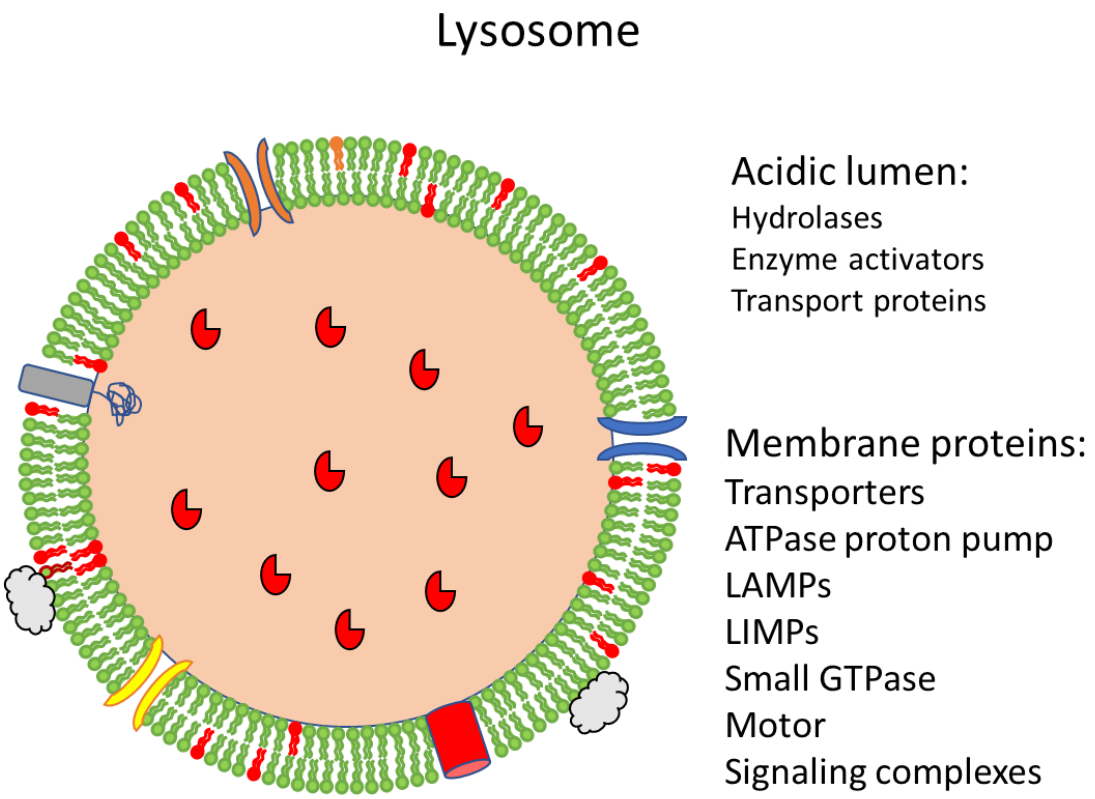


*Figure 15 Lysosome structure*

*The Lysosome is delimited by a bilayer lipid membrane and has an acidic lumen that contains acid hydrolases, enzyme activators, and transport factors. The lysosome membrane is associated with a specific set of proteins. For example, vacuolar ATPase (v-ATPase) maintains the acidic lumen. the highly glycosylated lysosome-associated membrane proteins (LAMPs) that protect the lysosomal membrane from degradation. Transporters for ions, sugars, nucleosides, AA ,and other products from lysosomal degradation. Small GTPase and motor that mediate the movement.*

## IV3.2 Lysosome positioning and motility

Lysosomes are highly dynamic structures (Bonifacino and Neefjes, 2017). Lysosomes are spread throughout the cytoplasm, although with a higher concentration in the perinuclear region. At any given time, some lysosomes are stationary, while others move bidirectionally along microtubule tracks. All lysosomes, however, are potentially motile, as over time some stationary lysosomes start to move, while some moving lysosomes stop moving. Several factors contribute to these dynamics, including immobilization by interactions with perinuclear ER (Jongsma et al., 2016a) and Golgi complex (Starling et al., 2016), or with peripheral actin filaments underlying the plasma membrane (Encarnação et al., 2016), as well as mobilization by interaction with microtubule motors (Harada et al., 1998; Nakata and Hirokawa, 1995). Whereas lysosomes movement from the cell periphery towards the perinuclear region (retrograde movement) is mediated by coupling to cytoplasmic dynein and its activator dynactin (Burkhardt et al., 1997; Harada et al., 1998), movement from the perinuclear region towards the cell periphery (anterograde movement) is mediated by coupling to several kinesins, including members of the kinesin 1 (KIF5) and kinesin 3 (KIF1) families (Guardia et al., 2016; Matsushita et al., 2004; Nakata and Hirokawa, 1995). Lysosomal transport and re-positioning appear to be adaptation mechanisms for changing environmental conditions. Growth factors (Dykes et al., 2016), nutrient availability (Korolchuk et al., 2011), and extracellular pH (Heuser, 1989) trigger the re-positioning of lysosomes which appears to be crucial for nearly all aspects of their functions (Neefjes et al., 2017; Pu et al., 2016).

## IV.3. 3 LD accumulation and lysosome dysfunction

The alterations of the lysosome are implicated in several diseases. Indeed, lysosomes have been implicated in the pathogenesis of various metabolic disorders as best exemplified by their roles in obesity and diabetes (Gilleron et al., 2019; Jaishy and Abel, 2016; Mészáros et al., 2018). The lipid overload that is characteristic of obesity impairs lysosomal function by various mechanisms (Jaishy and Abel, 2016). For instance, feeding of mice with a high-fat diet inhibits lysosomal acidification and acid hydrolase activity, and triggers permeabilization of the lysosomal membrane, with consequent impairment of lysosomal and autophagic functions in different tissues (Gornicka et al., 2012). Despite the harmful effects of a high-fat diet, lysosomal adaptation via the transcription factor EB (TFEB) and the transcription factor E3 (TFE3) can exert a protective effect on whole-body lipid and glucose homeostasis, thereby decreasing the tendency towards obesity and diabetes (Pastore et al., 2017). Lysosomes also participate in whole-body glucose regulation by maintaining the fitness of insulin-producing pancreatic β-cells (Mészáros et al., 2018). Early response of these cells to nutrient starvation is the degradation of nascent insulin granules by sequestration into Golgi complex-derived double-membraned structures that subsequently fuse with lysosomes-a process distinct from

canonical autophagy (Goginashvili et al., 2015). Lysosomal degradation of nascent insulin granules decreases the secretion of insulin and provides the β-cells with an alternative source of amino acids during fasting. When subjected to a high-fat diet, β-cells induce canonical autophagy, which protects them from ER stress and other harmful effects of lipid oversupply (Chu et al., 2015b). However, prolonged lipid overload overwhelms the protective effects of lysosomes and autophagy on metabolic homeostasis and eventually leads to lysosome damage, resulting in deterioration of lysosomal function and β-cell loss.

# V. Intracellular membrane trafficking and LDs

## V.1 Intracellular membrane trafficking

Intracellular membrane trafficking plays a critical role in diverse cellular functions including both developmental and pathological processes (Yarwood et al., 2020). In general, intracellular membrane trafficking involves the formation and budding of membrane vesicles from a donor membrane, their transport, and subsequent fusion with target membranes, leading to transport of cargo from the donor to the target organelle (Rothman, 2002; Søreng et al., 2018). Membrane trafficking can be divided into two basic pathways based on the direction of travel, the secretory pathway, and the endocytic pathway. The secretory pathways refer to the movement of cargoes of newly synthesized proteins, lipids, or carbohydrates moving from the ER via the Golgi to the cell membrane or extracellular space. Conversely, endocytic pathways are the movement of cargoes from the plasma membrane or extracellular space into the cell. This can be often used for the uptake of nutrients or to receive receptor-dependent cell signaling from the extracellular space. Another important function of the endocytic pathway is to direct cargoes for recycling or degradation. In the secretory pathway, newly synthesized proteins are translocated into the ER. ER-derived cargo enters the cis-Golgi complex and moves through the TGN to the target sites such as lysosome or plasm membrane. On the other hand, endocytic pathways start at the plasma membrane and use multiple ways for internalization, such as clathrin-dependent, caveolin-dependent internalization. Internalized cargo can traffic into early endosomes, where it is sorted either back to the surface of the cell by recycling or into multivesicular bodies (MVBs) and lysosomes for degradation. The caveolin-dependent internalized cargo termed caveolae could transport to the LD. (Figure 16)

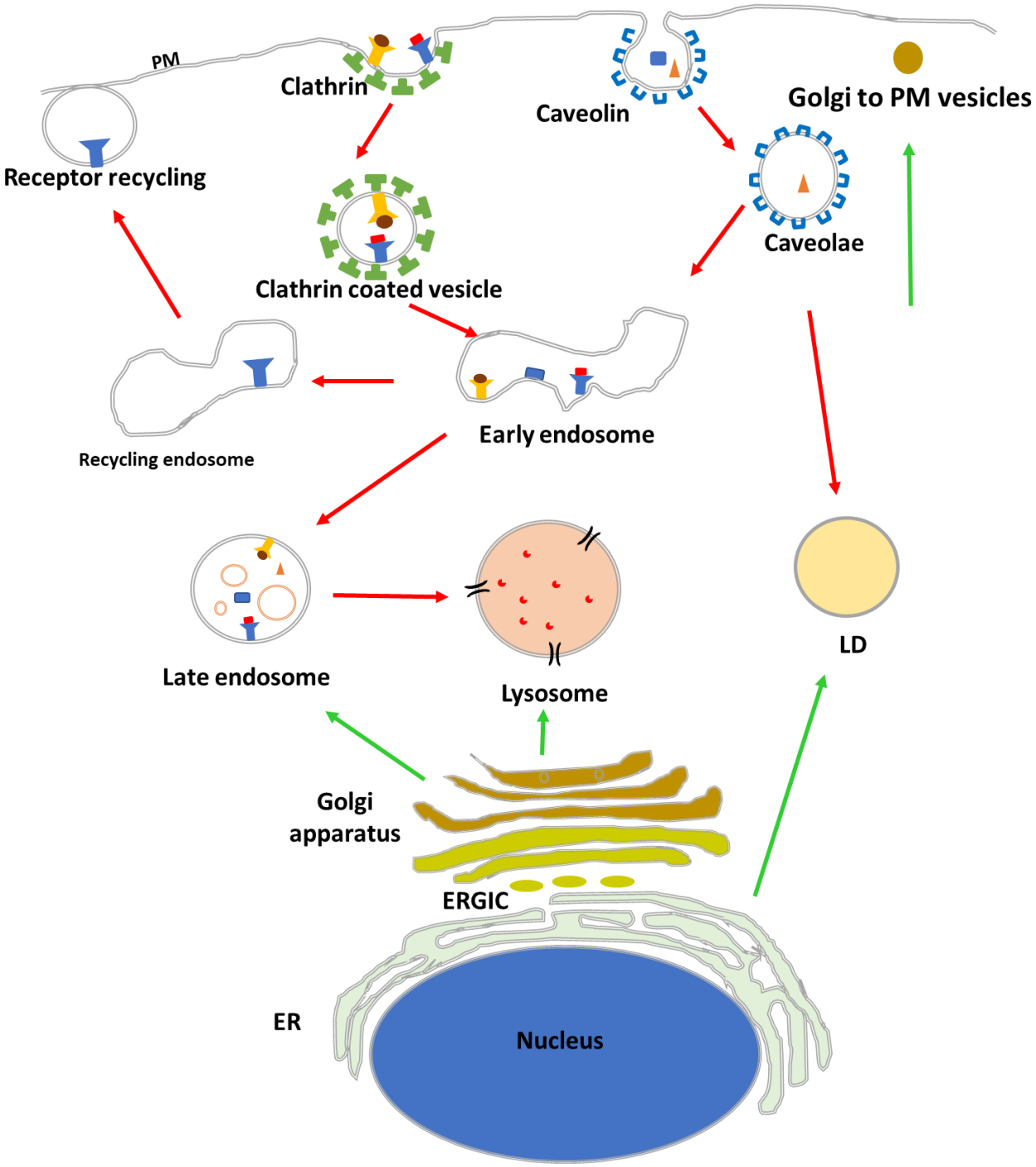


*Figure 16 Intracellular membrane trafficking.*

*Intracellular membrane trafficking is divided into two major routes: the secretory pathway (Green arrows), and endocytic pathways (Red arrows).*

## V.2 Phosphoinositides (PIs)

### V.2.1 PIs and their metabolism

The PIs are minor constituents of the cellular membranes, representing about 1% of total phospholipids with phosphatidylinositol representing about 10% (Payrastre et al., 2001). The inositol ring of PIs is a polyol cyclohexane of which positions 3, 4 and 5 can be phosphorylated to generate seven possible PIs: PtdIns3P, PtdIns4P, PtdIns5P, PtdIns(3,4)P2, PtdIns(3,5)P2, PtdIns(4,5)P2 and PtdIns(3,4,5)P3. Each PI interconversion reaction is regulated by specific kinases or phosphatases (Figure 17). In mammals, 18 PI interconversion reactions have been identified, and these reactions are mediated by 19 PI kinases and 28 PI phosphatases (De Craene et al., 2017; Nakada-Tsukui et al., 2019; Sasaki et al., 2009). Phosphoinositide Kinase (PI3K, PI4K, and PIP) use PtdIns as a substrate to generate PtdIns3P, PtdIns4P, and PtdIns5P, respectively. Mono-phosphorylated PIs are further phosphorylated by PIP kinases to generate PtdIns(3,4) P2, PtdIns (3,5)P2, and PtdIns(4,5)P2, which is further phosphorylated to generate PI(3,4,5)P3. Each PI is dephosphorylated by a series of PI phosphatases such as PtdIns 3-phosphatases (PTEN, MTM) PI4-phosphatases (INPP4, TMEM55), and PtdIns 5-phosphatases (SHIP). It was believed that the presence and levels of PIs in a given membrane are determined by lipid kinases and phosphatases specific to the different membranes which allow the spatiotemporal regulation of events, such as budding, membrane fusion, and dynamics (Balla, 2013; De Craene et al., 2017; Schink et al., 2016).

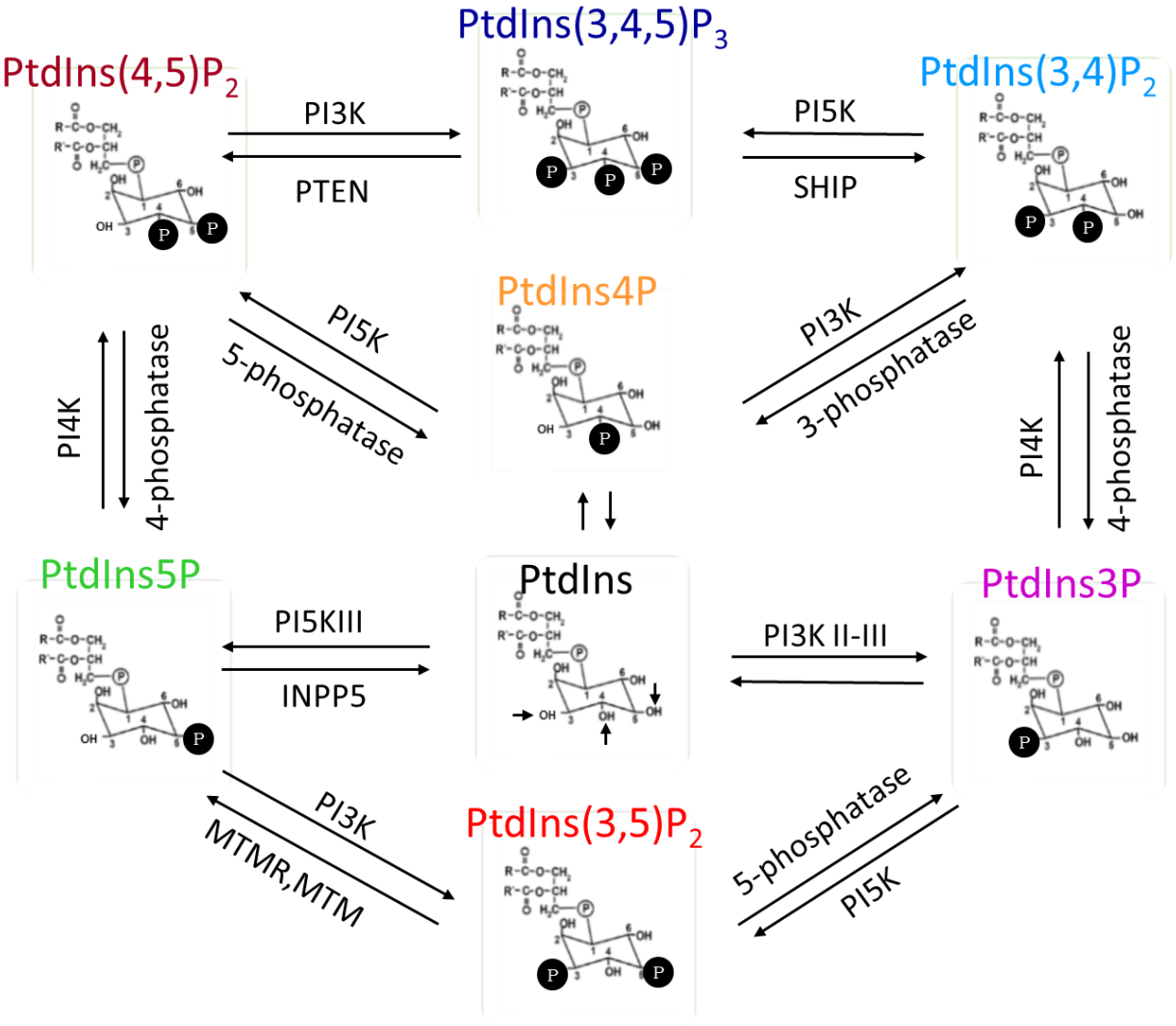


*Figure 17Phosphoinositides and their metabolism*

*Presentation of the 7 PIs and the enzymes involved in their metabolism. Phosphatidylinositol (PtdIns) has five free hydroxyl residues in positions 2,3,4,5 and 6 but only 3 are phosphorylatable, in positions 3, 4, and 5, probably due to steric hindrance. The different types of human lipid kinases and phosphatases that generate them are indicated.*

### V.2.2 PIs subcellular localization and membrane trafficking

Each PI type is enriched in a specific compartment (Balla, 2013; Pemberton and Balla, 2019; Schink et al., 2016) (Figure 18). Thus, PIs have been seen as the landmarks of distinct membranes and contribute to membrane identity (Balla, 2013). In particular, PtdIns4P and PtdIns(4,5)P2 are enriched on the plasma membrane, where PtdIns(3,4)P2 and PtdIns(3,4,5)P3 are transiently generated in situ in response to extracellular stimuli or intracellular signaling (Di Paolo and De Camilli, 2006). PtdIns4P is enriched in the Golgi apparatus, where it regulates both intra-Golgi trafficking and the subsequent transport to the plasma membrane or the endosomal system (De Matteis et al., 2013). PtdIns3P is enriched in early endosomes and is known to trigger the recruitment of a number of effector proteins important for early endosomal identity and function (Marat and Haucke, 2016; Schink et al., 2016). PtdIns(3,5)P2, converted from PtdIns3P, accumulates in the MVBs and late endosomes/lysosomes as early endosomes mature (Wallroth and Haucke, 2018; Wang et al., 2019). PtdIns5P is present in the nucleus, plasma membrane, ER and functions in cytoskeleton regulation, and stress signaling pathways (Hasegawa et al., 2017). All the PIs can localize in the nucleus which involving in transcription and chromatin remodeling (Poli et al., 2016; Ramos et al., 2020; Shah et al., 2013; Ye and Ahn, 2008).

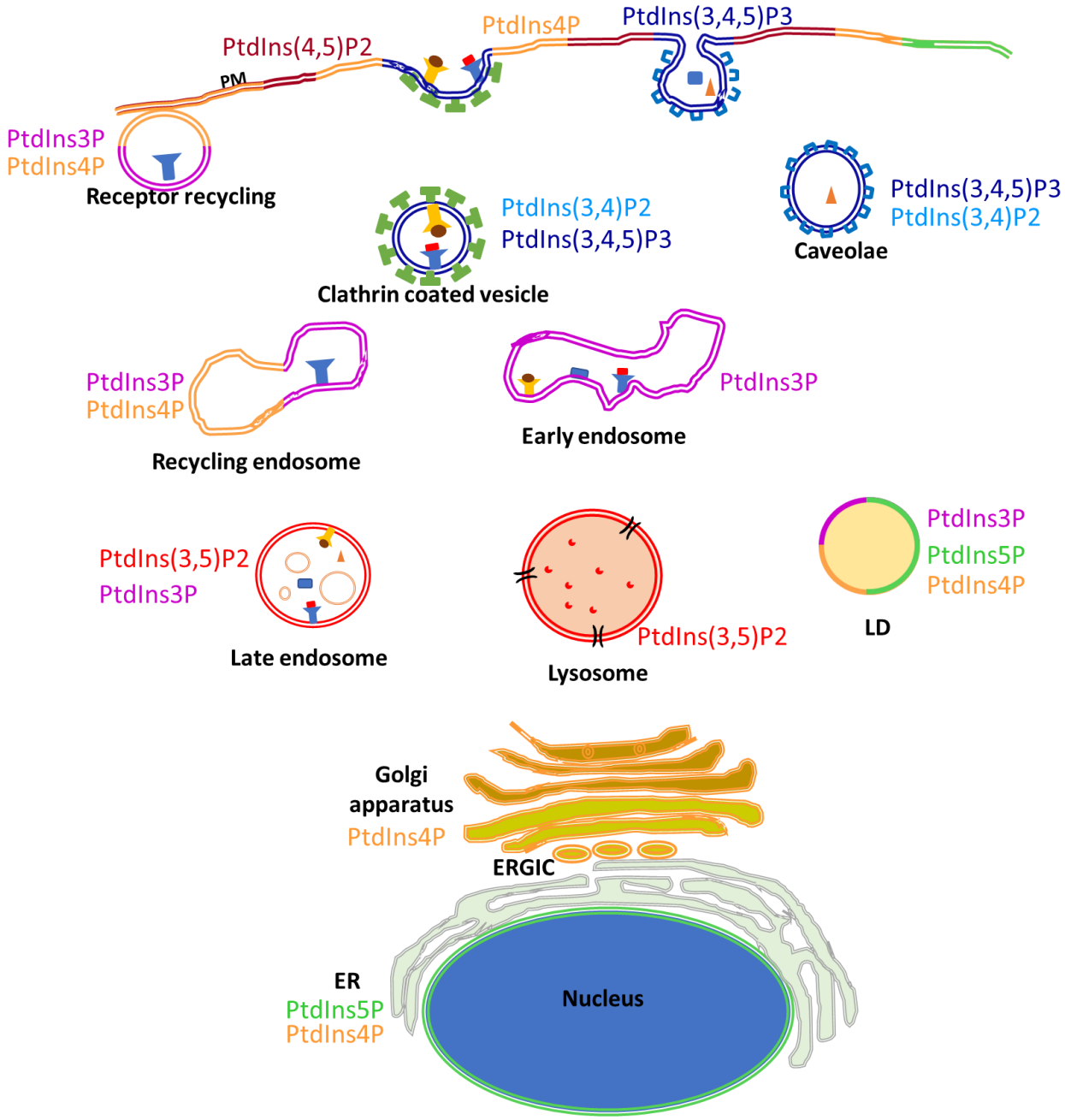


*Figure 18 Subcellular localization of PIs.*

*A typical cell showing the subcellular localization of different type of PIs. The seven PI species are depicted with different colors as indicated.*

The type and distribution of PIs in the membrane serve as a molecular tag to recruit specific effectors (Hammond and Balla, 2015; Várnai et al., 2017). These recruited effectors may contain PI-binding domains which include the PH (Pleckstrin Homology), PTB (phosphotyrosine-binding), PDZ (PSD-95, Discs Large, and ZO-1), GRAM (glucosyltransferases, Rab-like GTPase activators, and myotubularins), GLUE (GRAM-like ubiquitin-binding in EAP45), FERM (4.1, ezrin, radixin, and moesin), PX (phox homology), FYVE (Fab1p, YOTB, Vac1p, and EEA1), C2 (protein kinase C (PKC) conserved 2), Tubby, PROPPINs (β–propellers that bind phosphoinositides), ENTH

(Epsin N-terminal homology), ANTH (AP180 N-terminal homology), and BAR (Bin, Amphiphysin, and Rvs) domain families (Chandra et al., 2019; Pemberton and Balla, 2019; Singh et al., 2021; Yamamoto et al., 2020). While many proteins are recruited to PIs independently of those domains which could be mediated through multiple different molecular mechanisms, including polybasic motifs (Hammond and Burke, 2020). Furthermore, lipid kinases and phosphatases contain specific PI-binding domains contributing to their recruitment or dissociation to a specific membrane and leading to the dynamic changes of membrane PIs. Subsequently, these changes in membrane composition, control the profile of the membrane-associated proteins, thus, providing a fundamental role of PIs in the regulation of membrane trafficking.

## V.1 Rab proteins

Rab proteins are small guanosine triphosphatases (small GTPase) which also play crucial roles in regulating intracellular membrane trafficking. Rabs participate in vesicle budding, membrane fusion, and interactions with the cytoskeleton (McCaffrey et al., 2021). Over 70 members of the Rab family of proteins exist in the human genome, representing the largest portion of the Ras-related small GTPases (Barr, 2013; Mizuno-Yamasaki et al., 2012).

### V.1.1 Rabs Prenylation and membrane association

The membrane association of Rabs is ensured by prenylation, which is a posttranslational modification that adds one or two hydrophobic geranylgeranyl groups (20-carbon isoprenoid groups) to Rabs C-terminal cysteine residues (Pereira-Leal et al., 2001; Shinde and Maddika, 2017). The geranylgeranylation is mediated by Rab geranylgeranyl transferase (GGTase II) in cooperation with Rab escort protein (REP) (Leung et al., 2006). The REP chaperones the newly geranylgeranylated Rab GTPase to its correct target membranes (Alexandrov et al., 1994). The Rabs also exist in the cytosol in a soluble form which is achieved by interaction with the Rab GDP dissociation inhibitor (GDI). Rab GDI specifically recognizes Rabs in their GDP-bound form and thereby serves to solubilize Rabs from membranes once GTP hydrolysis has been completed (Goody et al., 2005; Zhen and Stenmark, 2015) (Figure 19).

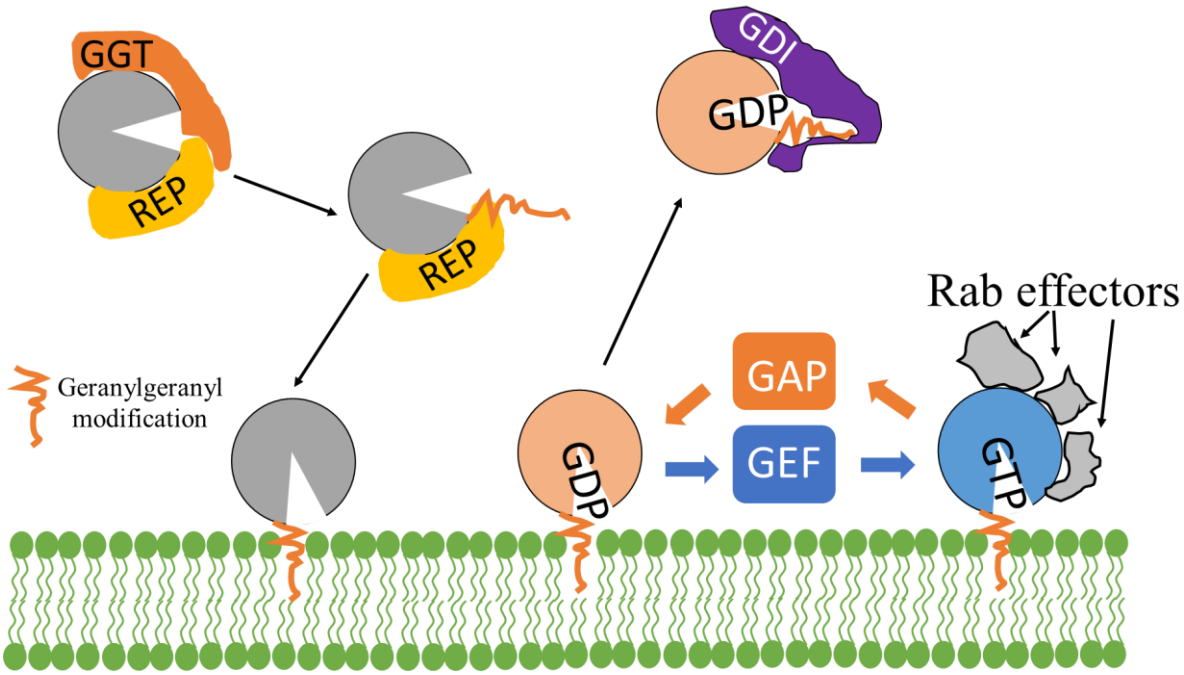


*Figure 19 Rab Prenylation and GTPase cycle.*

*Newly synthesized Rab associates with REP and RabGGTase. RGGTase catalyzes the transfer of prenyl groups to C-terminal cysteine residues. REP remains associated with prenylated Rab and targets it to the membrane. Rab GTPases are activated by GEFs and inactivated by GAPs. Inactive Rabs bind to GDP dissociation inhibitor (GDI) and are retained in the cytosol. Active Rabs are associated with intracellular membranes and recruit specific effector proteins that regulate various steps of membrane trafficking.*

### V.1.2 Rabs as molecular switches

The Rab proteins have important roles in the regulation of intracellular membrane trafficking pathways as molecular switches. Its function as molecular switches in the same manner as other small GTPases, cycling between GDP-bound and GTP-bound forms (Figure 19). Conversion of Rab proteins from inactive GDP-bound forms to active GTP-bound forms is facilitated by guanine nucleotide exchange factors (GEFs), and this conversion, in turn, recruits downstream effector proteins. GTPase-activating proteins (GAPs) convert Rab proteins back to an inactive, GDP-bound state by GTP hydrolysis (Barr and Lambright, 2010; Blümer et al., 2013; Lamber et al., 2019). In the GTP-bound active form, Rabs specifically interact with proteins that termed Rab effectors. These Rab effectors include molecular tethers, fusion regulators, motors, sorting adaptors, kinases, phosphatases, components of membrane contact sites and Rab regulators, and spatiotemporally recruitment of those effectors contributes to the regulation of the intracellular membrane trafficking (Gillingham et al., 2014; Homma et al., 2021).

Each Rab protein localizes to specific intracellular compartments (Figure 20). For example, in the secretory pathway, about one-third of known Rabs have been found associated with membranes at the ER/Golgi/TGN level (Liu and Storrie, 2012). In the endocytic pathway, the Rabs commonly identified are Rab4, Rab5, Rab7, and Rab11. Rab4, Rab5, and Rab11 function in the early endocytic pathway, whereas Rab7 and Rab9 regulate the later stages of endocytosis (Wandinger-Ness and Zerial, 2014). Rab5 primes the pathway by regulating the formation of coated vesicles, the fusion of vesicles with early endosomes, and the homophilic fusion between early endosomes (Bucci et al., 1992). Endosomal maturation into multivesicular bodies, followed by fusion to lysosomes is controlled by Rab7 (Bucci et al., 2000; Rink et al., 2005; Vanlandingham and Ceresa, 2009). Rab4, Rab 11, and Rab9 are the recycling GTPases and mediate retro-transport of the cargo to the plasma membrane and the Golgi complex (Arjonen et al., 2012; Dong et al., 2013). Rab11-mediates endosomal recycling is shown to be essential for the maintenance of cellular polarity (Jing and Prekeris, 2009). While these Rabs localize primarily to endosomal compartments were also shown associated with trans-Golgi network (TGN) compartments which reflects the dynamic nature of the interface between TGN membranes and endosomes (Goud et al., 2018).

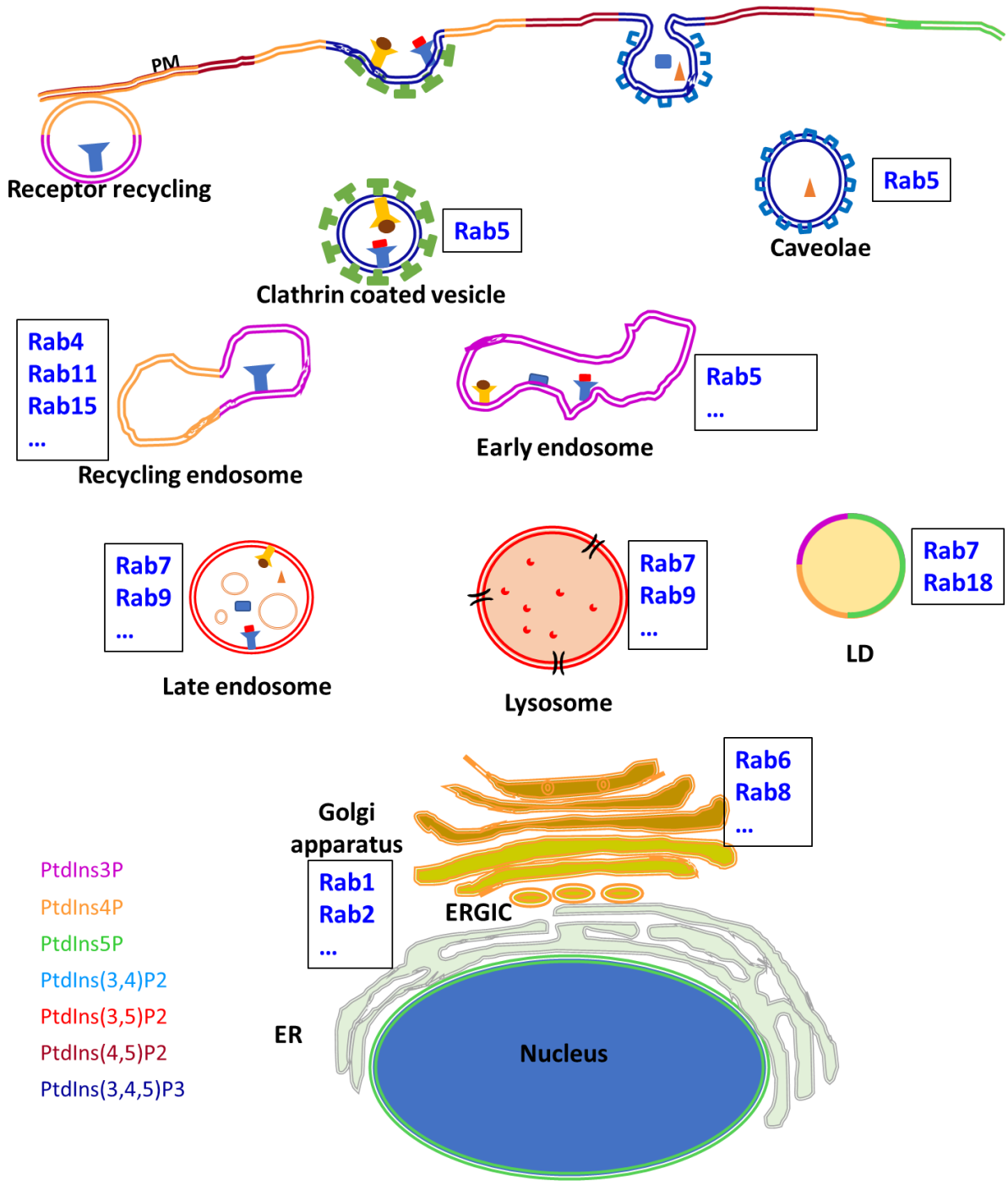


*Figure 20 The intracellular localization of Rabs.*

*A typical cell showing the intracellular localization and associated vesicle transport pathway of several Rab GTPases. Rab1 regulates ER-Golgi traffic while Rab2 is involved in recycling from Golgi and the ERGIC back to the ER. Rab6 regulates intra-Golgi traffic. Several Rabs including Rab8, -10, and -14 regulate biosynthetic traffic from the TGN to the PM. Most early endocytic steps rely on Rab5. Lysosome enriched Rab7. Rab15 directs membrane traffic from the early endosome to the recycling endosome. Rab4 and Rab11 regulate fast and slow endocytic recycling, respectively. Rab18 and lysosome-specific Rab7 mediate the regulation of LD.*

## V.3 Coordination between Rabs and PIs

Although Rabs and PIs are biochemically distinct, there are many striking similarities in their essential functions in membrane trafficking. Indeed, their intricate localization patterns and the well-established physical interactions between Rab and PIs regulators such as OCRL (Inositol Polyphosphate-5-Phosphatase) for Rab35 (Cauvin et al., 2016; Klinkert and Echard, 2016) and the PIs-mediated recruitment of Rab regulators such as the PtdIns3P and Rab5 interactor Rabaptin5 (Campa and Hirsch, 2017), all indicate the existence of coordination between Rab and PIs (Jean and Kiger, 2012).

### V.3.1 Rabs and PIs coordination in endo-lysosome maturation

A well-established example of the coordination between Rabs and PIs is the maturation of early endosome to the late endosome/lysosome. As described above, the Early endosomes are specified by the Rab5 and PtdIns3P whereas late endosomes/lysosomes are characterized by the Rab7 and PI(3,5)P2 (Wallroth and Haucke, 2018; Wang et al., 2019). Thus, the conversion of early endosomes to late endosomes requires the switching of Rab5 to Rab7 and PI3P to PI(3,5)P2. For the replacement of Rab5 with Rab7 on endosomes, a complex containing Mon1/SAND-1 and Ccz1/CCZ-1 has been reported. By sensing the membrane level and directly binding of PtdIns3P (Cabrera et al., 2014; Poteryaev et al., 2010), Mon1/SAND-1 localizes to early endosomes, where it displaces the GEF of Rab5, Rabex-5/RABX-5, thus preventing the continuous activation of Rab5 (Poteryaev et al., 2010). In the meantime, Mon1/SAND-1 forms a complex with Ccz1/CCZ-1, which functions as the GEF of Rab7 to promote its activation and membrane enrichment (Cabrera et al., 2014; Nordmann et al., 2010; Shinde and Maddika, 2016). The active GTP-bound Rab7 (GTP-Rab7) can recruit TBC-2, a Rab5 GTPase–activating protein, to help to inactivate GTP-bound Rab5 (Chotard et al., 2010; Li et al., 2009).

The PI conversion depends on PIKFYVE, a PI5K, which binds to PtdIns3P via its zing finger FYVE domain and converts it into PtdIns (3,5)P2 (Huotari and Helenius, 2011; Wallroth and Haucke, 2018). The endosomal PtdIns3P is generated by the class III phosphatidylinositol 3-kinase (PI3K) complex, which consists of Vps34, p150/Vps15, and Beclin1/Atg6 (Christoforidis et al., 1999; Funderburk et al., 2010) and both Rab5 and Rab7 are interacting with p150/Vps15. The active GTP-Rab5 promotes endosomal association of the PI3K complex and facilitates the generation of PtdIns3P on endosomes (Christoforidis et al., 1999; Murray et al., 2002). In contrast, active Rab7 recruit and directly interact with WDR91 (WD repeat domain 91), the homologues of *C. elegans* SORF-1, leading to the inhibition of Rab7-associated PI3K complex activity. This allows the turnover of endosomal PtdIns3P and consequently conversion of early endosomes to late endosomes (Liu et al., 2017).

### V.3.2 Rabs and PIs in lysosome positioning and motility

Several protein complexes have been implicated in the regulation of lysosomal positioning. For example, the anterograde movement of lysosomes is regulated by the multi-subunit complex BORC, the small GTPase Arl8, and its effector SKIP, which directly interacts with the kinesin light chain, thus linking lysosomes to the plus-end-directed microtubule motor kinesin (Pu et al., 2015; Rosa-Ferreira and Munro, 2011). The lysosomal transmembrane proteins such as LAMP1/2 (Huynh et al., 2007; Krzewski et al., 2013), TRPML1 (transient receptor potential cation channel, mucolipin subfamily, member 1) (Li et al., 2016), TMEM55B (Type 1 phosphatidylinositol 4,5-bisphosphate 4-phosphatase) (Willett et al., 2017) were also shown to regulate the retrograde lysosomal transport by recruitment of dynein-dynactin. Rab7 has been shown to play a fundamental role in both anterograde and retrograde movements of lysosomes. It seems that the PIs present in their membranes will determine which direction of movement Rab7 will involve-in (Figure 21). Indeed, active Rab7 were able to recruit effector proteins such as the Rab-interacting lysosomal protein (RILP), which binds to the p150glued subunit of dynactin and dynein light intermediate chain, then acquiring the dynein-dynactin complex for microtubule minus-end transport (Johansson et al., 2007; Rocha et al., 2009; Tan et al., 2011). In contrast, in combination with PtdIns3P, activated Rab7 can bind the effector FYCO1 (FYVE and coiled-coil domain containing protein 1) to recruit the kinesin-1 motor and then, regulate the anterograde directed motility and, hence, transport of late endosomes from the cytoplasm to the cell periphery (Pankiv et al., 2010). PtdIns3P also contributes to the formation of ER membrane contact sites with lysosomes by engaging ORP1L (Oxysterol-binding protein-related protein 1) and protrudin which interacts with late endosomal Rab7 to deliver the kinesin- 1 to FYCO1 (Johansson et al., 2005; Raiborg et al., 2015).

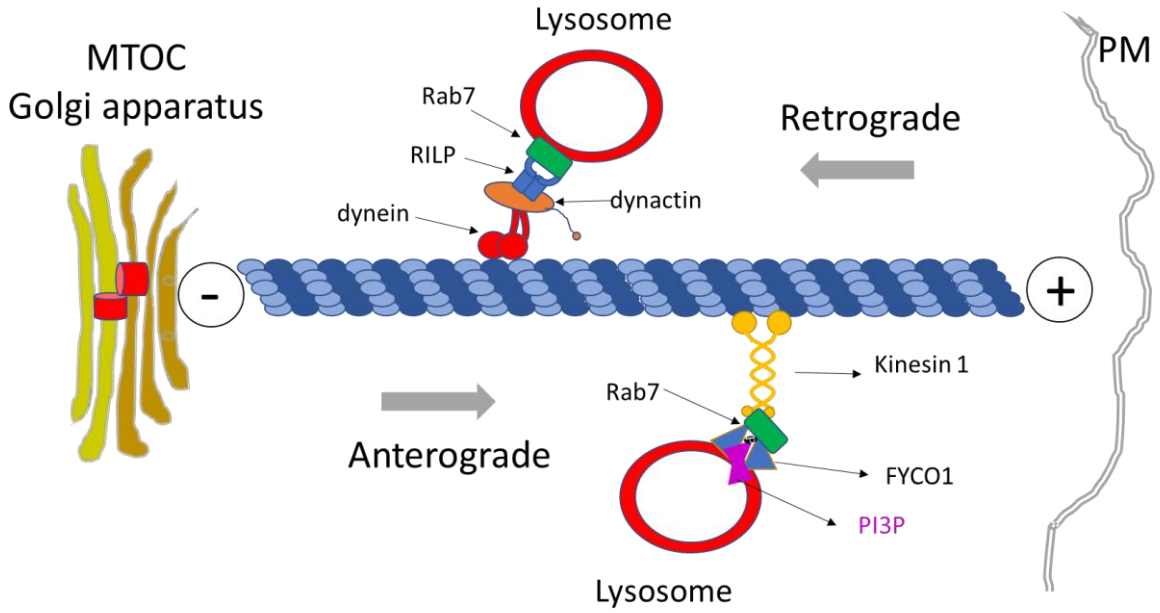


*Figure 21 Machineries involved in Rab7 and PI3P in lysosome motility*

*Rab7 interacts with RILP and recruits dynein for retrograde transport of lysosome to the MTOC/Golgi apparatus or in the presence of PtdIns3P interact with FYCO1 to mediate the anterograde transport of lysosome to the cell periphery. Adopted from(Ballabio and Bonifacino, 2019)*

## V.4 Rabs and PIs in LD regulation

### V .4.1 Rabs proteins and LDs

More than 30 Rab proteins have been shown to be associated with LDs through proteomic analysis in mammals (Bersuker et al., 2018; Brasaemle et al., 2004; Krahmer et al., 2013a). However, only a few of them have been reported to be functionally linked with LDs.

#### V .4.1.1 Rab18

Rab18 is the best characterized Rab family protein, with extensive evidence for a direct association with the monolayer surface of LDs (Gerondopoulos et al., 2014; Gronemeyer et al., 2013; Xu et al., 2018a). Both endogenous Rab18 and GFP- tagged Rab18 fusion proteins show ring- like staining surrounding a subset of LDs in adipocytes as well as non- adipocyte cells such as Vero, BHK, and C2C12 cells treated with oleic acid (Deng et al., 2021; Martin et al., 2005; Ozeki et al., 2005; Pulido et al., 2011). The association of LDs with Rab18 is regulated by its guanine nucleotide status, as only overexpressed wild- type and dominant- active, Rab18 localizes to LDs and not the dominant- negative (Martin et al., 2005) (Figure 22). Also, Rab18 could interact with PLIN2, PLIN2 facilities and stabilize the LD targeting of Rab18, which, in turn, promotes ACSL3 (acyl-CoA synthetase long-chain family member 3) recruitment onto LDs for acyl-CoA synthesis, which induce the LD growth and accumulation (Deng et al., 2021).

#### V.4.1.2 Rab7

As mentioned above, the Rab7 is associated with MVB and lysosomes. Interestingly, It has been demonstrated that Rab7 is involved in LD degradation via lipophagy (Schroeder et al., 2015). Nutrient deprivation activates Rab7 on the LD surface and in the late endocytic/autophagic compartments, promoting LD targeting of late endosomes/lysosomes and autophagosomes, ultimately resulting in lipophagic breakdown of LDs. Further studies have shown that the active, membrane-associated form of Rab7 interacts with RILP to connect lysosomes or autophagosomes to the microtubule network, promoting the fusion of LDs with lysosomes. Therefore, depletion of Rab7 significantly reduces the breakdown of LDs during starvation, although this impairment can be rescued by expression of wild- type and constitutively active (Q67L), but not dominant-negative (T22N), mutant forms of Rab7 (Schroeder et al., 2015) (Figure 22). Lipolysis stimulated by the β-adrenergic receptor (ADRB2) also requires autophagic machinery mediated by Rab7 (Lizaso et al., 2013). The localization of Rab7 to LDs is enhanced by ADRB2 stimulation, which then facilitates the fusion of LD-containing autophagic vacuoles with lysosomes. Depletion of Rab7 or expression of the dominant-negative mutant of Rab7 in 3T3-L1 adipocytes impairs autophagosome-lysosome association and in turn, reduces basal and ADRB2-stimulated lipolysis. In a follow-up study, it was observed that chronic ethanol exposure inhibits Rab7 activity, disrupts degradative compartment

morphology and motility, and causes reduced LD turnover during the process of lipophagy (Schulze et al., 2017). Taken together, these results indicate that Rab7 is essential in the auto-lysosomal pathway of lipolysis.

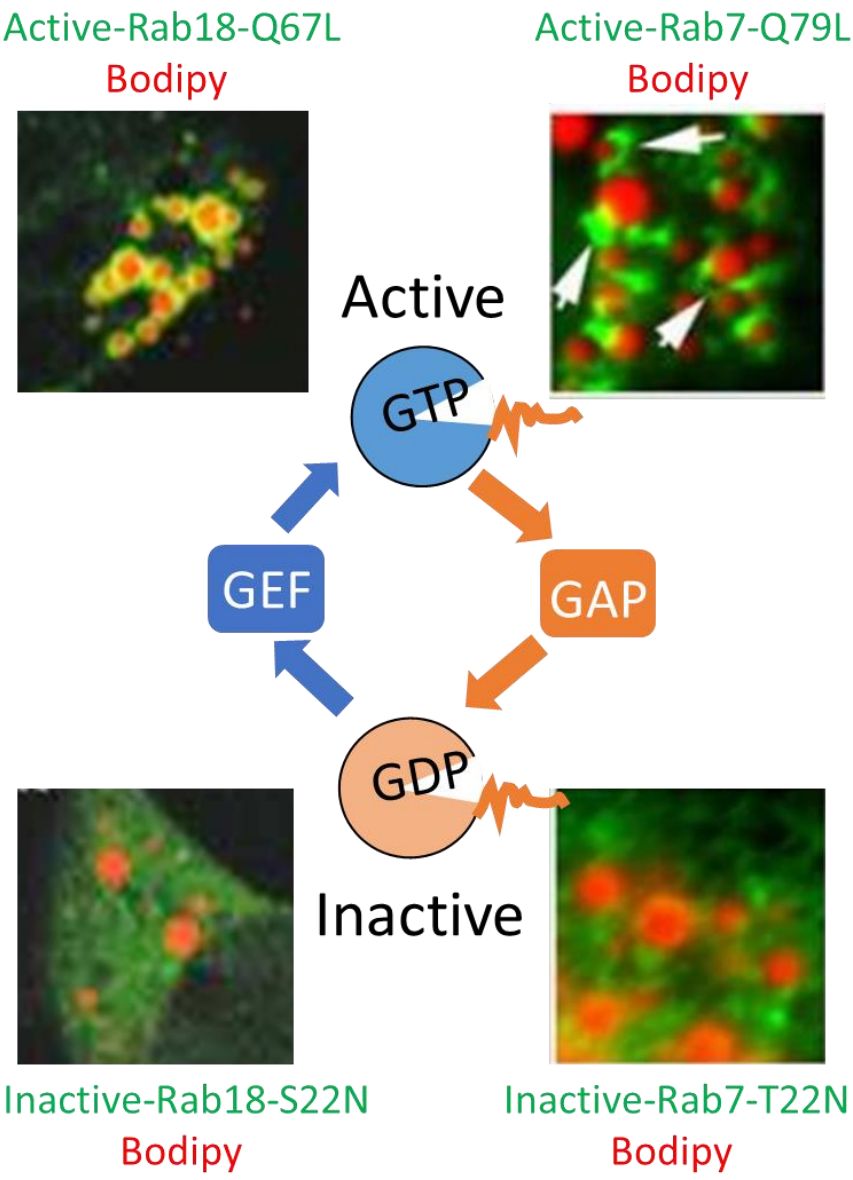


*Figure 22 The activation of Rab18 and Rab7 affect its association with LD.*
*Schematic representation of GTPase cycle of Rab18 and Rab7 and its association with LD. GEF, guanine nucleotide exchange factor; GAP, GTPase activating protein. Rab18 GTPase active (-Q67L) form and Rab7 GTPase active(-Q79L) form were found associated with LD, not the inactive forms. Images were adorpted from(Schroeder et al., 2015),(Ozeki et al., 2005).*

## V.4.2 PIs and LD

As mentioned above, the PIs are constituents of the phospholipid monolayer of LD, while their presence and their role have not been well documented so far. This is probably because their low level makes their detection difficult. But recent studies have shown that the PIs have an important role in regulating LDs and particularly in yeast. For example, in yeast, the sfh3, a nonclassical member of the Sec14-like phosphatidylinositol transfer protein (PITP) superfamily whose members help specify the outcomes of PI-signaling in cells, acts as a negative regulator of neutral lipid utilization. This requires its ability to bind PIs and to stimulate PtdIns4P production (Ren et al., 2014). In addition, we reported that the monophosphorylated PIs such as PtdIns3P, PtdIns4P, and PtdIns5P but not the PtdIns(4,5)P2, increases the LDs (Akil et al., 2016a). Consistent with our results, a recent paper has shown that the ORP5 (oxysterol binding protein and its related proteins), which is normally localized at the ER-LD contact sites to deliver PS to the LD surface and bring back PtdIns4P from LD to the ER, regulate LD. When depletion of ORP5 increases the level of PtdIns4P on LD and then increases LD size. Furthermore, they demonstrated that the PtdIns4P produced by PI4K2A is recruited on LDs (Du et al., 2020).

Overall, these reported data revealed that different PIs have different effects on LD. Thus, here again as shown for trafficking above, we can speculate that coordination may exist between Rabs and PIs to control LD behavior while this needs further investigations.

# Chapter III

# Septins

## I. Septin domains and subgroups

Septins are GTPases that are evolutionarily classified into the phylogenetic branch of P-loop NTPases, including the myosin/kinesin cytoskeleton motor superfamily and the Ras GTPase superfamily (Figure 23) (Leipe et al., 2002; Mostowy and Cossart, 2012). They have first discovered in the budding yeast Saccharomyces cerevisiae by Lee Hartwell in 1971, as cell division control proteins (CDC proteins) involved cytokinesis. The septins were subsequently found arranged into a highly ordered ring of 10-nm filaments by electron and immunofluorescence microscopy, and have been described as intimately associated with plasma membrane within the neck of the bud and formed during early bud emergence and disappear when cytokinesis begins (Byers and Goetsch, 1976). Because of their localization in the bud neck and their role in the septum, these proteins were named septins (Sanders and Field, 1994).

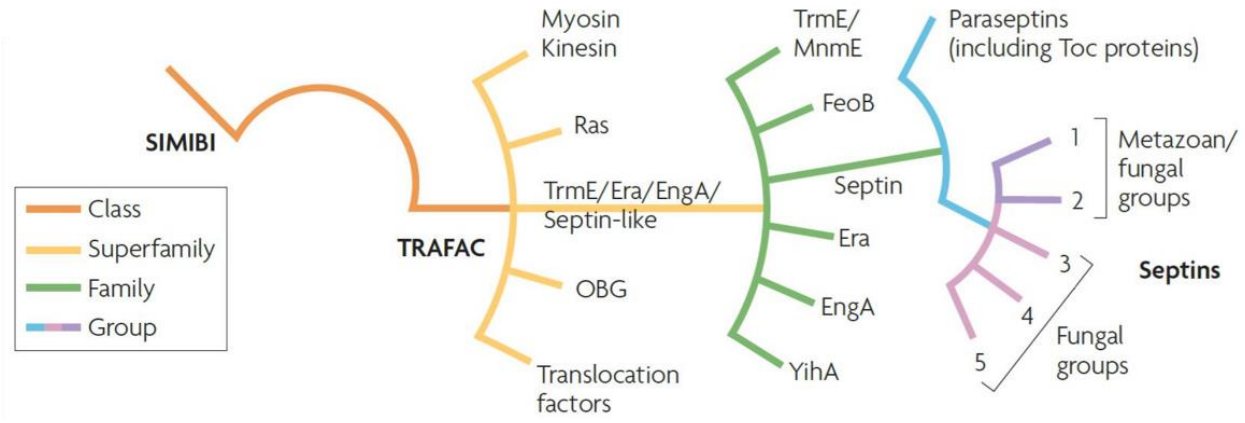


*Figure 23 Classification of septins.*

*A schematic diagram of the position of the septins in the P- loop NTPase superclass, which is divided into two classes, called SIMIBI (signal recognition particle, MinD and BioD), and TRAFAC (translation factor), on the basis of phylogenetic studies (Hall and Russell, 2004; Leipe et al., 2002) adopted form (Weirich et al., 2008).*

The number of septins genes in an organism varies widely. In humans, septins comprise a family of 13 members (septin1-septin12, septin14). This number of septins could be further amplified by the expression of isoforms which result from alternative splicing of the transcript on

the septin genes. For example, septin 4, 8, and 9, long or short N-terminal extensions have been identified (Kinoshita, 2003; Russell and Hall, 2011). Such diversity allows a vast repertoire of septin assembly, which could explain its multiplicity of localizations and sub-cellular functions.

## I. 1 Septin structure

All mammalian septins have a central core domain with a minimum sequence similarity of 70%. The core consists of a polybasic domain (PB), a GTP-binding domain, and 52 highly conserved amino acids of unknown function called the septin unique element (Cao et al., 2007; Pan et al., 2007). Their amino- and carboxy-terminal regions contain Pro-rich and coiled-coil domains, respectively, which vary in length and amino acid composition (within each septin group, the C-terminal regions share 50-60% sequence identity) (Figure 24) (Mostowy and Cossart, 2012).

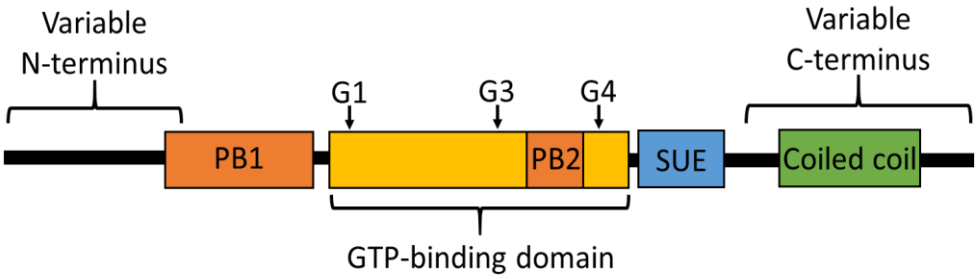


*Figure 24 Typical septin domains*

*Septins possess a GTP-binding domain with G1, G3, and G4 motifs. Between the N-terminus and the GTPase domain, there are highly conserved polybasic regions required for interactions with membranes. The C-terminus of the protein frequently contains a coiled-coil domain involved in protein-protein interactions. In addition, septins include the septin unique element.*

### I.1.1 GTP binding domain

Similar to the Ras proteins, the GTP-binding structure of septins consists of alternating α-helices, β-sheets, and loops (P-loops) that come in contact with the phosphate groups of GTP**.** Septins, however, contain additional helices and β-strands in the N- or C-terminal, which in part support tandem dimerization into oligomers and polymers (Macedo et al., 2013; Sirajuddin et al., 2007a, 2009). Assembly of these septin hetero-oligomers depends on GTP-binding and hydrolysis, which further stabilizes the dimerization interfaces through allosteric effects (McMurray, 2014; Zent and Wittinghofer, 2014; Zeraik et al., 2014). In contrast to the monomeric Ras GTPases, whose function relies on the hydrolysis and exchange of GTP by GAPs and GEFs, septins hydrolyze and exchange GTP on their own, albeit at very slow rates (Abbey et al., 2016, 2019).

### I.1.2 Septin unique domain

The septin unique domain (SUD) are highly conserved among septins, which distinguishes septins from other small GTP-binding proteins, is located near the C-terminus, and partly overlaps with the GTP-binding interface where it has been suggested from structural studies to participate in septin polymerization (Sirajuddin et al., 2009) and is known be required for the interaction of septin monomers during the assembly of complexes and filaments (Sirajuddin et al., 2007b). (Figure 24)

### I.1.3 Polybasic domain (PB)

A short polybasic region (PB) is present between the N-terminus and the GTPase domain in most septin sequences and binds directly to PtdIns(4,5)P2, and thus mediates interactions with plasma membranes (Casamayor and Snyder, 2003). Our laboratory reported that recombinant septin 9 bound specifically to mono-phosphorylated PtdIns (PtdIns3P, PtdIns4P, and PtdIns5P) while the strongest interaction was observed with PtdIns5P (Akil et al., 2016a). Subsequently, we further identified a second polybasic domain motif enriched in basic amino acids (aa 399–402 of human septin 9 isoforms 1, 586 residues). This second polybasic domain termed PB2 is conserved in all human septins (Omrane et al., 2019). (Figure 24)

### I.1.4 C-terminal region

The carboxyl-terminus of septins is often predicted to form coiled-coil structures, which are important determinants for filament assembly and stability and are important for recognition and binding of partner molecules (de Almeida Marques et al., 2012; Meseroll et al., 2012, 2013). For example, some septins interact with proteins such as Centromere-associated protein E/F (CENPE/F), Sorting Nexin 6 (SNX6) which are associated with intracellular trafficking and exocytosis or are part of the kinetochore via coiled-coil domains (Nakahira et al., 2010; Zhu et al., 2008). (Figure 24)

### I.1.5 N-terminal region

The amino-terminus of septins are different both in length and sequences, and may contain a proline-rich domain, which is important for protein-protein interactions and frequently involved in the interaction of proteins with cytoskeletal components (Bai et al., 2013; Kremer et al., 2005). In addition, our laboratory reported that the AH motif is also presented in this region which is crucial for septins to membrane binding. (Figure 24)

## I.2 The septin Homology-based subgroups

Based on their sequence similarity and the number of coiled-coil domains in their sequences, mammalian septins can be subdivided into four different groups (septin 2, septin3, septin 6, or septin 7) termed according to their founding member (Figure 25). The septin 2 subgroup (septin 1, 2, 4, 5) contains two coiled-coil domains. The septin 3 subgroup (septin 3, 9, 12) has no coiled-coil domain. The septin6 (septin 6, 8, 10, 11, 14) and the septin 7 subgroup (septin 7), respectively comprise one coiled-coil domain (Macara et al., 2002; Kinoshita, 2003b).

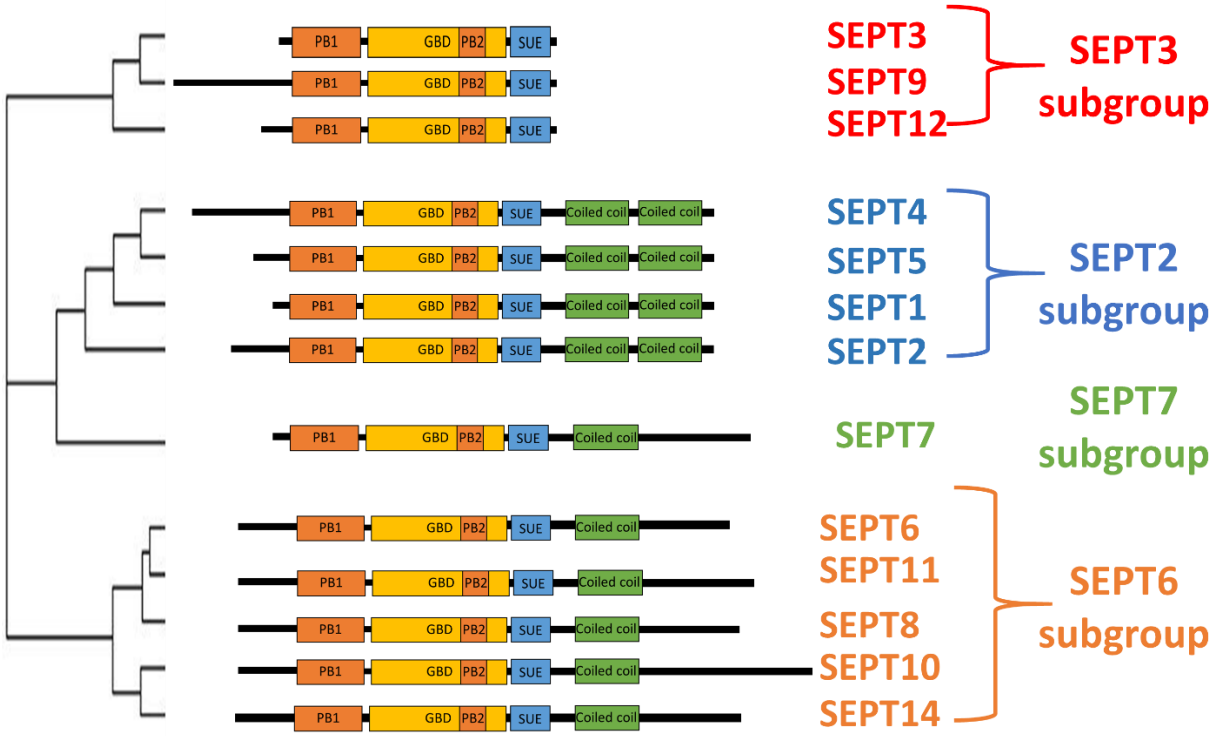


*Figure 25 Homology-based subgroups*

*The 13 human septins are classified into four subgroups (3, 2, 7, and 6) based on sequence homology and coiled-coil domains. Adopted from (Kinoshita, 2003; Macara et al., 2002; Neubauer and Zieger, 2017)*

# II. Septin complex assembly and regulation

## II.1 Septin complex assembly

Since their discovery, it has been suggested that septins work as complexes. The crystallographic structural study of the septin complex carried out by Sirajuddin and these colleagues in 2007 has greatly clarified our understanding of the interaction between the different septin (Sirajuddin et al., 2007b). The structure of human septin complexes revealed an apolar rod-shaped structure of the following order: 7 -6-2-2-6-7. In the meantime, this study also revealed that the filament-forming septin-septin interactions are mediated via their G-domains which form two alternating interfaces between the septin subunits of the filaments, namely G-G which is an interaction of the nucleotide-binding pocket and the flanking regions of the G-domain and N-C interface as N- and C-termini interactions of the G-domains (Sirajuddin et al., 2009). (Figure 26a)

In some cases, septins can also assemble into hetero octamers, which additionally contain a member of the septin3 group. It is currently viewed that septin 9 caps the ends of hetero-hexameric complexes by interacting with septin 7, resulting in a hetero-octameric composition arranged as 9-7-6-2-2-6-7-9 (Kim et al., 2011; Nakahira et al., 2010; Sandrock et al., 2011; Sellin et al., 2011). In addition, another type of assembly is proposed for octamer formation: Septin 9 can also interact with both septin 6 and septin 7 by associating laterally with a trimer (Sandrock et al., 2011; Versele and Thorner, 2005) (Figure 26b).

The hexameric and octameric septin complexes described above are considered as the building blocks of higher-order structures of septins. The protofilament is formed by the association of each oligomer end to end, those filaments can associate laterally, forming bundled filaments, which can, in turn, assemble into higher-order structures such as ring (Bertin et al., 2008; DeMay et al., 2011; Garcia et al., 2011a; John et al., 2007; Sirajuddin et al., 2007b) (Figure 26c). The filament formation is required for many functions performed by septins.

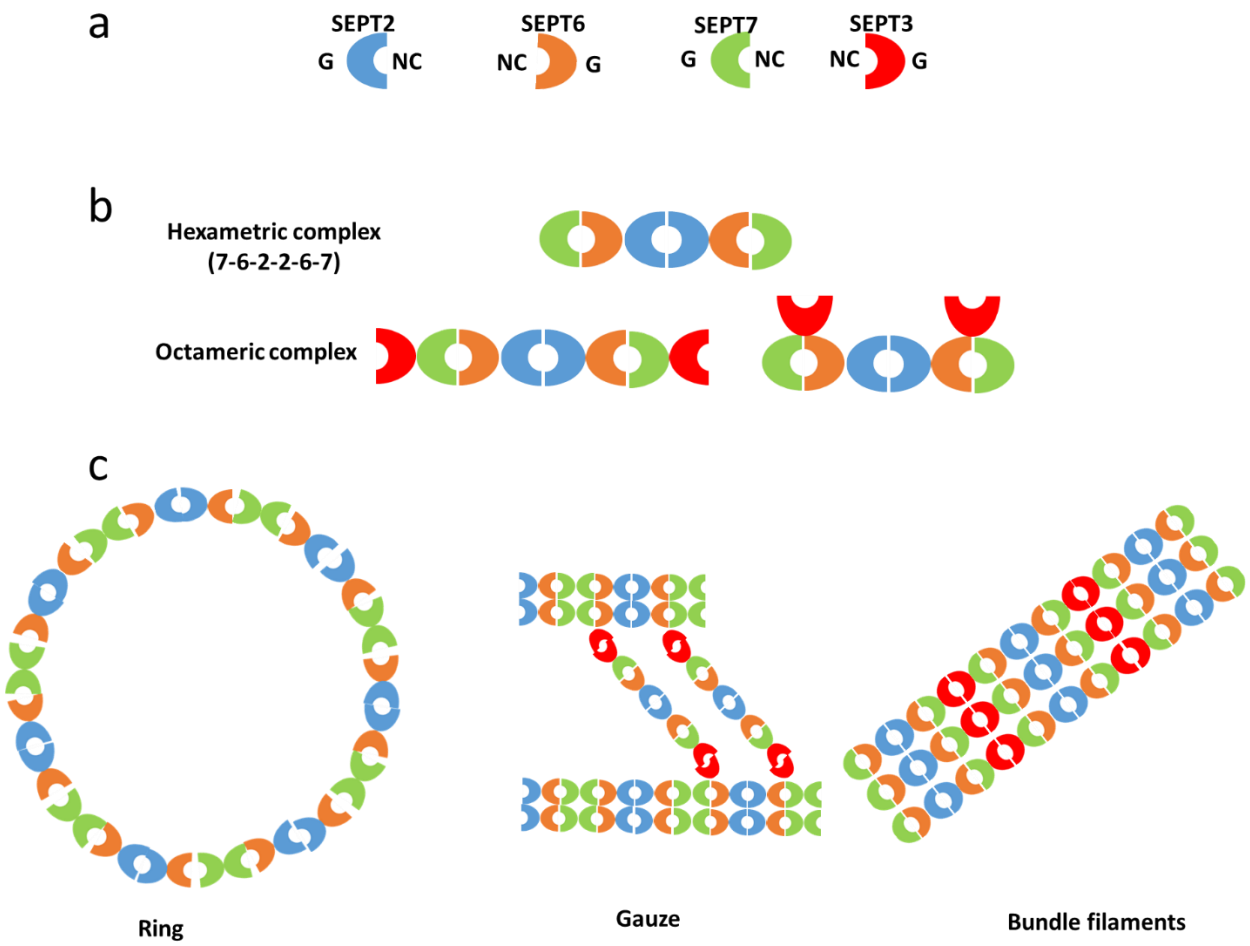


*Figure 26 Septins complex and high-order structures*

*Septins from different groups are shown in different colors.*

*a) Septins interact with other septins via their G- and NC interfaces; human septins can form hexametric or octameric complexes that contain three or four septins, where each septin group member is present in two copies.*

*b) Two types of assembly are proposed for octamer formation: Septin 9 can either be inserted between two septin 7 to form a linear complex or interact with both septin 6 and septin 7 by associating laterally with a trimer.*

*c) Further association of these oligomers leads to the assembly of non-polar polymers, such as filaments, rings, and cages.*

## II.2 Regulation of septins complex assembly

### II.2.1 GTP/GDP cycle

As mentioned above, septins polymerize and interact with other septins via two interfaces (G- and NC-interfaces). The G-interface comprises the GTP-binding domain whereas the NC-interfaces involve the N- and C-terminal regions, which are brought into close proximity upon folding (Sheffield et al., 2003). This means each septin subunit assembles and extends apolar filaments arranged in a palindromic order by alternating NC- and G-interface associations. Upon GTP-binding a conformational change in the switch regions is provoked, which affects the G- and the NC-interface. The GTP-binding capacity of septins is essential for septin-septin interactions and fundamental to ensure structural integrity, in a way that GTP-binding and its hydrolysis control assembly and disassembly of filaments and also the stability of the interface within the septin polymer (Zeraik et al., 2014). In the septin 2-6-7 complex, septin 2 and 7 bind to GDP, while septin 6 binds to GTP (de Almeida Marques et al., 2012). Moreover, a septin 11 mutant, which showed reduced GTPase activity, was unable to form filaments (Hanai et al., 2004).

### II.2.2 Protein interactor

The assembly and disassembly of septin filaments are also regulated by their interaction with other proteins. In mammalian cells, septins interact with the CDC42-binding Borg3 protein, and overexpression of Borg3 leads to the aggregation of septin filaments (G et al., 2001). Another example is the Orc6 protein in drosophila, an ORC subunit required for DNA replication, which binds to septin complexes in the stoichiometric ratio of two Orc6 molecules per hexamer and stimulates polymerization of filaments (Akhmetova et al., 2015; Huijbregts et al., 2009). Orc6 remains bound to the polymerized filaments and apparently stabilizes them due to Orc6-Orc6 dimerization (Akhmetova et al., 2015).

### II.2.3 Posttranslational modification

The dynamics of septin filaments *in vivo* may be regulated by various posttranslational modifications, such as SUMOylation, acetylation, and phosphorylation.

#### II.2.3.1 SUMOylation

SUMOylation is a posttranslational modification consisting of the covalent addition of a small ubiquitin-like modifier (SUMO) polypeptide into the lysine residues of the target proteins. This modification controls the subcellular localization, activity, and stability of many proteins. The SUMOylation process requires the E1-activating enzyme and the E2-conjugating enzyme, as well as

ATP. Ubc9 is one member of the E2 family that is involved in recognizing the SUMOylation motif on targeted proteins (Bernier-Villamor et al., 2002). SUMOylation plays a central role in the control of cell division and is the first posttranslational modification described for septins in yeast (Johnson and Blobel, 1999a).

Indeed, the *Saccharomyces cerevisiae* proteins Cdc3, Cdc11, and Shs1 (the homologous of mammalian septins) were found to be SUMOylated at the G2/M transition and deSUMOylated at cytokinesis. Mutation of all SUMO sites in Cdc3, Cdc11, and Shs1 prevented the disappearance of septin rings at division sites and blocks cytokinesis (Johnson and Blobel, 1999a; Takahashi, 2003; Takahashi et al., 1999a). Several studies have identified components of the SUMOylation machinery as putative interactors with human septins. They include the Ubc9/UBE2I, the E3 SUMO-protein ligase PIAS3 (Protein Inhibitor of Activated STAT3), or SUMO1 itself (Havugimana et al., 2012; Nakahira et al., 2010). High-throughput analyses of SUMOylated proteins have identified human septins as SUMO targets (Becker et al., 2013; Hendriks and Vertegaal, 2016). Furthermore, human SUMO proteome identified some of the SUMO-modified lysines in septin 2, septin 6, septin 7, septin 8, septin 9, and septin 10 (Hendriks et al., 2017). Indeed, a subsequent study reveals that there are SUMO sites in the C-terminal domain of septin 6 and septin 7 and in the N-terminal domain of septin 9. Additional SUMO sites were also identified in central domains of septin 6,7 and 9 but mutagenesis analysis suggests those sites do not constitute major SUMO sites (Ribet et al., 2017a). They further demonstrated that septin SUMOylation plays a critical role in the organization of septin filaments. But a lack of SUMOylation in septin 7 and septin 11 does not inhibit canonical septin complex formation which suggests that SUMOylation is not required for septin-septin interactions. However, they proposed that SUMOylation of septins is critical for the correct assembly of septin higher-order structures (Ribet et al., 2017a).

### II.2.3.1 Phosphorylation

Phosphorylation is the most characterized posttranslational modification in septins. In yeast, fifty-nine phosphorylation sites have been mapped. Phosphorylation of yeast septins is generally found in the N- and C-terminal regions. Loss of septin phosphorylation leads to defects in morphogenesis and cytokinesis. Thus, the phosphorylation state appears to regulate the dynamics of septin ring formation (Hernández-Rodríguez and Momany, 2012a). In mammals, several protein kinases have been involved in septin phosphorylation. Septin 4 is phosphorylated by GSK3. During the epididymal transit of spermatozoa, deficiency in septin 4 phosphorylation leads to a defective membrane diffusion barrier (Koch et al., 2015). The cyclin-dependent kinase 1 (Cdk1) phosphorylates septin 9 and this phosphorylation effect in Pin1 binding and is necessary for cytokinesis (Estey et al., 2013). The ERK3/MK5/septin 7signaling complex is activated by p21-activated protein kinases and contributes to neuronal morphogenesis (Brand et al., 2012). Upon

phosphorylation through mitogen-activated protein kinase-activated protein kinase 5 (MK5), phosphorylated septin 8 may be implicated in vesicle trafficking (Shiryaev et al., 2012).

### II.2.3.1 Acetylation

Regulation of septins by acetylation is probably the least studied posttranslational modification. In yeast, all mitotic septins, except Cdc11, are acetylated by the lysine acetyltransferase complex NuA4 (Mitchell et al., 2011). Septins became mislocalized during the nascent ring-to-hourglass transition in NuA4 complex deletion mutant strains, implying that acetylation of septins may regulate septin hourglass formation or its stability. The authors investigated how the loss of acetylation on specific septins could influence septin localization and function using a C-terminal truncation of Shs1 that loses a majority of acetylation sites. They conceded that many of their phenotypes associated with this truncation allele are complicated by the fact that this region of Shs1 is also heavily phosphorylated and SUMOylated.

# III Septin interaction with cytoskeleton and membrane

## III.1 Septin and Actin

Early in the identification and characterization of mammalian septins, septins were reported to colocalize with actin (G et al., 2001; Kinoshita et al., 1997; Surka et al., 2002) (Figure 27). In non-dividing cells, septins localize most prominently to actin stress fibers (SFs), which consist of bundles of linear actin filaments (Dolat et al., 2014a; F et al., 2015), and also been observed at lamellipodia, pseudopodia, and phagocytic cups, which contain branched actin filaments (Y et al., 2013; Yw et al., 2008). Recent work suggests that septins are also involved in the maintenance of a perinuclear actin network. On the ventral side of nuclei, septins form a dense network of filaments, which colocalizes with actin (Verdier-Pinard et al., 2017).

Initially, the interaction between septins and actin was considered as indirect and mediated by the adapter protein Anillin (Kinoshita et al., 2002), myosin II motor protein (Joo et al., 2007) as well as proteins of the BORG family (F et al., 2015). While, Sept1/Sept2/Pnut complexes in drosophila have been shown to directly interact and bind actin filaments together into curved bundles (M et al., 2014b). A similar effect was also shown in human septin 2/6/7 complexes on the bending of actin bundles *in vitro*. Subsequently, septin 9 binds directly to actin and promotes its crosslinking which contributes to the stabilization of developing focal contacts, and cell motility was also found in MDCK cells (Dolat et al., 2014a). The association of septin 9 with actin depends on the unique domain of its N-terminal domain and does not necessarily require the association in complexes with other septins. (Figure 27).

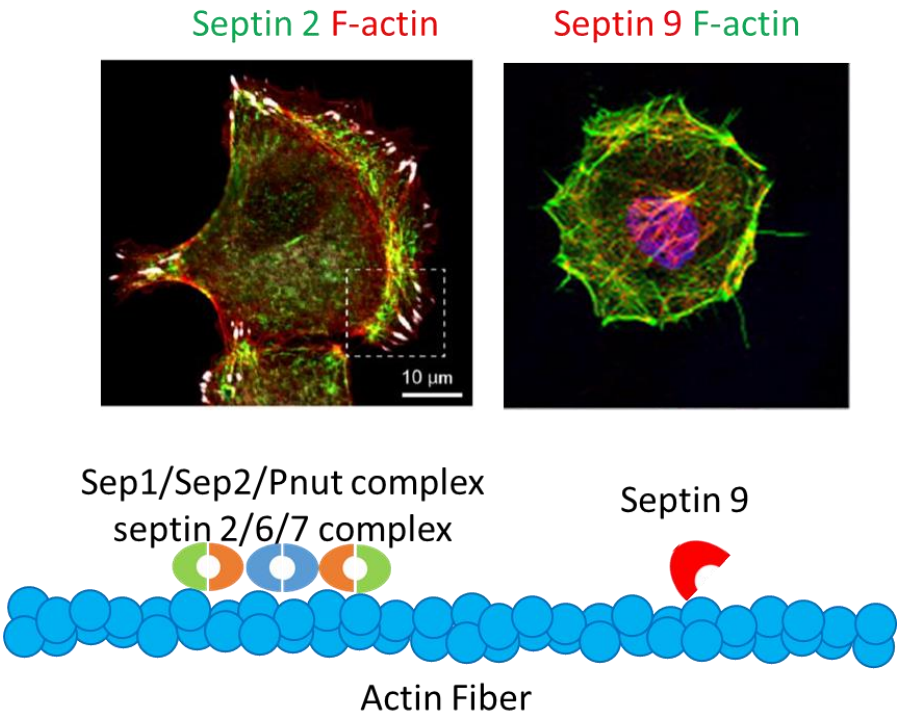


*Figure 27 Septins and actin colocalization and interaction*

*Septins colocalized with F-actin in actin-rich areas. Sep1/Sep2/Pnut complexes in drosophila, septin 2/6/7 complexes in humans directly interact with actin; septin 9 alone is also able to bind actin and promotes the actin fiber bundle. Image adapted from(Dolat et al., 2014a),(Mostowy et al., 2009a) and reproduced.*

Increasing reports suggest that septins influence actin organization by interacting directly with actin filaments and/or actin-binding proteins (ABPs), septins have also been implicated in the regulation of actin by the Rho-signaling GTPases Cdc42 and RhoA. Septin localization and function in actin SFs is dependent on Cdc42 activity, and the mammalian Borg (binding of Rho GTPases) family of Cdc42 effector proteins (Cdc42EPs), which regulates the formation of higher-order septin filaments in a Cdc42-dependent manner (Aj and F, 2017; F et al., 2015) as mentioned above.

## III.2 Septin and microtubule

The MT-associated septins localize to specific subsets of MTs, rather than decorating the entire MT network. In non-mitotic epithelial cells, septins associate with perinuclear MT bundles, Golgi-emanating MTs, peripheral focal adhesion-targeted MTs and/or ciliary MTs (Ghossoub et al., 2013; Jr et al., 2011; M et al., 2014a). In dividing cells, septins have been reported to localize to spindle poles, metaphase kinetochore MTs as well as MTs of the central spindle and the midbody (Menon et al., 2014; Surka et al., 2002) (Figure 28).

Among the 13 septins, septin 9 has been shown to bind to MTs directly (Bai et al., 2013). The N-terminal tail of septin 9 contains a series of tetrapeptide motifs with the sequence Lys/Arg-Arg/x-x-Asp/Glu. Detailed biochemical analysis suggests that the basic residues (Lys/Arg) of these motifs interact with the acidic amino acids of the C-terminal tail of βII-tubulin (Bai et al., 2013). It is unknown whether other septins associate with MTs through similar repeat motifs, but the N-terminal tail of septin 9 is unique among all septins. Notably, the N-terminal sequence of septin 9 is alternatively spliced, resulting in septin 9 isoforms that lack MT-binding motifs (septin 9_i4, i5) or contain unique N-terminal sequences upstream of them (septin 9_i2, i3) (Figure 28).

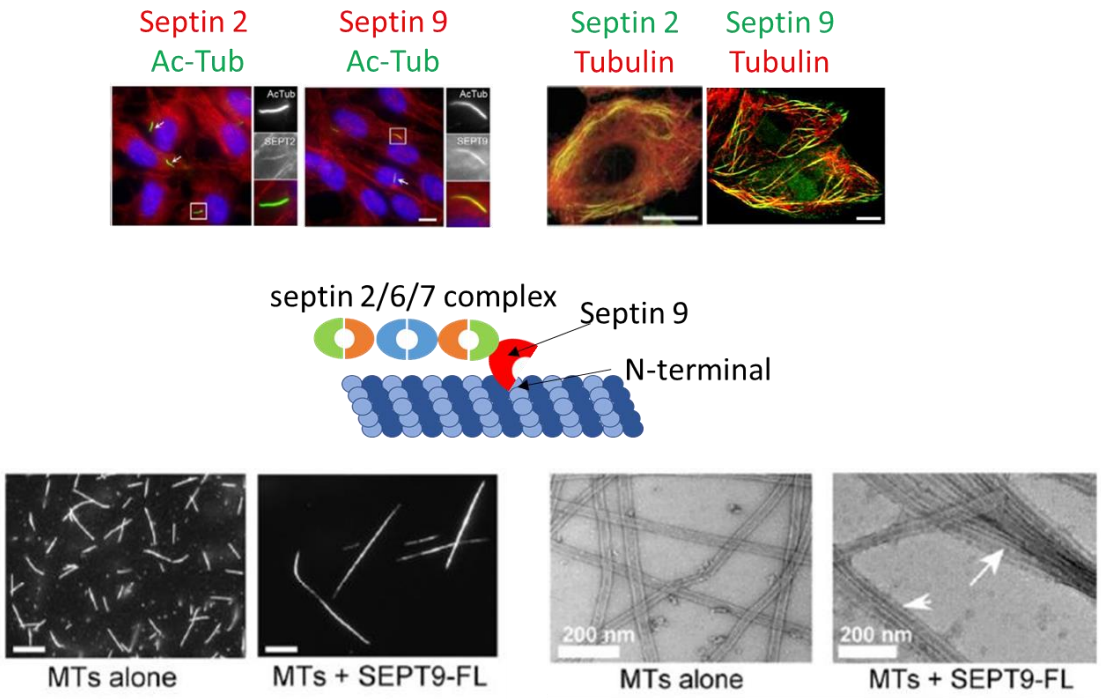


*Figure 28 Septins and tubulin colocalization and interaction*

*Septins colocalized with microtubules (MTs) in specific subsets of MTs such as the cilia and peripheric MTs. septin 9 using the tetrapeptide motifs in the N-terminal to bind the C-terminal tail of βII-tubulin promotes the MTs bundle. Image adapted from(Ghossoub et al., 2013),(Bai et al., 2013),(Targa et al., 2019) and reproduced.*

Septins also have the capacity to regulate MT dynamics. For example, in MDCK epithelial cells, septin 2 depletion increases the catastrophic shrinkage of perinuclear and peripheral MTs and decreases the growth of peripheral MTs (Bowen et al., 2011). In primary neurons, MT plus-end growth rates were similarly reduced by septin 7 knockdown, suggesting that septins suppress MT catastrophe events and promote MT growth (Ageta-Ishihara et al., 2013). Interestingly, depletion of septin 7 also increased the MT acetylation, a feature of MT stability, through modulating the interaction of MTs with MAP4 (Kremer et al., 2005).

## III.3 Septin and membrane

The association of septins with membranes was mediated by an interaction between their PB1 and the recently identified PB2 domain and PI lipids (Omrane et al., 2019; Tanaka-Takiguchi et al., 2009; Zhang et al., 1999a). Recently, several studies have revealed that the septins were also able to directly associate with the membranes through their AH motifs. An evolutionarily conserved septin AH motif was identified at the C-terminus of the yeast septin Cdc12 and shown to be necessary and sufficient for curvature preference *in vitro*. When the authors made an equivalent truncation mutation in the *Ashbya* homologue of Cdc12, septin association with curved membranes in vivo was drastically reduced (Cannon et al., 2019) (Figure 29a). As in our team, we performed a bioinformatics screening for AHs in the full sequence of septin 9. Two striking sequences emerged from our analysis as being the most prominent AHs (aa 274 to 294 and aa 370 to 402). Surprisingly, these AHs were directly adjacent to PB1 and PB2, respectively. And MD simulation showed that this portion of the protein indeed folded as an α-helix and was well-positioned to bind membranes. The AH close to PB2 was folded but oriented toward the interior of the protein unless a conformational switch occurred. These AHs contain very hydrophobic residues, such as tyrosine, tryptophan, and phenylalanine, a feature that enhances membrane association. Our analysis, therefore, suggested that septin 9 has at least one PB-adjacent AH associated with PB1 that can mediate its physical association with membranes. In addition, for the other septins, we also found flagrant AHs juxtaposed with the PB2 of septins 2, 6, and 7 with which septin 9 interacts to form the octamer (Omrane et al., 2019) (Figure 29 b-c).

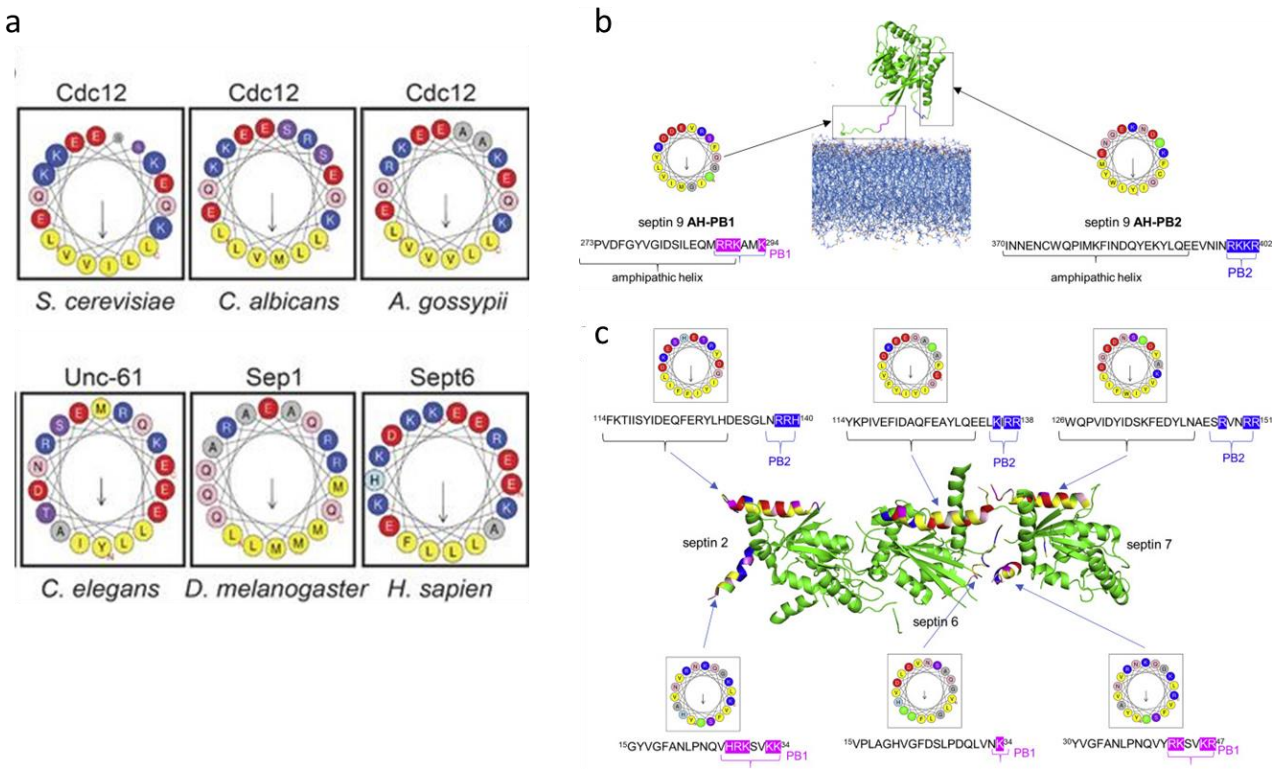


*Figure 29 Septins have Amphipathic Helices mediating its binding to the membrane.*
*a), AHs found in the C-terminal extensions of septins in multiple species represented through helical wheel diagrams.*
*b) Crystal structural model of septin 9 (PDB code 5cyp) showing the predicted amphipathic helices as opposed to PB1 and PB2 and their helical wheel representation generated using Heliquest.*
*c) Structural model of the (NC2G/G6NC/NC7G) septin complex published by Sirajuddin et al. showing the predicted amphipathic helices opposed to PB2 and the helical wheel representation of these helices generated using Heliquest. The sequence of each predicted helix is presented; the corresponding helical wheel and PB1 basic residues are highlighted in magenta and those of PB2 in blue. Image adapted from(Cannon et al., 2019),(Omrane et al., 2019) and reproduced.*

AHs do not generally require specific phospholipids for membrane association, and septin curvature preference in vitro is at least partially independent of phospholipid identity (McMurray, 2019). However, when human septins bind to the curved ends of rod-shaped bacterial cells in the context of bacterial infection, they are recruited there by cardiolipin, a curvature-specific bacterial membrane lipid (Krokowski et al., 2018). And, we proposed that the septin PB domains may interact with specific PI lipids to dock the protein on specific organelles since we have already shown that septin specifically binds to LDs and Golgi apparatus, which are enriched of PI5P and PI4P, respectively (Akil et al., 2016a; Omrane et al., 2019).

# IV. The cellular processes involving septins

Thanks to their ability to form filaments and their binding to cell membranes and cytoskeleton, the septins frequently serve as a scaffold for a wide range of proteins. These included membrane-bound receptors, cytoskeletal proteins, thus providing them a diffusion barrier function involved in various cell processes (Figure 30), such as cytokinesis, and cell polarity.

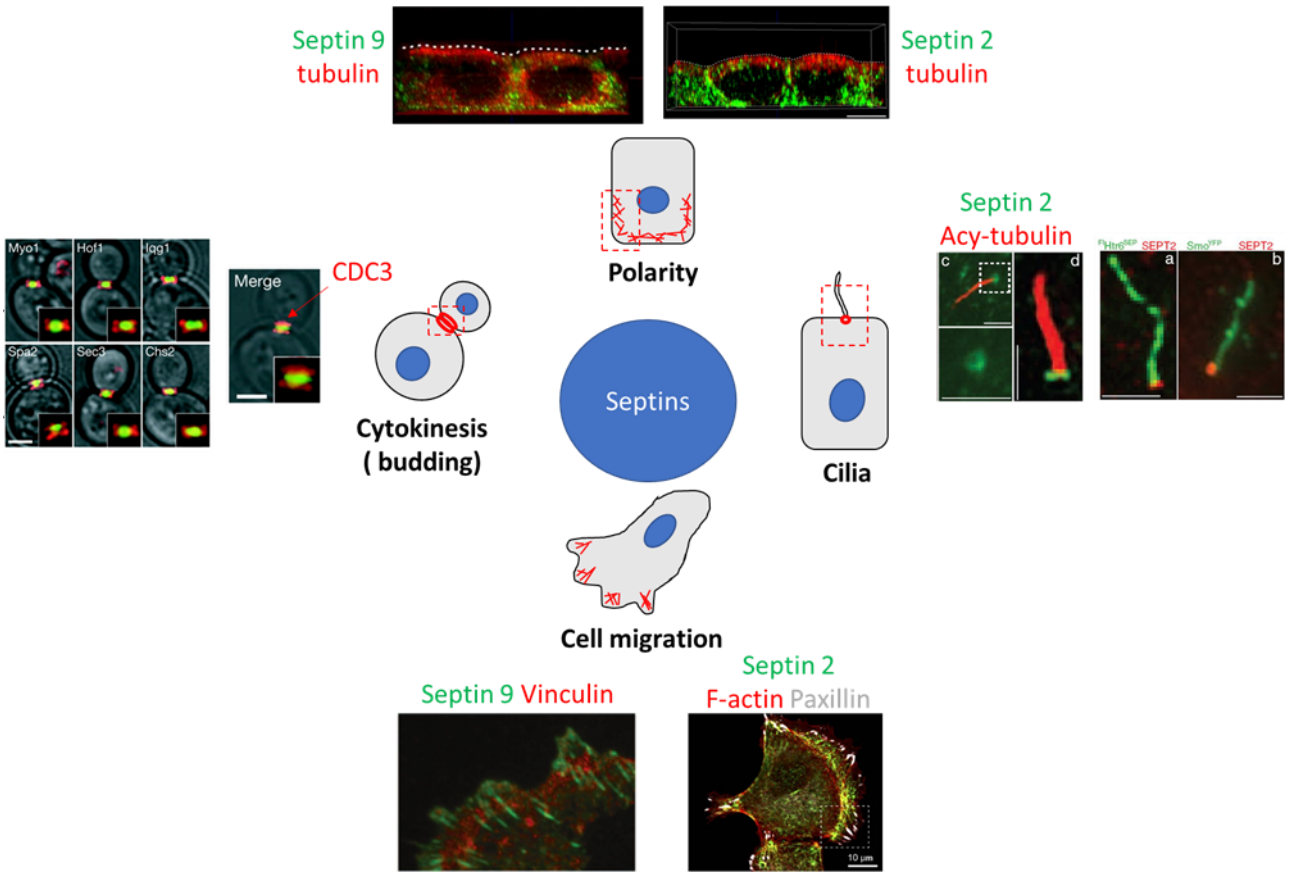


*Figure 30 septins role as diffusion barrier and protein scaffold in various biological processes. Septins localization was shown in the polarization of epithelial cells; cleavage furrow in yeast budding; in cilia; in protrusion of migration cells. Images were adopted and reproduced from (T et al., 2016),(Dobbelaere and Barral, 2004),(Hu et al., 2010),(Kuo et al., 2012),(Dolat et al., 2014a; Marcus et al., 2019; Mostowy and Cossart, 2012).*

## IV.1 Cytokinesis

In yeast, upon entering a new cell cycle, five septins (CDC3, CDC10, Cdc11, CDC12 and Shs1) are recruited to the bud site (Iwase et al., 2006). Septins are initially organized into clusters and then form a dynamic cortical ring (Longtine and Bi, 2003) (Figure 30 Cytokinesis). The budding ring structure serves as a platform for approximately 40 proteins (Douglas et al., 2005;

Gladfelter et al., 2001), for example, it served for the proteins Bud3, Bud4, and Axl2/Bud10, which determine the direction of the division axis in a yeast cell, as well as for Bud5 and Bud2 factors, which regulate the accuracy of budding (Douglas et al., 2005). This ring structure also represents a physical barrier that prevents the free diffusion of certain proteins between daughter and mother cells. For instance, during budding, Ist2p, a protein of the internal membrane which is only found in the daughter cell, but if the septin ring was destroyed, Ist2p spread into the maternal cell (Douglas et al., 2005; Takizawa et al., 2000). The septins diffusion barrier is also critical for preventing the segregation of misfolded proteins from the mother to daughter compartment (Chao et al., 2014; Clay et al., 2014).

In mammals, cytokinesis is usually accompanied by the formation of a septin ring that serves as a platform for signaling effectors and some other proteins (Joo et al., 2005; Kinoshita and Noda, 2001). In mammalian fibroblasts, mouse embryonic epithelial cells, or human HeLa cells, cytokinesis is impossible in the absence of septins. Different mammalian septins control different stages of cytokinesis; for instance, in HeLa cells, septin 2, septin 7, or septin 11 deficiency impairs the early stages of cytokinesis, while the lack of septin 9 affects the last stage of cell division (Estey et al., 2010).

## IV.2 Ciliogenesis

In addition to the cytokinesis, the role of septins in cilia was reported. Cilia are organelles involved in the motion of the intercellular fluid at different stages of ontogenesis. Although the ciliary membrane is continuous to the cell plasma membrane, it is nevertheless distinct from it since the membrane proteins could not circulate freely between the two membranes (Hu and Nelson, 2011). A septin ring is frequently present at the base of both primary (immotile) and motile cilia (Dash et al., 2014; Ghossoub et al., 2013; Hu et al., 2010; Kim et al., 2010) (Figure 30 Cilia). Septin 2, septin 7, or septin 9 depletion in human retinal pigmented epithelial cells, which represent a canonical model for the study of primary cilia, resulted in the decrease of cilia length and number (Ghossoub et al., 2013). The depletion of septin 2 in kidney epithelial cells or in mouse embryonic fibroblasts enhances the diffusion of membrane proteins between cilia and the remaining cell membrane, which demonstrates the importance of the septin diffusion barrier in ciliogenesis (Hu et al., 2010). Further studies also showed that different septins had distinct localizations in motile cilia of human respiratory epithelial cells. Septin 2, 7, 9 were found both at the ciliary base and the axoneme, while some were only at the base (septin 6, 8) or the axoneme (septin 11) (Fliegauf et al., 2014). This raises the possibility that distinct septin complexes could carry out different functions within cilia in the same cell.

## IV.3 Cell polarity

Cellular polarity is characterized by an asymmetry in the composition of the plasma membrane, in the distribution of intracellular organelles, and in the cytoskeleton. Subsequently, in epithelial cells, the intracellular and membrane contents are divided into two functionally different domains that consist of apical and basolateral domains. The apical domain faces the lumen of the organ while the basolateral membrane which is enriched with intercellular junctional complexes composed of tight junctions, adherent junctions and desmosomes, establishes the contacts between cells in its lateral part and also with the extracellular matrix (ECM) in the basal part (Rodriguez-Boulan and Macara, 2014; Shin and Margolis, 2006). In Madin Darby canine kidney (MDCK) cells, it has been shown that MTs carrying trafficking vesicles are guided by septin protofilaments. Depletion of septin 2 decreases the transport of vesicles from the TGN to the plasma membrane. As a result, apical and basolateral membrane markers accumulate in the cytoplasm and the cells fail to adopt the characteristic morphology of a polarized epithelial cell (Spiliotis et al., 2008). In addition, in polarized human colon adenocarcinoma (Caco-2) cells, both septin 2 and septin 9 have been shown mainly localized in the basolateral domain (T et al., 2016) (Figure 30 Polarity), Although a link between septin and junctional complex localization was still not reported, the junctional complexes bind to the actin cytoskeleton via adapter proteins in their cytoplasmic side (Fanning et al., 2012; Mège and Ishiyama, 2017). Thus, we can speculate that septin may affect intercellular junctional complexes localization via affecting the actin cytoskeleton, thus, regulate cell polarity.

## IV.4 Cell shape and motility.

The septins also participate in the maintenance and regulation of the cell shape and motility (Dolat et al., 2014b; Gilden et al., 2012; Kremer et al., 2007; Tooley et al., 2009). Membrane-associated septins interact with other components of the cytoskeleton and determine the rigidity of the cell. In the absence of septin 2 or septin 11, rigidity and cortical plasticity of HeLa cells decreased (Mostowy et al., 2011). Septin 7 depletion in mouse amoeboid T cells significantly damaged their morphology but did not alter the cell volume. Cells lacking the septins can squeeze through narrow openings, which may facilitate the progression and metastasis of malignant tumors (Tooley et al., 2009). In addition, several studies demonstrate that loss of septin 2, septin 7, and septin 9 consistently attenuate wound healing in cultured epithelial and cancer cell monolayers, as well as in *Xenopus embryo* (Dolat et al., 2014a; Shindo et al., 2018; Zeng et al., 2019; Zhang et al., 2016a). The observed promigratory activity of the septin cytoskeleton may be mediated by different mechanisms such as control of cortical MT assembly at the migrating cell edge (Shindo et al., 2018), formation of basal actin-based stress fibers (Dolat et al., 2014a), stabilization of FAs (Dolat

et al., 2014a; Zeng et al., 2019), and activation of mitogen-activated protein (MAP) kinase signaling (Zhang et al., 2016a). Interestingly, septin 2 and septin 9 are not only essential for focal adhesion maturation but also regulate the assembly of other adhesion structures such as podosomes which mediate matrix degradation (Collins et al., 2020; Møller et al., 2018) (Figure 30 Migration).

## IV.5 Membrane trafficking

Septins also have been shown to participate in the membrane trafficking process (Figure 31). Membrane traffic relies on the formation of transport carriers, which depend on the concentration of cargo in confined membrane areas. Furthermore, select machinery needs to be assembled to aid membrane deformation into highly curved vesicles, and to promote fission from the donor compartment (Figure 16). Given the proposed scaffolding and diffusion barrier function of septin filaments, and their well-established roles in membrane curve sensors and binding property (Bridges et al., 2016; Cannon et al., 2019; McMurray, 2019), it is conceivable that septins contribute to carrier formation, for instance by shielding membrane subdomains, by imposing or sensing membrane curvature, or by recruiting appropriate effector proteins assisting vesicle generation (Song et al., 2016). For example, accumulating evidence suggests that septins are associated with membranes of the endo-lysosomal system. A proteomic approach identified several septins together with bona fide endosomal proteins on early endosome-like liposomes (T et al., 2008). Later, septin 6 and septin 7 on endosomes regulate the biogenesis of MVBs in a process involving the adaptor complex AP-3 and ESCRT proteins were also demonstrated (S et al., 2014). Depletion of septin 2 or septin 11 in macrophages perturbs phagocytic uptake of opsonized latex beads (Yw et al., 2008), and at sites of phagosome formation both septin family members co-localize with actin-rich structures. Similarly, several septins have been found to assemble in close proximity to actin at the entry site of several pathogens in human non-phagocytic cells, and have been proven important for their internalization (Qt et al., 2013; S and P, 2011). During the endosome to MVBs maturation, septin 2 was recruited by $PI(4,5)P_2$ to fusion sites on Rab7-positive macropinosomes, while, septin 2 depletion does not impair docking between macropinosomes, but reduces their fusion (Dolat and Spiliotis, 2016). In addition, in our primary studies, we have found that the endogenous septin 9 is present in septin structures associated with the Golgi apparatus, depletion of septin 9 by a specific siRNA promoted Golgi fragmentation and impede Golgi dependent secretory pathways, thus septins also play a critical role in the control of the Golgi apparatus compactness and its subsequent function in cellular trafficking (Omrane et al., 2019) (Figure 31).

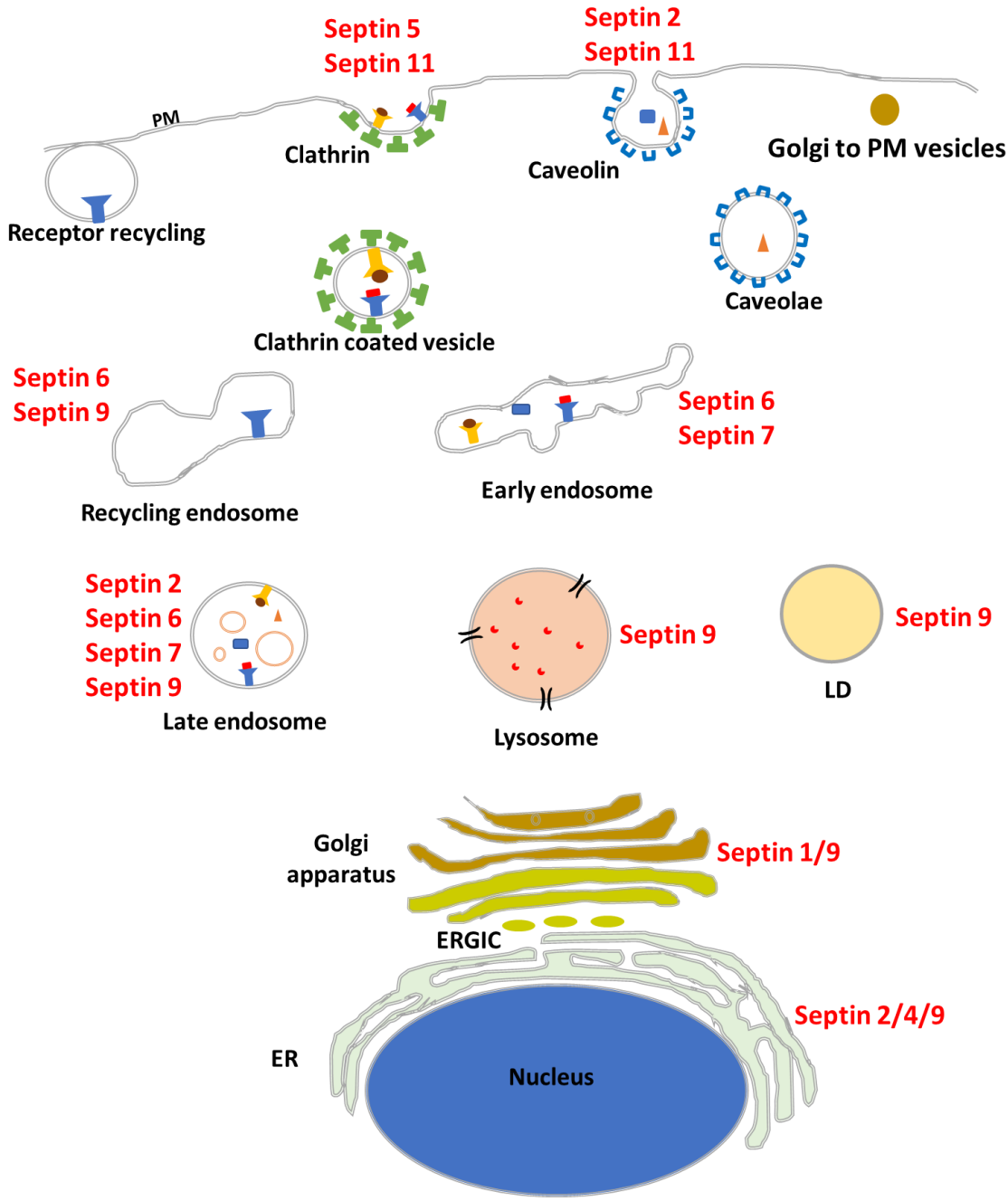


*Figure 31 Septins involved membrane trafficking processes*

*Septins associated with nearly all the membrane structure organelles within the cells. Septin 5/11 associated with clathrin-mediated endocytosis (Maimaitiyiming et al., 2013); septin 2/11 associated with caveolae (Hau et al., 2019; Moreno-Castellanos et al., 2017); Septin 6/7 facilitates MVB biogenesis (S et al., 2014); septin 2/6/7/9 related to late lysosome sorting (Dolat and Spiliotis, 2016); septin 9 as a scaffold recruit dynein and dynamin protein for lysosome movement (Kesisova et al., 2020); septin1/9 maintain the proper structure and transport function of Golgi apparatus (Omrane et al., 2019; Song et al., 2019); Septin 2/6/7 associated with ER (Akil et al., 2016a; Katz et al., 2019; Luedeke et al., 2005). septin 9 interact with LDs (Akil et al., 2016a).*

# V. Septins associated diseases

Given the range of cellular functions attributed to septins, it is not surprising that the septins might be linked to a variety of diseases due to the loss or gain of such cellular functions.

## V.1 Neurological Diseases

The septins are thought to be involved in both neurodegenerative and neurobehavioral disorders. Alzheimer's disease is a progressive neurodegenerative disorder that is histopathologically characterized by the presence of senile plaques as well as neurofibrillary alterations. Septin 2, septin 1, and septin 4 have been shown to be concentrated in the neurofibrillary tangles of Alzheimer's patient brains, potentially suggesting a role in the neurodegenerative process (Kinoshita et al., 1998). In another common neurodegenerative disorder, Parkinson's disease, septin 4 is thought to have a role in cell death and the formation of Lewy body cytoplasmic inclusions containing α-synuclein (Ihara et al., 2003; Shehadeh et al., 2009). Proteomic studies performed on postmortem brains of patients with schizophrenia and bipolar disorder demonstrated differential expression of septins in both diseases (Pennington et al., 2008). Deregulation of several proteins in the cerebral cortex of fetuses with Down syndrome included a decrease in the level of septin 7, suggesting involvement in the developmental and cognitive impairment in this disease (Engidawork et al., 2003). The mass-spectrometry findings that postsynaptic densities contain several members of the septin gene family (Tada et al., 2007; Walikonis et al., 2000) support their possible implication in neurodegeneration and loss of cognitive function.

## V.2 Septin and cancer

Septin 9 was the first septin implicated in cancer in the late 1990s, as a fusion partner of the mixednlineage leukemia (MLL) gene, which translocates to various chromosomal loci, giving rise to chimeras that promote the oncogenic potential of MLL (Osaka et al., 1999). Subsequently, the murine SL-3 retrovirus that causes T-cell lymphomas was found to preferentially integrate into the septin 9 gene locus (Sørensen et al., 2000). In the meantime, the human septin 9 gene was mapped to the chromosomal locus 17q25.3, which is frequently deleted in sporadic ovarian and breast cancers (Kalikin et al., 2000). Following these early findings, an increasing number of studies began to report the overexpression and down-regulation of specific septins in a variety of hematological malignancies and solid tumors. Though, alterations in septin expression have been reported in brain tumors, skin, kidney, colorectal, lung, and hormonally regulated cancers such as prostate, breast,

ovarian and endometrial cancers (Dolat et al., 2014b; Hall and Russell, 2004; Montagna et al., 2015). In the vast majority of these cancers, septins are overexpressed, but occasionally downregulation, ectopic expression, and epigenetic alterations have also been reported (Liu et al., 2010; Shen et al., 2012; Tanaka et al., 2001). Although septins function as hetero-oligomers, several studies show that abnormalities of the expression levels of a single septin could promote tumorigenic phenotypes (Connolly et al., 2011; Dolat et al., 2014a; García-Fernández et al., 2010; Gonzalez et al., 2009; Marcus et al., 2019). By contrast to classical tumor suppressors and oncogenes, the role of septins in cancer is not due to loss and gain of function mutations. Septins are thought to affect tumorigenesis as a consequence of altered expression by alternate slicing (Hall and Russell, 2004).

Given the advances in the cell biological function of septins, it is now evident that septins are linked to the molecular mechanisms that underlie hallmarks of cancer such as resistance to cell death, proliferation, angiogenesis, invasion, and metastasis. For example, septin 4 is regarded as a pro-apoptotic tumor suppressor, whose down-regulation in leukemia could render resistance to pro-apoptotic stimuli (García-Fernández et al., 2010). Septin 9_i1 binds and prevents the degradation of the c-Jun-N-terminal kinase (JNK), which promotes tumor cell proliferation (Gonzalez et al., 2009). Similarly, septins have also been reported to suppress the degradation of the epidermal growth factor receptor (EGFR) and the receptor-protein tyrosine kinase Erb2/HER2, which are linked to signaling pathways that trigger cell proliferation and migration (Diesenberg et al., 2015; Marcus et al., 2016).

Multiple studies have shown that over-expression of septin 9 isoforms enhances cell motility and invasion (Connolly et al., 2011; Dolat et al., 2014b; Marcus et al., 2019; Verdier-Pinard et al., 2017; Xu et al., 2018b). Septin 2 and septin7 have also been implicated in the migration and invasion of breast cancer and glioblastoma cells (Zhang et al., 2016b). While septin 7 appears to have the opposite role in gliomas (He et al., 2019; Jiang et al., 2014; Zhang et al., 2016b).

## V.3 Septin and infections

### V.3.1 Bacterial infections

A role for septins in bacterial infection was first suggested from studying *L. monocytogenes* invasion approximately 20 years ago in the laboratory of Pascale Cossart (Pizarro-Cerdá et al., 2002). Since then, septins have been associated with a wide variety of bacterial pathogens, including *Chlamydia trachomatis, Clostridium difficile, Salmonella Typhimurium and enteropathogenic Escherichia coli* (Boddy et al., 2018; Lee et al., 2017; T et al., 2016; Volceanov et

al.) The accumulation at the bacterial entry site of septins and induced morphology changes of the host cell surface to promote efficient invasion (Boddy et al., 2018; Mostowy et al., 2009b, 2011). After entry into the cell, bacteria replication may take place in the cytoplasm or within vacuoles (Castanheira and García-Del Portillo, 2017). And, at the bacterial surface, actin tails are formed enabling bacteria to move in the cytoplasm, escape to defense mechanisms of the host cell and infect adjacent cells (Welch and Way, 2013). However, the epithelial cell may activate defense mechanisms by inducing the reorganization of septins into cage-like structures around the intracellular bacteria (Mostowy et al., 2010). Enclosed in septin cages, bacteria lose the actin-based motility and are prone to degradation by autophagy(Krokowski et al., 2018). Thus, they may participate in the cellular defense against intracellular bacterial infections. Interestingly, septin cages are not formed around dead cytosolic bacteria (Sirianni et al., 2016), this may result from the insufficient release of *Salmonell*a pathogenicity effectors, such as SopB, which is a protein that I worked with during my master. This protein is encoded in the pathogenicity islands (SPI) -1 of *Salmonella* with inositol phosphatase activity that hydrolyzes a variety of PIs and inositol phosphates at the host cell membrane during Salmonella invasion (Hu et al., 2017).

## V.3.2 Virus infections

### V.3.2.1. Vaccinia Virus Infection

Vaccinia virus, a member of the *Orthopoxviruses* genus, is well known for its use as a vaccine to successfully eradicate smallpox (Walsh and Dolin, 2011). Following host cell invasion, vaccinia replicates in the cytoplasm and is wrapped by two membranes derived from the trans-Golgi network or endosomal cisternae to form an intracellular enveloped virus (IEV). IEV is transported to the cell periphery in an MT-dependent manner, where the outermost membrane of IEV fuses with the plasma membrane. After fusion of IEVs with the plasma membrane, two modes of viral spread are possible (Leite and Way, 2015). Either they are released from the cell as an extracellular enveloped virus (EEV) promoting the long-range spread, or they remain attached to the cell membrane as so-called cell-associated enveloped viruses (CEV). CEVs are then capable of signaling back into the cell to induce the polymerization of actin tails, facilitating spreading into and infecting adjacent cells (Leite and Way, 2015).

The involvement of septins in vaccinia infection was originally reported by two human genome-wide RNAi screens which suggested that knockdown septins enhance vaccinia replication and/or spread (Beard et al., 2014; Sivan et al., 2013). A subsequent study confirmed that depletion of septins (2,9,11) led to a significantly increased release of the vaccinia virus (Pfanzelter et al., 2018). High-resolution confocal microscopy showed that septins are recruited to viral particles only after their fusion with the plasma membrane and that septin 7 forms ring-like structures, thereby

entrapping extracellular CEV. Actin tail formation takes place after the recruitment of septins to CEVs. Upon starting the actin polymerization, septins rapidly disappear from the viral particles. These results suggest that septin complexes control vaccinia infection by suppressing actin tail formation, viral release, and cell-to-cell spreading (Pfanzelter et al., 2018).

### V.3.2.2. Hepatitis C Virus (HCV) Infection

As mentioned in chapter I (liver section), HCV is an enveloped, single-stranded RNA virus of the genus *Hepacivirus*, and the family *Flaviviridae*. The HCV genome encodes a large polyprotein precursor subject to proteolytic cleavage by viral and host proteases to generate both structural and non-structural proteins (Beeck and Dubuisson, 2003; Kato, 2000). In a study for seeking proteins interacting with NS5B, a nonstructural HCV protein that functions as RNA-dependent RNA polymerase, the heterogeneous nuclear ribonucleoprotein A1 (hnRNP A1) and septin 6 have been identified. Knockdown of either septin 6 or hnRNP A1 inhibited HCV replication. They proposed that septin 6 may act as a scaffolding molecule in the replication complex connecting NS5B and hnRNP A1 via protein-protein interactions and hnRNP A1 and viral RNA via RNA-protein interaction. Since hnRNP A1 is an RNA-binding protein, they also proposed that it may direct the HCV RNA replication complex to the proper region(s) of the genomic RNA. (Kim et al., 2007).

Our group also provided evidence that septins are necessary for regulateing HCV replication. In HCV-induced cirrhosis samples, the expression of most septins was modified compared to normal liver samples. Infection of Huh7.5 cells with HCV JFH-1 (Japanese fulminate hepatitis 1), we have shown that the expression level of septin 9 increased. Knocking down septin 9 using siRNAs reduced HCV genomic RNA. HCV-infected Huh7.5 cells exhibited a well-developed microtubule network compare to non-infected cells which colocalized with septins filaments. The siRNA-induced silencing of septin 9 disintegrated the MT network. Septin 9_i1 promoted perinuclear recruitment of LDs surface-associated proteins such as PLIN2, PLIN3, as well as the HCV core and non-structural NS5A. Thus, we concluded that HCV optimizes the conditions for its replication by hijacking host septin 9 to modulate the growth of LDs and build up a lipid-enriched environment (Akil et al., 2016a).

# Chapter IV

# Experimental results

## I. Septin 9 and phosphoinositides regulate lysosome cellular localization and their association with lipid droplets for degradation

**Summary**

The liver plays a crucial role in the homeostasis of lipids (Bechmann et al., 2012) and thus alterations of the processes involved in their metabolism due to stressful conditions may induce an accumulation of lipid in the liver and the subsequent development of diseases that include steatosis, non-alcoholic steatohepatitis (NASH) which can progress in cirrhosis and cancer (Benedict and Zhang, 2017; Michelotti et al., 2013). The progression from steatosis to fibrosis/cirrhosis and even liver cancers are an extremely complex process. But the initiation of liver disease is clearer which is always associated with hepatocyte metabolism dysfunction and/or death induced by multiple factors. Since one of the hallmark features for liver disease occurrence is excessive lipid LD accumulation, understanding the underlying molecular mechanisms is essential to prevent the development of liver disease.

LDs consist of a hydrophobic core of neutral lipids (primarily composed of triacylglycerols and cholesterol esters) surrounded by a monolayer of phospholipid and cholesterol in which proteins are embedded. These proteins are dominated by enzymes involved in lipid metabolism and members of the PLIN family. However, proteins with other functions such as membrane trafficking, like small Rab-GTPases are also well represented. In addition, Rab GTPases and PIs present in discrete membrane domains on the different organelles and intracellular trafficking vesicles, facilitate endosomal functions to ensure the maintenance and coordination of membrane trafficking (Jean and Kiger, 2012). The Regulatory role of Rabs and PIs on LDs have been demonstrated respectively (Akil et al., 2016a; Ozeki et al., 2005; Schroeder et al., 2015), while, whether they are working in a coordinated manner and how they will be regulated are challenging issues.

Septins belong to a highly conserved family of GTP-binding proteins with 13 members in eukaryotes (Nishihama et al., 2011). Septins assemble in hetero-oligomeric complexes and form nonpolar filaments or rings that bind to actin and MTs (Kim et al., 2011; Kinoshita et al., 2002; Sellin et al., 2011). Septins are therefore essential for cytoskeleton-dependent cell processes and are considered as the fourth component of the cytoskeleton (Bai et al., 2013; Joo et al., 2007; Mostowy

and Cossart, 2012; Smith et al., 2015 ). Septins are also associated with a variety of PIs at different intracellular membranes through polybasic domains (PB) (Akil et al., 2016a; Dolat and Spiliotis, 2016; Omrane et al., 2019; Pagliuso et al., 2016; Zhang et al., 1999b). Once attached to the membranes, septins can act as a scaffold that recruits cytosolic proteins and other cytoskeletal elements to control numerous cellular functions such as cytokinesis, ciliogenesis, vesicle trafficking, cell polarity (Akil et al., 2016a; Bridges et al., 2016; Fung et al., 2014; Gassama-Diagne et al., 2006; Mostowy and Cossart, 2012; Song et al., 2016; Tanaka-Takiguchi et al., 2009). Alterations of the expression of septins are associated with several diseases including infectious diseases and cancer (Angelis and Spiliotis, 2016; Henzi et al., 2021; Krokowski et al., 2018).

We reported a high expression of septin 9 in hepatitis C virus (HCV)-induced cirrhosis. We also showed that septin 9 is hijacked by HCV to induce the perinuclear accumulation of LDs by a PtdIns5P and MT-dependent mechanism (Akil et al., 2016a).

While the increase of LDs within cells is controlled by two major pathways of metabolism: the pathway of anabolism which involves the synthesis of TG and CE and the catabolism pathway which results in the reduction of the lipid content through β oxidation, lipolysis by lipases, autophagy-dependent on lysosome and export of lipids through secretion. (Bessone et al., 2019; Koo, 2013; Kwanten et al., 2014).

As described in Chapters II and IV, the lysosome plays a central role in LD catabolism and its dysfunction contributes to LD accumulation and has been associated with steatosis in different studies (Inami et al., 2011; Miyagawa et al., 2016; Wang et al., 2018).

According to these main points, we hypothesized that septin 9 may regulate lysosome trafficking and its activity to impair LD degradation and promote their perinuclear accumulation dependent on PI and Rabs (Figure 32).

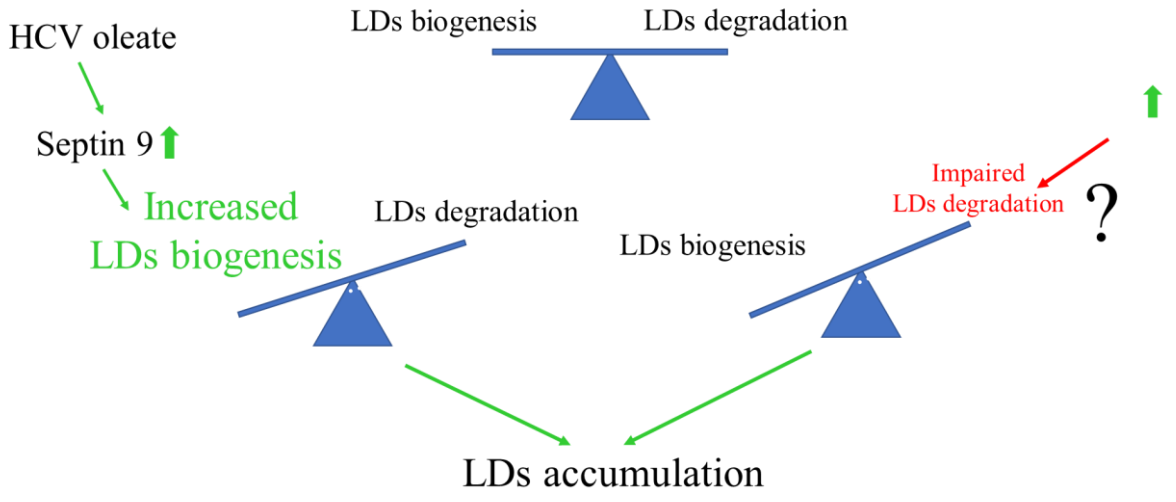


Figure 32 Hypothesis for thesis

In this thesis, we used Huh7 cells loaded with oleate as a model system to study the role of septin 9 in LD accumulation. We showed that after the addition of oleate to the cells, we observed a dramatic Spatio-temporal rearrangement of LDs which showed a perinuclear clustering of LD in the first hours following oleate addition (0-100μM) and later the LD dispersed towards the cell periphery. However, with a higher concentration of oleate (200-400μM), this dynamic of LDs was disrupted, and LD remained accumulated in the perinuclear region. We observed a similar distribution and change in dynamic of the lysosomes which are associated with LDs. Interestingly, the depletion of septin 9 in oleate treated cells, dispersed the oleate-induced lysosome perinuclear clusters while overexpression of septin 9_i1 maintain lysosome perinuclear clusters. Furthermore, we found that the perinuclear lysosomes are colocalized with Golgi structure and this colocalization is relied on MTs dynamic and enhanced centrosome MTs polymerization which are both regulated by septin 9.

Subsequently, we observed that Rab7 protein was also clustered in the perinuclear region with Golgi whereas the contact between Rab7 and perinuclear LDs clusters was reduced. In such conditions, a high level of septin 9 was found associated with the large LDs. Conversely, when the LDs and lysosomes were dispersed in the cytoplasm, an association between Rab7 and LDs was observed and revealed the increase of the contact of LDs with the lysosomes to permit their degradation. Furthermore, the addition of PtdIns5P or transfection of the cells with MTMR3 which hydrolyses PtdIns(3,5)P2 to form PtdIns5P, strongly increased the cell content of LDs and the perinuclear clustering of Rab7 as observed with septin 9 expression and increase oleate concentration. Interestingly, treatment of cells with PtdIns(3,5)P2 gave opposite data and Rab7 was seen around the LDs. Together, these results indicated that the presence of specific PIs is important for the intracellular distribution of LDs and their interaction with lysosomes for their degradation. To conclude, our results have uncovered the role of septin 9 and PIs in LDs behavior and their interaction with lysosomes which identified molecular machinery that links lipid metabolism to organelle homeostasis.

**Résumé**

Le foie joue un rôle crucial dans l'homéostasie des lipides (Bechmann et al., 2012) et donc les altérations des processus impliqués dans leur métabolisme dues à des conditions stressantes peuvent induire une accumulation de lipides dans le foie et le développement ultérieur de maladies qui incluent la stéatose, la stéatohépatite non alcoolique (NASH) qui peut évoluer en cirrhose et en cancer (Benedict et Zhang, 2017 ; Michelotti et al., 2013). La progression de la stéatose vers la fibrose/cirrhose et même les cancers du foie sont un processus extrêmement complexe. Mais l'initiation de la maladie hépatique est plus claire et est toujours associée à un dysfonctionnement du métabolisme des hépatocytes et/ou à leur mort induite par de multiples facteurs. L'accumulation excessive de GLs lipidiques étant l'une des caractéristiques de l'apparition de la maladie du foie, il est essentiel de comprendre les mécanismes moléculaires sous-jacents pour prévenir le développement de la maladie du foie.

Les GLs sont constituées d'un noyau hydrophobe de lipides neutres (principalement composé de triacylglycérols et d'esters de cholestérol) entouré d'une monocouche de phospholipides et de cholestérol dans laquelle sont intégrées des protéines. Ces protéines sont dominées par les enzymes impliquées dans le métabolisme des lipides et les membres de la famille PLIN. Cependant, des protéines ayant d'autres fonctions comme le trafic membranaire, comme les petites Rab-GTPases sont également bien représentées. De plus, les Rab GTPases et PIs présentes dans des domaines membranaires discrets sur les différents organites et vésicules de trafic intracellulaire, facilitent les fonctions endosomales pour assurer le maintien et la coordination du trafic membranaire (Jean et Kiger, 2012). Le rôle régulateur des Rabs et des PIs sur les GLs a été démontré respectivement (Akil et al., 2016a ; Ozeki et al., 2005 ; Schroeder et al., 2015), alors que, s'ils travaillent de manière coordonnée et comment ils seront régulés sont des questions difficiles.

Les septines appartiennent à une famille hautement conservée de protéines de liaison au GTP qui compte 13 membres chez les eucaryotes (Nishihama et al., 2011). Les septines s'assemblent en complexes hétéro-oligomériques et forment des filaments ou des anneaux non polaires qui se lient à l'actine et aux MTs (Kim et al., 2011 ; Kinoshita et al., 2002 ; Sellin et al., 2011). Les septines sont donc essentielles aux processus cellulaires dépendant du cytosquelette et sont considérées comme le quatrième composant du cytosquelette (Bai et al., 2013 ; Joo et al., 2007 ; Mostowy et Cossart, 2012 ; Smith et al., 2015). Les septines s'associent également à une variété de PI au niveau de différentes membranes intracellulaires par le biais de domaines polybasiques (PB) (Akil et al., 2016a ; Dolat et Spiliotis, 2016 ; Omrane et al., 2019 ; Pagliuso et al., 2016 ; Zhang et al., 1999b). Une fois attachées aux membranes, les septines peuvent agir comme un échafaudage qui recrute des protéines cytosoliques et d'autres éléments du cytosquelette pour contrôler de nombreuses fonctions cellulaires telles que la cytokinèse, la ciliogenèse, le trafic de vésicules, la polarité cellulaire (Akil et al, 2016a ; Bridges et al., 2016 ; Fung et al., 2014 ; Gassama-Diagne et al., 2006 ; Mostowy et Cossart, 2012 ;

Song et al., 2016 ; Tanaka-Takiguchi et al., 2009). Les altérations de l'expression des septines sont associées à plusieurs maladies dont les maladies infectieuses et le cancer (Angelis et Spiliotis, 2016 ; Henzi et al., 2021 ; Krokowski et al., 2018).

Nous avons rapporté une forte expression de la septine 9 dans la cirrhose induite par le virus de l'hépatite C (VHC). Nous avons également montré que la septine 9 est détournée par le VHC pour induire l'accumulation périnucléaire des GLs par un mécanisme dépendant de PtdIns5P et de MT (Akil et al., 2016a).

Alors que l'augmentation des GLs au sein des cellules est contrôlée par deux voies majeures du métabolisme : la voie de l'anabolisme qui implique la synthèse de TG et CE et la voie du catabolisme qui se traduit par la réduction du contenu lipidique par β oxydation, lipolyse par les lipases, autophagie dépendante du lysosome et exportation des lipides par sécrétion (Bessone et al., 2019 ; Koo, 2013 ; Kwanten et al., 2014).

Comme décrit dans le chapitre II, IV, le lysosome joue un rôle central dans le catabolisme des GLs et son dysfonctionnement contribue à l'accumulation des GLs et a été associé à la stéatose dans différentes études (Inami et al., 2011 ; Miyagawa et al., 2016 ; Wang et al., 2018b).

Selon ces principaux points, nous avons émis l'hypothèse que la septine 9 pourrait réguler le trafic des lysosomes et son activité pour altérer la dégradation des GLs et favoriser leur accumulation périnucléaire dépendante de PI et Rabs (Figure 32).

Dans cette thèse, nous avons utilisé les cellules Huh7 chargées en oléate comme système modèle pour étudier le rôle de la septine 9 dans l'accumulation des GLs. Nous avons montré qu'après l'addition d'oléate aux cellules, nous avons observé un réarrangement spatio-temporel spectaculaire des GLs qui a montré un regroupement périnucléaire des GLs dans les premières heures suivant l'addition d'oléate (0-100µM) et ensuite les GLs se sont dispersés vers la périphérie des cellules. Cependant, avec une concentration plus élevée d'oléate (200-400µM), cette dynamique des GLs a été perturbée, et les GLs sont restés accumulés dans la région périnucléaire. Nous avons observé une distribution similaire et un changement dans la dynamique des lysosomes qui sont associés aux GLs. Il est intéressant de noter que la déplétion de la septine 9 dans les cellules traitées à l'oléate disperse les amas périnucléaires de lysosomes induits par l'oléate, tandis que la surexpression de la septine 9_i1 maintient les amas périnucléaires de lysosomes. De plus, nous avons constaté que les lysosomes périnucléaires sont colocalisés avec la structure de Golgi et cette colocalisation repose sur la dynamique des MTs et la polymérisation accrue des MTs du centrosome qui sont toutes deux régulées par la septine 9.

Par la suite, nous avons observé que la protéine Rab7 était également regroupée dans la région périnucléaire avec le Golgi alors que le contact entre Rab7 et les groupes de GLs périnucléaires était réduit. Dans ces conditions, un niveau élevé de septine 9 a été trouvé associé

aux grands GLs. Inversement, lorsque les GLs et les lysosomes étaient dispersés dans le cytoplasme, des associations entre Rab7 et les GLs ont été observées et ont révélé l'augmentation du contact des GLs avec le lysosome pour permettre leur dégradation. De plus, l'ajout de PtdIns5P ou la transfection des cellules avec MTMR3 qui hydrolyse PtdIns(3,5)P2 pour former PtdIns5P, a fortement augmenté le contenu cellulaire des GLs et le regroupement périnucléaire de Rab7 comme observé avec l'expression de la septine 9 et l'augmentation de la concentration d'oléate. De façon intéressante, le traitement des cellules avec PtdIns(3,5)P2 a donné des données opposées et Rab7 a été vu autour des GLs. Ensemble, ces résultats indiquent que la présence de PIs spécifiques est importante pour la distribution intracellulaire des GLs et leur interaction avec les lysosomes pour leur dégradation. En conclusion, nos résultats ont mis en évidence le rôle de la septine 9 et des IP dans le comportement des GLs et leur interaction avec les lysosomes, ce qui a permis d'identifier la machinerie moléculaire qui relie le métabolisme des lipides à l'homéostasie des organites.

**Septin 9 and phosphoinositides regulate lysosome cellular localization and their association with lipid droplets for degradation**

Pei Xuan Song[1,2], Juan Peng[1,2], Mohyeddine Omrane[1,2], Christophe Desterke[1], Didier Samuel[1,2,3], Ama Gassama-Diagne[1,2*],

1. Unité 1193, INSERM, Villejuif F-94800, France
2. UMR-S 1193, Université Paris-Sud, Villejuif F-94800, France
3. AP-HP Hôpital Paul-Brousse, Centre Hépato-Biliaire, Villejuif F-94800, France.

*Correspondence to[ama.gassama@inserm.fr]

Keywords: Lipid droplet, septin 9, Lysosome, Golgi apparatus, Phosphoinositides

**Summary**

The accumulation of lipid droplets (LDs) in the liver is a hallmark of steatosis, often associated with lysosome dysfunction. Nevertheless, the underlying mechanisms remain unclear. Here using Huh7 cells loaded with oleate as a model to study LD metabolism, we show that cellular content and distribution of LDs are correlated to those of the lysosome and regulate by oleate and septin 9. High expression of septin 9 promotes perinuclear clustering of lysosomes which co-localized with Golgi and not with their surrounding LDs. Inversely, knock-down of septin 9 disperses the two organelles which colocalize at the cell periphery. The GFP-rab7 is present all around these peripheral LDs. PtdIns5P which binds septin 9, and MTMR3 which converts PtdIns(3,5)P2 into PtdIns(5) recapitulate the effects of septin 9. By contrast PtdIns(3,5)P2 promotes LD/lysosome co-localization. Overall, our data reveal a phosphoinositide/septin 9 dependent mechanism that regulates LD behavior through the control of their association with lysosome.

**Introduction**

The liver plays a crucial role in the homeostasis of lipids (Bechmann et al., 2012) and thus alterations of the processes involved in their metabolism due to stressful conditions, such as exposure to a high-fat diet, alcohol, or infection by pathogens such as hepatitis C virus, may induce an accumulation of lipid in the liver and the subsequent development of diseases that include steatosis, non-alcoholic steatohepatitis (NASH) which can progress in cirrhosis and cancer (Benedict and Zhang, 2017; Michelotti et al., 2013). Most of the lipids within the liver are stored in the hepatocytes in the form of cytosolic lipid droplets (LDs). LDs perform diverse cellular functions, which include sequestering the toxic lipids and acting as dynamic lipid storage that enables the rapid mobilization of fatty acids for energy (Herms et al., 2015; Rambold et al., 2015), membrane biosynthesis (Chauhan

et al., 2015; Kurat et al., 2009) and lipid signaling pathways (Haemmerle et al., 2011; Tang et al., 2013). LDs also associate with other organelles to maintain cell homeostasis (Barbosa and Siniossoglou, 2017; Barbosa et al., 2015; Schuldiner and Bohnert, 2017).

LDs consist of a hydrophobic core of neutral lipids (primarily composed of triacylglycerols and cholesterol esters) surrounded by a monolayer of phospholipid and cholesterol in which proteins are embedded. The lipid droplet proteins are dominated by enzymes involved in lipid metabolism and members of the perilipin family. However, proteins with other functions such as membrane trafficking, like small Rab-GTPases, and proteins for degradation are also well represented (Bersuker and Olzmann, 2017; Krahmer et al., 2013). There are about 70 human Rab GTPases, which are mostly involved in membrane trafficking and act as master regulators of organelle biogenesis and cellular homeostasis. The targeting of Rab to the membrane depends on the binding of their corresponding GEF (Guanosine Exchange factor) to specific phospholipids/phosphoinositides (PIs) (Blümer et al., 2013). Specific combinations of Rab GTPases and PIs in discrete membrane domains on the organelles and vesicles, facilitate endosomal functions to ensure the maintaining and coordination of membrane trafficking (Jean and Kiger, 2012). Therefore, identifying the regulators of the mechanisms behind this complex regulation of Rabs and PIs combination and function on organelles such as LDs and their contribution to cellular homeostasis is a challenging issue.

Septins belong to a family of GTP-binding proteins with 13 members and highly conserved in eukaryotes (Nishihama et al., 2011). Septins assemble in hetero-oligomeric complexes and form nonpolar filaments or rings that bind to actin and microtubules (MTs) (Kim et al., 2011; Kinoshita et al., 2002; Sellin et al., 2011). Septins are therefore essential for cytoskeleton-dependent cell processes and are considered as the fourth component of the cytoskeleton (Bai et al., 2013; Joo et al., 2007; Mostowy and Cossart, 2012; Smith et al., 2015 ). Septins associate with a variety of PIs at different intracellular membranes through a polybasic domain (PB1) (Akil et al., 2016; Dolat and Spiliotis, 2016; Pagliuso et al., 2016; Zhang et al., 1999). Recently, we reported that septin 9 has a second polybasic domain (PB2) conserved in the human septin family. This newly identified domain is critical to septin binding to PIs, filament formation, and the assembly and functionality of the Golgi apparatus (Omrane et al., 2019). Once attached to the membranes, septins can act as a scaffold that recruits cytosolic proteins and other cytoskeletal elements to control numerous cellular functions such as cytokinesis, ciliogenesis, vesicle trafficking, cell polarity (Akil et al., 2016; Bridges et al., 2016; Fung et al., 2014; Gassama-Diagne et al., 2006; Mostowy and Cossart, 2012; Song et al., 2016; Tanaka-Takiguchi et al., 2009). Therefore, alterations of the expression of septins are associated with several diseases including infectious diseases and cancer (Angelis and Spiliotis, 2016; Henzi et al., 2021; Krokowski et al., 2018).

We reported a high expression of septin 9 in hepatitis C virus (HCV)-induced cirrhosis. We

also showed that septin 9 is hijacked by HCV to induce the perinuclear accumulation of LDs by a phosphatidylinositol-5-phosphate and microtubule-dependent mechanism (Akil et al., 2016).

Excessive intracellular accumulation of LDs in liver cells generally results from increased uptake of hepatic free fatty acids (FFA), enhanced de novo lipogenesis, or impaired lipid catabolism (Bessone et al., 2019; Koo, 2013; Kwanten et al., 2014). The autophagy pathway plays an important role in lipid degradation and depends on the activities of the lysosome which dysfunction has been associated with steatosis in different studies (Inami et al., 2011; Miyagawa et al., 2016; Wang et al., 2018).

Lysosomes are highly dynamic organelles that are subject to bidirectional movements along microtubules between the center and periphery of cells and represent the main degradative compartments of eukaryotic cells (Cabukusta and Neefjes, 2018). Lysosomes movements are also modulated by contacts with other organelles such as the endoplasmic reticulum (ER) (Jongsma et al., 2016; Raiborg et al., 2015), trans-Golgi network (TGN) (Wang and Hong, 2002) and peroxisomes (Chu et al., 2015).

Thus, according to the binding capacities of septin 9 to PI and its critical role in the microtubule-dependent assembly of Golgi and vesicle trafficking, we made a hypothesis that septin 9 could control LD perinuclear accumulation by regulating the lysosomes. Our data validated this hypothesis.

**Results**

**Kinetic study of oleate-treated cells indicates that the size and perinuclear accumulation of LDs are related to lysosome localization and depend on oleate concentration**

To understand how hepatocytes could respond to lipid overload and the mechanisms behind the cytoplasmic LD accumulation, we used hepatocellular carcinoma derived Huh7 cells. The cells were treated with sodium oleate at 50,100, 200 and 400µM and analyzed after 12h, 24, 48, and 72h of treatment. First, we used BODIPY, to stain LDs and assess their total intensity and their time course distribution within cells. Immunofluorescence data revealed non-significant time-dependent changes of the LD behavior in non-treated (0µM) cells. However, at the different concentrations of oleate, the intensity of LDs significantly increased up to 24h after the treatment and then continued to decrease until 72h. However, while the increase of LD intensity increased in an oleate dose-dependent manner to reach the maximum at 24h, the decrease was inverse correlated to the dose of oleate and almost no change was observed in the kinetic for the dose of 400 µM of oleate (Fig 1A-B), (Table 1-2). Furthermore, we showed a correlation between the strong increase in the total intensity of LDs and their perinuclear localization (Fig 1C) (Table 3). Indeed, at 400µM of oleate, no significant change was observed over time for LDs distribution. In fact, nearly 83% of LDs consistently distributed in the perinuclear area (Fig 1C).

Lysosomes are broadly distributed throughout the cytoplasm, although a higher pool was found in the perinuclear region near the microtubule-organizing center (MTOC) and a very dynamic pool was at the periphery of the cells. These spatial different pools of lysosomes contribute to different biological roles (Cabukusta and Neefjes, 2018). Subsequently, we studied both the total intensity and the intracellular distribution of lysosomes by staining LAMP1 (Lysosomal-associated membrane protein 1). Surprisingly, no significant changes were observed on the total intensity of LAMP1 whatever the oleate concentration and the time after treatment (Fig 1D). Nevertheless, the increase of oleate concentration affected the intracellular distribution of LAMP1 which was mainly compact and formed a cluster in the perinuclear region. The maximum perinuclear distribution of LAMP1 was for the dose of 400 µM of oleate (Fig 1E) as observed for LDs (Fig 1C). Then we stained the cells using the red LysoTracker® probe which is a fluorescent probe for labeling and tracking acidic organelles in live cells such as lysosomes (Supplemental Fig. 1A). Data revealed a profile of LysoTracker® distribution in the cells similar to LAMP1 distribution. Thus, suggesting that the lysosomal components present in the cells and mainly those accumulated in the perinuclear area are still acidic.

Lysosomes accomplish their catabolic function through a wide range of enzymes including proteases, lipases, nucleases, and other hydrolytic enzymes that break down complex macromolecules (Perera and Zoncu, 2016; Settembre et al., 2013). Thus, to get further insights into the function of lysosomes in oleate treated cells, we analyzed by RT-PCR the mRNA expression of several lysosomal proteins at 24 and 72h after the treatment of the cells with 0, 100 and 400 µM of oleate. Surprisingly, we observed an increase of the transcripts of those genes after treatment compared to non-treated cells (Supplemental figure 2A), indicating that the accumulation of LDs and lysosome in the perinuclear region is not associated with a decrease in the expression of lysosomal enzymes but probably to the organelle clustering which could not be associated with LDs for their degradation. Indeed, we observed that when LAMP1 were clustered in the perinuclear area, which was observed in the cells treated with 100, 400µM oleate for 24h or 400µM for 72h, there is less interaction between LAMP1 and LD compared to the control cells and 100µM oleate treated for 72h whose LAMP1 displays disperse distribution (Supplemental figure 2B).

**Septin 9 regulates oleate induced lysosome perinuclear clustering**

In line with our results described above, and given our previous report on the role of septin 9 in HCV infection or oleate treatment-induced LD perinuclear accumulation (Akil et al., 2016), we hypothesized that septin 9 might control the dynamic of LDs in our kinetic studies through changes in lysosome distribution. To validate that, Huh7 cells were transfected with cDNA of either the isoform 1 of septin 9 (septin 9_i1) or with the empty vector (EV) as a control and treated with 100µM

of oleate. In EV transfected cells, the LD intensity and the perinuclear distribution increased until 24h and then decreased up to 72h after the treatment (Fig 2B-C) as shown in Fig1A. However, expression of septin 9_i1 in those cells blocked the decrease of LDs and accumulated them in the perinuclear region and sustain the perinuclear cluster of LAMP1 (Fig 2B-C). Subsequently, knockdown of septin 9 with septin 9 siRNA before treatment with 100µM oleate for 24h significantly decreased the intensity of cellular LDs and the clustering of lysosome in the perinuclear region and the latter was dispersed throughout the cytoplasm (Fig 2D-F). This effect of septin 9 knockdown were also confirmed in cell treated with 400µM oleate (Supplemental figure 3). We, therefore, concluded that septin 9 regulated oleate-induced lysosome clustering in the perinuclear area.

**Septin 9 and MTs regulate oleate induced co-localization of perinuclear lysosomes with Golgi**

Several studies have shown that the cellular localization of lysosomes is regulated by the Golgi (Tapia et al., 2019; Wang and Hong, 2002). For example, the activation of KDELR, which has been described as the Golgi-localized G protein-coupled receptor (GPCR) which regulates Golgi homeostasis, induces lysosome redistribution in the perinuclear area (Tapia et al., 2019). Besides, we reported that septin 9 co-localizes with Golgi, while depletion of septin 9 promotes Golgi fragmentation, thus impairing Golgi-dependent secretion (Omrane et al., 2019). Accordingly, we co-stained the cells treated with 100µM of oleate with LAMP1 and the trans-Golgi network marker (TGN46). As expected, after oleate treatment, the perinuclear lysosome co-localized with TGN46 at 12h and 24h whereas the LAMP1 signal re-localized to the peripheral area of the cells from 48 to 72h and its co-localization with Golgi decreased (Fig. 3A-B). Interestingly, knocked down of septin 9 using siRNA markedly decreased LAMP1 perinuclear signal and its co-localization with Golgi which was also dispersed in the cytoplasm as previously reported (Omrane et al., 2019) (Fig 3C-D). By opposite, overexpression of septin 9_i1 significantly increased the colocalization of LAMP1 with Golgi at 72h of 100µM treatment (Supplemental Fig 4). Taken together, these data revealed that oleate induced the septin 9-dependent perinuclear clustering of lysosomes which colocalized with the Golgi. Because lysosome trafficking is heavily reliant on MTs, nocodazole treatment was performed to assess whether lysosome to Golgi clustering at 24h post-treatment was reliant on MTs. Interestingly, nocodazole treatment disrupted the perinuclear clustering and the co-localization of both lysosomes and Golgi (Fig 3E-F). Thus, indicating that oleate induced LAMP1 perinuclear clustering and its co-localization with the Golgi is dependent on MTs.

**Oleate induces MT polymerization at MTOC**

Subsequently, we sought to determine the potential effect of oleate treatment on MTs by

staining the β-tubulin. The data indicated that oleate enhance MT network around the MTOC (Supplemental figure 5A), suggesting that LD accumulation may have a positive effect on MT polymerization. We subsequently examined the effect of LDs on tubulin polymerization *in vitro* using Paclitaxel and nocodazole treatments as positive and negative controls respectively. Immunoblots for soluble (S) and polymerized (P) tubulin fractions showed that oleate treatment promoted a dose-dependent polymerization of MTs compared to control cells (Supplemental figure 5B), which were consistent with the observation of tubulin staining (Supplemental figure 5A).

Next, by co-staining septin 9 and β-tubulin at 24 and 72h after the treatment of the cells with 0, 100 and 400 μM of oleate (Fig 4A), we observed that the MTs are both enhanced in cells treated with 100,400μM oleate for 24h, while, after 72h treatment, the MT enhancement decrease in 100μM oleate treated cell compared to 24h, But not in the 400μM (Fig 4B). In the meantime, we observed that the endogenous septin 9 are increased in the perinuclear area and colocalize with the enhanced MT (Fig 4B). Furthermore, by co-staining LAMP1 and β-tubulin, we found that the perinuclear cluster of LAMP1 associated with the MT network enhancement around the MTOC (Supplemental Figure 5C). Interestingly the treatment of cells with the siRNA of septin 9 impaired the MTOC accumulation of MT (Fig 4C-D). Thus, these data revealed that LD accumulation enhanced MT stabilization that involved septin 9.

**Septin 9 regulates Rab7 intracellular distribution and its association with LDs**

In line with our results described above, we wondered if septin 9 association with LDs might also change over time. Subsequently, we stained endogenous septin 9 and LDs under conditions similar to that described to analyze MT in Fig 4. As shown in Fig 5A-B, in the cells treated with 100 or 400μM oleate, septin 9 was found around the LDs at 24h for both conditions. Interestingly, at 72h, the LD size decreased as well as their association with septin 9 in cells treated with 100μM oleate. Whereas septin 9 was still present around the large LDs in cells treated with 400μM oleate (Fig 5B).

Rab7 is an important regulator of lysosome biogenesis (Bucci et al., 2000). It has been reported that when placed under nutrient deprivation, Rab7 is markedly recruited to LDs and is required to promote direct physical interactions between lysosomes and LDs which is essential for the subsequent utilization of LDs (Schroeder et al., 2015). Therefore, to further determine how septin 9 controlled the fate of LDs and lysosomes in oleate treated cells we studied Rab7. For that, Huh7 cells were transfected with the construct of GFP-Rab7 and treated with oleate. First, we validated the association of Rab7 with lysosome staining with LAMP1. In the control cells, both LAMP1 and GFP-Rab7 were co-distributed throughout the cytoplasm and treatment with oleate induced the colocalization and clustering of both proteins in the perinuclear area (Supplemental Fig 6). Next, we treated the cells expressing GFP-Rab7 with 100μM and 400μM oleate for 24h and 72h and we

analyzed the GFP-Rab7 and LDs (Fig 6A-B). In control cells, the GFP-Rab7 was consistently dispersed distribute within the cytoplasm and low levels of Rab7 could be resolved surrounding the LDs surfaces. When treated with either 100µM or 400µM oleate for 24h, Rab7 was clustered in the perinuclear region and surrounded by large LDs. However, after 72h treatment, in cells treated with 100µM oleate, Rab7 signal was dispersed in the cytoplasm and appeared clearly around the LDs, whereas both LDs and Rab7 remained clustered in the perinuclear region when cells are treated with 400µM oleate (Fig. 6A-B), consistent with data obtained with LAMP1 staining (Fig1). Strikingly, knock down of septin 9 in the cell treated with 400µM oleate at 72h re-localized Rab7 on LDs (Fig 6C). Those results were also validated for endogenous Rab7 (Supplemental figure 7). We also showed a co-localization of the perinuclear Rab7 cluster with Golgi and treatment with siRNA of septin 9 disrupt the colocalization (Supplemental Fig 8A-B).

Since the utilization of LDs by Rab7 were related to the autophagy process, we also checked the autophagy markers, like P62 and LC3B, in the same condition (Supplemental figure 8). As expected, there are more P62/LC3B puncta formed in cells treated with 100µM oleate for 72h or septin 9 knock down cells compared to control cells or LD accumulated cells (Supplemental figure 9).

Together, these data strongly suggested that a high dose of oleate promoted the accumulation of LDs by inducing the clustering of lysosomes, thus, impairing the association of lysosomes with LDs for their degradation. These data also highlighted a difference between Rab7 and septin 9 association with LDs. While septin 9 was found around the large and perinuclear LDs, Rab7 was found associated with dispersed and smaller LDs. Thus, strongly suggested that septin 9 inhibit Rab7 associated LD degradation by promoting Rab7 perinuclear cluster and by binding to LDs.

**PtdIns(3,5)P2 and PtdIns(5)P regulate Rab7 and septin 9 association with LDs respectively**

We reported that different PIs have distinct effects on the LD size and their interaction with endogenous septin 9 and particularly PtdIns5P had the highest effects (Akil et al., 2016). To note, Rab7 is associated with lysosome, which membrane is enriched in PtdIns(3,5)P2. Therefore, we hypothesized that the presence of distinct PIs might regulate Rab7 distribution and its interaction with LDs. To explore this, we treated the cells which expressed GFP-Rab7 with PtdIns(5)P and PtdIns(3,5)P2. Consistent with our primary results, we observed a strong increase of LDs and a perinuclear clustering of Rab7 within the cells treated with PtdIns(5)P compared to non-treated (NT) cells. Interestingly, treatment of cells with PtdIns(3,5)P2 slightly decreased LD size and Rab7 was seen around the LDs (Fig. 7A-B). The effects of PtdIns(5)P and PtdIns(3,5)P2 on Rab7/LDs interaction was also validated in the cells pretreated with oleate (Fig. 7A-B). In addition, the effect of PtdIns(3,5)P2 on septin 9 and LD association were also checked for endogenous septin 9 and septin

9_i1 overexpression. Consistent with our primary results, adding of PtdIns(5)P promotes septin 9 interact with LD in perinuclear area and promotes septin 9 filament formation surrounding LD at least in septin 9_i1 overexpression cells. While, adding PtdIns(3,5)P2 ,decrease LD and septin 9 on LD surface (Supplemental figure 10). The effect of PIs on MT were also analyzed, the data showed that the MTs are enhanced in cells treated with PtdIns(5)P, but not in the PtdIns(3,5)P2 treated cells (Supplemental figure 11). In the meantime, endogenous septin 9 are increased in the perinuclear area and colocalize with the enhanced MT (Supplemental figure 11). To further confirm these data, we also performed experiments using MTMR3 (Myotubularin Related Protein 3) which is a phosphatase that converts the endogenous PtdIns(3,5)P2 into endogenous PtdIns(5)P. As expected, overexpression of MTMR3 increased PtdIns(5)P, LDs and promoted LAMP1, Rab7 perinuclear clustering and promoted the septin 9 increasing in perinuclear area and MT enhancement (Fig. 8A-B).

In addition, in our primary works, we showed that septin 9 bind PIs via the polybasic domains (PBs). Thus, we further analysis if those PtdIns(5)P binding domains are important for septin 9 induced-lysosome distribution change. Therefore, we transfected cells with septin 9_i1 and septin 9 PBs-deleted mutant (septin 9_ΔΔ). Expression of septin 9_i1 promoted Rab7 and LAMP1 in the perinuclear area compared to empty vector cells (Supplemental figure12A-D). In contrast, septin 9_ΔΔ expression nearly have no effect on Rab7 and LAMP1 distribution compared to empty vector (Supplemental figure12A-D). Together, these results indicated that the presence of specific PI and the septin 9 PIs binding domains are important for the intracellular distribution of LDs and their interaction with lysosomes for their degradation.

**Discussion**

The lipids stored in LDs within cells are controlled by two major metabolic pathways that involved the synthesis of lipids to increase the lipid content of LDs and the catabolism pathway that results in a reduction in the lipid content through β-oxidation, lipolysis by lipases and lipophagy. The latter is dependent on lysosomes and the export of lipids via secretory pathways (Ballabio and Bonifacino, 2019; Olzmann and Carvalho, 2019). We had already provided evidence regarding the role of septin 9 in the growth and perinuclear accumulation of LDs (Akil et al., 2016). In the present study, we showed that septin 9 impaired LD catabolism and particularly we demonstrated that septin 9 regulated the intracellular localization of lysosomes and the interaction of lysosomal protein Rab7 and LDs. We also showed that there is a shift between septin 9 or Rab7 localization with LD, their specific localization on LDs is controlled by PIs and then influenced the LD behaviors (Fig 8).

The perinuclear clustering and growth of LDs often occur simultaneously. For example, in adipocytes, LDs arise from the peripheral lamellipodia and grow as they move towards the cell center (Nagayama et al., 2007). Conversely, when lipolysis is chronically stimulated in adipocytes, their

large perinuclear LDs fragment into small droplets dispersed throughout the cell (Marcinkiewicz et al., 2006). The dispersed to clustered redistribution of LDs may also result from infection by diverse intracellular pathogens (Cocchiaro et al., 2008; Toledo et al., 2016) such as hepatitis C virus (HCV) (Akil et al., 2016). Furthermore, it has been reported that these changes in the cellular distribution of LDs also contribute to their interaction with other organelles including the endoplasmic reticulum, mitochondria, peroxisomes, and autophagic lysosomes (Herms et al., 2015; Jin et al., 2021). A recent study demonstrated that interfering with the perinuclear accumulation of lysosomes can impair LD turnover (Tapia et al., 2019). Although our results revealed that when we increased oleate concentration or overexpressed septin 9, in such conditions, both LDs and lysosomes were clustered in the perinuclear region, where they appeared to occupy distinct regions. The clustered lysosomes were co-localized with the Golgi apparatus, which occupied the core region, while the LDs seem to be tightly packed around this core region (Figure 1 and 4). The Rab7 protein, which is a lysosomal component also found in LDs plays an important role in initiating lysosome-dependent lipophagy. We observed that Rab7 was also clustered in the core region with Golgi and then the contact between Rab7 and LDs was reduced. Therefore, we could speculate that the interaction of Rab7 with LDs for their degradation is impaired. In addition, a high level of septin 9 was found associated with the large clusters of LDs surrounding the core region formed with lysosomal proteins and Golgi. Conversely, when the LD and lysosome behaved more dispersed distributed in the cytoplasm, which has been observed under the condition such as 72h after treatment of cells knockdown of septin 9, we observed more interaction between Rab7 and LDs (Figure 6) which could further enhance the contact between lysosome and LD thus permitted LD degradation. Interestingly, a recent study showed that in the liver, the process involved in LD degradation is dependent on LD size, and indeed, large LDs were not preferentially degraded through lysosomes and remained the targets of cytoplasmic lipases (Schott et al., 2019). Thus, in line with our data, we could speculate that large perinuclear clustered LDs, which have more association with septin 9, have less chance to contacts lysosomes and therefore could not be degraded via the lipophagy pathway.

We also demonstrated that MTs played a crucial role in lysosome perinuclear clustering and its association with Golgi (Figure 4). Further, we showed that perinuclear LDs are surrounded by organized MT filaments and MT polymerization enhanced particularly in the MTOC where LAMP is clustered (Figure 5). The strong MT network might form a barrier to block contacts between LDs and lysosomes and thus impaired LD degradation and promote their perinuclear growth. Septin 9 control MTs and therefore, an increase of septin 9 could also contribute to lysosome clustering by affecting the MTs dynamics as reported recently (Kesisova et al., 2020). Furthermore, the composition of the monolayer of phospholipid surrounding the core of LDs plays an important role in the regulation of the interaction of LDs with proteins or other organelles (Thiam and Dugail, 2019).

Indeed, we have shown that PtdIns5P was able to promote the interaction between LD and septin 9 (Akil et al., 2016). Here our results revealed that the addition of PtdIns5P on Huh7 cells promoted the perinuclear clustering of Rab7 and reduced the Rab7/LD interaction. On the contrary, PtdIns(3,5)P2 which is enriched in lysosomes promoted the dispersion of LDs through the cytoplasm and increased their interaction with Rab7. In addition, MTMR3 which converts PtdIns(3,5)P2 to PtdIns5P recapitulates the effects of PtdIns5P on both LD and lysosomes perinuclear distribution. These data strongly highlighted the critical role of PI metabolism in the regulation of LD behavior and septin 9 functions.

LDs are dynamic organelles that are essential for cell homeostasis and participate in processes that maintain cell structure and energy homeostasis. To perform their functions, the interactions of LDs with multiple organelles such as the endoplasmic reticulum, Golgi, mitochondria, peroxisomes, and lysosomes are required. Therefore, to fully understand the biological function of LDs and their alterations during the pathogenesis of LD-associated diseases, their impacts on other organelles needed detailed analysis. Our results have uncovered the role of septin 9 and PIs in LDs behavior and their interaction with lysosomes. To conclude, we have identified molecular machinery that links lipid metabolism to organelle homeostasis. Indeed, understanding how LDs, lysosomes are coordinated both spatially and temporally might help in gaining a clearer understanding of the pathogenesis of LD-associated diseases such as steatosis, cirrhosis or even cancer.

**Materials and methods**

**Chemicals** Sodium oleate Cat#o-7501 purchased from Sigma-Aldrich. Albumin BSA FFA Cat#126575 was from Calbiochem. Nocodazole Cat#487928 from Calbiochem.

**Cell line and culture conditions** Human haptocarcinoma cells Huh7 was used. Cells were maintained in Dulbecco's modified Eagle's medium (DMEM; Invitrogen) containing 1g/L glucose and supplemented with 10% heat-inactivated fetal bovine serum, 1% nonessential amino acids (GibcoBRL) and 1% penicillin/streptomycin (GibcoBRL). Cells were tested for mycoplasma contamination weekly.

**Cell treatments** Cell treatment with oleate: complexes of sodium oleate with BSA were prepared as previously reported. Briefly, the solution containing 20 mM sodium oleate and 2.4 mM bovine serum albumin-fatty acid free (BSA FFA) was heated to 55 °C. The obtained complex was diluted in a pre-warmed culture medium at indicated concentration before addition to the cells. The treated cells were maintained in culture and collected either for immunoblot or immunofluorescence experiments depends on the treated time.

Cells treatment with PIs: PIs as a lyophilized powder were solubilized at 500 mM in water by vortex. The solution was then diluted in Dulbecco's phosphate-buffered saline (DPBS) to the concentration indicated in the legends of the experiment. Cells were washed with DPBS and the PIs solution was added to the cell for indicated time.

**Reverse transcription and real-time PCR analysis** Total RNA was isolated using RNeasy Mini Kit 50 (Cat# 74104 QIAGEN) and applied to reverse transcription using RevertAid First Strand cDNA Synthesis Kit (Cat#K1612 Thermo Scientific). The cDNA was analyzed by qPCR using QuantiTect SYBR Green PCR Kit (Cat#204143 QIAGEN) and a Light Cycler 480 Real-Time PCR System (Roche). Reaction parameters were Preincubation 10 min at 95 °C, followed by 45 cycles of 15 s at 95 °C, 30 s at 55 °C and 15 s at 72 °C. The triplicate mean values were calculated using GAPDH gene transcription as reference for normalization. Used RT–PCR primers sequences are presented in the Table 4.

**siRNA, plasmids and transfection reagents**. siRNAs from septin 9 were a Stealth RNAi siRNA (si1: Cat#SEPT9HSS173895, si2: Cat# SEPT9HSS173896 and si3: Cat# SEPT9HSS173897) from Invitrogen and non-targeting siRNA (Cat#sc-37007) was from Santa Cruz. The sequences targeting septin 9 are presented in the Table 5.

The cDNA of septin 9 isoform 1 transcript within pcDNA3.1/V5-His-TOPO vector (cDNA septin 9_i1) was a gift from Dr Russell (CCRCB, Queens University Belfast). The GFP-Rab7 cDNA plasmid was a gift from Dr Goud (Institut Curie, PSL Research University, CNRS UMR 144, Paris, France) The transfection of cDNA and siRNA were performed using X-tremeGENE 9 DNA Transfection Reagent (Roche Diagnostics) following the manufacturer's protocol. The transfection

was performed for 24 h unless indicated otherwise in the text.

**Primary antibodies**. Anti LAMP1 Cat#ab25630 (WB:1/500, IF:1/25), anti septin 9 Cat#ab38314 (WB:1/500, IF:1/25), anti α tubulin Cat#ab15246 (WB:1/1,000, IF:1/100), mouse and rabbit anti-V5 tag Cat#ab27671 (WB:1/1,000, IF:1/400), Cat#ab9116 (WB:1/1,000, IF:1/400) respectively and anti PLIN2 Cat#ab52355 (WB:1/2,000, IF:1/100) were from abcam; anti β tubulin Cat# T5201 (WB:1/1,000, IF:1/100), anti TGN46 Cat# NBP1-49643(IF:1/100) from Novus Biologicals; anti GM130 Cat# 610822 (IF: 1/100) from BD Biosciences; anti-Actin Cat#sc-1616 (WB:1/1,000) and anti-PLIN2 Cat#sc-32450 (WB:1/250, IF:1/25) from Santa Cruz Biotechnology.

**Secondary antibodies and dyes**. Anti mouse IgG-HRP and anti rabbit IgG-HRP form GE healthcare (WB:1/1,000). Anti-goat IgG-HRP Cat#sc-2020 (WB:1/1,000) from Santa Cruz. Alexa Fluor 546 Cat#A11003, A11010 and A10040 (IF:1/100), Alexa Fluor 488 Cat#A11001, A21206 and A21202 (IF:1/100), acidic vesicles were stained with LysoTracker Red DND-99 Cat# L7528, lipid droplet were stained with BODIPY 493/503 or BODIPY 576/589 (ThermoFisher) and nuclei with Hoechst Cat#H21486 (IF:1/5,000), both are from Invitrogen.

**Immunofluorescence**. Cells were grown on coverslips, fixed with paraformaldehyde 4% for 20 min and permeabilized for 30 min at 37 °C using the permeabilizing buffer (PFS): DPBS containing saponin (Cat#10294440 Fisher scientific) 0.025% m.v-1, gelatin from cold water fish skin (Cat#G7041 Sigma 0.7% m.v-1). Then cells were incubated with primary antibody for 2 h washed three times for 5min with PFS and incubated with the appropriate secondary antibodies or with the dye for 90 min. The coverslips were mounted using Prolong Gold (Cat#P36934 Invitrogen). For Lysotracker staining, the cells on coverslips were treated, then, cells were cultured in the same medium contains 75 nM Lysotracker for 1h, after incubation, cells were fixed and performed as described above.

**Immunoblot** Cells were washed with ice-cold DPBS and lysed on ice using the following buffer: 20mM Tris, HCl, 100mM NaCl, 1% Triton X-100 at PH 7.4 containing protease inhibitors (cOmplete ULTRA Cat#05892970001 Roche). The proteins were separated on SDS–PAGE and electro-transferred onto nitrocellulose membrane. After transfer, the membrane was saturated in DPBS containing 0.1% Tween 20 and 5% milk. Primary antibodies were added overnight at 4 C or for 2 h at room temperature depending on the antibody. The membranes were washed with DPBS and incubated for 1 h at room temperature with appropriate secondary antibody coupled with peroxidase. ECL plus kit (Cat#32132 Thermo Scientific) was used for protein detection. Chemiluminescent signal was detected by G:BOX Chemi Fluorescent & Chemiluminescent Imaging System from SYNGENE. Blot quantification was done using ImageJ software.

**Tubulin polymerization assay**. Fraction of soluble and polymerized tubulin were performed as described before. Briefly, soluble tubulin extraction buffer A (1mM MgCl2, 2 mM EGTA, 0.5%

NP40, 2 mM PMSF, 20 mM Tris-HCl[pH=6.8], protease inhibitor cocktail) was added to cells at 4°C for 5 min, plates were gently swirled two to three times, and buffer was removed and saved as soluble fraction. Immediately after, polymerized tubulin extraction buffer B (A + 1% SDS) was added for 2 min, cells were scraped, and the polymerized fraction was sonicated briefly and incubated on ice for 30 min. Soluble and polymerized fractions were loaded on a gel and transferred to nitrocellulose membranes to probe with specific antibody as indicated. Cells treated with nocodazole or Taxol alone served as control for efficient extraction of soluble and polymerized tubulin. ImageJ was used to quantify the intensity of beta-tubulin bands from each blot. Further, the percentage of polymerized tubulin was determined by dividing the densitometry value of polymerized tubulin by the total tubulin content (the sum of the densitometry values of soluble and polymerized tubulin).

**Images acquisition and analysis**. Images were acquired with a Leica TCS SP5 AOBS tandem confocal microscope. For colocalization analysis, images were treated by ImageJ software, the plugin 'Intensity Correlation Analysis' was used to generate the Pearson's correlation coefficient (Rr) which range from -1 (perfect exclusion) to +1 (perfect correlation).

To calculate the total intensity of LAMP1 and LDs, images obtained by confocal microscopy were processed cell ROI by free hand selection tool according to thresholding image, then total intensity of LAMP1 and LDs were measured by ImageJ analyses. The line plot for LAMP1 and Bodipy was generated by ImageJ software function 'Plot profile'.

To determine LAMP1, LDs and Rab7 distribution in cells, the plugin 'Radial profile Angle' was used. For analysis, the individual cell total area was generated by free hand selection tool according the thresholding image, then a circle which center is located in the center of the cell nucleus was defined at the periphery of each cell. Then, the plugin produces a profile plot of normalized integrated intensities around concentric circles as a function of distance from a point in the image, where considered as the center of the cell. The concentric circles were assembled in three circle bands, the first corresponding to the area of the nuclei and the rest corresponding to the cytoplasm was divided in two equal bands (the band near the nuclei is considered as the 'perinuclear' and the other the 'periphery'. The intensity in each band was calculated from the total integrated intensities around concentric circles present in the band. A diagram of this analysis was present in Supplemental Fig 14A.

To measure the mean intensity of Rab7 or septin 9 associated with LD, the Fiji function 'Analyze particles' were performed on the LDs image to obtain the areas occupied by LDs and marked as area1, then enlarge those areas by 0.5µm, and marked this new area as area 2. Apply those two areas on the target signal image and analyze the total area value and intensity of the target signal. Then calculate. A diagram of this analysis was present in Supplemental Fig 14B.

**Statistical analyses**. Unpaired Student's t-tests were used, and statistical significance was

determined at *P<0.05; **P<0.001, ***P<0.0001.

**Acknowledgements**

We thank B,Goud and S.Miserey-Lenkei (CNRS U144,institute Curie, Paris) for advices on intracellular trafficking and providing the reagents. We thank L.Amazit from the imagery services at Paul Brousse hospital, Villejuif).

**Author contributions**

PX.S contributed to design and performed most of the experiments, analyzed the data and wrote the manuscript. J.P. and M.O. analyzed and discussed the data. D.S discussed data. A.G-D. conceived and supervised the project, designed experiments, and wrote the manuscript.

**Competing interests**

The authors declare that they have no conflict of interest.

**Funding**

PX,S was supported by a scholarship from Chinese Scholarship Council. This work was supported by INSERM and University Paris Saclay.

**References**

Akil, A., Peng, J., Omrane, M., Gondeau, C., Desterke, C., Marin, M., Tronchère, H., Taveneau, C., Sar, S., Briolotti, P., et al. (2016). Septin 9 induces lipid droplets growth by a phosphatidylinositol-5-phosphate and microtubule-dependent mechanism hijacked by HCV. *Nat Commun* 7,.

Angelis, D. and Spiliotis, E. T. (2016). Septin Mutations in Human Cancers. *Front Cell Dev Biol* 4, 122.

Bai, X., Bowen, J. R., Knox, T. K., Zhou, K., Pendziwiat, M., Kuhlenbäumer, G., Sindelar, C. V. and Spiliotis, E. T. (2013). Novel septin 9 repeat motifs altered in neuralgic amyotrophy bind and bundle microtubules. *J Cell Biol* 203, 895–905.

Ballabio, A. and Bonifacino, J. S. (2019). Lysosomes as dynamic regulators of cell and organismal homeostasis. *Nat Rev Mol Cell Biol* 1–18.

Barbosa, A. D. and Siniossoglou, S. (2017). Function of lipid droplet-organelle interactions in lipid homeostasis. *Biochimica et Biophysica Acta (BBA) - Molecular Cell Research* 1864, 1459–1468.

Barbosa, A. D., Savage, D. B. and Siniossoglou, S. (2015). Lipid droplet-organelle interactions: emerging roles in lipid metabolism. *Curr. Opin. Cell Biol.* 35, 91–97.

Bechmann, L. P., Hannivoort, R. A., Gerken, G., Hotamisligil, G. S., Trauner, M. and Canbay, A. (2012). The interaction of hepatic lipid and glucose metabolism in liver diseases. *J. Hepatol.* 56, 952–964.

Benedict, M. and Zhang, X. (2017). Non-alcoholic fatty liver disease: An expanded review. *World J Hepatol* 9, 715–732.

Bersuker, K. and Olzmann, J. A. (2017). Establishing the lipid droplet proteome: Mechanisms of

lipid droplet protein targeting and degradation. *Biochim Biophys Acta* 1862, 1166–1177.

Bessone, F., Razori, M. V. and Roma, M. G. (2019). Molecular pathways of nonalcoholic fatty liver disease development and progression. *Cell. Mol. Life Sci.* 76, 99–128.

Blümer, J., Rey, J., Dehmelt, L., Mazel, T., Wu, Y.-W., Bastiaens, P., Goody, R. S. and Itzen, A. (2013). RabGEFs are a major determinant for specific Rab membrane targeting. *J Cell Biol* 200, 287–300.

Bridges, A. A., Jentzsch, M. S., Oakes, P. W., Occhipinti, P. and Gladfelter, A. S. (2016). Micron-scale plasma membrane curvature is recognized by the septin cytoskeleton. *J Cell Biol* 213, 23–32.

Bucci, C., Thomsen, P., Nicoziani, P., McCarthy, J. and van Deurs, B. (2000). Rab7: A Key to Lysosome Biogenesis. *Mol Biol Cell* 11, 467–480.

Cabukusta, B. and Neefjes, J. (2018). Mechanisms of lysosomal positioning and movement. *Traffic*.

Chauhan, N., Visram, M., Cristobal-Sarramian, A., Sarkleti, F. and Kohlwein, S. D. (2015). Morphogenesis checkpoint kinase Swe1 is the executor of lipolysis-dependent cell-cycle progression. *Proc. Natl. Acad. Sci. U.S.A.* 112, E1077-1085.

Chu, B.-B., Liao, Y.-C., Qi, W., Xie, C., Du, X., Wang, J., Yang, H., Miao, H.-H., Li, B.-L. and Song, B.-L. (2015). Cholesterol transport through lysosome-peroxisome membrane contacts. *Cell* 161, 291–306.

Cocchiaro, J. L., Kumar, Y., Fischer, E. R., Hackstadt, T. and Valdivia, R. H. (2008). Cytoplasmic lipid droplets are translocated into the lumen of the Chlamydia trachomatis parasitophorous vacuole. *Proceedings of the National Academy of Sciences* 105, 9379–9384.

Dolat, L. and Spiliotis, E. T. (2016). Septins promote macropinosome maturation and traffic to the lysosome by facilitating membrane fusion. *J. Cell Biol.* 214, 517–527.

Fung, K. Y. Y., Dai, L. and Trimble, W. S. (2014). Chapter Seven - Cell and Molecular Biology of Septins. In *International Review of Cell and Molecular Biology* (ed. Jeon, K. W.), pp. 289–339. Academic Press.

Gassama-Diagne, A., Yu, W., Beest, M. ter, Martin-Belmonte, F., Kierbel, A., Engel, J. and Mostov, K. (2006). Phosphatidylinositol-3,4,5-trisphosphate regulates the formation of the basolateral plasma membrane in epithelial cells. *Nat Cell Biol* 8, 963–970.

Haemmerle, G., Moustafa, T., Woelkart, G., Büttner, S., Schmidt, A., van de Weijer, T., Hesselink, M., Jaeger, D., Kienesberger, P. C., Zierler, K., et al. (2011). ATGL-mediated fat catabolism regulates cardiac mitochondrial function via PPAR-α and PGC-1. *Nat. Med.* 17, 1076–1085.

Henzi, T., Lannes, N. and Filgueira, L. (2021). Septins in Infections: Focus on Viruses. *Pathogens* 10,.

Herms, A., Bosch, M., Reddy, B. J. N., Schieber, N. L., Fajardo, A., Rupérez, C., Fernández-Vidal, A., Ferguson, C., Rentero, C., Tebar, F., et al. (2015). AMPK activation promotes lipid droplet dispersion on detyrosinated microtubules to increase mitochondrial fatty acid oxidation. *Nature Communications* 6, 1–14.

Inami, Y., Yamashina, S., Izumi, K., Ueno, T., Tanida, I., Ikejima, K. and Watanabe, S. (2011). Hepatic steatosis inhibits autophagic proteolysis via impairment of autophagosomal acidification

and cathepsin expression. *Biochemical and Biophysical Research Communications* 412, 618–625.

Jean, S. and Kiger, A. A. (2012). Coordination between RAB GTPase and phosphoinositide regulation and functions. *Nat Rev Mol Cell Biol* 13, 463–470.

Jin, Y., Ren, Z., Tan, Y., Zhao, P. and Wu, J. (2021). Motility Plays an Important Role in the Lifetime of Mammalian Lipid Droplets. *Int J Mol Sci* 22,.

Jongsma, M. L. M., Berlin, I., Wijdeven, R. H. M., Janssen, L., Janssen, G. M. C., Garstka, M. A., Janssen, H., Mensink, M., van Veelen, P. A., Spaapen, R. M., et al. (2016). An ER-Associated Pathway Defines Endosomal Architecture for Controlled Cargo Transport. *Cell* 166, 152–166.

Joo, E., Surka, M. C. and Trimble, W. S. (2007). Mammalian SEPT2 Is Required for Scaffolding Nonmuscle Myosin II and Its Kinases. *Developmental Cell* 13, 677–690.

Kesisova, I. A., Robinson, B. P. and Spiliotis, E. T. (2020). A septin GTPase scaffold of dynein-dynactin motors triggers retrograde lysosome transport. *bioRxiv* 2020.06.01.128488.

Kim, M. S., Froese, C. D., Estey, M. P. and Trimble, W. S. (2011). SEPT9 occupies the terminal positions in septin octamers and mediates polymerization-dependent functions in abscission. *J Cell Biol* 195, 815–826.

Kinoshita, M., Field, C. M., Coughlin, M. L., Straight, A. F. and Mitchison, T. J. (2002). Self- and Actin-Templated Assembly of Mammalian Septins. *Developmental Cell* 3, 791–802.

Koo, S.-H. (2013). Nonalcoholic fatty liver disease: molecular mechanisms for the hepatic steatosis. *Clin Mol Hepatol* 19, 210–215.

Krahmer, N., Hilger, M., Kory, N., Wilfling, F., Stoehr, G., Mann, M., Farese, R. V. and Walther, T. C. (2013). Protein correlation profiles identify lipid droplet proteins with high confidence. *Mol. Cell Proteomics* 12, 1115–1126.

Krokowski, S., Lobato-Márquez, D., Chastanet, A., Pereira, P. M., Angelis, D., Galea, D., Larrouy-Maumus, G., Henriques, R., Spiliotis, E. T., Carballido-López, R., et al. (2018). Septins Recognize and Entrap Dividing Bacterial Cells for Delivery to Lysosomes. *Cell Host & Microbe* 24, 866-874.e4.

Kurat, C. F., Wolinski, H., Petschnigg, J., Kaluarachchi, S., Andrews, B., Natter, K. and Kohlwein, S. D. (2009). Cdk1/Cdc28-dependent activation of the major triacylglycerol lipase Tgl4 in yeast links lipolysis to cell-cycle progression. *Mol. Cell* 33, 53–63.

Kwanten, W. J., Martinet, W., Michielsen, P. P. and Francque, S. M. (2014). Role of autophagy in the pathophysiology of nonalcoholic fatty liver disease: a controversial issue. *World J. Gastroenterol.* 20, 7325–7338.

Marcinkiewicz, A., Gauthier, D., Garcia, A. and Brasaemle, D. L. (2006). The Phosphorylation of Serine 492 of Perilipin A Directs Lipid Droplet Fragmentation and Dispersion. *J. Biol. Chem.* 281, 11901–11909.

Mas, V. R., Maluf, D. G., Archer, K. J., Yanek, K., Kong, X., Kulik, L., Freise, C. E., Olthoff, K. M., Ghobrial, R. M., McIver, P., et al. (2009). Genes involved in viral carcinogenesis and tumor initiation in hepatitis C virus-induced hepatocellular carcinoma. *Mol Med* 15, 85–94.

Michelotti, G. A., Machado, M. V. and Diehl, A. M. (2013). NAFLD, NASH and liver cancer.

*Nature Reviews Gastroenterology & Hepatology* 10, 656–665.

Miyagawa, K., Oe, S., Honma, Y., Izumi, H., Baba, R. and Harada, M. (2016). Lipid-Induced Endoplasmic Reticulum Stress Impairs Selective Autophagy at the Step of Autophagosome-Lysosome Fusion in Hepatocytes. *The American Journal of Pathology* 186, 1861–1873.

Mostowy, S. and Cossart, P. (2012). Septins: the fourth component of the cytoskeleton. *Nature Reviews Molecular Cell Biology* 13, 183–194.

Nagayama, M., Uchida, T. and Gohara, K. (2007). Temporal and spatial variations of lipid droplets during adipocyte division and differentiation. *J. Lipid Res.* 48, 9–18.

Nishihama, R., Onishi, M. and Pringle, J. R. (2011). New insights into the phylogenetic distribution and evolutionary origins of the septins. *Biol. Chem.* 392, 681–687.

Olzmann, J. A. and Carvalho, P. (2019). Dynamics and functions of lipid droplets. *Nat Rev Mol Cell Biol* 20, 137–155.

Omrane, M., Camara, A. S., Taveneau, C., Benzoubir, N., Tubiana, T., Yu, J., Guérois, R., Samuel, D., Goud, B., Poüs, C., et al. (2019). Septin 9 has Two Polybasic Domains Critical to Septin Filament Assembly and Golgi Integrity. *iScience* 13, 138–153.

Pagliuso, A., Tham, T. N., Stevens, J. K., Lagache, T., Persson, R., Salles, A., Olivo-Marin, J.-C., Oddos, S., Spang, A., Cossart, P., et al. (2016). A role for septin 2 in Drp1-mediated mitochondrial fission. *EMBO reports* 17, 858–873.

Perera, R. M. and Zoncu, R. (2016). The Lysosome as a Regulatory Hub. *Annu. Rev. Cell Dev. Biol.* 32, 223–253.

Raiborg, C., Wenzel, E. M., Pedersen, N. M., Olsvik, H., Schink, K. O., Schultz, S. W., Vietri, M., Nisi, V., Bucci, C., Brech, A., et al. (2015). Repeated ER-endosome contacts promote endosome translocation and neurite outgrowth. *Nature* 520, 234–238.

Rambold, A. S., Cohen, S. and Lippincott-Schwartz, J. (2015). Fatty acid trafficking in starved cells: regulation by lipid droplet lipolysis, autophagy, and mitochondrial fusion dynamics. *Dev. Cell* 32, 678–692.

Schott, M. B., Weller, S. G., Schulze, R. J., Krueger, E. W., Drizyte-Miller, K., Casey, C. A. and McNiven, M. A. (2019). Lipid droplet size directs lipolysis and lipophagy catabolism in hepatocytes. *J Cell Biol* 218, 3320–3335.

Schroeder, B., Schulze, R. J., Weller, S. G., Sletten, A. C., Casey, C. A. and McNiven, M. A. (2015). The small GTPase Rab7 as a central regulator of hepatocellular lipophagy. *Hepatology* 61, 1896–1907.

Schuldiner, M. and Bohnert, M. (2017). A different kind of love - lipid droplet contact sites. *Biochim Biophys Acta Mol Cell Biol Lipids* 1862, 1188–1196.

Sellin, M. E., Sandblad, L., Stenmark, S. and Gullberg, M. (2011). Deciphering the rules governing assembly order of mammalian septin complexes. *MBoC* 22, 3152–3164.

Settembre, C., Fraldi, A., Medina, D. L. and Ballabio, A. (2013). Signals from the lysosome: a control centre for cellular clearance and energy metabolism. *Nat. Rev. Mol. Cell Biol.* 14, 283–296.

Smith, C., Dolat, L., Angelis, D., Forgacs, E., Spiliotis, E. T. and Galkin, V. E. (2015). Septin 9

Exhibits Polymorphic Binding to F-Actin and Inhibits Myosin and Cofilin Activity. *J. Mol. Biol.* 427, 3273–3284.

Song, K., Russo, G. and Krauss, M. (2016). Septins As Modulators of Endo-Lysosomal Membrane Traffic. *Front Cell Dev Biol* 4, 124.

Tanaka-Takiguchi, Y., Kinoshita, M. and Takiguchi, K. (2009). Septin-Mediated Uniform Bracing of Phospholipid Membranes. *Current Biology* 19, 140–145.

Tang, T., Abbott, M. J., Ahmadian, M., Lopes, A. B., Wang, Y. and Sul, H. S. (2013). Desnutrin/ATGL activates PPARδ to promote mitochondrial function for insulin secretion in islet β cells. *Cell Metab.* 18, 883–895.

Tapia, D., Jiménez, T., Zamora, C., Espinoza, J., Rizzo, R., González-Cárdenas, A., Fuentes, D., Hernández, S., Cavieres, V. A., Soza, A., et al. (2019). KDEL receptor regulates secretion by lysosome relocation- and autophagy-dependent modulation of lipid-droplet turnover. *Nature Communications* 10, 735.

Thiam, A. R. and Dugail, I. (2019). Lipid droplet–membrane contact sites – from protein binding to function. *J Cell Sci* 132,.

Toledo, D. A. M., D'Avila, H. and Melo, R. C. N. (2016). Host Lipid Bodies as Platforms for Intracellular Survival of Protozoan Parasites. *Front Immunol* 7,.

Wang, T. and Hong, W. (2002). Interorganellar Regulation of Lysosome Positioning by the Golgi Apparatus through Rab34 Interaction with Rab-interacting Lysosomal Protein. *Mol Biol Cell* 13, 4317–4332.

Wang, X., Zhang, X., Chu, E. S. H., Chen, X., Kang, W., Wu, F., To, K.-F., Wong, V. W. S., Chan, H. L. Y., Chan, M. T. V., et al. (2018). Defective lysosomal clearance of autophagosomes and its clinical implications in nonalcoholic steatohepatitis. *The FASEB Journal* 32, 37–51.

Zhang, J., Kong, C., Xie, H., McPherson, P. S., Grinstein, S. and Trimble, W. S. (1999). Phosphatidylinositol polyphosphate binding to the mammalian septin H5 is modulated by GTP. *Current Biology* 9, 1458–1467.

**Figure legends**

**Figure 1 The kinetic of LD and lysosome intracellular distributions are correlated and dependent of oleate concentration**

**A**. Huh7 cells were grown overnight. Then culture medium was supplemented without or with 50, 100, 200 and 400 μM sodium oleate complex for different time (12h, 24h, 48h, 72h), then stained for LDs(green) and LAMP1(red). Scale bar, 20μm.

**B**. LDs intensity were analyzed in 25 cells from three experiments performed as described in A.

**C**. The percentage of LD intensity in Perinuclear and Peripheric are present in 25 cells from three experiments performed as described in A.

**D**. LAMP1 intensity of 25 cells from 3 independent experiments performed as described in A.

**E**. The percentage of LAMP1 intensity in Perinuclear and Peripheric are present in 25 cells from three experiments performed as described in A.

Data information: Bar graphs present Mean ± SEM. Student's t-test was used. *P < 0.05, **P< 0.001, ***P<0.0001.

**Figure 2 Septin 9 regulates oleate induced lysosome perinuclear clustering**

**A**. Huh7 cells were transfected with EV or septin 9_I1 for 48h then analysis the expression of septin 9_i1 by Immunoblot for V5-tag, β-Actin was used for loading control.

**B**. Huh7 cells were transfected with EV or septin 9_I1 were grown for 24h. Then culture medium was supplemented with 100 μM sodium oleate complex for different time points (0 h, 12h, 24h, 48h, 72h), after treatment, cells were stained for LDs(green) and LAMP1(red). Scale bar, 20μm.

**C**. Fluorescence intensity of LDs and the percentage of LAMP1 in perinuclear area were analyzed in 25 cells from three experiments performed as described in **B**.

**D**. Huh7 cells were transfected with or not septin 9-siRNA for 48h then analysis the expression of septin 9 by Immunoblot, β-Actin was used for loading control.

**E**. Huh7 cells were transfected with or not septin 9-siRNA for 24h then culture with medium supplemented with or not 100 μM oleate for 24h. Then stained for BODIPY (green) and LAMP1 (red). Scale bar, 20μm.

**F**. Fluorescence intensity of LDs and the percentage of LAMP1 in perinuclear area were analyzed in 25 cells from three experiments performed as described in **D**.

Data information: Bar and line graphs present Mean ± SEM. Student's t-test was used. *P < 0.05, **P< 0.001, ***P<0.0001.

**Figure 3 Septin 9 induced-perinuclear cluster of lysosomes colocalizes with Golgi structure**

**A**. Huh7 cells were cultured overnight. Then culture medium was supplemented with or without 100 μM sodium oleate complex for different time points (12h, 24h, 48h, 72h), after treatment, cells were stained for TGN46 (green) and LAMP1(red). Scale bar, 20μm.

**B**. Bar graphs show percentage of LAMP1 in perinuclear area and Pearson's correlation coefficient (Rr) for co-localization between LAMP1 and TGN46 of 30 cells from 3 independent experiments performed as described in A.

**C**. Huh7 cells were transfected with or not septin 9-siRNA for 24h then culture with medium supplemented with or not 100 μM oleate for 24h and stained for TGN46 (green) and LAMP1 (red). The dot squares indicate the zoomed area shown right, TGN46 and LAMP1 were shown below. Scale bar, 5μm.

**D**. Bar graphs show percentage of LAMP1 in perinuclear area and Pearson's correlation coefficient (Rr) for co-localization between LAMP1 and TGN46 of 28 cells from 3 independent experiments performed as described in C.

**E**. Huh7 cells were culture medium supplemented with or without 100 μM oleate for 24h. 4h before fixing, added 33 nM of nocodazole. After incubation cells were stained for LAMP1 (red) and TGN46

(green). The dot squares indicate the zoomed area shown right, TGN46 and LAMP1 were shown below. Scale bar, 5μm.
**F**. Bar graphs show Pearson's correlation coefficient (Rr) for co-localization between LAMP1 and TGN46 of 30 cells from 3 independent experiments performed as described in C.
Data information: Bar graphs present Mean ± SEM. Student's t-test was used. *P < 0.05, **P< 0.001, ***P<0.0001.

**Figure 4 LD accumulation regulates microtubule polymerization**
**A.** Huh7 cells were culture with medium supplemented with 0,100 or 400 μM oleate complex for 24h or 72h then stained for β tubulin(green) and septin 9 (red). Scale bar, 20μm.
**B**. Bar graphs show mean intensity of β tubulin in MTOC area, mean intensity of septin 9 in perinuclear area and Pearson's correlation coefficient (Rr) for co-localization between β tubulin and septin 9 of 18 cells from 3 independent experiments performed as described in A.
**C**. Huh7 cells were transfected with or not septin 9-siRNA for 24h then culture with medium supplemented with 0,100 or 400 μM oleate complex for 24h or 72h then stained for β tubulin(green) and Bodipy (red). Scale bar, 20μm.
D. Bar graphs show intensity of β tubulin in MTOC area of 24 cells from 3 independent experiments performed as described in C.
Data information: Bar graphs present Mean ± SEM. Student's t-test was used. *P < 0.05, **P< 0.001, ***P<0.0001.

**Figure 5** Septin 9 is associated with large LDs in the perinuclear area.
A. Huh7 cells were grown overnight. Then culture medium was supplemented without or with 100 and 400 μM sodium oleate complex for different time (24h, 72h), then stained for LDs(red) and septin 9 (green). Scale bar, 20μm.
B. Dot rectangles in A are presented in higher magnification. Scale bar, 5μm.Bar graphs show total intensity of LD and Mean intensity of Rab7 on LDs.
Data information: Bar and line graphs present Mean ± SEM. Student's t-test was used. *P < 0.05, **P< 0.001, ***P<0.0001.

**Figure 6 Septin 9 regulates the intracellular distribution of Rab7 and its interaction with LDs**
**A**. Huh7 cells transfected with GFP-Rab7 were grown for 24h. Then culture medium was supplemented without or with 100 and 400 μM sodium oleate complex for different time (24h, 72h), then stained for LDs (red). Scale bar, 20μm.
**B**. Dot rectangles in A are presented in higher magnification. Scale bar, 5μm. Bar graphs show total intensity of LD and Mean intensity of Rab7 on LDs of 24 cell from 3 independent experiments performed as described in A.
**C**. Huh7 cells were transfected with or not septin 9-siRNA for 24h then culture with medium supplemented with or not 400 μM oleate for 72h then stained for LD (red). The dot squares indicate the zoomed area shown right. Scale bar, 5μm. Bar graphs show total intensity of LD and Mean intensity of Rab7 on LDs of 15 cells from 3 independent experiments performed as described.
Data information: Bar graphs present Mean ± SEM. Student's t-test was used. *P < 0.05, **P< 0.001, ***P<0.0001.

**Figure 7 PIs regulate LD behavior and intracellular distribution of lysosomal proteins**
**A**. Huh7 cells transfected with GFP-Rab7 were pretreated with or without 100μM oleate for 24h, then treated with cell-permeant PtdIns5P or PtdIns (3,5) P2 at 30 mM for 15 min before fixing and staining for LDs (red). The dot squares indicate the zoom area. Scale bar, 5μm.
**B**. Bar graphs show the percentage of Rab7 in perinuclear area and Mean intensity of Rab7 on LDs of 24 cells from three independent experiments performed as described in A.

**Figure 8 Overexpression of MTMR3 increases PtdIns5P, promotes LD accumulation,**

**perinuclear clustering of lysosome, septin 9 perinuclear increasing and MT enhancement.**
**A**. Huh7 cells were transfected with EV or MTMR3 were grown for 48h. Then, cells were stained for 2XPHD (green)/ Flag (red), BODIPY (red)/ Flag (green), LAMP1 (red)/ Flag (green), Rab7 (green)/ MTMR3 (red), septin 9 (green)/ MTMR3 (red) and MTs (green)/ Flag (red). Scale bar, 20μm.
**B**. Bar graphs show total intensity of 2XPHD, LD size and percentage of LAMP1 and Rab7 in perinuclear area, mean intensity of septin 9 in perinuclear are and mean MTs intensity in MTOC area from 3 independent experiments performed as described in A.
Data information: Bar and line graphs present Mean ± SEM. Student's t-test was used. *P < 0.05, **P< 0.001, ***P<0.0001.
**C**. Normally, the cell contains few LDs which are dispersed distributed throughout the cytoplasm and lysosomes also dispersed distributed, Rab7 were able to bind to LD, thus, initiate the LD degradation. When LDs are accumulated within cells, the LDs are clustered around nucleus, enrich of PtdIns5P, and associated with high level of septin 9. And the lysosomal protein, LAMP1 and Rab7 are colocalized with Golgi apparatus, which have no contact with LD.

Tables

Table 1 Analysis of Bodipy distribution

| LD | | Mean | | | | | SEM | | | | |
|---|---|---|---|---|---|---|---|---|---|---|---|
| Position | Dosage(μM) | 0h | 12h | 24h | 48h | 72h | 0h | 12h | 24h | 48h | 72h |
| Perinuclear | 0 | 0.5134 | 0.5102 | 0.5061 | 0.4975 | 0.5124 | 0.0865 | 0.0592 | 0.0522 | 0.0509 | 0.0534 |
| | 50 | 0.5242 | 0.5822 | 0.6424 | 0.6112 | 0.4545 | 0.0507 | 0.0342 | 0.0302 | 0.0294 | 0.0308 |
| | 100 | 0.5234 | 0.7542 | 0.8143 | 0.7288 | 0.5215 | 0.0605 | 0.0734 | 0.0668 | 0.0402 | 0.0986 |
| | 200 | 0.5454 | 0.7945 | 0.8262 | 0.7126 | 0.6124 | 0.0623 | 0.0704 | 0.0572 | 0.0462 | 0.0598 |
| | 400 | 0.5545 | 0.8457 | 0.8571 | 0.8414 | 0.8349 | 0.0615 | 0.0318 | 0.0234 | 0.0254 | 0.0167 |
| Peripheric | 0 | 0.4866 | 0.4898 | 0.4939 | 0.5025 | 0.4876 | 0.0865 | 0.0592 | 0.0522 | 0.0509 | 0.0534 |
| | 50 | 0.4758 | 0.4178 | 0.3576 | 0.3888 | 0.5455 | 0.0507 | 0.0342 | 0.0302 | 0.0294 | 0.0308 |
| | 100 | 0.4766 | 0.2458 | 0.1857 | 0.2712 | 0.4785 | 0.0605 | 0.0734 | 0.0668 | 0.0402 | 0.0986 |
| | 200 | 0.4546 | 0.2055 | 0.1738 | 0.2874 | 0.3876 | 0.0623 | 0.0704 | 0.0572 | 0.0462 | 0.0598 |
| | 400 | 0.4455 | 0.1543 | 0.1429 | 0.1586 | 0.1651 | 0.0615 | 0.0318 | 0.0234 | 0.0254 | 0.0167 |

Table 2 Analysis of LAMP1 distribution

| LAMP1 | | Mean | | | | | SEM | | | | |
|---|---|---|---|---|---|---|---|---|---|---|---|
| Position | Dosage(μM) | 0h | 12h | 24h | 48h | 72h | 0h | 12h | 24h | 48h | 72h |
| Perinuclear | 0 | 0.6955 | 0.7119 | 0.6935 | 0.7022 | 0.6922 | 0.6955 | 0.7119 | 0.6935 | 0.7022 | 0.6922 |
| | 50 | 0.7074 | 0.8096 | 0.8148 | 0.7022 | 0.7012 | 0.7074 | 0.8096 | 0.8148 | 0.7022 | 0.7012 |
| | 100 | 0.7046 | 0.8604 | 0.9201 | 0.8364 | 0.7361 | 0.7046 | 0.8604 | 0.9201 | 0.8364 | 0.7361 |
| | 200 | 0.6976 | 0.9024 | 0.9128 | 0.8476 | 0.7725 | 0.6976 | 0.9024 | 0.9128 | 0.8476 | 0.7725 |
| | 400 | 0.6992 | 0.9095 | 0.9117 | 0.9008 | 0.9018 | 0.6992 | 0.9095 | 0.9117 | 0.9008 | 0.9018 |
| Peripheric | 0 | 0.3045 | 0.2881 | 0.3065 | 0.2978 | 0.3078 | 0.6955 | 0.7119 | 0.6935 | 0.7022 | 0.6922 |
| | 50 | 0.2926 | 0.1904 | 0.1852 | 0.2978 | 0.2988 | 0.7074 | 0.8096 | 0.8148 | 0.7022 | 0.7012 |
| | 100 | 0.2954 | 0.1396 | 0.0799 | 0.1636 | 0.2639 | 0.7046 | 0.8604 | 0.9201 | 0.8364 | 0.7361 |
| | 200 | 0.3024 | 0.0976 | 0.0872 | 0.1524 | 0.2275 | 0.6976 | 0.9024 | 0.9128 | 0.8476 | 0.7725 |
| | 400 | 0.3008 | 0.0905 | 0.0883 | 0.0992 | 0.0982 | 0.6992 | 0.9095 | 0.9117 | 0.9008 | 0.9018 |

Table 3 Analysis of the correlation between LD and lysosomes distribution

| Position | Dosage(μM) | Correlation Bodipy/LAMP1 |
|---|---|---|
| Perinuclear | 0 | -0.209482214 |
| | 50 | 0.614718853 |
| | 100 | 0.984182479 |
| | 200 | 0.992128811 |
| | 400 | 0.999520416 |
| Peripheric | 0 | -0.209482214 |
| | 50 | 0.614718853 |
| | 100 | 0.984182479 |
| | 200 | 0.992128811 |
| | 400 | 0.999520416 |

**Table 4 Primers sequences**

| Primer name | Sequence (5’ to 3’) |
|---|---|
| LAMP1 Forward | ACGTTACAGCGTCCAGCTCAT |
| LAMP1 Reverse | TCTTTGGAGCTCGCATTGG |
| LIPA Forward | CTGACAAAGGTCCCAAACCAG |
| LIPA Reverse | GCAAGAATGAAGCCCAGGC |
| GNS Forward | CCCATTTTGAGAGGTGCCAGT |
| GNS Reverse | TGACGTTACGGCCTTCTCCTT |
| GBA Forward | GGGCAAAGGTGGTACTGACAG |
| GBA Reverse | GCATGGTGTTGGGGAACAG |
| MCOLN1 Forward | TTGCTCTCTGCCAGCGGTACTA |
| MCOLN1 Reverse | GCAGTCAGTAACCACCATCGGA |
| TMEM55B Forward | GTTCGATGCCCCTGTAACTGTC |
| TMEM55B Reverse | CCCAGGTTGATGATTCTTTTGC |
| ATP6V1E1 Forward | AAAGGTCGGCTTGTGCAAACCC |
| ATP6V1E1 Reverse | GGTCATCTCTTGCTCTGAGGAC |
| GAPDH Forward | CCACATCGCTCAGACACCAT |
| GAPDH Reverse | CCAGGCGCCCAATACG |

**Table 5 siRNA sequences**

| siRNA Name | Sequence (5' to 3') |
|---|---|
| si RNA1 (SEPT9HSS173895) Forward | AGGCGUACCGUGUGAAGCGCCUCAA |
| si RNA1 (SEPT9HSS173895) Reverse | UUGAGGCGCUUCACACGGUACGCCU |
| si RNA2 (SEPT9HSS173896) Forward | AGGCGCCUGCAUCACGGAACGAGAA |
| si RNA2 (SEPT9HSS173896) Reverse | UUCUCGUUCCGUGAUGCAGGCGCCU |
| si RNA3 (SEPT9HSS173897) Forward | GCCAUGAAGCAGGGCUUCGAGUUCA |
| si RNA3 (SEPT9HSS173897) Reverse | UGAACUCGAAGCCCUGCUUCAUGGC |

**Supplemental**

**Figure 1 Oleate treatment induces acidic vesicles redistribution**

A. Huh7 cells were grown for 24h. the culture medium was supplemented with or without 100, 200 μM sodium oleate complex for different time points (12h, 24h, 48h, 72h), then stained with Lysotracker(red). Scale bar, 20μm.

**Figure 2 Analysis of lysosomal genes in oleate treated cells and LAMP1-Bodipy interaction**

**A**. Huh7 cells were grown overnight. Then culture medium was supplemented without or with 100 and 400 μM sodium oleate complex for different time (24h, 72h), mRNA was extracted, and RT-PCR were performed for LAMP1, TMEM55B, MCOLN1, GBA, GNS, LIPA and ATP6V1E1.

**B.** The line plots for LAMP1 and BODIPY were performed for cells treated with 0,100 and 400 μM sodium oleate complex for different time (24h, 72h).

**Figure 3 Knockdown of septin 9 disrupts oleate-induced LDs accumulation and lysosome perinuclear cluster**

A. Huh7 cells were transfected with or not septin 9-siRNA for 24h then culture with medium supplemented with or not 400 μM oleate for different time. Then stained for BODIPY (green) and LAMP1 (red). Scale bar, 20μm.

B. Fluorescence intensity of LDs and the percentage of LAMP1 in perinuclear area were analyzed in 25 cells from two experiments performed as described in A.

**Figure 4 Septin 9_i1 overexpression maintains the colocalization of LAMP1 and TGN46**

A. Huh7 cells were transfected with EV or septin 9_i1 were grown for 24h. Then culture medium was supplemented with 100 μM sodium oleate complex for 72h, after treatment, cells were stained for TGN46 (green) and LAMP1 (red). Scale bar, 20μm.

B. Bar graphs show Pearson's correlation coefficient (Rr) for co-localization between LAMP1 and TGN46.

Data information: Bar and line graphs present Mean ± SEM. Student's t-test was used. *P < 0.05, **P< 0.001, ***P<0.0001.

**Figure 5 MT enhance in LD accumulating cells and associated with LAMP1 perinuclear cluster**

**A.** Huh7 cells were culture with medium supplemented with 0, 50, 100 or 200 μM oleate complex for 24h then stained for β tubulin (green) and LDs (red). White squares are presented in higher magnification. Scale bar, 5μm.

**B**. Immunoblot analysis of soluble β tubulin and polymerized β tubulin in Huh7 cells treated with oleate. Taxol and nocodazole were used as polymerized positive and negative control. Bar graph presents the densitometry analysis of the percentage of polymerized β tubulin in total β tubulin (P/(S+P)) from three independent experiments.

C. Huh7 cells were grown overnight. Then culture medium was supplemented without or with 100 and 400 μM sodium oleate complex for different time (24h, 72h), then stained for LAMP1 (red) and β tubulin (green). Scale bar, 20μm.

**Figure 6 Oleate treatment promotes colocalization of Rab7 with LAMP1 in the perinuclear area**

A. Huh7 cells expressed GFP-Rab7 were culture medium supplemented with or without 100 μM oleate for 24h, then stained for LAMP1 (red).

**Figure 7 Septin 9 regulates the intracellular distribution of endogenous Rab7**

A. Huh7 cells were transfected with or not septin 9-siRNA for 24h then culture with medium supplemented with or not 100, 400 μM oleate for different time (24, 72h). Then stained for Rab7 (green) and BODIPY (red). Scale bar, 20μm.

B. Bar graphs show the percentage of Rab7 intensity in perinuclear area from two different

experiments.

**Figure 8 Septin 9 regulates the formation of autophagosomes**
A. Huh7 cells were transfected with or not septin 9-siRNA for 24h then culture with medium supplemented with or not 100, 400 μM oleate for different time (24, 72h). Then stained for P62 (green) and BODIPY (red). Scale bar, 20μm.
B. Bar graphs show the number of P62 puncta per cells from two different experiments.
C. Huh7 cells were transfected with or not septin 9-siRNA for 24h then culture with medium supplemented with or not 100, 400 μM oleate for different time (24, 72h). Then stained for LC3B (green) and BODIPY (red). Scale bar, 20μm.
D. Bar graphs show the number of LC3B puncta per cells from two different experiments.
Data information: Bar and line graphs present Mean ± SEM. Student's t-test was used. *P < 0.05, **P< 0.001, ***P<0.0001.

**Figure 9 Septin 9 is responsible for Rab7 perinuclear cluster and Golgi colocalization**
A. GFP-Rab7 expressed Huh7 cells were transfected with or not septin 9-siRNA for 24h then culture with medium supplemented with or not 400 μM oleate for 72h then stained for TGN46(red). Scale bar, 20μm.
B. Bar graphs show show Pearson's correlation coefficient (Rr) for co-localization between Rab7 and TGN46.
Data information: Bar graphs present Mean ± SEM. Student's t-test was used. *P < 0.05, **P< 0.001, ***P<0.0001.

**Figure 10 PIs regulates septin 9 association with LDs**
A. Huh7 cells treated with cell-permeant PtdIns5P or PtdIns (3,5) P2 at 30 mM for 15 min before fixing and staining for endogenous septin 9 (green) and LDs (red). The dot squares indicate the zoom area. Scale bar, 5μm.
B. Bar graphs show the mean intensity of endogenous septin 9 on LDs from two independent experiments performed as described in A.
C. Huh7 cells transfected with or without septin 9_i1 were cultured for 24h. Then, cells were treated with cell-permeant PtdIns5P or PtdIns (3,5) P2 at 30 mM for 15 min before fixing and staining for V5-tag (green) and LDs (red). The dot squares indicate the zoom area. Scale bar, 5μm.
D. Bar graphs show the mean intensity of V5-tag on LDs from two independent experiments performed as described in A.
Data information: Bar graphs present Mean ± SEM. Student's t-test was used. *P < 0.05, **P< 0.001, ***P<0.0001.

**Figure 11 PIs regulate microtubules in MTOC area**
A. Huh7 cells treated with cell-permeant PtdIns5P or PtdIns (3,5) P2 at 30 mM for 15 min before fixing and staining for endogenous septin 9 (red) and β tubulin (red). Scale bar, 20μm.
B. Bar graphs show mean intensity of β tubulin in MTOC area, mean intensity of septin 9 in perinuclear area and Pearson's correlation coefficient (Rr) for co-localization between β tubulin and septin 9 from two independent experiments performed as described in A.

**Figure 12 Septin 9 PBs are important for its function in lysosome regulation**
A. Huh7 cells were transfected with EV, septin 9_i1 or Septin 9_ΔΔ for 48h and then stained for Rab7 (green) and V5-tag (red).
B. Bar graphs show the percentage of Rab7 in perinuclear area from two independent experiments performed as described in A.
C. Huh7 cells were transfected with EV, septin 9_i1 or Septin 9_ΔΔ for 48h and then stained for LAMP1 (red) and V5-tag (green).
D. Bar graphs show the percentage of LAMP1 in perinuclear area from two independent experiments

performed as described in A.

**Figure 13 Uncropped blots**

**Figure 14 Diagrams for the method of image calculation**

Figure 1

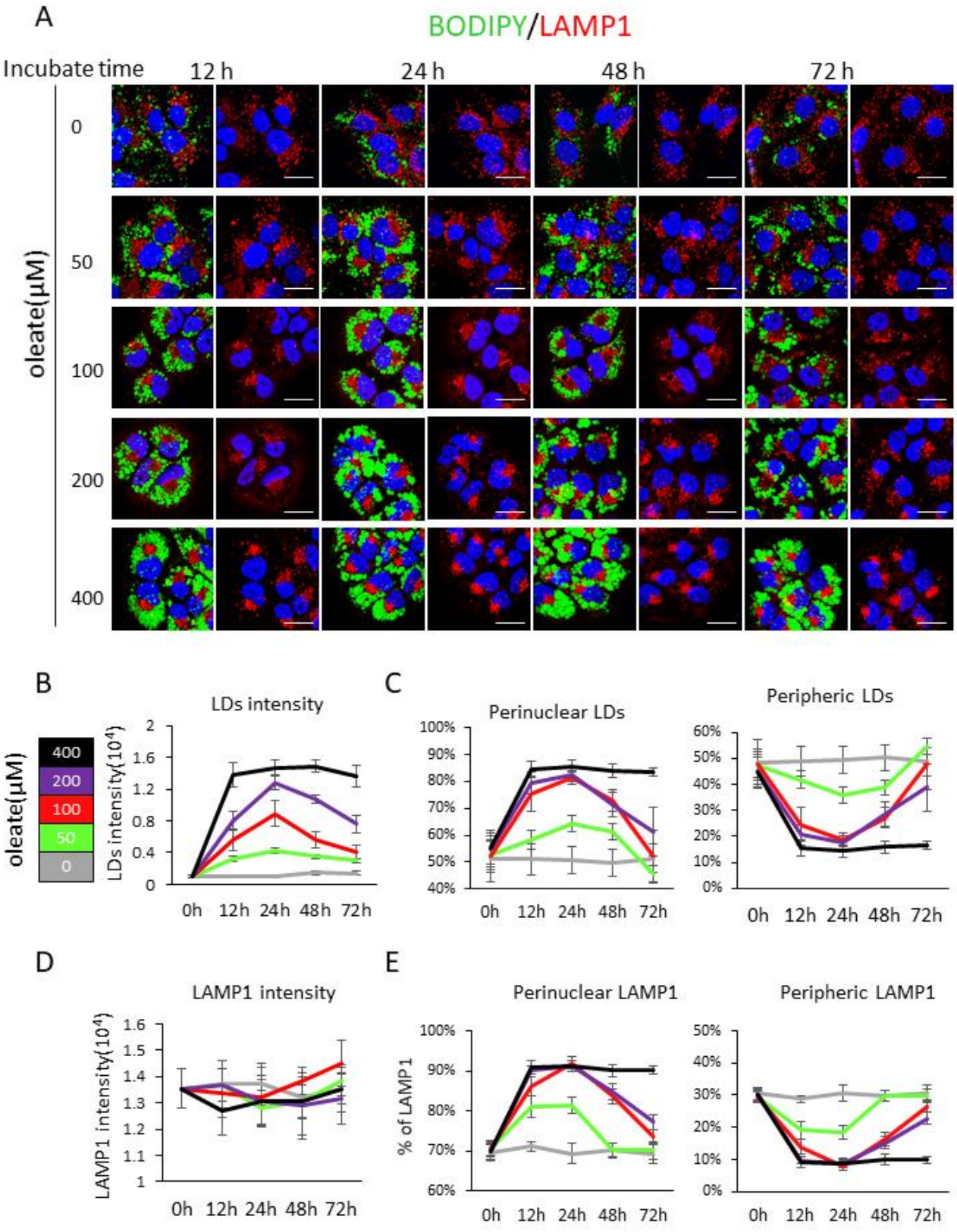
A
BODIPY/LAMP1
Incubate time
12 h
24 h
48 h
72 h
oleate(μM)
0
50
100
200
400
B
LDs intensity
oleate(μM)
400
200
100
50
0
LDs intensity(10⁴)
0h 12h 24h 48h 72h
C
Perinuclear LDs
Peripheric LDs
0h 12h 24h 48h 72h
D
LAMP1 intensity
LAMP1 intensity(10⁴)
0h 12h 24h 48h 72h
E
Perinuclear LAMP1
Peripheric LAMP1
% of LAMP1
0h 12h 24h 48h 72h

Supplemental Figure 1

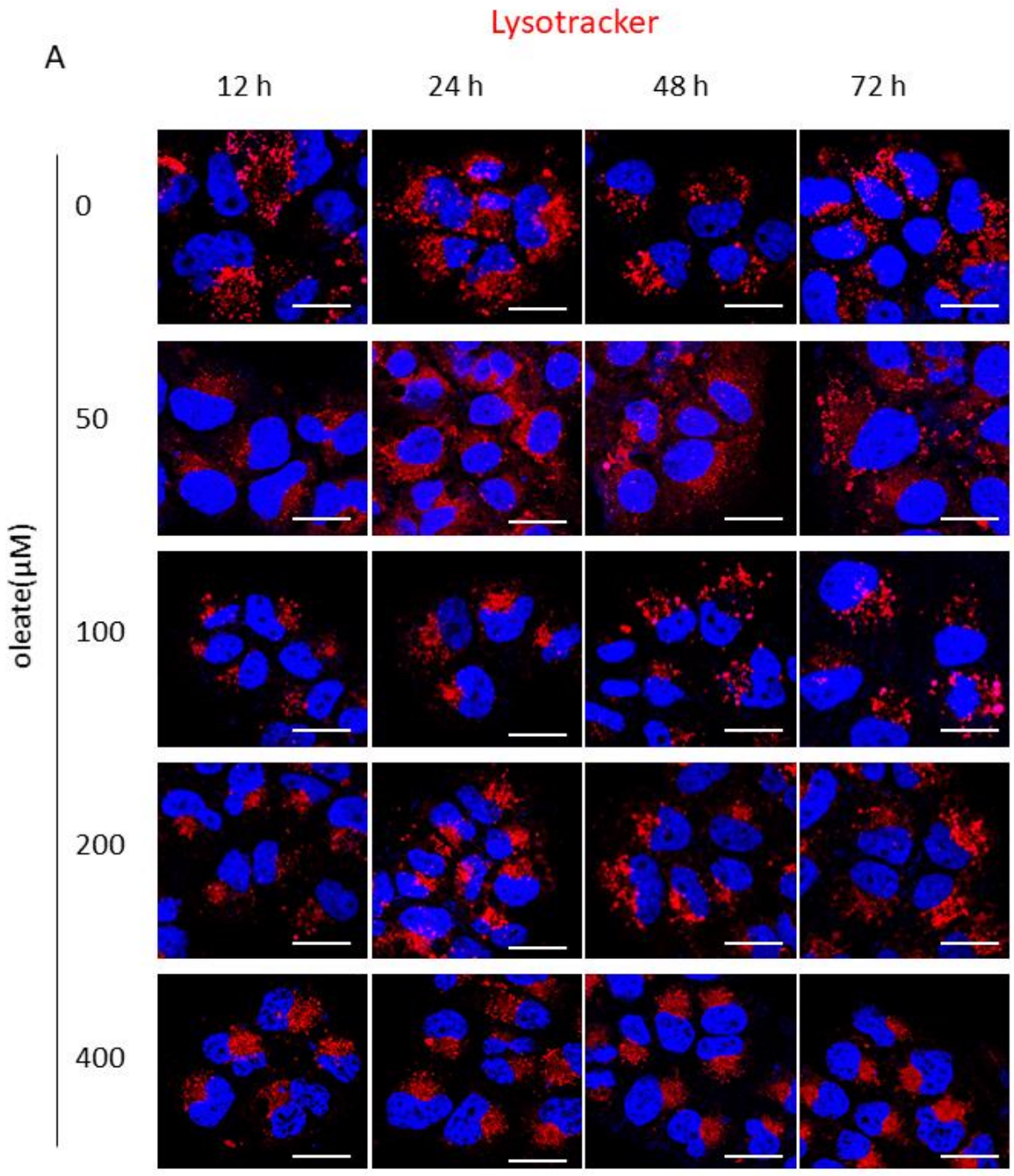

Supplemental Figure 2

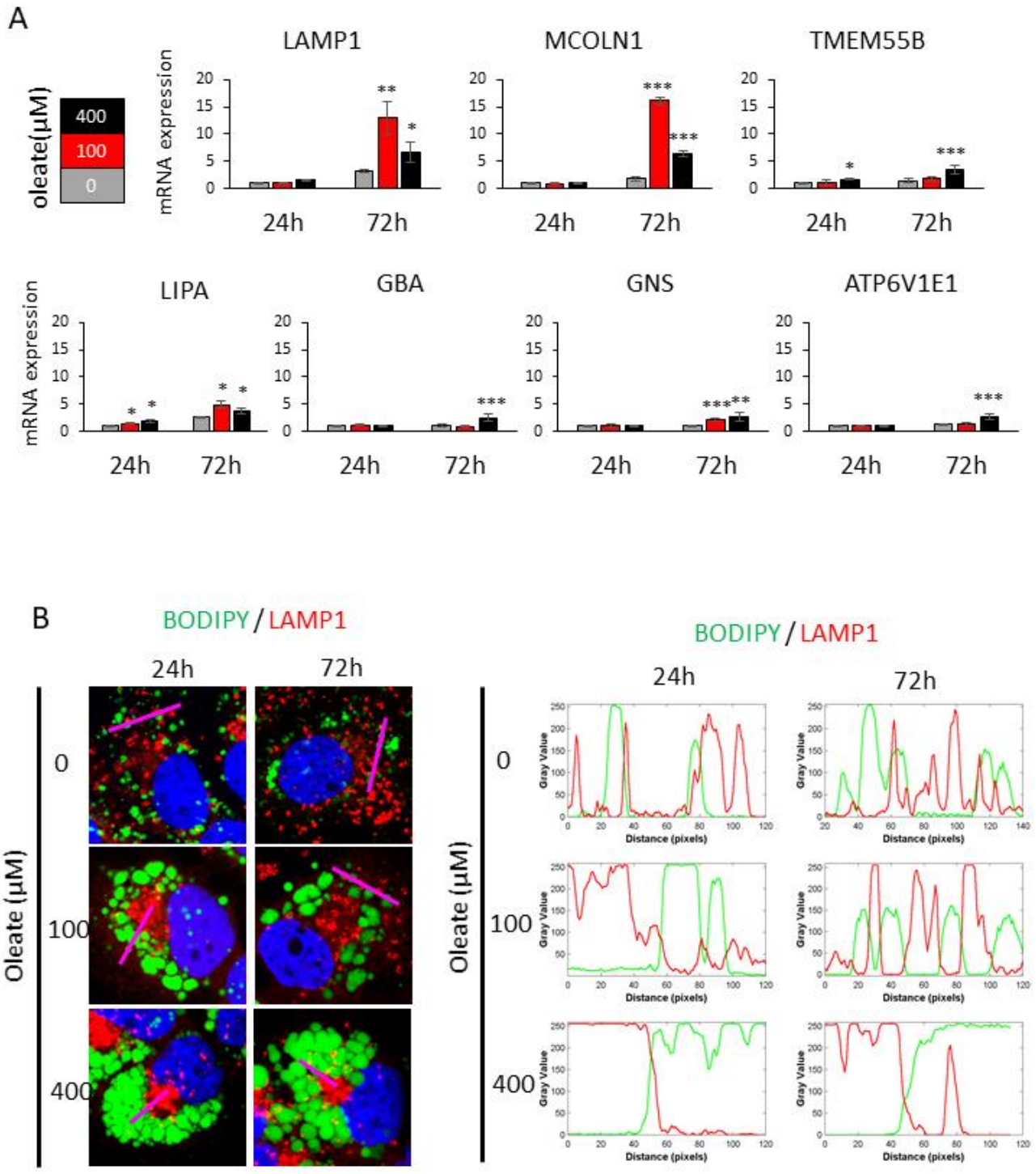

Figure 2

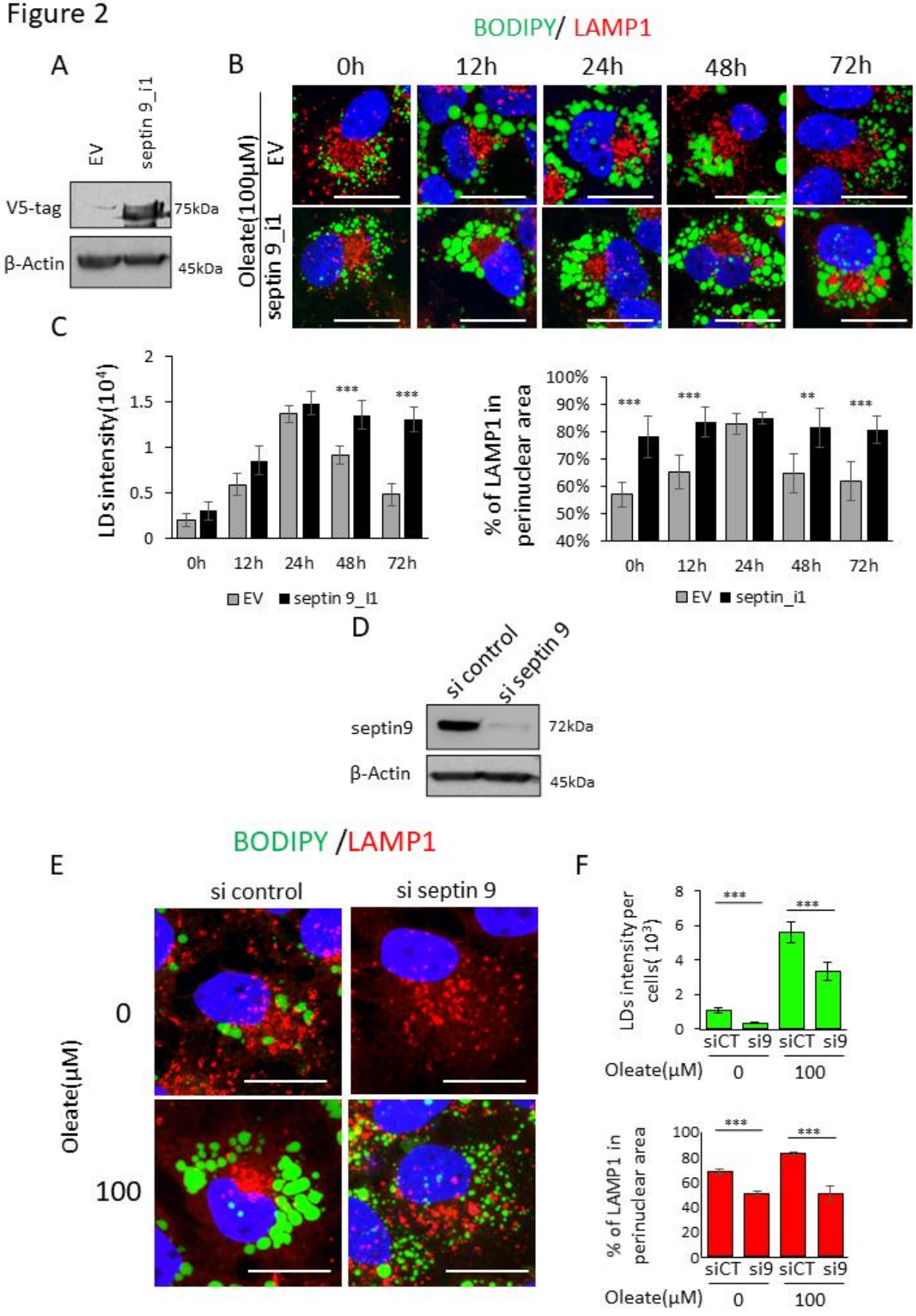
BODIPY/ LAMP1
A
EV
septin 9_i1
V5-tag
75kDa
β-Actin
45kDa
B
0h
12h
24h
48h
72h
Oleate(100μM)
EV
septin 9_i1
C
LDs intensity(10⁴)
% of LAMP1 in perinuclear area
EV
septin 9_I1
septin_i1
D
si control
si septin 9
septin9
72kDa
β-Actin
45kDa
BODIPY /LAMP1
E
si control
si septin 9
Oleate(μM)
0
100
F
LDs intensity per cells( 10³)
% of LAMP1 in perinuclear area
siCT
si9
Oleate(μM)
0
100

Supplemental Figure 3

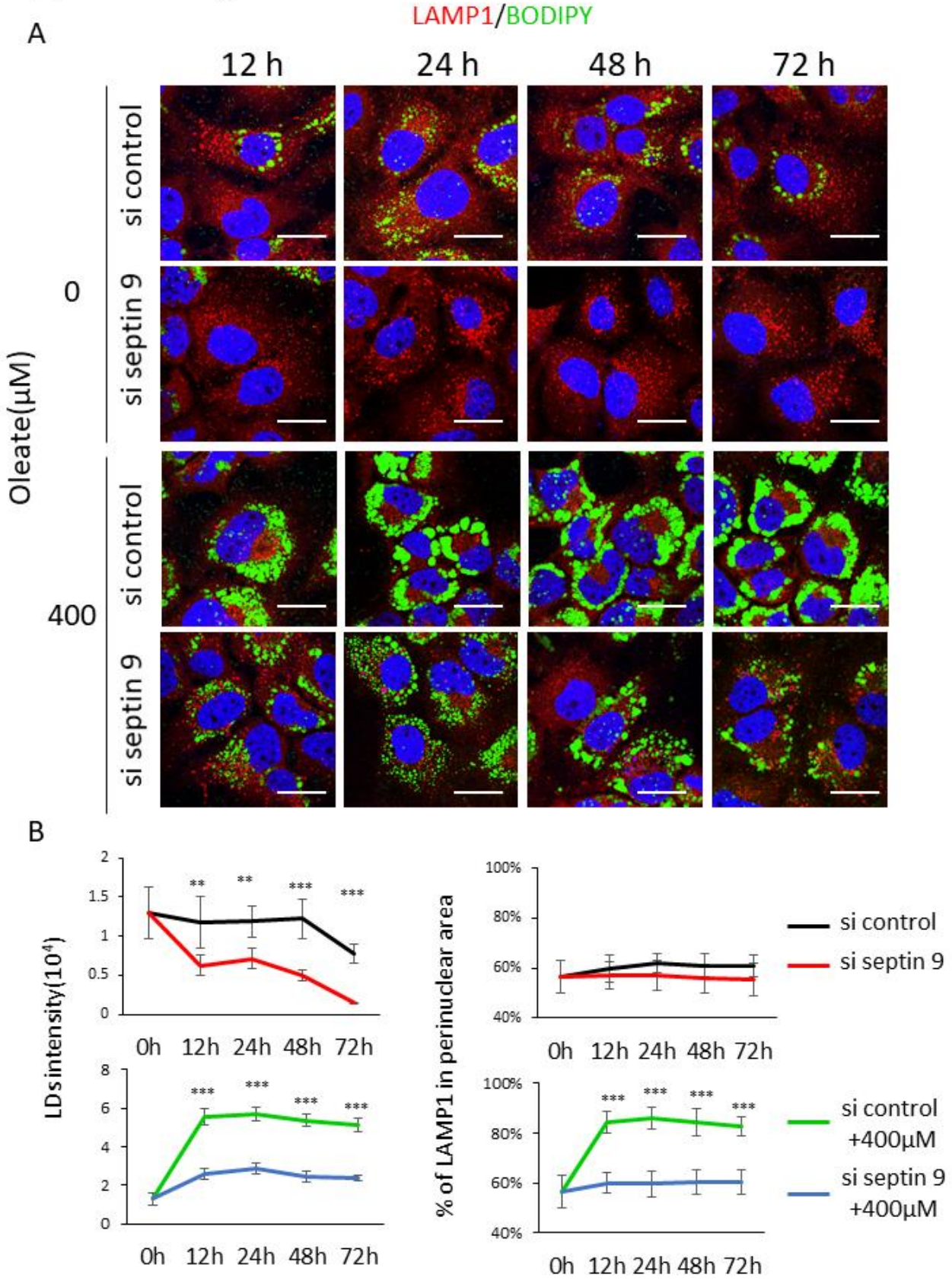

Figure 3

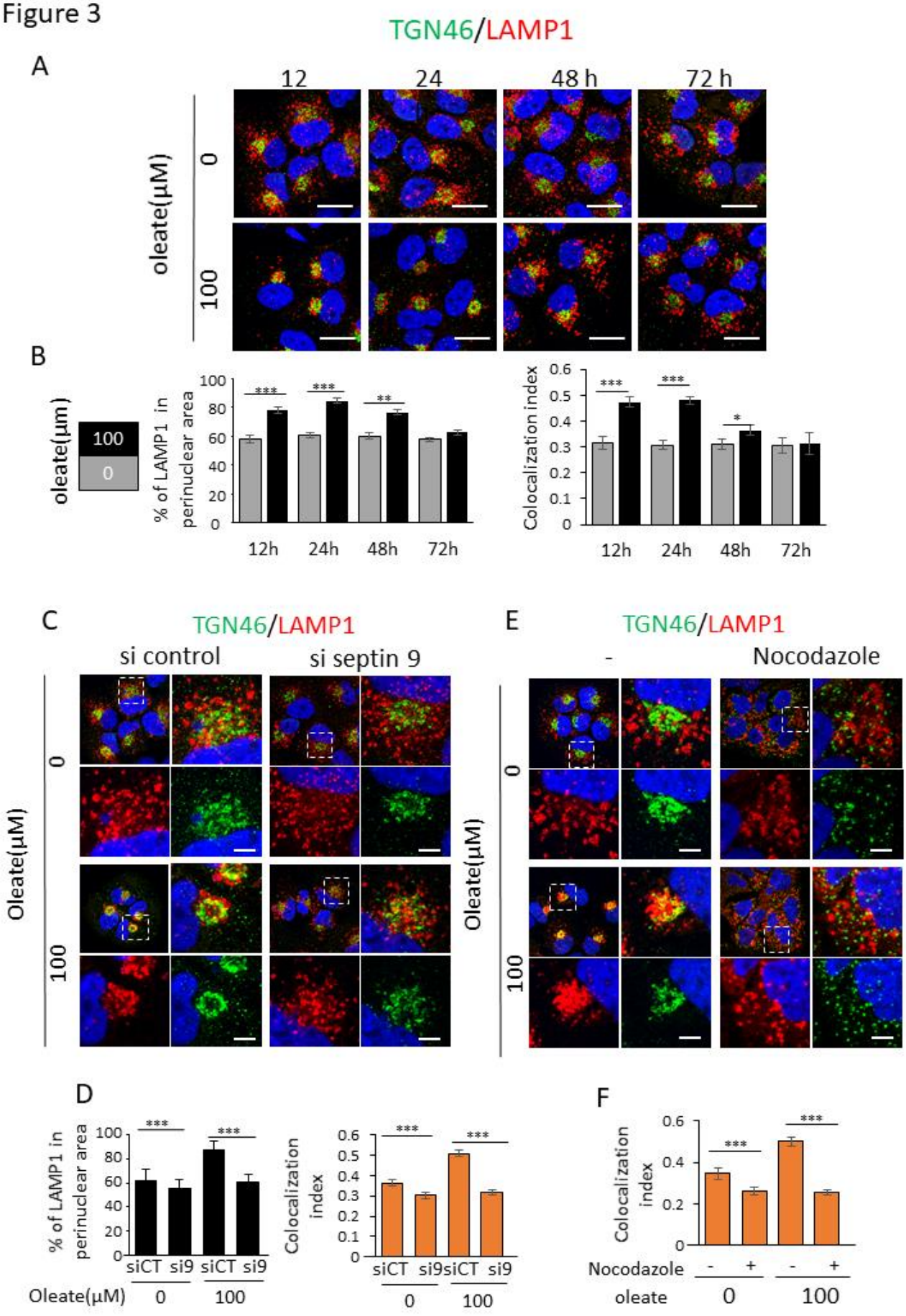
TGN46/LAMP1
A
12
24
48 h
72 h
oleate(µM)
0
100
B
oleate(µm)
100
0
% of LAMP1 in perinuclear area
Colocalization index
12h
24h
48h
72h
C
TGN46/LAMP1
si control
si septin 9
Oleate(µM)
0
100
D
% of LAMP1 in perinuclear area
Colocalization index
siCT
si9
Oleate(µM)
0
100
E
TGN46/LAMP1
-
Nocodazole
F
Colocalization index
Nocodazole
oleate

Supplemental Figure 4

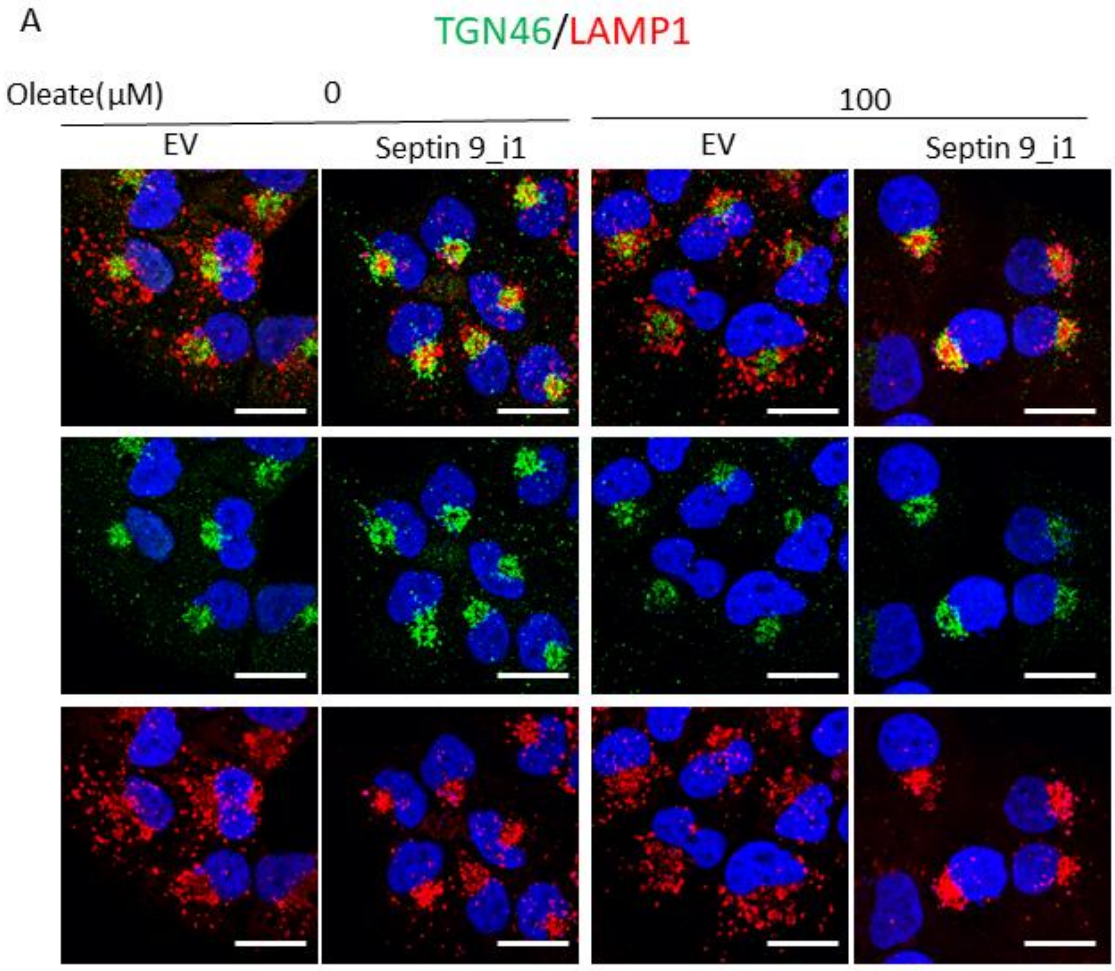


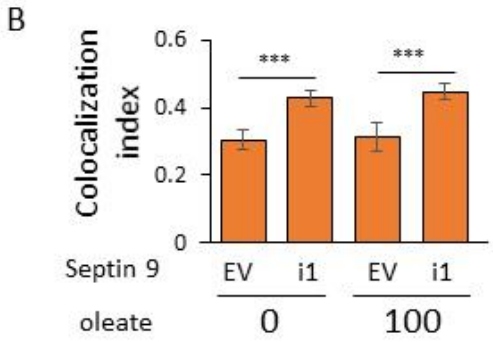

Supplemental Figure 5

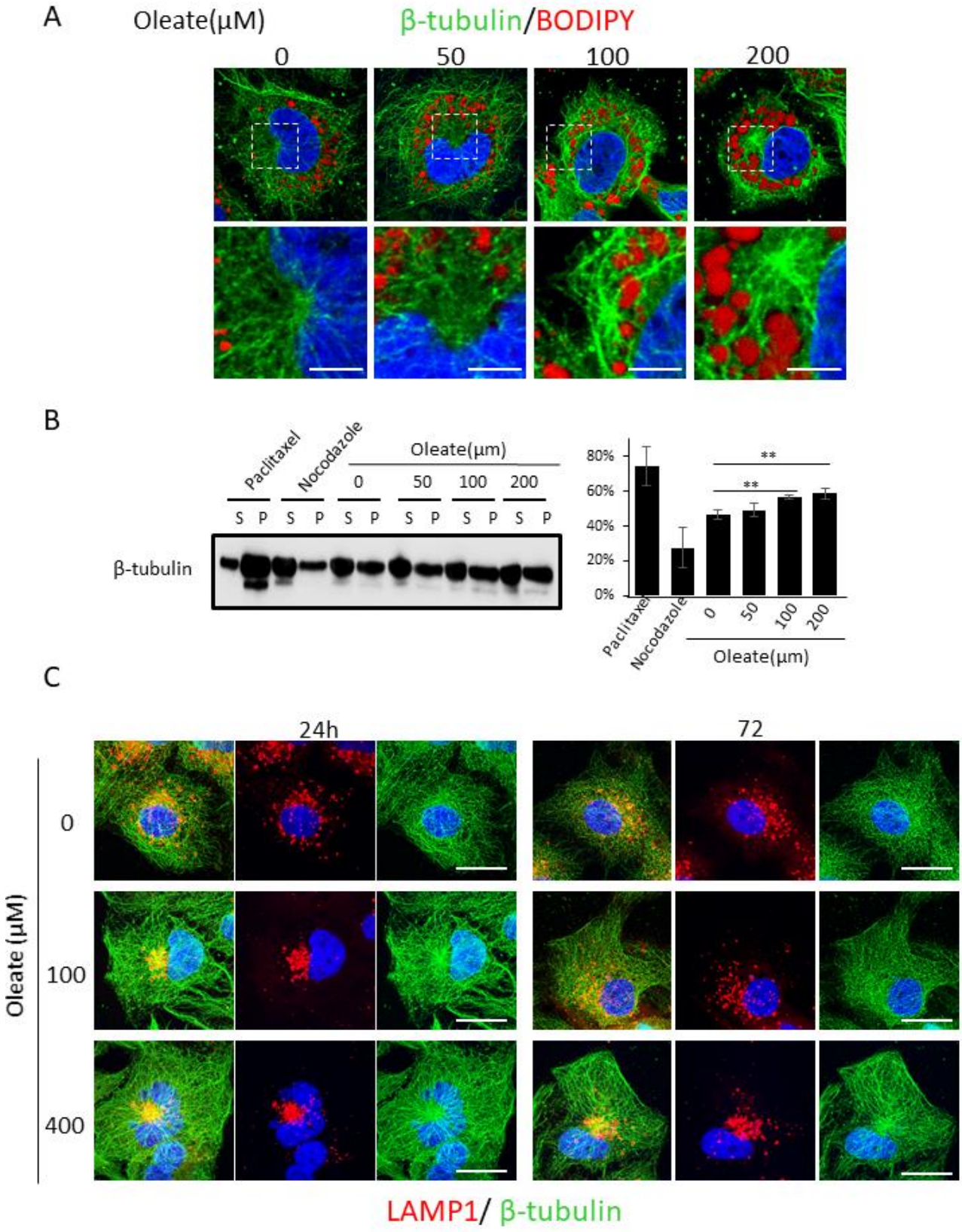

Figure 4

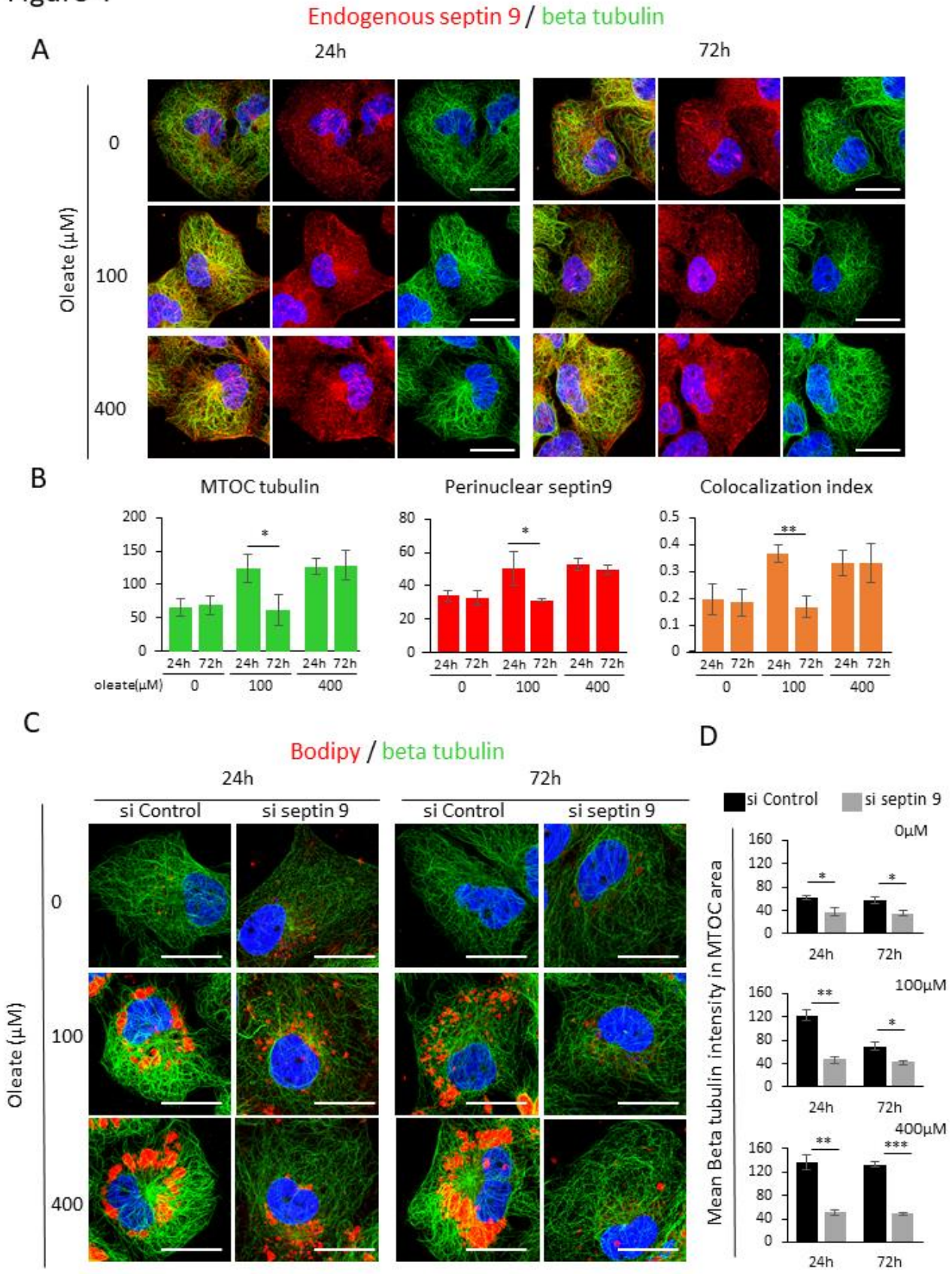
Endogenous septin 9 / beta tubulin
A
24h
72h
Oleate (µM)
0
100
400
B
MTOC tubulin
Perinuclear septin9
Colocalization index
oleate(µM)
C
Bodipy / beta tubulin
si Control
si septin 9
D
Mean Beta tubulin intensity in MTOC area
0µM
100µM
400µM

Figure 5

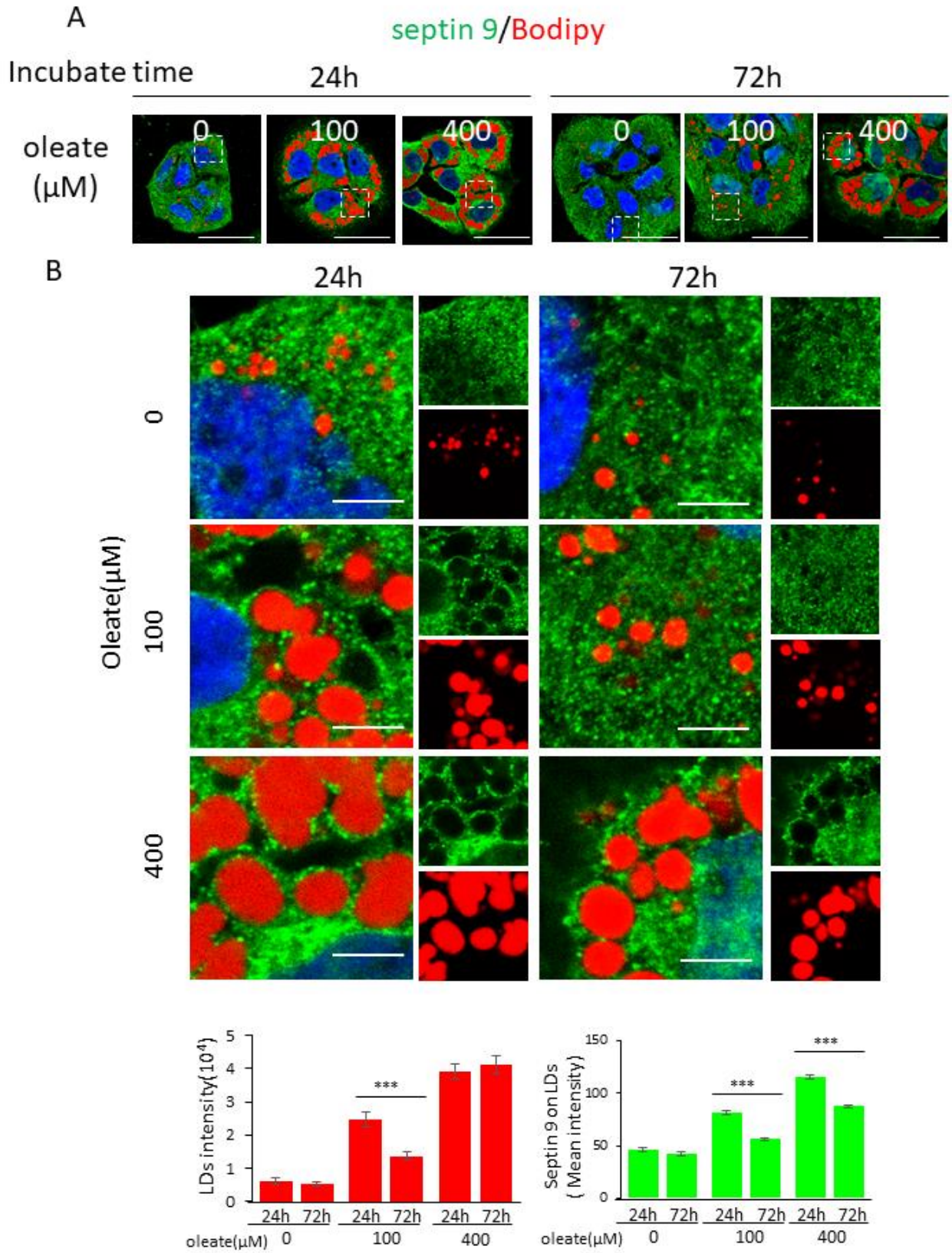
A
septin 9/Bodipy
Incubate time
24h
72h
oleate (μM)
0
100
400
B
24h
72h
Oleate(μM)
0
100
400
LDs intensity(10⁴)
***
24h 72h 24h 72h 24h 72h
oleate(μM) 0 100 400
Septin 9 on LDs ( Mean intensity)
***
***
24h 72h 24h 72h 24h 72h
oleate(μM) 0 100 400

Supplemental figure 6

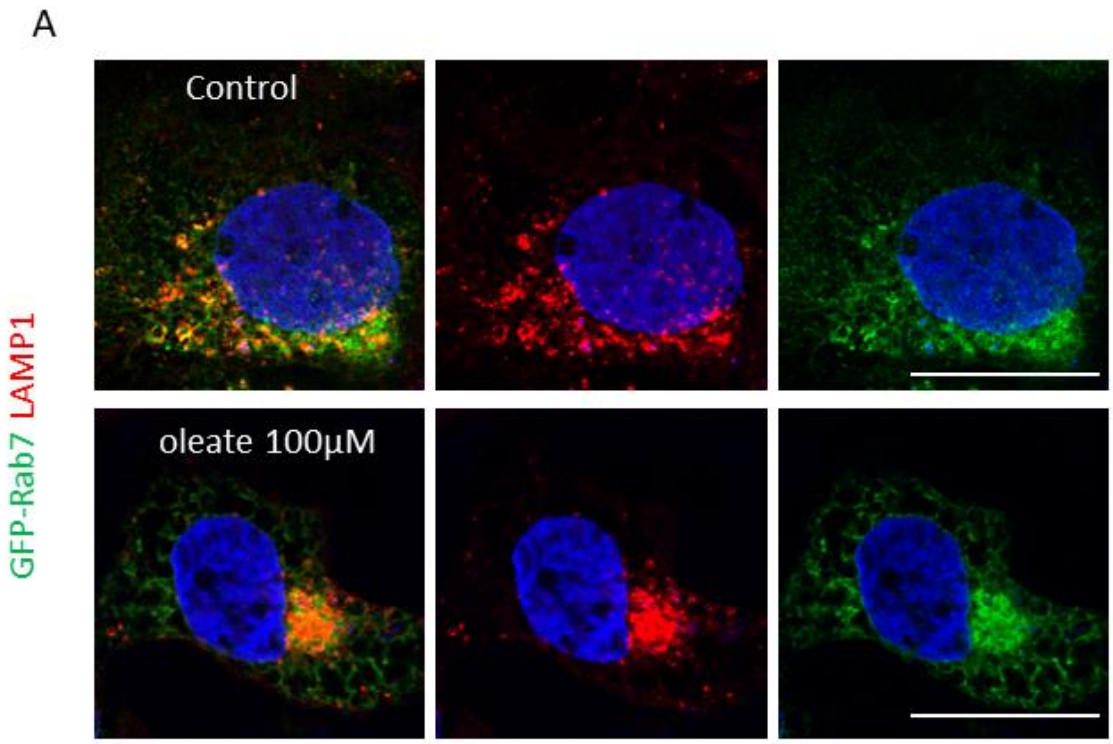

Figure 6

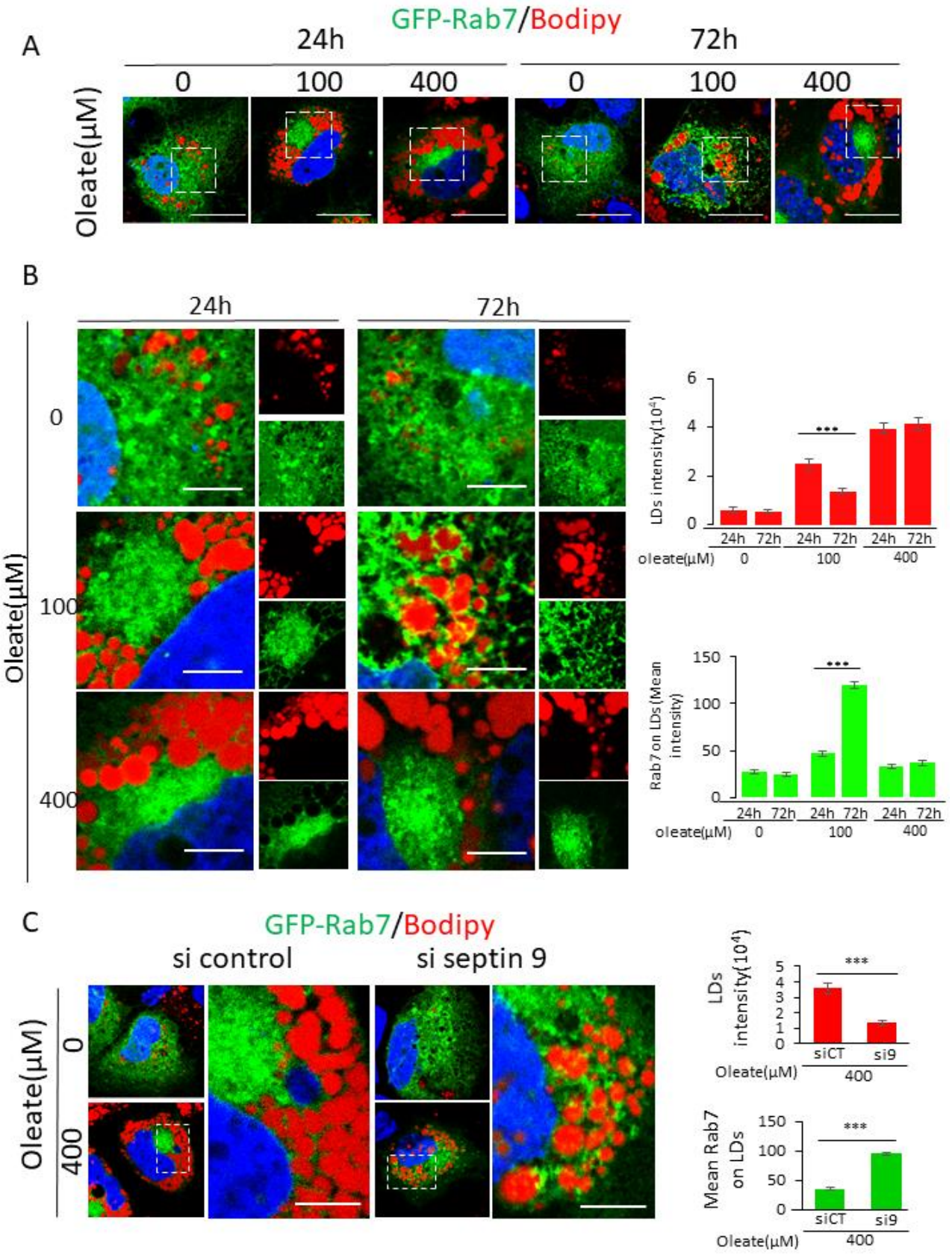
A
GFP-Rab7/Bodipy
24h
72h
0
100
400
0
100
400
Oleate(µM)
B
24h
72h
Oleate(µM)
0
100
400
LDs intensity(10⁴)
6
4
2
0
***
24h 72h 24h 72h 24h 72h
oleate(µM) 0 100 400
Rab7 on LDs (Mean intensity)
150
100
50
0
***
24h 72h 24h 72h 24h 72h
oleate(µM) 0 100 400
C
GFP-Rab7/Bodipy
si control
si septin 9
Oleate(µM)
0
400
LDs intensity(10⁴)
5
4
3
2
1
0
***
siCT
si9
Oleate(µM)
400
Mean Rab7 on LDs
150
100
50
0
***
siCT
si9
Oleate(µM)
400

Supplemental Figure 7

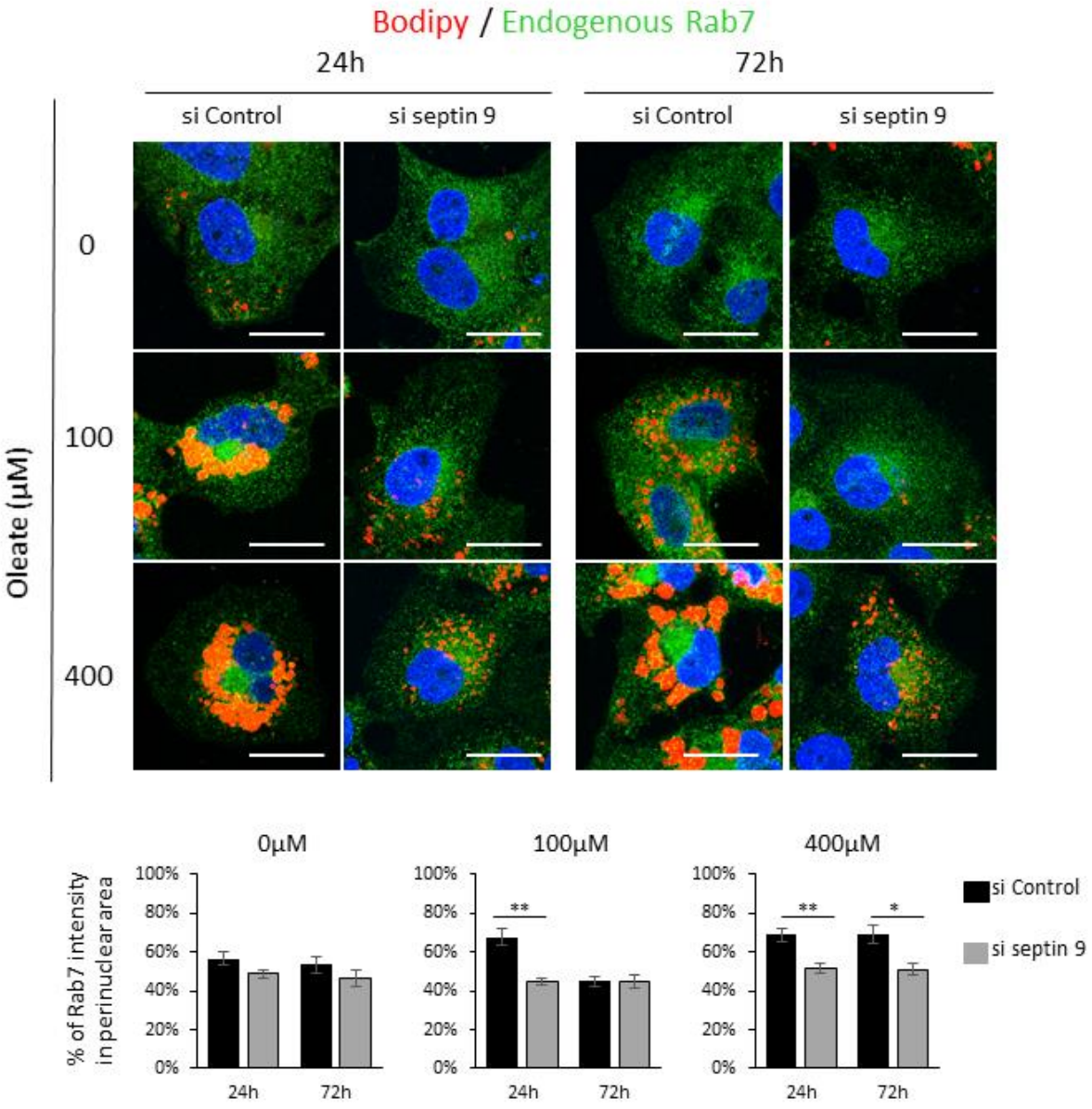

Supplemental figure 8

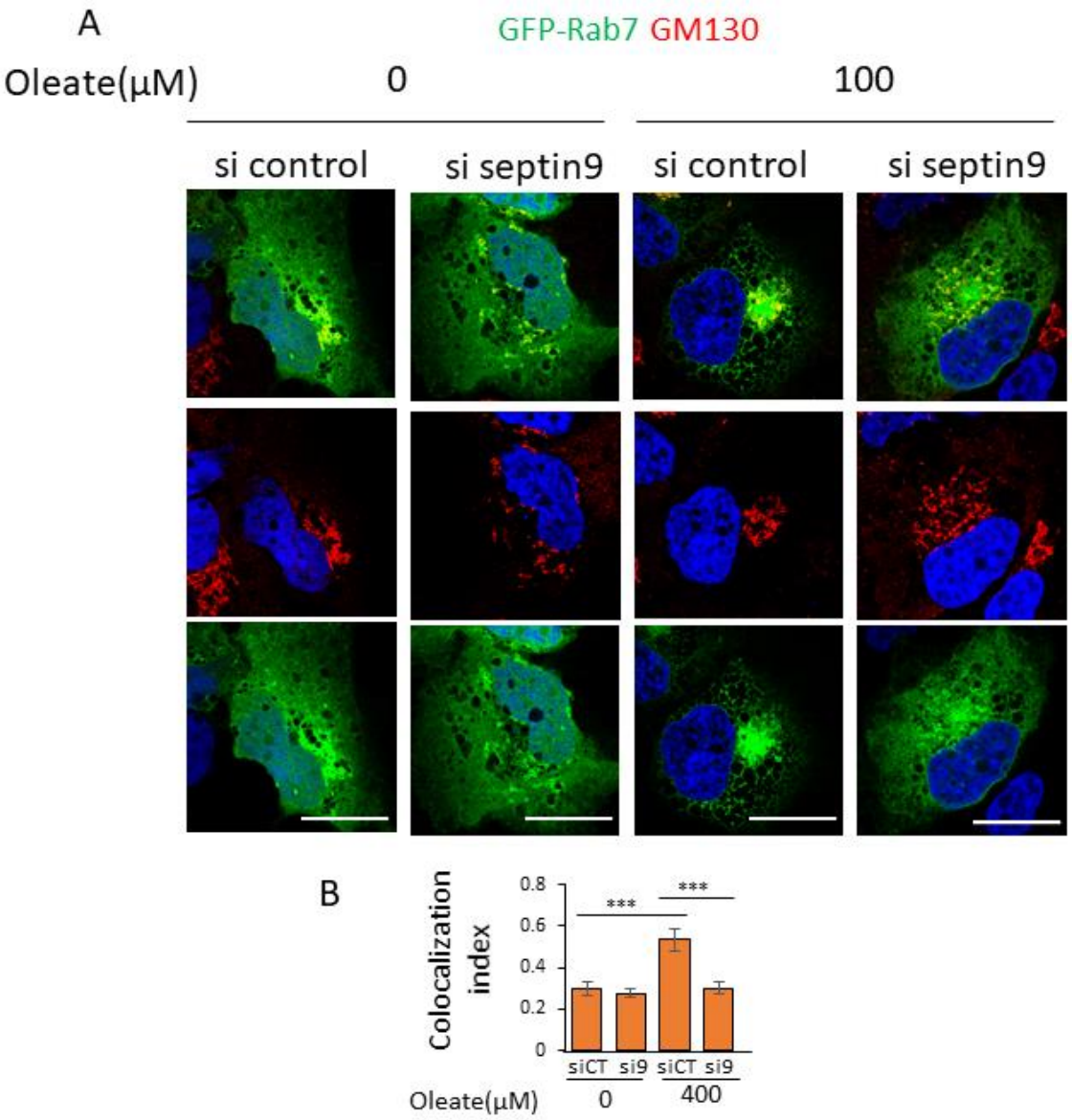

Supplemental figure 9

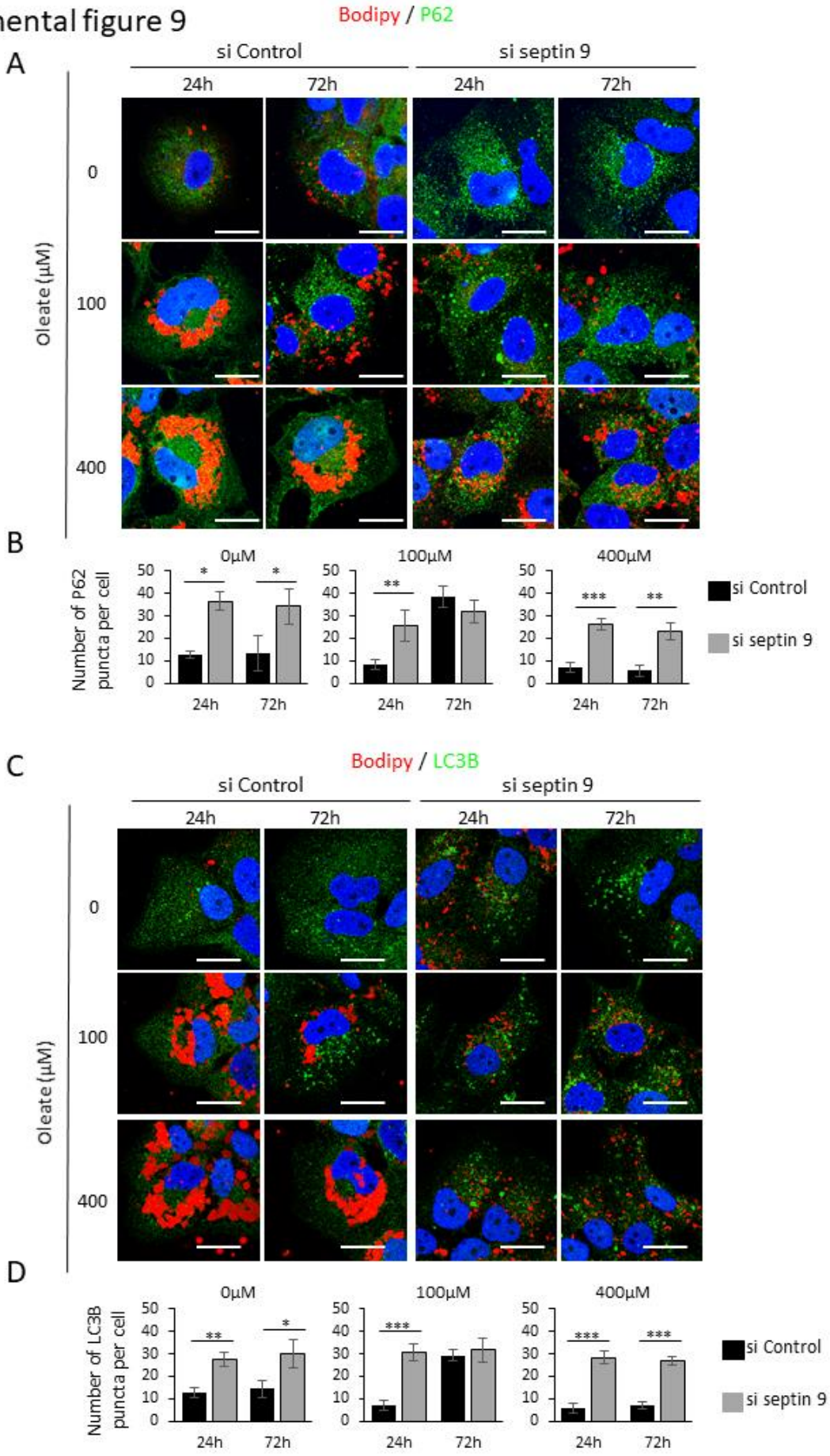

Figure 7

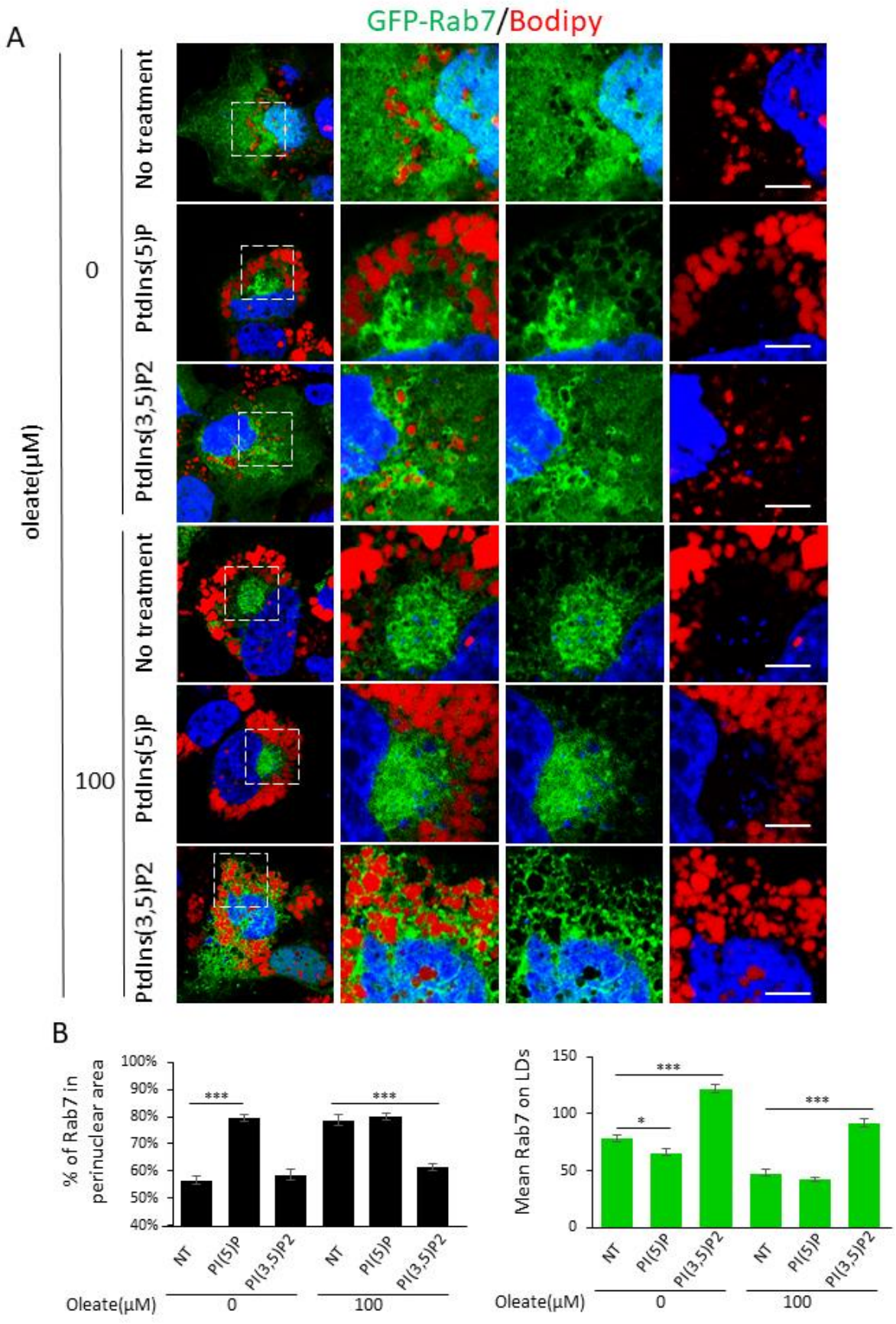
A
GFP-Rab7/Bodipy
oleate(μM)
0
100
No treatment
PtdIns(5)P
PtdIns(3,5)P2
No treatment
PtdIns(5)P
PtdIns(3,5)P2
B
% of Rab7 in perinuclear area
100%
90%
80%
70%
60%
50%
40%
***
***
NT
PI(5)P
PI(3,5)P2
NT
PI(5)P
PI(3,5)P2
Oleate(μM)
0
100
Mean Rab7 on LDs
150
100
50
0
***
*
***
NT
PI(5)P
PI(3,5)P2
NT
PI(5)P
PI(3,5)P2
Oleate(μM)
0
100

Supplemental Figure 10

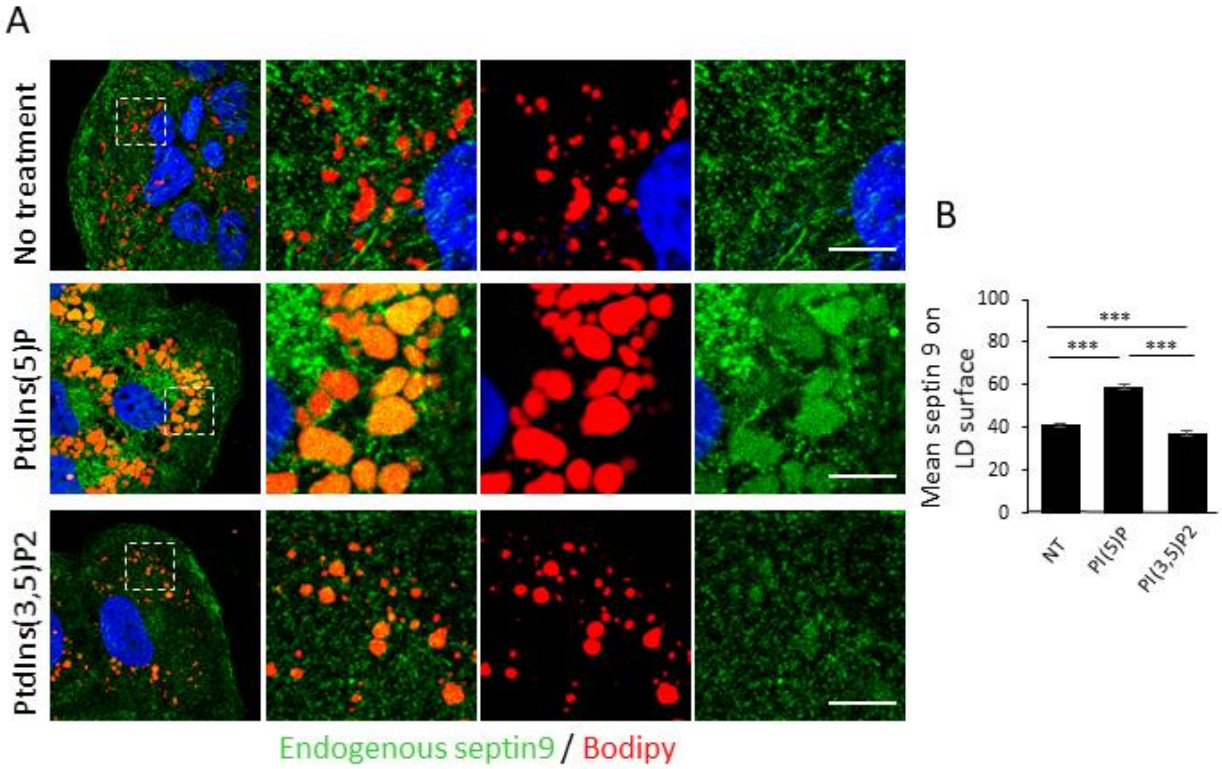

Supplemental Figure 11

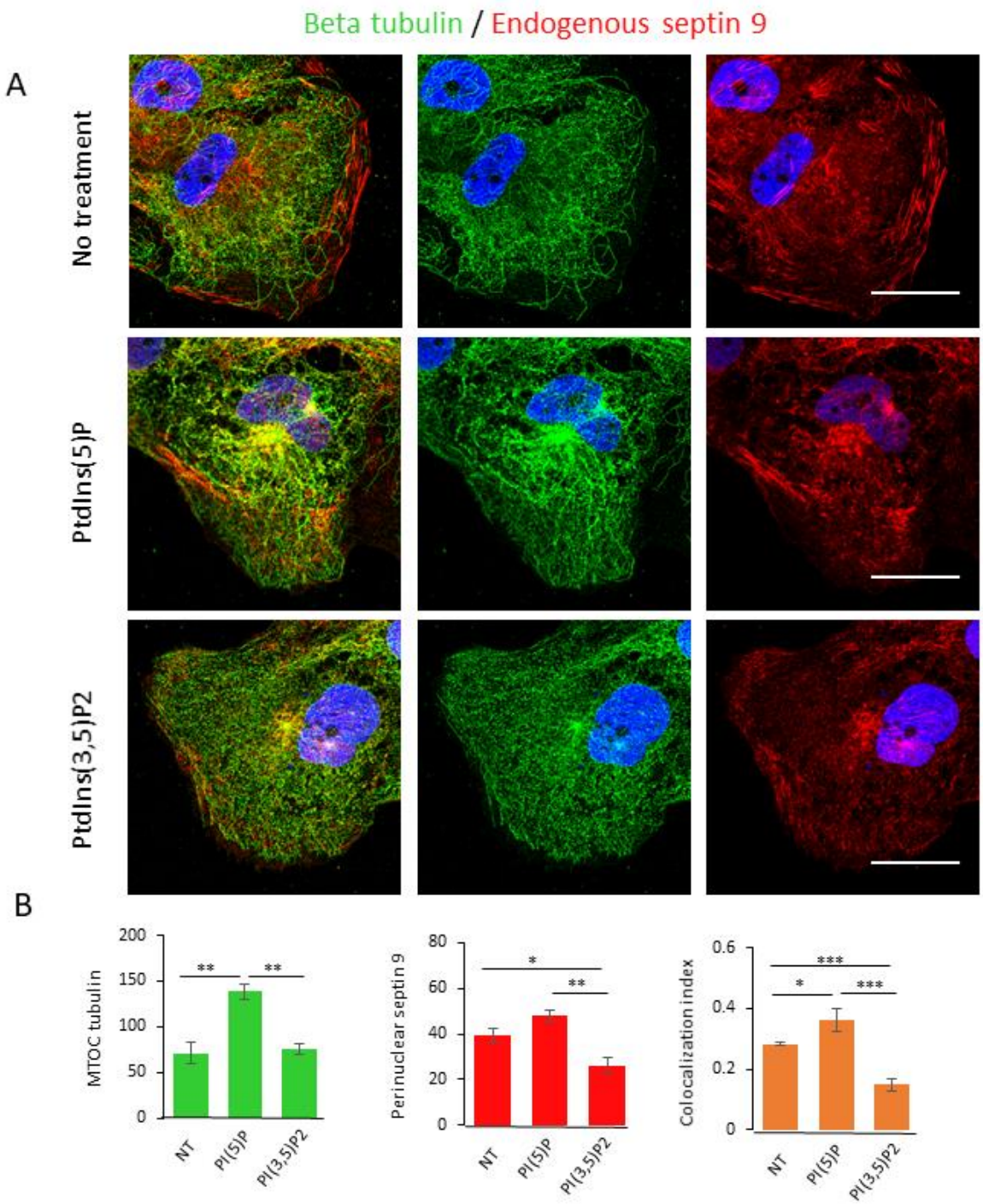

Figure 8

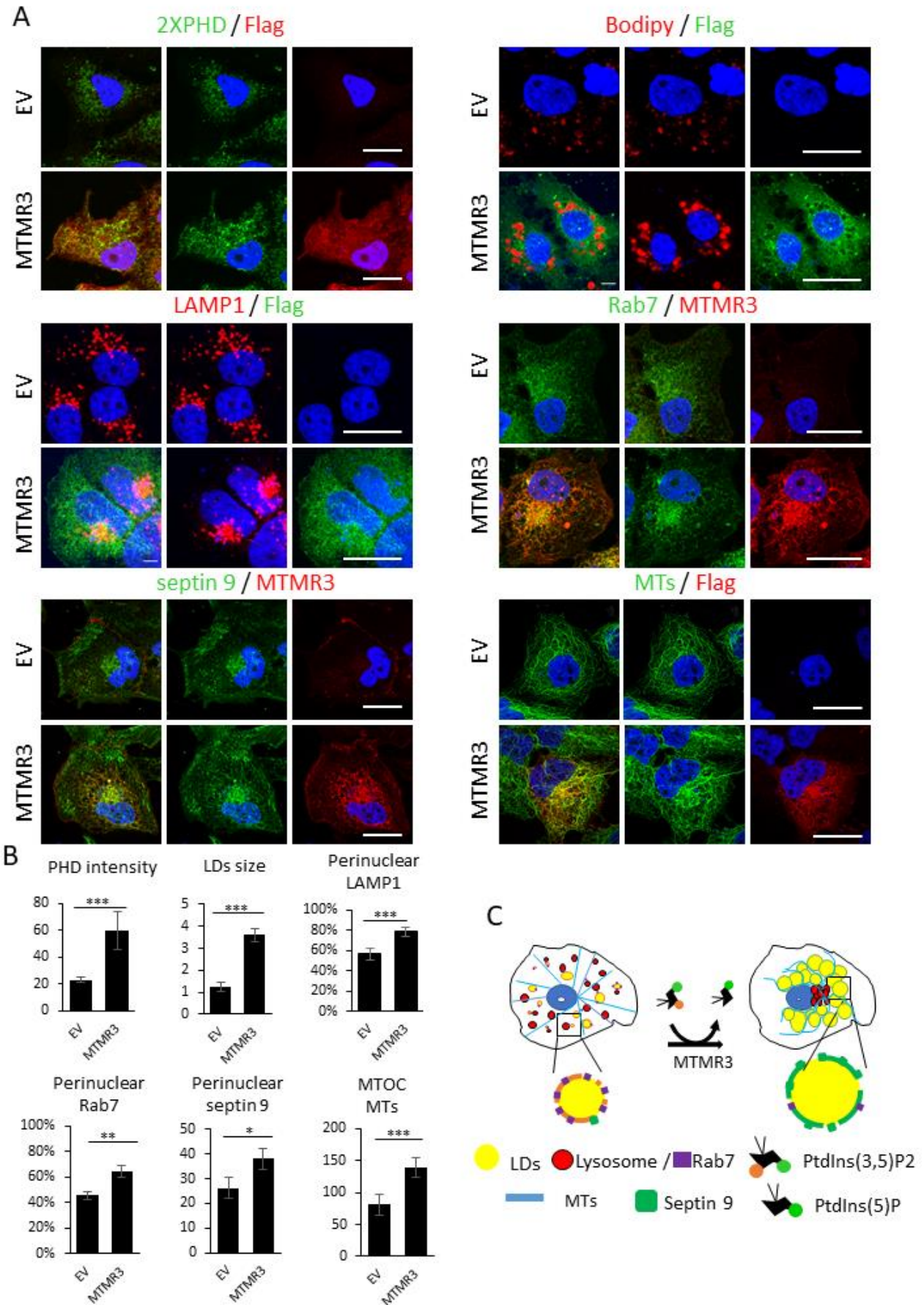
A
2XPHD / Flag
Bodipy / Flag
LAMP1 / Flag
Rab7 / MTMR3
septin 9 / MTMR3
MTs / Flag
EV
MTMR3
B
PHD intensity
LDs size
Perinuclear LAMP1
Perinuclear Rab7
Perinuclear septin 9
MTOC MTs
***
**
*
EV
MTMR3
C
MTMR3
LDs
Lysosome / Rab7
PtdIns(3,5)P2
MTs
Septin 9
PtdIns(5)P

Supplemental Figure 12

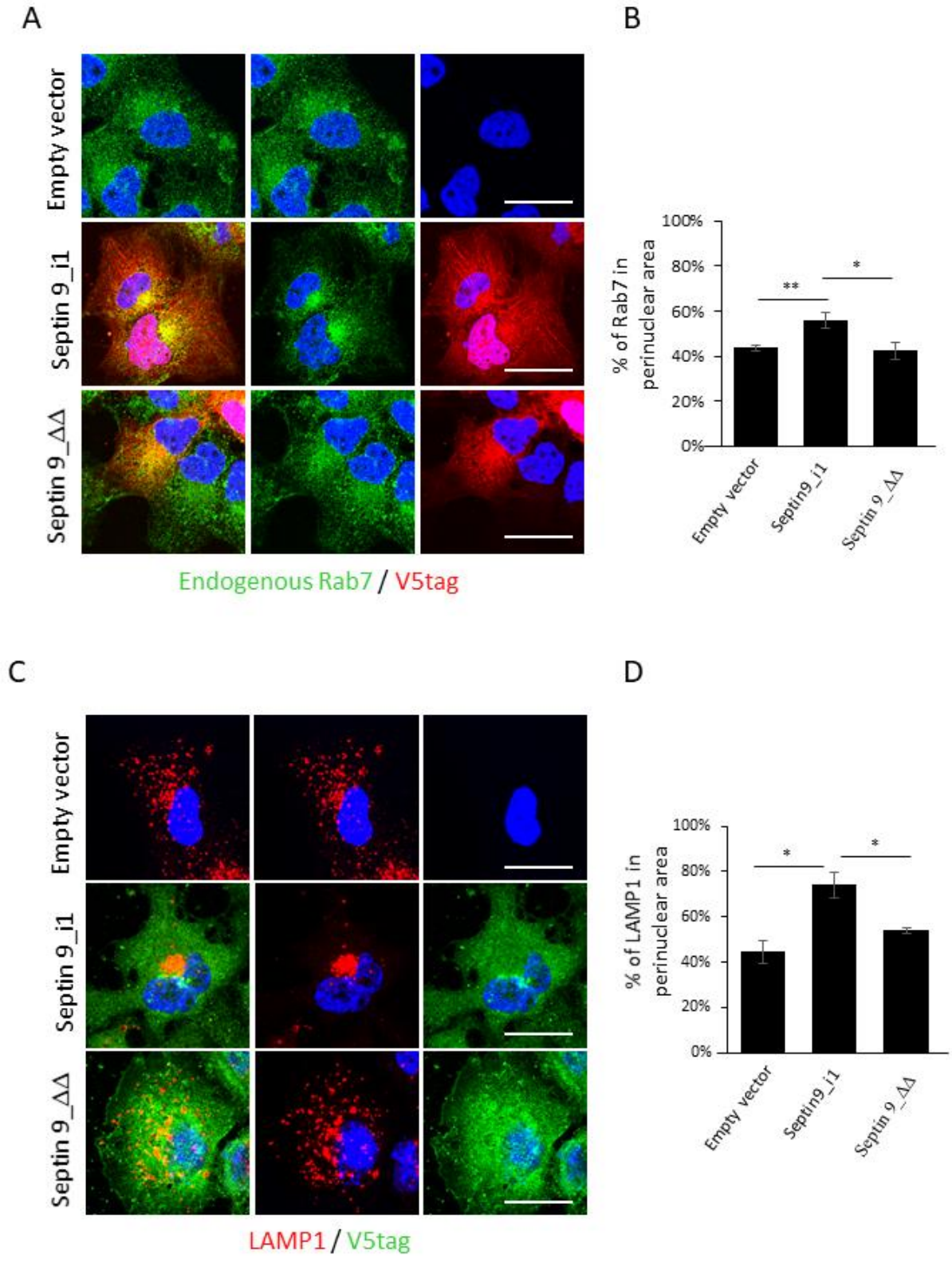

Supplemental figure 13

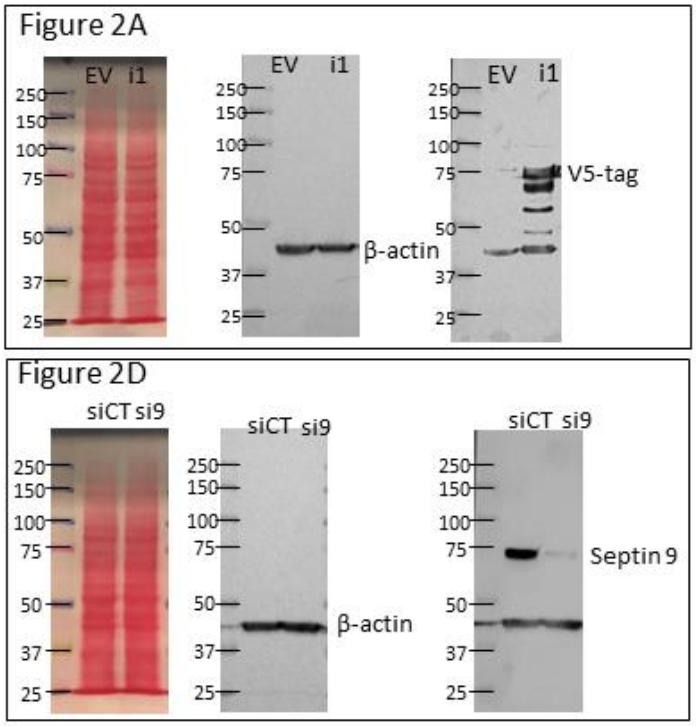


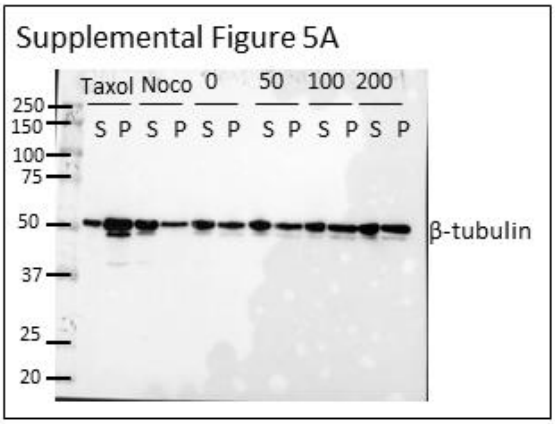

Supplemental Figure 14

A. Methods for protein signal in perinuclear and perinuclear area.

A.1 Steps

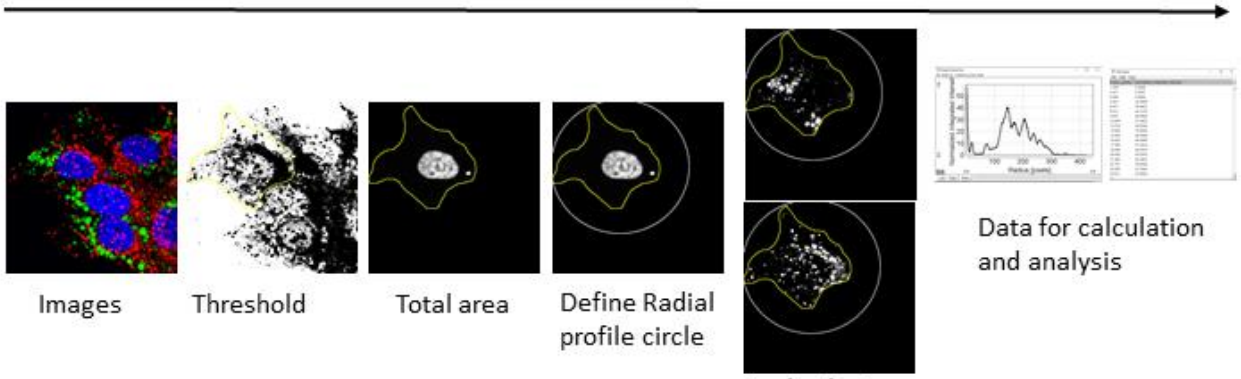


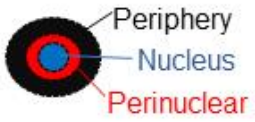


$$\%\ \text{of intensity in perinuclear area} = \frac{\text{Intensity within perinuclear area}}{\text{Intensity within total cell area}} \times 100\%$$

B. Method for protein signal around LDs.

Steps

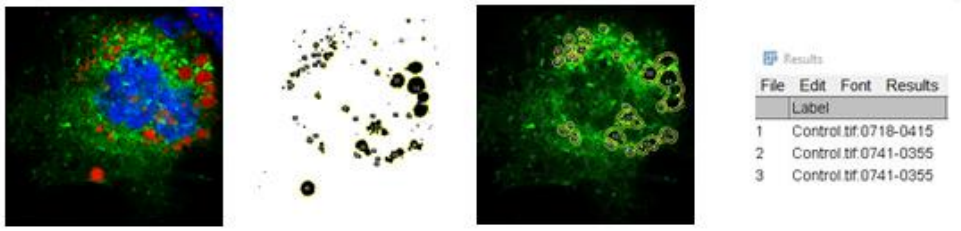


$$\text{Mean intensity} = \frac{(\text{Intensity within Area2})-(\text{Intensity within Area1})}{(\text{Area2 value})-(\text{Area1 value})}$$

## II. PIAS1 regulates Hepatitis C virus-induced lipid droplet accumulation through control of septin 9 and microtubule filament assembly

**Summary**

As described in chapter I, HCV infection is a major risk factor for the development of hepatocellular carcinoma (HCC) (Alqahtani and Colombo, 2020). Although new therapeutic approaches (direct acting antivirals (DAA)) seem to eradicate HCV, it does not completely eliminate the risk of HCC, especially in patients with advanced cirrhosis (Wu et al., 2019). We previously also reported that septin 9 contributes to HCV replication and controls LD biogenesis which is needed for the proper assembly of septins complex (Akil et al., 2016a), and further We also identified a second polybasic PB domain in septin 9 which is conserved in all the mammalian septins and involved in interaction with phosphoinositides (PI) and membrane binding and play a crucial role for septin filament assembly and maintain the proper function of Golgi structure (Omrane et al., 2019). Whether other factors that responsible for septin assembly could affect LDs were unknown.

As discirbed in chapter III, the assembly of septins may be regulated by several molecules or post-translational modifications (Hernández-Rodríguez and Momany, 2012b) such as SUMOylation (Hernández-Rodríguez and Momany, 2012b),(Takahashi et al., 1999b)(Garcia et al., 2011b). SUMOylation is a posttranslational modification that involves the covalent addition of a small ubiquitin-like modifier (SUMO) polypeptide to the target proteins. In yeast, septins were among the first proteins reported as being modified by SUMOylation (Takahashi et al., 1999b),(Johnson and Blobel, 1999b). This SUMOylation is mediated by the yeast Siz proteins, the homologous of mammalian protein inhibitor of activated STAT1 (PIAS1) (Johnson and Gupta, 2001). PIAS family consists of four genes, PIAS1, PIAS2 (PIASx), PIAS3, and PIASy (PIAS4) which mainly function as small ubiquitin-like modifiers (SUMO) E3 ligase and regulate the function of many transcription factors thereby regulating diverse cellular processes, including cell proliferation (Hoefer et al., 2012), DNA damage responses (Morozko et al., 2021; Zlatanou and Stewart, 2010), and inflammation responses (Liu and Shuai, 2008; Rytinki et al., 2009; Shuai, 2006). In mammals, the critical role of SUMO modification of specific septins 6, 7, and 11 in septin filament formation and cell division was reported. (Ribet et al., 2017b). Nevertheless, the role of SUMO ligase such as PIAS1 on the assembly and the functions of mammalian septins was not investigated.

In this study, we demonstrated a role of PIAS1 independently of IFN/STAT signaling. We showed the upregulation of PIAS1 expression upon infection by HCV, which is in agreement with data showing overexpression of this protein in liver biopsies from HCV patients (Bautista et al., 2007). In addition, we observed colocalization of HCV core and PIAS1 in the perinuclear region. Our results revealed that PIAS1, in turn, controlled the accumulation of LDs and the replication of

HCV. The progression of chronic HCV infection involves the development of steatosis. LDs play a crucial role in the HCV life cycle and mostly the interactions between HCV proteins, especially the core protein and LDs are required for the morphogenesis and production of infectious HCV (Miyanari et al., 2007; Paul et al., 2014). Our study revealed that PIAS1 modulated the redistribution of LDs and their association with HCV core (Figure 2) and thus contributed to establishing a lipid environment required for virus replication and production. Furthermore, we found that PIAS1 directly interacts with septin9_i1 and controls both the filamentous structures of septins and MT in the presence of HCV genomic replicon which is crucial for HCV-induced LD accumulation. Therefore, we suggested that, in addition to its role as a STAT signalling regulator for HCV immune escape, the PIAS1 is also hijacked by HCV to promote LDs accumulation through regulation of MT and septin 9 which are necessary for HCV replication.

To conclude, this work provided fundamental data on the functional features of PIAS1 beyond its action mediated by inhibition of STAT1 transcriptional activity, and it also brought significant insights on the host cellular machinery exploited by HCV for its replication. Thus, targeting PIAS1 may provide new antiviral approaches to combat HCV infection.

**Résumé**

Comme décrit dans le chapitre I, l'infection par le VHC est un facteur de risque majeur pour le développement du carcinome hépatocellulaire (CHC) (Alqahtani et Colombo, 2020). Bien que de nouvelles ap-proches thérapeutiques (antiviraux à action directe (AAD)) semblent éradiquer le VHC, elles n'éliminent pas complètement le risque de CHC, notamment chez les patients atteints de cirrhose avancée (Wu et al., 2019). Nous avons également rapporté précédemment que la septine 9 contribue à la réplication du VHC et contrôle la biogenèse de la GL, nécessaire à l'assemblage correct du complexe de septines (Akil et al., 2016), et nous avons également identifié un second domaine PB polybasique dans la septine 9, qui est conservé dans toutes les septines de mammifères et impliqué dans l'interaction avec les phosphoinositides (PI) et la liaison à la membrane, et joue un rôle crucial dans l'assemblage des filaments de septine et le maintien de la fonction correcte de la structure de Golgi (Omrane et al., 2019). On ne savait pas si d'autres facteurs responsables de l'assemblage des septines pouvaient affecter les GL.

Comme discuté au chapitre III, l'assemblage des septines peut être régulé par plusieurs molécules ou modifications post-traductionnelles (Hernández-Rodríguez et Momany, 2012b) telles que la SUMOylation (Hernández-Rodríguez et Momany, 2012b)(Takahashi et al., 1999b)(Garcia et al., 2011b). La SUMOylation est une modification post-traductionnelle qui implique l'addition covalente d'un petit polypeptide modificateur de type ubiq-uitin (SUMO) aux protéines cibles. Chez la levure, les septines ont été parmi les premières protéines signalées comme étant modifiées par SUMOylation (Takahashi et al., 1999b)(Johnson et Blobel, 1999b). Cette SUMOylation est médiée par les protéines Siz de la levure, homologues de la protéine inhibitrice de STAT1 activé (PIAS1) des mammifères (Johnson et Gupta, 2001). La famille PIAS se compose de quatre gènes, PIAS1, PIAS2 (PIASx), PIAS3 et PIASy (PIAS4) qui fonctionnent principalement comme une petite ubiquitine-like modifiers (SUMO) E3 ligase et régulent la fonction de nombreux facteurs de transcription, régulant ainsi divers processus cellulaires, notamment la prolifération cellulaire (Hoefer et al..., 2012), les réponses aux dommages de l'ADN (Morozko et al., 2021 ; Zlatanou et Stewart, 2010) et les réponses à l'inflammation (Liu et Shuai, 2008 ; Rytinki et al., 2009 ; Shuai, 2006). Chez les mammifères, le rôle critique de la modification SUMO de septines spécifiques 6, 7 et 11 dans la formation des filaments de septine et la division cellulaire a été ré-établi. (Ribet et al., 2017b). Néanmoins, le rôle de la SUMO ligase telle que PIAS1 sur l'assemblage et les fonctions des septines de mammifères n'a pas été étudié.

Dans cette étude, nous avons démontré un rôle de PIAS1 indépendamment de la signalisation IFN/STAT. Nous avons montré la régulation à la hausse de l'expression de PIAS1 lors d'une infection par le VHC, ce qui est en accord avec les données montrant une surexpression de cette protéine dans les biopsies hépatiques de patients atteints du VHC (Bautista et al., 2007). De

plus, nous avons observé une colocalisation du noyau du VHC et de PIAS1 dans la région périnucléaire. Nos résultats ont révélé que PIAS1 contrôlait à son tour l'accumulation des GL et la réplication du HCV. La progression de l'infection chronique par le VHC implique le développement d'un foie gras. Les GLs jouent un rôle crucial dans le cycle de vie du VHC et la plupart des interactions entre les protéines du VHC, en particulier la protéine centrale et les GLs, sont nécessaires pour la morphogenèse et la production du VHC infectieux (Miyanari et al., 2007 ; Paul et al., 2014). Notre étude a révélé que PIAS1 modulait la redistribution des LDs et leur association avec le noyau du VHC et contribuait ainsi à établir un environnement lipidique nécessaire à la réplication et à la production du virus. De plus, nous avons découvert que PIAS1 interagit directement avec septin9_i1 et contrôle à la fois les structures filamenteuses des septines et de la MT en présence du réplicon génomique du VHC, ce qui est crucial pour l'accumulation des GL induite par le VHC. Par conséquent, nous avons suggéré que, en plus de son rôle de régulateur de la signalisation STAT pour l'échappement immunitaire du VHC, le PIAS1 est également détourné par le VHC pour promouvoir l'accumulation des GL par la régulation de la MT et de la septine 9 qui sont nécessaires à la réplication du VHC.

En conclusion, ce travail a fourni des données fondamentales sur les caractéristiques fonctionnelles de PIAS1 au-delà de son action médiée par l'inhibition de l'activité transcriptionnelle de STAT1, et il a également apporté des informations importantes sur les machineries cellulaires de l'hôte exploitées par le VHC pour sa réplication. Ainsi, le ciblage de PIAS1 pourrait fournir de nouvelles approches antivirales pour combattre l'infection par le VHC.

pathogens

MDPI

*Article*

# PIAS1 Regulates Hepatitis C Virus-Induced Lipid Droplet Accumulation by Controlling Septin 9 and Microtubule Filament Assembly

**Abdellah Akil [1,2,3], Peixuan Song [1,2], Juan Peng [1,2], Claire Gondeau [4,5], Didier Samuel [1,2,6] and Ama Gassama-Diagne [1,2,*]**

[1] Unité 1193, INSERM, F-94800 Villejuif, France; akil@uab.edu (A.A.); songpx027@gmail.com (P.S.); sammialone999@hotmail.com (J.P.); didier.samuel@aphp.fr (D.S.)
[2] UMR-S 1193, Université Paris-Saclay, F-94800 Villejuif, France
[3] Department of Radiation Oncology, University of Alabama at Birmingham, Birmingham, Al 35205, USA
[4] Unité 1183, INSERM, Université Montpellier 1, F-34293 Montpellier, France; claire.gondeau@inserm.fr
[5] Department of Hepato-Gastroenterology A, Institute of Research in Biotherapy, CHU Montpellier, Hopital Saint Eloi, F-34293 Montpellier, France
[6] Centre Hépato-Biliaire, Hôpital Paul-Brousse, Assistance Publique-Hôpitaux de Paris, Université Paris-Saclay, F-94800 Villejuif, France
* Correspondence: ama.gassama@inserm.fr; Tel: +33-014-559-6070

**Abstract:** Chronic hepatitis C virus (HCV) infection often leads to fibrosis and chronic hepatitis, then cirrhosis and ultimately hepatocellular carcinoma (HCC). The processes of the HVC life cycle involve intimate interactions between viral and host cell proteins and lipid metabolism. However, the molecules and mechanisms involved in this tripartite interaction remain poorly understood. Herein, we show that the infection of HCC-derived Huh7.5 cells with HCV promotes upregulation of the protein inhibitor of activated STAT1 (PIAS1). Reciprocally, PIAS1 regulated the expression of HCV core protein and HCV-induced LD accumulation and impaired HCV replication. Furthermore, PIAS1 controlled HCV-promoted septin 9 filament formation and microtubule polymerization. Subsequently, we found that PIAS1 interacted with septin 9 and controlled its assembly on filaments, which thus affected septin 9-induced lipid droplet accumulation. Taken together, these data reveal that PIAS1 regulates the accumulation of lipid droplets and offer a meaningful insight into how HCV interacts with host proteins.

**Keywords:** HCV; PIAS1; septin 9; lipid droplets

**Citation:** Akil, A.; Song, P.; Peng, J.; Gondeau, C.; Samuel, D.; Gassama-Diagne, A. PIAS1 Regulates Hepatitis C Virus-Induced Lipid Droplet Accumulation by Controlling Septin 9 and Microtubule Filament Assembly. *Pathogens* **2021**, *10*, 1327. https://doi.org/10.3390/pathogens10101327

Academic Editor: Fabrizio Fabrizi

Received: 7 September 2021
Accepted: 13 October 2021
Published: 15 October 2021



## 1. Introduction

Hepatitis C virus (HCV) infection is a major risk factor for the development of hepatocellular carcinoma (HCC) [1]. Although new therapeutic approaches (such as direct acting antivirals; DAAs) seem to eradicate HCV, they do not completely eliminate the risk of HCC, especially in patients with advanced cirrhosis [2]. The role of hepatic steatosis in the pathogenesis of chronic hepatitis C, including fibrosis, cirrhosis, and hepatocellular carcinoma (HCC), has been shown. Although there have been several reports on the processes potentially involved, the mechanisms underlying the development of steatosis in the context of HCV infection require further investigation [3,4]. A hallmark of HCV infection is the presence of steatosis with an accumulation of lipid droplets (LDs) in the liver, which can be detected in up to 70% of infected individuals [5].

LDs are dynamic organelles that contribute to a variety of cellular functions, including the sequestration of toxic lipids [6,7], membrane biosynthesis [8,9], and lipid signaling pathways [10,11]. LDs also interact with other organelles to fulfil diverse functions and maintain cellular homeostasis [12–14]. We previously reported an elevated expression of

septin 9 in HCV-induced cirrhosis: HCV infection increased septin 9 expression and promoted its assembly into filaments, and septin 9 regulated LD growth, dependent on microtubules (MTs). We also showed that these effects of septin 9 depend on its binding to phosphoinositides (PIs) [15].

Septins form a family of GTP-binding proteins that comprise 13 identified members in mammals [16,17]. Septins form hetero-oligomeric complexes and higher-order structures (including filaments and rings), associate with cell membranes, and organize actin and microtubule cytoskeletons [16,18–21]. Septin assembly is necessary to assure their multiple cellular functions and contribute to pathological conditions, including neurological diseases [22–25], infection by several pathogens [26–31], and cancer [32–37]. Nevertheless, while many studies have provided data on the structural organization of septins, little is known about the cellular factors responsible for septin assembly [38–42]. We recently identified a second polybasic PB domain in septin 9, which is conserved in all mammalian septins and is involved in their interactions with PIs and their filamentous assembly [43]. Alongside their regulation by PIs, the assembly of septins is regulated by several molecules or post-translational modifications [44] such as SUMOylation [41,42,44–46], which involves the covalent addition of a small ubiquitin-like modifier (SUMO) polypeptide to target proteins. In yeast, septins were among the first proteins reported as being modified by SUMOylation [46,47], a process mediated by yeast Siz proteins, which are homologous with the mammalian protein inhibitor of activated STAT1 (PIAS1) [48]. The PIAS family of proteins consists of four members: PIAS1, PIAS2 (PIASx), PIAS3, and PIASy (PIAS4), which mainly function as small ubiquitin-like modifier (SUMO) E3 ligases, regulating the function of numerous transcription factors and hence diverse cellular processes, including cell proliferation [49], DNA damage responses [50,51], and inflammation responses [52–54]. In mammals, the critical role of SUMO modification of the specific septins 6, 7, and 11 in septin filament formation and cell division has been reported. [42]. Nevertheless, the effects of SUMO ligases such as PIAS1 on the assembly and functions of mammalian septins have not been investigated.

In this study, we explored the potential role of PIAS1 as a regulator of septin 9 assembly and its function in HCV pathogenesis. We demonstrated the upregulation of PIAS1 expression following infection by HCV. PIAS1 colocalized with the HCV core in the perinuclear region. The knockdown of PIAS1 affected LD growth and HCV replication. PIAS1 interacted with septin 9 and regulated the formation of its filamentous structure and MT organization. Finally, we demonstrated that PIAS1 is an essential regulator of septin 9 function in HCV-infected cells.

## 2. Result

### *2.1. HCV Infection Increases the Expression of PIAS1, Which Co-localizes with Its Core Protein*

We previously reported that septin 9 plays a role in HCV pathogenesis [15] and we hypothesized that this might be mediated by its modification by PIAS1. We therefore investigated the role of PIAS1 in HCV infection, using a cell culture infection system based on Huh7.5 cells infected with the JFH-1 (Japanese fulminant hepatitis 1) strain. We inoculated Huh7.5 cells with JFH1 particles for 72 h and the cells were fixed, stained for HCV core and PIAS1, and then analyzed by confocal microscopy (Figure 1a). In non-infected cells (Uninfected), PIAS1 displayed a fine punctate distribution, while in cells infected with HCV-JFH1 (JFH1), PIAS1 expression increased and colocalized with the HCV core protein in the perinuclear region (Figure 1b), although an increase in the nuclear staining of PIAS1 was also observed (Figure 1a). We further analyzed the expression of PIAS1 by immunoblotting (Figure 1c); HCV infection increased PIAS1 expression and promoted its colocalization with the HCV core protein in the perinuclear region. PIAS1 regulates HCV-induced LD accumulation and HCV replication, and LDs play a crucial role in HCV replication and its pathogenesis [55]. Therefore, in order to assess the role of PIAS1 in the HCV life cycle, Huh7.5 cells were transfected with PIAS1-specific siRNA and then infected

with JFH1 particles. As presented in Figure 2a, LDs were dispersed in the cytoplasm in the control cells (Uninfected + siCtrl), whereas in the JFH1-infected cells (JFH1 + siCtrl), there was an increase in and redistribution of LDs, as they are clustered and colocalized with the core protein in the perinuclear region (Figure 2a,b). The knockdown of PIAS1 strongly reduced the intensity of LDs and the HCV core, as well as the formation of their colocalized perinuclear clusters (Figure 2a,b). Interestingly, these findings are similar to those reported for septin 9 knockdown [15]. We also validated the protein decrease in PIAS1 and the HCV core using immunoblotting (Figure 2c). Subsequently, we examined the contribution of PIAS1 to HCV replication. Thus, Huh7.5 cells were first treated with PIAS1 siRNA and then infected with JFH1 particles, after which the total mRNA was isolated and analyzed by RT-PCR. As the results showed, the knockdown of PIAS1 induced a decrease in HCV RNA (Figure 2d), and analysis of the PIAS1 mRNA levels was used as a control for siRNA efficiency. Taken together, these different results indicate that PIAS1 contributes to the intracellular accumulation of LDs and the replication of HCV.

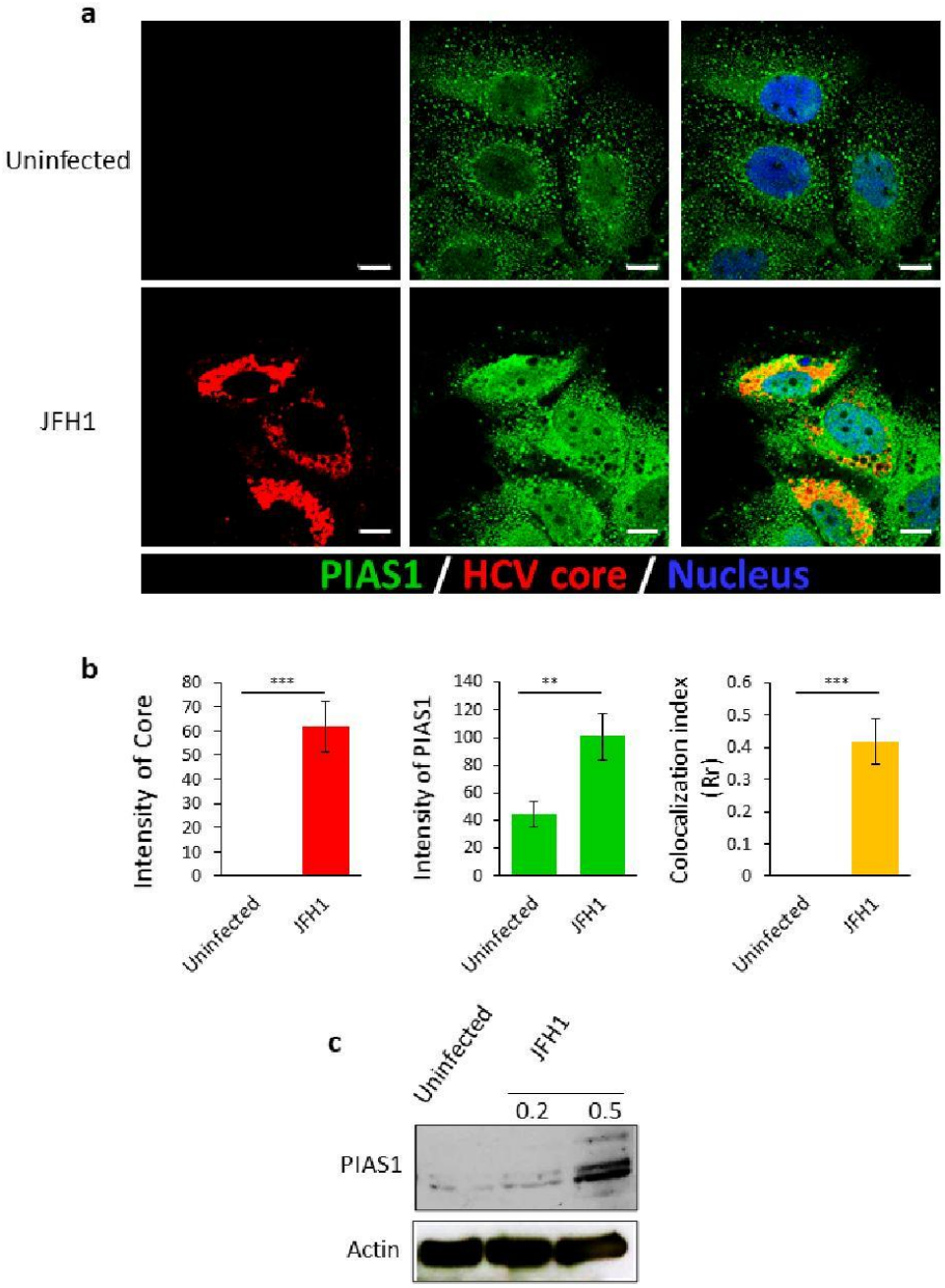


**Figure 1.** HCV infection upregulates PIAS1 expression. (**a**) Huh7.5 cells were grown overnight. The cells were then infected or not with JFH1 (0.5 Geq/cell) for 72 h, then stained for PIAS1 (green) and the HCV core (red). Scale bar, 10 µm. (**b**) The HCV core and PIAS1 intensity and the colocalization index were analyzed between the HCV core and PIAS1 of at least 30 cells from the experiments, as described in (**a**). (**c**) Huh7.5 cells were grown overnight. The cells were then infected or not with JFH1 for 0.2 or 0.5 Geq/cell for 72 h, and then analyzed by immunoblotting for PIAS1. Data information: Bar graphs present the mean ± SEM. A Student's *t*-test was used: ** $p < 0.001$, and *** $p < 0.0001$.

cells transfected with control siRNA (siCtrl) or PIAS1 siRNA (siPIAS1) (100 pmoles/assay) and JFH1-infected cells. Data information: Bar graphs present the mean ± SEM. A Student's *t*-test was used: ** $p < 0.001$.

### *2.2. PIAS1 Regulates the HCV-Induced Stabilization of Microtubules and Endogenous Septin 9 Filaments*

The dynamic microtubule (MT) network is critical for HCV infection [56]. Indeed, microtubules are necessary for the virus to enter cells and for particle assembly. The HCV core protein binds directly to tubulin and enhances microtubule polymerization [56]. Moreover, the redistribution of LDs induced by the HCV core protein is dependent on MTs and dynein [57], and we previously reported that septin 9 regulates the formation of MT filaments in HCV-infected cells [15]. According to these different reports and the data above, we postulated that PIAS1 might control septin 9 and MT filament formation. First, we validated the presence of the HCV core protein, which was co-stained with MTs in JFH1-infected cells (Figure 3a). We then stained septin 9 and MT filaments, which subsequently formed filaments that partly co-localized (Figure 3b), as previously reported [15]. Strikingly, the treatment of HCV-infected cells with PIAS1 siRNA abolished both MT and septin 9 filaments, and septin 9 displayed a vesicular structure instead (Figure 3b), thus indicating the critical role of PIAS1 in the formation of endogenous septin 9 and MT filaments.

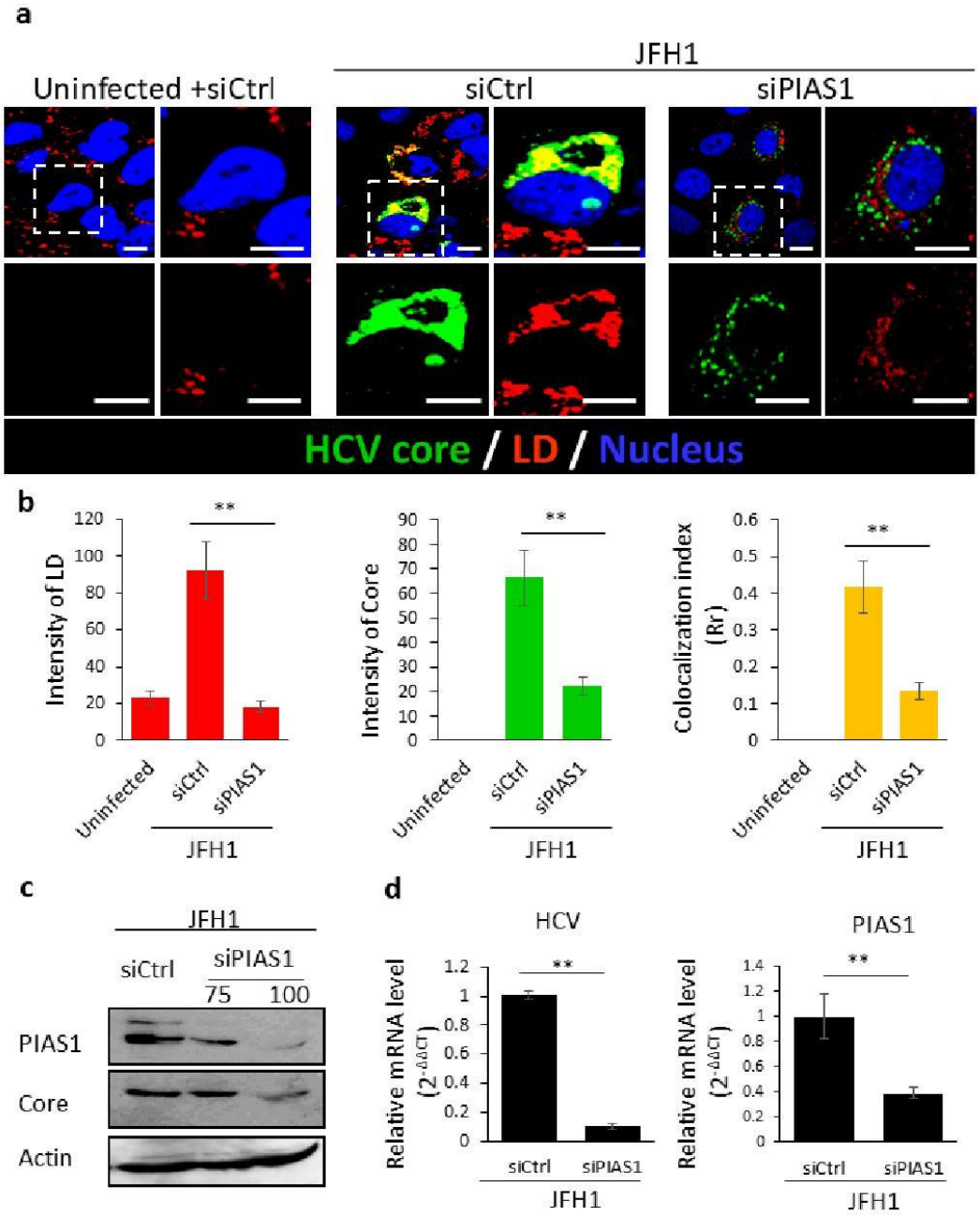


**Figure 2.** Knockdown of PIAS1 downregulates HCV replication and induces LD accumulation. (**a**) Huh7.5 cells were grown overnight. The cells were then transfected with control siRNA (siCtrl) or PIAS1 siRNA (siPIAS1) and infected or not with JFH1 for 72 h, before being stained for the HCV core (green) and LD (red), Scale bar, 10 µm. (**b**) LDs, the HCV core intensity, and the colocalization index were analyzed between the HCV core and LDs of at least 30 cells from the experiments described in (**a**). (**c**) Huh7.5 cells were grown overnight. The cells were then transfected with control siRNA (siCtrl) or PIAS1 siRNA (siPIAS1) (75 or 100 pmoles/assay), infected with JFH1 for 72 h and then analyzed by immunoblotting for PIAS1 and the HCV core. (**d**) RT-PCR assays were used to analyze PIAS1 mRNA and HCV RNA isolated from

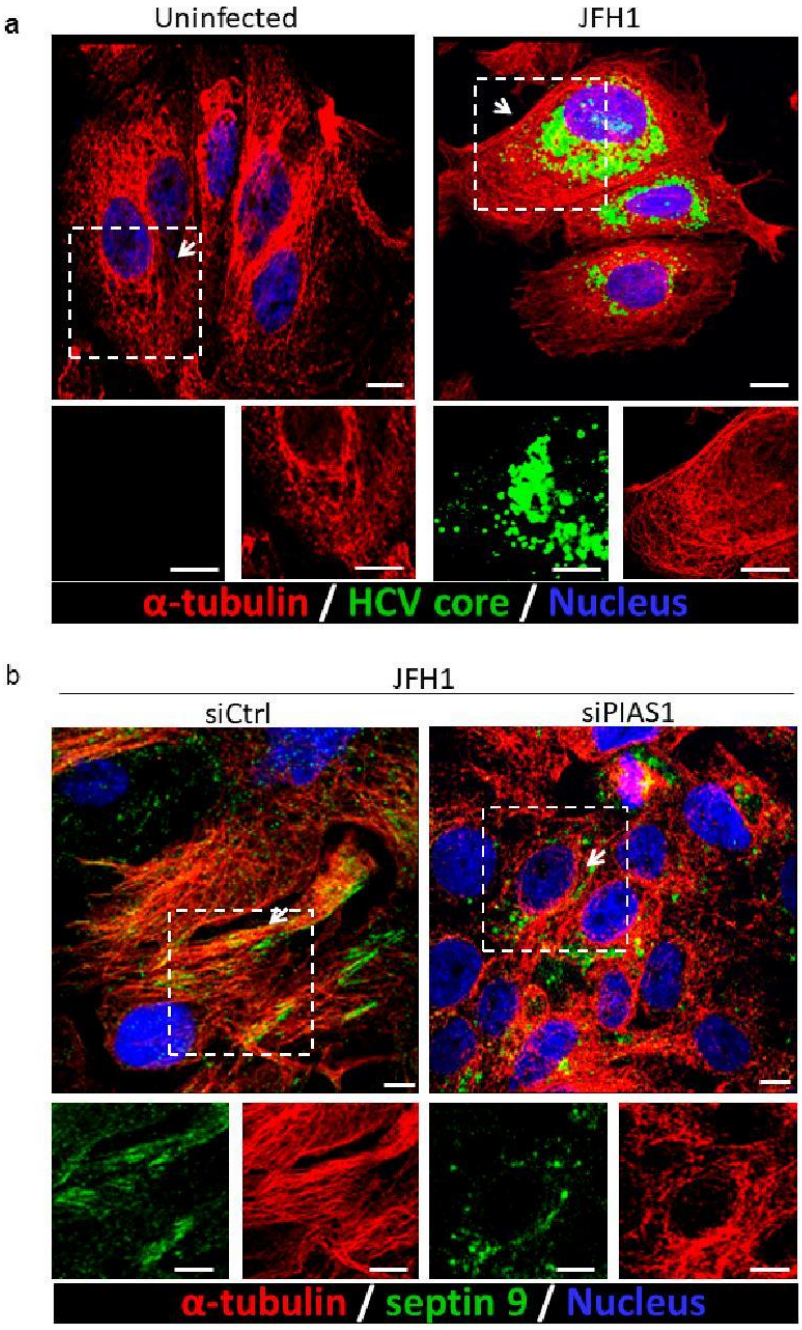


**Figure 3.** Knockdown PIAS1 disrupts HCV-induced septin 9 filament formation and MT association (**a**). Huh7.5 cells were grown overnight. The cells were then infected or not with JFH1 for 72 h and stained for the HCV core (green) and α-

tubulin (red). Scale bar, 10 μm. (**b**) Huh7.5 cells were grown overnight. The cells were transfected with control siRNA or PIAS1 siRNA and infected with JFH1 for 72 h, then stained for septin 9 (green) and β-tubulin (red). Scale bar, 10 μm.

### *2.3. PIAS1 Interacts with Septin 9_i1 and Controls its Filamentous Structure Formation and MT Organization in the Presence of the HCV Genomic Replicon*

To confirm the data obtained with endogenous septin 9 using the JFH1 model, and to further investigate the relationship between septin 9, PIAS1, and HCV, we used Huh7 cells stably expressing the HCV genomic replicon (Huh7R) [58] to perform further mechanistic studies. First, we tried to determine probable interactions between septin 9 and PIAS1 by performing immunoprecipitation (IP). Huh7R cells were transfected with the cDNA of an empty vector (EV) and the isoform 1 of septin 9 (septin 9_i1), which has the highest expression in HCV-infected cells among the five characterized septin 9 isoforms [15]. As shown in Figure 4a, PIAS1 was revealed by immunoblotting in the immunoprecipitated of septin 9_i1 using the V5 tag antibody, thus indicating a cellular interaction between septin 9 and PIAS1 (Figure 4a). We further confirmed the presence of an endogenous PIAS1 signal associated with septin 9_i1 filament by immunofluorescence performed on cells transfected with septin 9_v1 (Figure 4b). Subsequently, we validated the effect of PIAS1 on MT and septin 9 filaments in septin 9_i1-transfected Huh7R cells. The septin 9_i1 formed clear filaments that partly colocalized with MTs (Figure 4c), and treatment with PIAS1 siRNA impaired the formation of septin 9_i1 filaments (Figure 4c). In this case, septin 9_i1 gave rise to vesicular structures, which colocalized with non-assembled MTs, as observed for endogenous septin 9 in JFH1-infected cells (Figure 3b). Interestingly, treating septin 9_i1-transfected cells with nocodazole (which depolymerizes microtubules) disrupted the association between septin 9_i1 and MTs, while septin 9_i1 formed notable stress fibers (Figure 4c), as previously been reported [59]. Conversely, the treatment of cells with Taxol, which stabilizes microtubule filaments, induced the formation of stronger septin 9_i1 filaments (Figure 4c), indicating that septin_i1 filament assembly is regulated by the microtubule network. We further used the septin 9_i1-transfected Huh7R cells transfected with PIAS1 siRNA (siPIAS1) to analyze the effect of PIAS1 knockdown on septin 9_i1 expression, revealed by immunoblotting using the V5 tag antibody. The results showed that PIAS1 knockdown decreased septin 9_i1 expression in the band detected at 75 kDa (Figure 4d). Together, these data indicate that PIAS1 also regulates septin 9_i1 filament formation.

overnight. The cells were then transfected with septin 9_i1 cDNA plasmids and control siRNA (siCtrl) or PIAS1 siRNA (siPIAS1) for 48 h, and analyzed by immunoblotting for PIAS1 and the V5 tag, with actin being used as a loading control.

### *2.4. PIAS1 Regulates Septin 9-Induced LD Accumulation*

According to the effects of PIAS1 on septin 9 and MT filaments, we assessed the effect of PIAS1 depletion on the accumulation of LDs induced by septin 9_i1 (Figure 5a). Indeed, compared to cells transfected with an empty vector and control siRNA (Empty vector + siCtrl), the cells expressing septin 9_i1 (septin 9_i1 + siCtrl) displayed a higher content of LDs that formed a well-organized cluster surrounded by septin 9_v1 filaments. However, in cells co-transfected with septin 9_i1 and PIAS1 siRNA, the LDs were smaller than in septin 9_i1 cells and no clusters were observed. As expected, the formation of septin 9 filaments was also disrupted (Figure 5a,b). Here, again, these findings are very similar to those obtained with endogenous septin 9 in JFH1-infected cells (Figure 2) and reinforce the role of PIAS1 as a regulator of septin 9 filament organization, as well as its involvement in the accumulation and distribution of LDs.

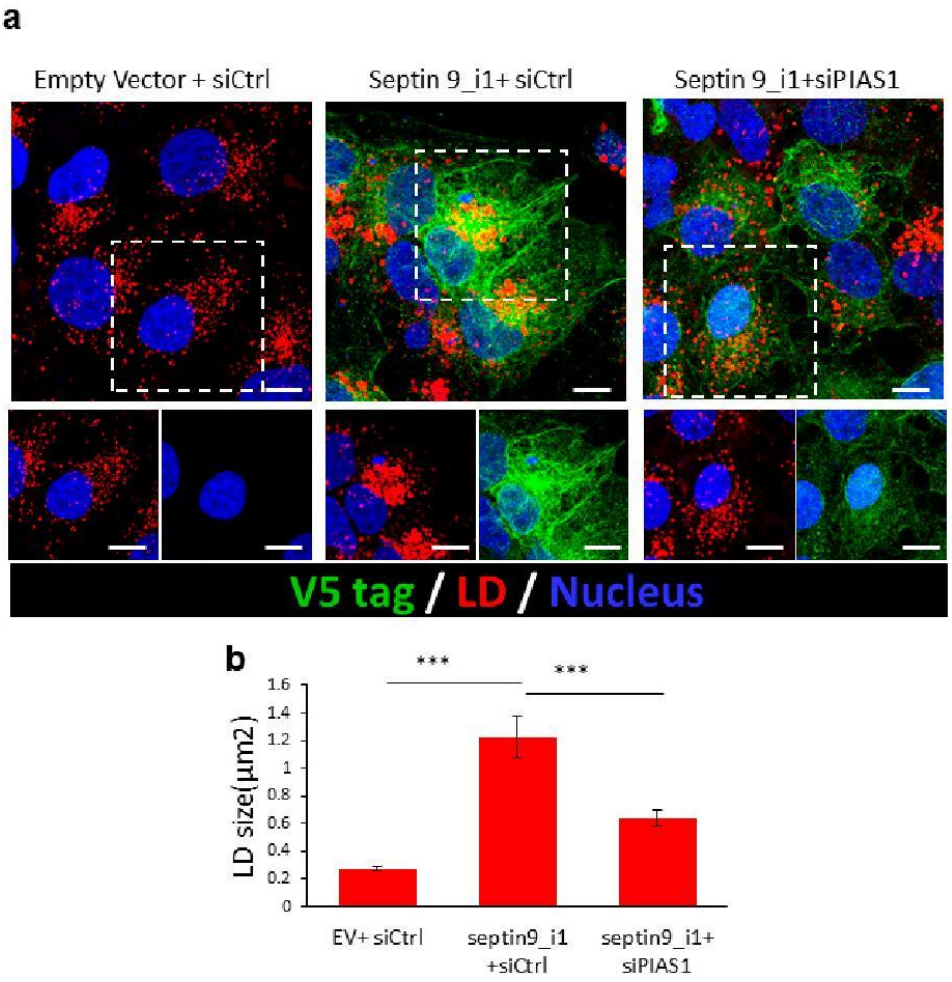

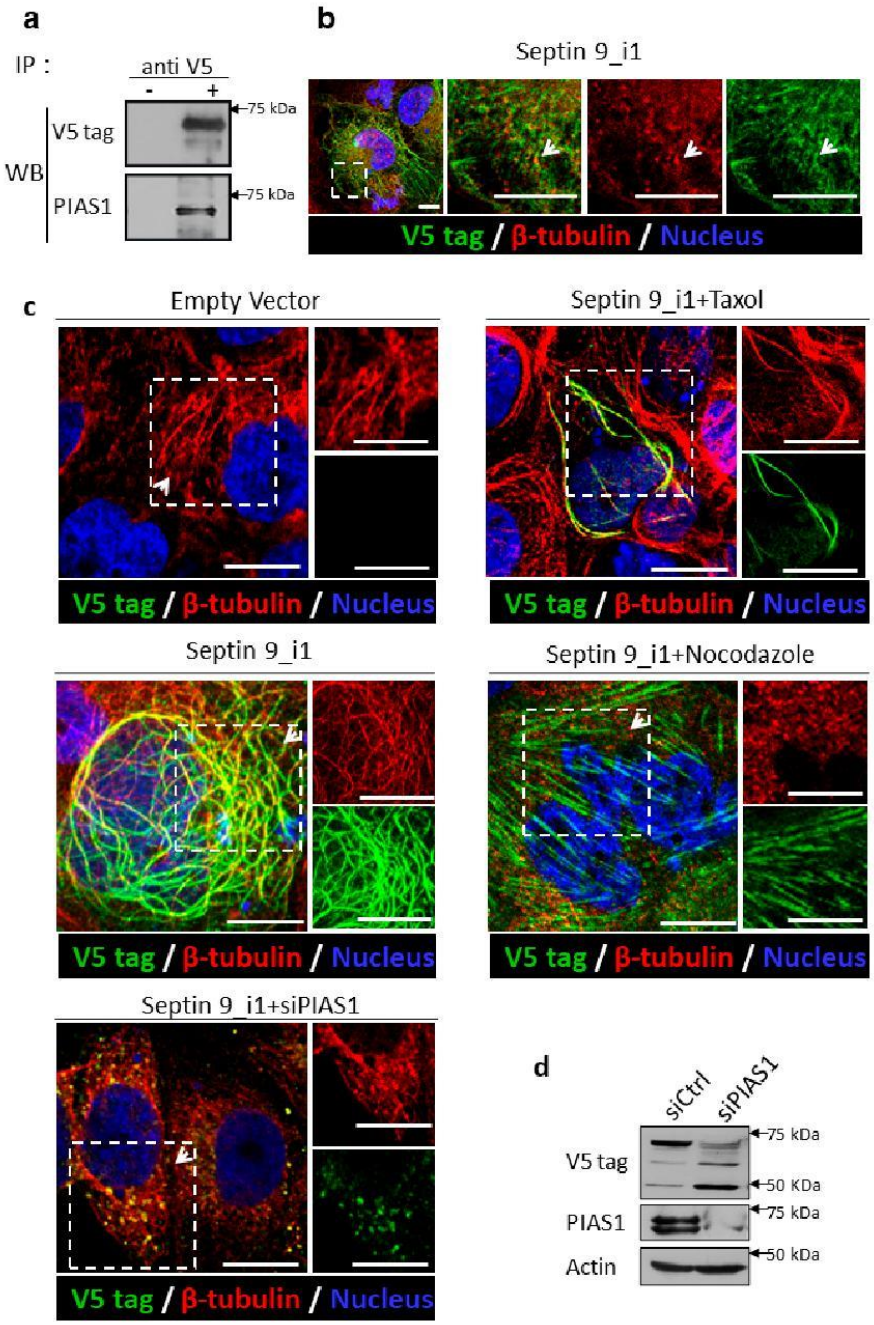


**Figure 4.** PIAS1 interacts with septin 9_v1 and affects septin 9_v1 filament formation. (**a**) Huh7R cells were transfected with septin 9_i1 and IP was performed for V5 and PIAS1. (**b**) Huh7R cells were transfected with septin 9_i1 and stained for V5 (green) and PIAS1 (red). Scale bar, 10 µm. (**c**) Huh7R cells were transfected with an empty vector or septin 9_i1 with or without PIAS1 siRNA, and stained for V5 (green) and α-tubulin (red). Scale bar, 10 µm. For the nocodazole and Taxol treatments, 33 nM nocodazole or 500 nM Taxol were added to the cells 2 h before fixation. (**d**) Huh7R cells were grown

**Figure 5.** Knockdown of PIAS1 downregulates septin 9 and induces LD accumulation. (**a**) Huh7R cells were transfected with an empty vector or septin 9_i1 with or without PIAS1 siRNA, and stained for V5 (green) and LD (red). Scale bar, 10 µm. (**b**) The size of LDs was analyzed for at least 30 cells from the experiments described in (**a**). Data information: Bar graphs present the mean ± SEM. A Student's *t*-test was used: *** $p < 0.0001$.

## 3. Discussion

The progression of chronic HCV infection involves the development of fatty liver with the accumulation of LDs in hepatocytes. LDs play a crucial role in the HCV life cycle and, in most cases, interactions between HCV proteins (particularly the HCV core protein) and LDs are required for morphogenesis and the production of infectious HCV [55,60]. Although hundreds of cellular factors have been identified as being involved in the HCV life cycle [61], how they contribute to HCV pathogenesis remains unknown.

The involvement of the PIAS1 protein in HCV infection has already been demonstrated, and it is believed that the main function of PIAS1 during HCV infection is linked to its role as a negative regulator of STAT signaling. Thereby, the upregulation of PIAS1 expression alters that of the interferon (IFN) target genes that are important to cellular defenses against HCV [62,63]. During this study, we investigated the contribution of PIAS1 in HCV replication using a different approach. We first revealed the upregulation of PIAS1 expression following infection by HCV, which is in line with data that show an overexpression of this protein in liver biopsies from HCV patients [64]. In addition, we observed a colocalization of the HCV core and PIAS1 in the perinuclear region (Figure 1). Then, we demonstrated that PIAS1, in turn, controls the accumulation of LDs and the replication of HCV (Figure 2). Furthermore, our study revealed that PIAS1 modulates the redistribution of LDs and their association with the HCV core (Figure 2) and thus contributes to establishing a lipid environment appropriate for viral replication and production.

Another important finding was the identification of PIAS1 as a regulator of septin 9 assembly in filaments, as the knockdown of PIAS1 disrupted the filamentous structure of septin 9, which became vesicular (Figure 3). Herein, we also provided evidence regarding the interaction between septin 9 and PIAS1, since PIAS1 was found in septin 9_i1-immunoprecipitated proteins and, furthermore, the partial colocalization of septin_i1 and PIAS1 was observed by the immunofluorescence study of cells containing the HCV genomic replicon (Figure 4). In our previous study, we demonstrated the role of MTs and septin 9 in HCV infection [15]. Given the fact that septin filament assembly is tightly regulated by its SUMOylation [59], and, in yeast, this SUMOylation is mediated by yeast Siz proteins, the homologs of PIAS1 [48], further studies to reveal the role of PIAS1 in mammalian septin 9 SUMOylation and the pathogenesis of HCV are required. Overall, we suggest that in addition to its role as a STAT signaling regulator for HCV immune escape, PIAS1 is also hijacked by HCV to promote LD accumulation through the regulation of MT and septin 9, which are necessary for HCV replication.

To conclude, this work has provided fundamental data on the functional features of PIAS1 as a regulator of cytoskeleton elements such as MT and septin 9 and LD metabolism. This study also offers significant insights into the host cellular machineries exploited by HCV to enable its replication. Targeting PIAS1 may therefore enable new antiviral approaches to combat HCV infection.

## 4. Materials and Methods

### *4.1. Antibodies and Reagents*

Anti-mouse β-actin came from Sigma, and anti-rabbit PIAS1, anti-V5 tag, and anti-mouse HCV core were obtained from Abcam. Anti-mouse Alexa Fluor 488 or 546 came from Invitrogen. Nuclei were stained with Hoechst from Invitrogen. Nocodazole and Taxol were obtained from Sigma. For immunoblotting and immunofluorescence, the antibody was diluted at a ratio of 1:500 and 1:100, respectively.

### *4.8. RNA Extraction and RT-PCR Analysis*

Total RNA was isolated using an RNAble solution (Eurobio, Les Ulis, France) and intracellular levels of positive strand HCV RNA were quantified using a strand-specific qRT-PCR technique with a Light Cycler Fast Start DNA MasterPlus SYBR Green I mix (Roche, Mannheim, Germany) on a Light Cycler 480 Real-Time PCR System (Roche, Mannheim, Germany). The triplicate mean values were calculated according to the Ct quantification method using GAPDH gene transcription as the reference for normalization. Details on the methods using specific primers and probes are available on request. The average levels of HCV RNA compared to the positive control, obtained during triplicate experiments, are shown.

### *4.9. Image Acquisition and Analysis*

Images were acquired with a Zeiss 510 LSM confocal microscope or Leica TCS SP5 (Leica Microsystems, available on April, 2016). For colocalization analysis, images were treated by ImageJ software, and plugin "Intensity Correlation Analysis" was used to generate the Pearson's correlation coefficient (Rr), which ranged from −1 (perfect exclusion) to +1 (perfect correlation).

To calculate the total intensity of the HCV core and LDs, images obtained by confocal microscopy were processed by cell ROI using the freehand selection tool, then the total intensity of the HCV core and LDs were measured by ImageJ analyses.

### *4.10. Statistical Analyses*

Comparisons of mean values were conducted using unpaired Student's *t*-tests. Statistical significance was determined at * $p < 0.05$, ** $p < 0.001$, and *** $p < 0.0001$.

**Author Contributions:** A.A. contributed to the design, performed experiments, analyzed the data, and wrote the manuscript. P.S. performed the experiments, analyzed the data, and wrote the manuscript. J.P. analyzed and discussed the data. C.G. performed the infection of cells using the JFH1 virus particles and discussed the data. D.S. discussed the data. A.G.-D. conceived and supervised the project, designed the experiments, and wrote the manuscript. All authors have read and agreed to the published version of the manuscript.

**Funding:** This work was supported by grants from the French ANRS (Agence Nationale pour la Recherche sur le SIDA et les hépatites virales) and Association pour la Recherche sur le Cancer (ARC/SUBV/CKLQ6) to A.G.-D., A.A. was supported by a fellowship of RII Pasteur, University of Paris XI and CHB association. P.S. was supported by a scholarship from Chinese Scholarship Council. C.G. was supported by a grant from French ANRS.

**Institutional Review Board Statement:** Not applicable.

**Informed Consent Statement:** Not applicable.

**Data Availability Statement:** The data presented in this study are available in the main text, figures, tables.

**Conflicts of Interest:** The authors declare that they have no conflicts of interest.

## References

1. Alqahtani, S.A.; Colombo, M. Viral Hepatitis as a Risk Factor for the Development of Hepatocellular Carcinoma. *Hepatoma Res.* **2020**, *6*, 58, doi:10.20517/2394–5079.2020.49.
2. Wu, P.-S.; Chang, T.-S.; Lu, S.-N.; Su, H.-J.; Chang, S.-Z.; Hsu, C.-W.; Chen, M.-Y. An Investigation of the Side Effects, Patient Feedback, and Physiological Changes Associated with Direct-Acting Antiviral Therapy for Hepatitis C. *Int. J. Environ. Res. Public Health* **2019**, *16*, 4981, doi:10.3390/ijerph16244981.
3. Asselah, T.; Rubbia-Brandt, L.; Marcellin, P.; Negro, F. Steatosis in Chronic Hepatitis C: Why Does It Really Matter? *Gut* **2006**, *55*, 123–130, doi:10.1136/gut.2005.069757.
4. Koike, K. Steatosis, Liver Injury, and Hepatocarcinogenesis in Hepatitis C Viral Infection. *J. Gastroenterol.* **2009**, *44* (Suppl. 19), 82–88, doi:10.1007/s00535-008-2276-4.

### 4.2. Cell Culture

Huh7.5, Huh7 cells harboring the HCV genome-length replicon, and Huh7.5-infected cells were cultured in Dulbecco's Modified Eagle's Medium (DMEM; Invitrogen, Paisley, UK) containing 4.5 g/L of glucose supplemented with 10% heat-inactivated fetal bovine serum, 1% nonessential amino acids (Invitrogen, Paisley, UK), and 1% penicillin/streptomycin (Invitrogen, Paisley, UK).

### 4.3. siRNAs and Cell Transfection

The endogenous expression of PIAS1 was silenced by transfection with a pool of specific siRNAs PIAS1 (si1: sc-36219 and si2: sc-36220; Santa Cruz, Dallas, TX, USA). Huh7.5 cells were grown in 12-well plates or on glass coverslips and transiently transfected with 75/100 pmol siRNA oligonucleotide of PIAS1 at 40–50% confluence using Lipofectamine RNAiMAX (Invitrogen, Paisley, UK) according to the manufacturer's protocol. Control non-targeting siRNAs were used as a negative control (Genecust, Boynes, France). Depending on the experiments, cells were lysed in lysis buffer containing a cocktail of protease inhibitors (Roche, Meylan, France), fixed with 3.7% paraformaldehyde for immunofluorescence staining or used for the isolation of total RNA with RNAble solution (Eurobio, Les Ulis, France).

### 4.4. Immunoblotting

Cells were collected on ice, washed and lysed in 20 mM Tris, HCl, 100 mM NaCl, 1% Triton X100, and 10 mM EDTA at pH 7.4 containing a protease and phosphatase inhibitor cocktail (Roche Diagnostics). The proteins were separated on SDS-PAGE, blotted onto a PVDF membrane, and visualized using a chemiluminescence reagent (Amersham, Darmstadt, Germany).

### 4.5. Immunofluorescence Staining

Huh7.5 cells were grown on glass coverslips in 12-well plates, treated depending on the experiments, fixed with 3.7% paraformaldehyde, permeabilized, and saturated with PBS supplemented with 0.7% fish gelatin and 0.025% saponin. Primary antibodies were diluted with permeabilization solution and incubated with the cells. After several washes, staining was performed with fluorescent secondary antibodies and Hoechst. The lipophilic fluorescence dye LD 540 was used to stain the lipid droplets. For the nocodazole and Taxol treatments, the cells were cultured with 33 nM nocodazole or 500 nM Taxol containing medium 2 h prior to fixation.

### 4.6. JFH1/HCVcc Inoculation

Cells were infected with HCV at 37 °C for 3 h, and then the unbound viruses were removed by aspiration and by washing the cells three times with PBS. At 48 h post-infection, the infected cells were either lysed in lysis buffer (used for the isolation of total RNA) or fixed with 3.7% paraformaldehyde. The levels of HCV proteins in the HCV-infected cells were determined by Western blotting, while the levels of HCV RNA were quantified using the reverse transcription polymerase chain reaction (RT-PCR) method, and IFA staining was performed with fluorescent secondary antibodies.

### 4.7. Determination of Infectious HCV Titer

Serially diluted HCV was used to infect naive Huh-7.5 cells in 24-well plates. Three days post-infection, focus-forming units (FFUs) were determined by IFA staining using a specific monoclonal antibody. The infectious HCV titer was calculated from the average number of NS5A-positive FFU/mL in triplicate assays.

5. Leandro, G.; Mangia, A.; Hui, J.; Fabris, P.; Rubbia-Brandt, L.; Colloredo, G.; Adinolfi, L.E.; Asselah, T.; Jonsson, J.R.; Smedile, A.; et al. Relationship between Steatosis, Inflammation, and Fibrosis in Chronic Hepatitis C: A Meta-Analysis of Individual Patient Data. *Gastroenterology* **2006**, *130*, 1636–1642, doi:10.1053/j.gastro.2006.03.014.
6. Herms, A.; Bosch, M.; Reddy, B.J.N.; Schieber, N.L.; Fajardo, A.; Rupérez, C.; Fernández-Vidal, A.; Ferguson, C.; Rentero, C.; Tebar, F.; et al. AMPK Activation Promotes Lipid Droplet Dispersion on Detyrosinated Microtubules to Increase Mitochondrial Fatty Acid Oxidation. *Nat. Commun.* **2015**, *6*, 1–14, doi:10.1038/ncomms8176.
7. Rambold, A.S.; Cohen, S.; Lippincott-Schwartz, J. Fatty Acid Trafficking in Starved Cells: Regulation by Lipid Droplet Lipolysis, Autophagy, and Mitochondrial Fusion Dynamics. *Dev. Cell* **2015**, *32*, 678–692, doi:10.1016/j.devcel.2015.01.029.
8. Kurat, C.F.; Wolinski, H.; Petschnigg, J.; Kaluarachchi, S.; Andrews, B.; Natter, K.; Kohlwein, S.D. Cdk1/Cdc28-Dependent Activation of the Major Triacylglycerol Lipase Tgl4 in Yeast Links Lipolysis to Cell-Cycle Progression. *Mol. Cell* **2009**, *33*, 53–63, doi:10.1016/j.molcel.2008.12.019.
9. Chauhan, N.; Visram, M.; Cristobal-Sarramian, A.; Sarkleti, F.; Kohlwein, S.D. Morphogenesis Checkpoint Kinase Swe1 Is the Executor of Lipolysis-Dependent Cell-Cycle Progression. *Proc. Natl. Acad. Sci. USA* **2015**, *112*, E1077–E1085, doi:10.1073/pnas.1423175112.
10. Haemmerle, G.; Moustafa, T.; Woelkart, G.; Büttner, S.; Schmidt, A.; van de Weijer, T.; Hesselink, M.; Jaeger, D.; Kienesberger, P.C.; Zierler, K.; et al. ATGL-Mediated Fat Catabolism Regulates Cardiac Mitochondrial Function via PPAR-α and PGC-1. *Nat. Med.* **2011**, *17*, 1076–1085, doi:10.1038/nm.2439.
11. Tang, T.; Abbott, M.J.; Ahmadian, M.; Lopes, A.B.; Wang, Y.; Sul, H.S. Desnutrin/ATGL Activates PPARδ to Promote Mitochondrial Function for Insulin Secretion in Islet β Cells. *Cell Metab.* **2013**, *18*, 883–895, doi:10.1016/j.cmet.2013.10.012.
12. Schuldiner, M.; Bohnert, M. A Different Kind of Love—Lipid Droplet Contact Sites. *Biochim. Biophys. Acta Mol. Cell Biol. Lipids* **2017**, *1862*, 1188–1196, doi:10.1016/j.bbalip.2017.06.005.
13. Barbosa, A.D.; Siniossoglou, S. Function of Lipid Droplet-Organelle Interactions in Lipid Homeostasis. *Biochim. Biophys. Acta BBA Mol. Cell Res.* **2017**, *1864*, 1459–1468, doi:10.1016/j.bbamcr.2017.04.001.
14. Barbosa, A.D.; Savage, D.B.; Siniossoglou, S. Lipid Droplet-Organelle Interactions: Emerging Roles in Lipid Metabolism. *Curr. Opin. Cell Biol.* **2015**, *35*, 91–97, doi:10.1016/j.ceb.2015.04.017.
15. Akil, A.; Peng, J.; Omrane, M.; Gondeau, C.; Desterke, C.; Marin, M.; Tronchère, H.; Taveneau, C.; Sar, S.; Briolotti, P.; et al. Septin 9 Induces Lipid Droplets Growth by a Phosphatidylinositol-5- Phosphate and Microtubule-Dependent Mechanism Hijacked by HCV. *Nat. Commun.* **2016**, *7*, 12203, doi:10.1038/ncomms12203.
16. Kim, M.S.; Froese, C.D.; Estey, M.P.; Trimble, W.S. SEPT9 Occupies the Terminal Positions in Septin Octamers and Mediates Polymerization-Dependent Functions in Abscission. *J. Cell Biol.* **2011**, *195*, 815–826, doi:10.1083/jcb.201106131.
17. Marcus, E.A.; Tokhtaeva, E.; Turdikulova, S.; Capri, J.; Whitelegge, J.P.; Scott, D.R.; Sachs, G.; Berditchevski, F.; Vagin, O. Septin Oligomerization Regulates Persistent Expression of ErbB2/HER2 in Gastric Cancer Cells. *Biochem. J.* **2016**, *473*, 1703–1718, doi:10.1042/BCJ20160203.
18. Kinoshita, M.; Field, C.M.; Coughlin, M.L.; Straight, A.F.; Mitchison, T.J. Self- and Actin-Templated Assembly of Mammalian Septins. *Dev. Cell* **2002**, *3*, 791–802, doi:10.1016/S1534-5807(02)00366-0.
19. Mostowy, S.; Cossart, P. Septins: The Fourth Component of the Cytoskeleton. *Nat. Rev. Mol. Cell Biol.* **2012**, *13*, 183–194, doi:10.1038/nrm3284.
20. Sellin, M.E.; Sandblad, L.; Stenmark, S.; Gullberg, M. Deciphering the Rules Governing Assembly Order of Mammalian Septin Complexes. *Mol. Biol. Cell* **2011**, *22*, 3152–3164, doi:10.1091/mbc.e11-03-0253.
21. Barral, Y.; Kinoshita, M. Structural Insights Shed Light onto Septin Assemblies and Function. *Curr. Opin. Cell Biol.* **2008**, *20*, 12–18, doi:10.1016/j.ceb.2007.12.001.
22. Ihara, M.; Tomimoto, H.; Kitayama, H.; Morioka, Y.; Akiguchi, I.; Shibasaki, H.; Noda, M.; Kinoshita, M. Association of the Cytoskeletal GTP-Binding Protein Sept4/H5 with Cytoplasmic Inclusions Found in Parkinson's Disease and Other Synucleinopathies. *J. Biol. Chem.* **2003**, *278*, 24095–24102, doi:10.1074/jbc.M301352200.
23. Shehadeh, L.; Mitsi, G.; Adi, N.; Bishopric, N.; Papapetropoulos, S. Expression of Lewy Body Protein Septin 4 in Postmortem Brain of Parkinson's Disease and Control Subjects. *Mov. Disord.* **2009**, *24*, 204–210, doi:10.1002/mds.22306.
24. Pennington, K.; Beasley, C.L.; Dicker, P.; Fagan, A.; English, J.; Pariante, C.M.; Wait, R.; Dunn, M.J.; Cotter, D.R. Prominent Synaptic and Metabolic Abnormalities Revealed by Proteomic Analysis of the Dorsolateral Prefrontal Cortex in Schizophrenia and Bipolar Disorder. *Mol. Psychiatry* **2008**, *13*, 1102–1117, doi:10.1038/sj.mp.4002098.
25. Tada, T.; Simonetta, A.; Batterton, M.; Kinoshita, M.; Edbauer, D.; Sheng, M. Role of Septin Cytoskeleton in Spine Morphogenesis and Dendrite Development in Neurons. *Curr. Biol.* **2007**, *17*, 1752–1758, doi:10.1016/j.cub.2007.09.039.
26. Pizarro-Cerdá, J.; Jonquières, R.; Gouin, E.; Vandekerckhove, J.; Garin, J.; Cossart, P. Distinct Protein Patterns Associated with Listeria Monocytogenes InlA- or InlB-Phagosomes. *Cell Microbiol.* **2002**, *4*, 101–115, doi:10.1046/j.1462-5822.2002.00169.x.
27. Boddy, K.C.; Gao, A.D.; Truong, D.; Kim, M.S.; Froese, C.D.; Trimble, W.S.; Brumell, J.H. Septinregulated Actin Dynamics Promote Salmonella Invasion of Host Cells. *Cell Microbiol.* **2018**, *20*, e12866, doi:10.1111/cmi.12866.
28. Lee, P.P.; Lobato-Márquez, D.; Pramanik, N.; Sirianni, A.; Daza-Cajigal, V.; Rivers, E.; Cavazza, A.; Bouma, G.; Moulding, D.; Hultenby, K.; et al. Wiskott-Aldrich Syndrome Protein Regulates Autophagy and Inflammasome Activity in Innate Immune Cells. *Nat. Commun.* **2017**, *8*, 1576, doi:10.1038/s41467-017-01676-0.
29. Mostowy, S.; Cossart, P. Cytoskeleton Rearrangements during Listeria Infection: Clathrin and Septins as New Players in the Game. *Cell Motil.* **2009**, *66*, 816–823, doi:10.1002/cm.20353.

30. Mostowy, S.; Janel, S.; Forestier, C.; Roduit, C.; Kasas, S.; Pizarro-Cerdá, J.; Cossart, P.; Lafont, F. A Role for Septins in the Interaction between the Listeria Monocytogenes INVASION PROTEIN InlB and the Met Receptor. *Biophys. J.* **2011**, *100*, 1949–1959, doi:10.1016/j.bpj.2011.02.040.
31. Pfanzelter, J.; Mostowy, S.; Way, M. Septins Suppress the Release of Vaccinia Virus from Infected Cells. *J. Cell Biol.* **2018**, *217*, 2911–2929, doi:10.1083/jcb.201708091.
32. Dolat, L.; Hu, Q.; Spiliotis, E.T. Septin Functions in Organ System Physiology and Pathology. *Biol. Chem.* **2014**, *395*, 123–141, doi:10.1515/hsz-2013-0233.
33. Montagna, C.; Sagie, M.; Zechmeister, J. Mammalian Septins in Health and Disease. *Res. Rep. Biochem.* **2015**, *2015*, 59–72, doi:10.2147/RRBC.S59060.
34. Marcus, J.; Bejerano-Sagie, M.; Patterson, N.; Bagchi, S.; Verkhusha, V.V.; Connolly, D.; Goldberg, G.L.; Golden, A.; Sharma, V.P.; Condeelis, J.; et al. Septin 9 Isoforms Promote.Tumorigenesis in Mammary Epithelial Cells by Increasing Migration and ECM Degradation through Metalloproteinase Secretion at Focal Adhesions. *Oncogene* **2019**, *38*, 5839–5859, doi:10.1038/s41388-019-0844-0.
35. Diesenberg, K.; Beerbaum, M.; Fink, U.; Schmieder, P.; Krauss, M. SEPT9 Negatively Regulates Ubiquitin-Dependent Down-regulation of EGFR. *J. Cell Sci.* **2015**, *128*, 397–407, doi:10.1242/jcs.162206.
36. Xu, D.; Liu, A.; Wang, X.; Chen, Y.; Shen, Y.; Tan, Z.; Qiu, M. Repression of Septin9 and Septin2 Suppresses Tumor Growth of Human Glioblastoma Cells. *Cell Death Dis.* **2018**, *9*, 514, doi:10.1038/s41419-018-0547-4.
37. Zhang, N.; Liu, L.; Fan, N.; Zhang, Q.; Wang, W.; Zheng, M.; Ma, L.; Li, Y.; Shi, L. The Requirement of SEPT2 and SEPT7 for Migration and Invasion in Human Breast Cancer via MEK/ERK Activation. *Oncotarget* **2016**, *7*, 61587–61600, doi:10.18632/oncotarget.11402.
38. Nagata, K.; Asano, T.; Nozawa, Y.; Inagaki, M. Biochemical and Cell Biological Analyses of a Mammalian Septin Complex, Sept7/9b/11. *J. Biol. Chem.* **2004**, *279*, 55895–55904, doi:10.1074/jbc.M406153200.
39. Sirajuddin, M.; Farkasovsky, M.; Hauer, F.; Kühlmann, D.; Macara, I.G.; Weyand, M.; Stark, H.; Wittinghofer, A. Structural Insight into Filament Formation by Mammalian Septins. *Nature* **2007**, *449*, 311–315, doi:10.1038/nature06052.
40. Spiliotis, E.T.; Nelson, W.J. Here Come the Septins: Novel Polymers That Coordinate Intracellular Functions and Organization. *J. Cell Sci.* **2006**, *119*, 4–10, doi:10.1242/jcs.02746.
41. Hendriks, I.A.; Lyon, D.; Young, C.; Jensen, L.J.; Vertegaal, A.C.O.; Nielsen, M.L. Site-Specific Mapping of the Human SUMO Proteome Reveals Co-Modification with Phosphorylation. *Nat. Struct. Mol. Biol.* **2017**, *24*, 325–336, doi:10.1038/nsmb.3366.
42. Ribet, D.; Boscaini, S.; Cauvin, C.; Siguier, M.; Mostowy, S.; Echard, A.; Cossart, P. SUMOylation of Human Septins Is Critical for Septin Filament Bundling and Cytokinesis. *J. Cell Biol.* **2017**, *216*, 4041–4052, doi:10.1083/jcb.201703096.
43. Omrane, M.; Camara, A.S.; Taveneau, C.; Benzoubir, N.; Tubiana, T.; Yu, J.; Guérois, R.; Samuel, D.; Goud, B.; Poüs, C.; et al. Septin 9 Has Two Polybasic Domains Critical to Septin Filament Assembly and Golgi Integrity. *iScience* **2019**, *13*, 138–153, doi:10.1016/j.isci.2019.02.015.
44. Hernández-Rodríguez, Y.; Momany, M. Posttranslational Modifications and Assembly of Septin Heteropolymers and Higher-Order Structures. *Curr. Opin. Microbiol.* **2012**, *15*, 660–668, doi:10.1016/j.mib.2012.09.007.
45. Takahashi, Y.; Iwase, M.; Konishi, M.; Tanaka, M.; Toh-e, A.; Kikuchi, Y. Smt3, a SUMO-1 Homolog, Is Conjugated to Cdc3, a Component of Septin Rings at the Mother-Bud Neck in Budding Yeast. *Biochem. Biophys. Res. Commun.* **1999**, *259*, 582–587, doi:10.1006/bbrc.1999.0821.
46. Garcia, G.; Bertin, A.; Li, Z.; Song, Y.; McMurray, M.A.; Thorner, J.; Nogales, E. Subunit-Dependent Modulation of Septin Assembly: Budding Yeast Septin Shs1 Promotes Ring and Gauze Formation. *J. Cell Biol.* **2011**, *195*, 993–1004, doi:10.1083/jcb.201107123.
47. Johnson, E.S.; Blobel, G. Cell Cycle-Regulated Attachment of the Ubiquitin-Related Protein SUMO to the Yeast Septins. *J. Cell Biol.* **1999**, *147*, 981–994.
48. Johnson, E.S.; Gupta, A.A. An E3-like Factor That Promotes SUMO Conjugation to the Yeast Septins. *Cell* **2001**, *106*, 735–744, doi:10.1016/S0092-8674(01)00491-3.
49. Hoefer, J.; Schäfer, G.; Klocker, H.; Erb, H.H.H.; Mills, I.G.; Hengst, L.; Puhr, M.; Culig, Z. PIAS1 Is Increased in Human Prostate Cancer and Enhances Proliferation through Inhibition of P21. *Am. J. Pathol.* **2012**, *180*, 2097–2107, doi:10.1016/j.ajpath.2012.01.026.
50. Morozko, E.L.; Smith-Geater, C.; Monteys, A.M.; Pradhan, S.; Lim, R.G.; Langfelder, P.; Kachemov, M.; Hill, A.; Stocksdale, J.T.; Cullis, P.R.; et al. PIAS1 Modulates Striatal Transcription, DNA Damage Repair, and SUMOylation with Relevance to Huntington's Disease. *Proc. Natl. Acad. Sci. USA* **2021**, *118*, e2021836118, doi:10.1073/pnas.2021836118.
51. Zlatanou, A.; Stewart, G.S. A PIAS-Ed View of DNA Double Strand Break Repair Focuses on SUMO. *DNA Repair* **2010**, *9*, 588–592, doi:10.1016/j.dnarep.2010.02.003.
52. Liu, B.; Shuai, K. Targeting the PIAS1 SUMO Ligase Pathway to Control Inflammation. *Trends Pharm. Sci.* **2008**, *29*, 505–509, doi:10.1016/j.tips.2008.07.008.
53. Shuai, K. Regulation of Cytokine Signaling Pathways by PIAS Proteins. *Cell Res.* **2006**, *16*, 196–202, doi:10.1038/sj.cr.7310027.
54. Rytinki, M.M.; Kaikkonen, S.; Pehkonen, P.; Jääskeläinen, T.; Palvimo, J.J. PIAS Proteins: Pleiotropic Interactors Associated with SUMO. *Cell Mol. Life Sci.* **2009**, *66*, 3029–3041, doi:10.1007/s00018-009-0061-z.

55. Miyanari, Y.; Atsuzawa, K.; Usuda, N.; Watashi, K.; Hishiki, T.; Zayas, M.; Bartenschlager, R.; Wakita, T.; Hijikata, M.; Shimotohno, K. The Lipid Droplet Is an Important Organelle for Hepatitis C Virus Production. *Nat. Cell Biol.* **2007**, *9*, 1089–1097, doi:10.1038/ncb1631.
56. Roohvand, F.; Maillard, P.; Lavergne, J.-P.; Boulant, S.; Walic, M.; Andréo, U.; Goueslain, L.; Helle, F.; Mallet, A.; McLauchlan, J.; et al. Initiation of Hepatitis C Virus Infection Requires the Dynamic Microtubule Network. *J. Biol. Chem.* **2009**, *284*, 13778–13791, doi:10.1074/jbc.M807873200.
57. Boulant, S.; Douglas, M.W.; Moody, L.; Budkowska, A.; Targett-Adams, P.; McLauchlan, J. Hepatitis C Virus Core Protein Induces Lipid Droplet Redistribution in a Microtubule- and Dynein-Dependent Manner. *Traffic* **2008**, *9*, 1268–1282, doi:10.1111/j.1600-0854.2008.00767.x.
58. Blight, K.J.; Kolykhalov, A.A.; Rice, C.M. Efficient Initiation of HCV RNA Replication in Cell Culture. *Science* **2000**, *290*, 1972–1974, doi:10.1126/science.290.5498.1972.
59. Surka, M.C.; Tsang, C.W.; Trimble, W.S. The Mammalian Septin MSF Localizes with Microtubules and Is Required for Completion of Cytokinesis. *Mol. Biol. Cell* **2002**, *13*, 3532–3545, doi:10.1091/mbc.e02-01-0042.
60. Paul, D.; Madan, V.; Bartenschlager, R. Hepatitis C Virus RNA Replication and Assembly: Living on the Fat of the Land. *Cell Host Microbe* **2014**, *16*, 569–579, doi:10.1016/j.chom.2014.10.008.
61. Li, H.-C.; Yang, C.-H.; Lo, S.-Y. Cellular Factors Involved in the Hepatitis C Virus Life Cycle. *World J. Gastroenterol.* **2021**, *27*, 4555–4581, doi:10.3748/wjg.v27.i28.4555.
62. El-Saadany, S.; Ziada, D.H.; El Bassat, H.; Farrag, W.; El-Serogy, H.; Eid, M.; Abdallah, M.; Ghazy, M.; Salem, H.A. The Role of Hepatic Expression of STAT1, SOCS3 and PIAS1 in the Response of Chronic Hepatitis C Patients to Therapy. *Can. J. Gastroenterol.* **2013**, *27*, e13–e17, doi:10.1155/2013/562765.
63. Duong, F.H.T.; Filipowicz, M.; Tripodi, M.; La Monica, N.; Heim, M.H. Hepatitis C Virus Inhibits Interferon Signaling through Up-Regulation of Protein Phosphatase 2A. *Gastroenterology* **2004**, *126*, 263–277, doi:10.1053/j.gastro.2003.10.076.
64. Bautista, D.; Bermúdez-Silva, F.J.; Lasarte, J.J.; Rodriguez-Fonseca, F.; Baixeras, E. Liver Expression of Proteins Controlling Interferon-Mediated Signalling as Predictive Factors in the Response to Therapy in Patients with Hepatitis C Virus Infection. *J. Pathol.* **2007**, *213*, 347–355, doi:10.1002/path.2214.

# Discussion and Perspective

To avoid paraphrasing what was said in the discussion of the articles presented above, I will summarize this work simply by saying that the present work further deepens our understanding of the role of septin 9 and its interactor PIs effect on LD. In particular, we have learned that septin 9 and PIs not only participate in the processes for LD biogenesis (Akil et al., 2016b), but they also affect the LD degradation through regulating the intracellular distribution of lysosome, and its interaction with LD. Of course, many fascinating questions arise and deserve to be explored further.

In this thesis, we observed that the high expression of septin 9 promotes the perinuclear cluster of both LD and lysosomes. The directed motion of either LDs or lysosomes is typically brought about by cytoskeletal motors, such as kinesin, dynein, and myosin (Pu et al., 2016; Welte, 2009; Welte and Gould, 2017). For example, movement of LDs towards the MTOC is mediated by the cytoplasmic retrograde motor dynein (Boulant et al., 2008) and as described in chapter III, lysosomes move to the perinuclear area by enhancing dynein–dynactin-dependent retrograde transport. Interestingly, recent work has shown that septin 9 was able to promote lysosome perinuclear cluster in a dynein-driven dependent way. It's shown that septin as a membrane-associated GTPase could directly interact with dynein in a GDP-bound state. Septin 9 provides a GDP-activated scaffold for the recruitment of multiple dynein-dynactin complexes (Kesisova et al., 2020). Although the direct interaction of septin 9 with dynein is not found by us, at least, consistent with our results, it demonstrates that upregulated septin 9 promotes the perinuclear cluster of lysosomes. Moreover, instead of direct interaction, septin 9 could also regulate vesicle transport as a microtubule-associated protein (MAPs) that bind along microtubules and modulate the interaction of motors with the microtubule surface. For example, septin 9 localizes specifically in dendrites in neurons, impedes axonal cargo of kinesin-1, and boosts kinesin-3 motor cargo further into dendrites (Karasmanis et al., 2018).

## Septins and Golgi dependent protein trafficking

In addition, we observed that the perinuclear lysosomes are colocalized with Golgi structure which could be arisen from the failure of lysosomal protein exit from the Golgi apparatus. Our preliminary data based on the vesicular stomatitis virus G glycoprotein (VSVG) based assay showed that LDs accumulation itself impacted Golgi compactness and inhibited post-Golgi secretion (Figure). In oleate-treated cells, the VSVG remained in the Golgi apparatus while it reached the membrane in non-treated cells (Figure 33). Notably, our group recently revealed that septin 9 is particularly necessary for Golgi assembly and its function, as the absence of septin 9 provoked Golgi dissociation and impairs secretory pathways as reported also elsewhere (Joshi, Bekier, and Wang 2015) and shown below (Figure siRNA). Given the results, as shown, we thought that the increased septin 9 in the perinuclear area, which promotes Golgi apparatus more compact, also led to the impairment of the Golgi secretion pathway. Thus, either fragmentation or high compactness of Golgi structure could impair Golgi secretion function. Thus, during the functional regulation of the Golgi apparatus, the localization and expression of septin 9 in the Golgi apparatus or the MT that is regulated by septins need to be strictly controlled to ensure the normal Golgi secretion (Figure 34).

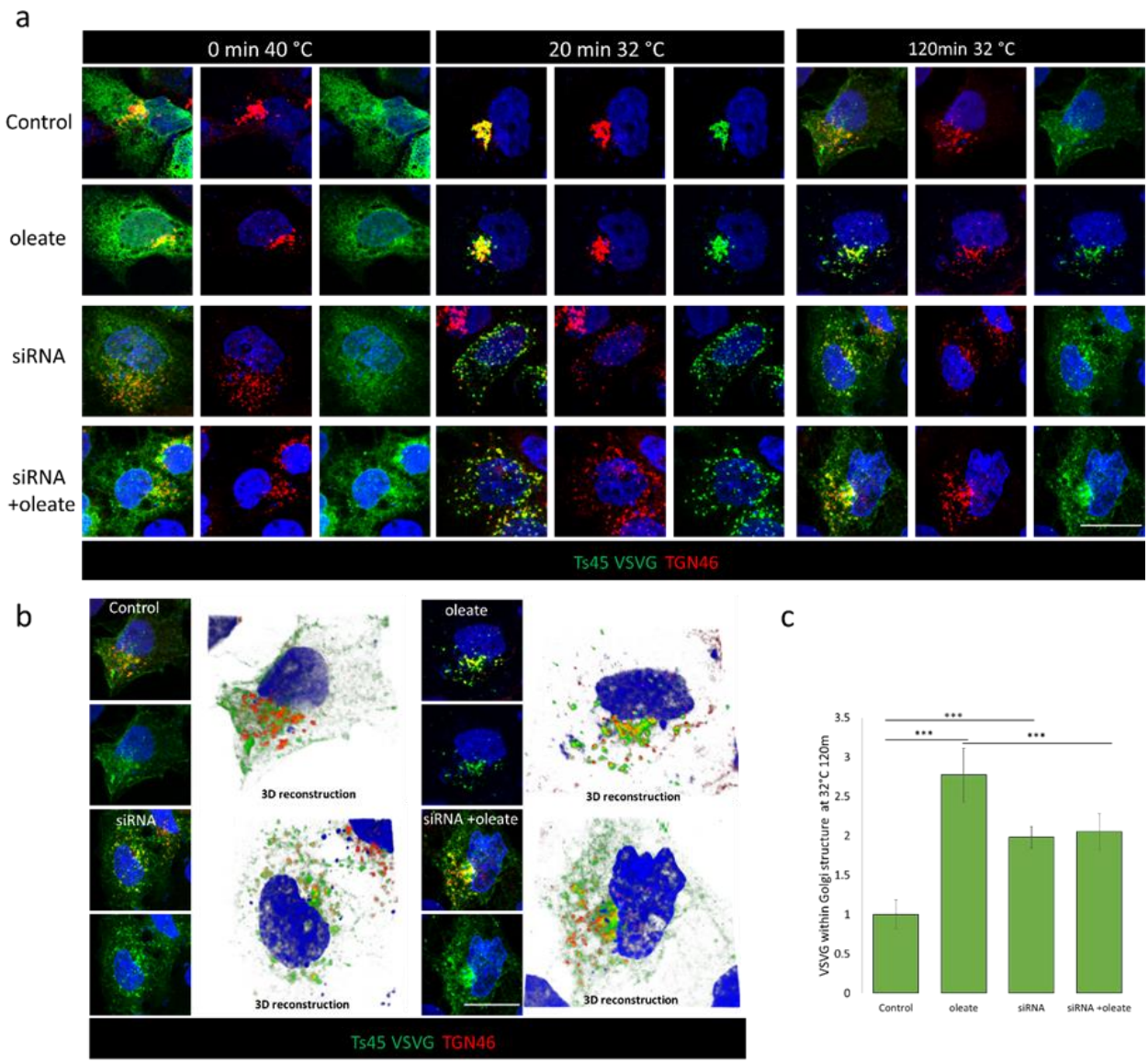


*Figure 33 Septin 9 regulates the VSVG trafficking*

***a**. Huh7 cells were transfected with or not septin 9-siRNA for 24h then transfected with Ts VSVG and cultured with medium supplemented with or not 100 µM oleate for 24h under 40°C. And move from 40°C to 32°C at different times, stained for TGN46(red). Scale bar, 5µm.*

***b**. 3D reconstruction images were shown for different conditions as described for 120min in a.*

***c**. Bar graphs show the Fold changes of VSVG intensity within Golgi structure cells from 3 independent experiments performed as described in a.*

*Data information: Bar graphs present Mean ± SEM. Student's t-test was used. *P < 0.05, **P< 0.001, ***P<0.0001.*

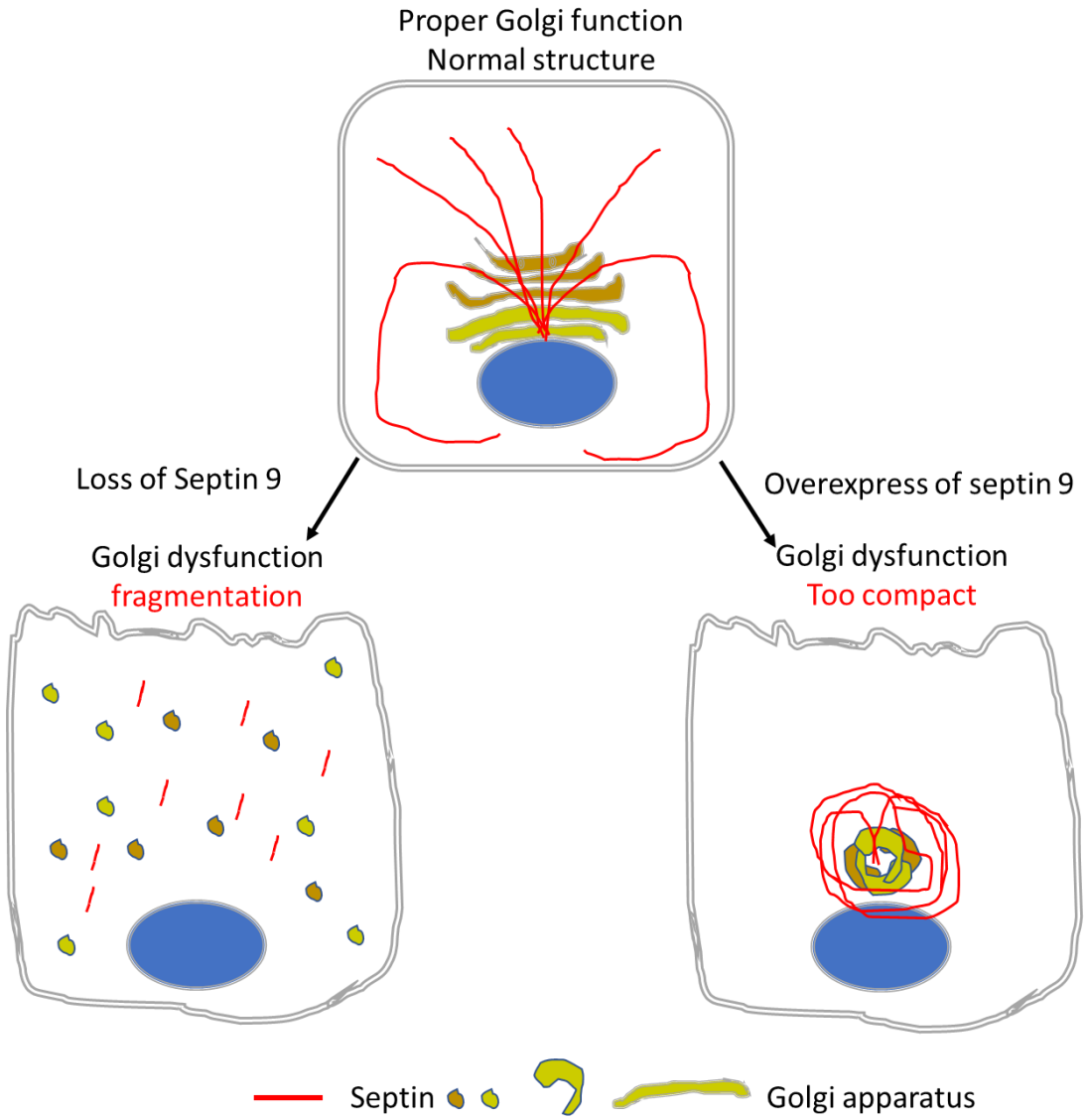


*Figure 34 Septin 9 regulates Golgi-dependent protein trafficking.*

*A model shows the role of septin 9 in Golgi-dependent proteins trafficking. The localization and expression of septin 9 in the Golgi apparatus need to be strictly controlled to ensure normal Golgi secretion. Ether, depletion of septin 9 induces the fragmentation of Golgi or upregulated septin 9 expression induced Golgi high compactness, leading to the dysfunction of Golgi dependent protein trafficking.*

In fact, besides MTs, actin-based cytoskeleton also plays a critical role in regulating the structure and function of the Golgi apparatus. For example, Golgi compactness is consistently seen when actin and its partners present at the Golgi complex are perturbed, such as after the treatment of actin depolymerization drugs (Lázaro-Diéguez et al., 2006), the depletion of the Arp2/3 activator WHAMM (WASP homolog associated with actin, Golgi membranes, and MTs) (Campellone et al., 2008), cortactin (Kirkbride et al., 2012), or myosin 18A (Ng et al., 2013). Thus, besides MTs, septin 9 may also affect post-Golgi secretion through regulating the association between actin filaments and Golgi structure (Figure 35).

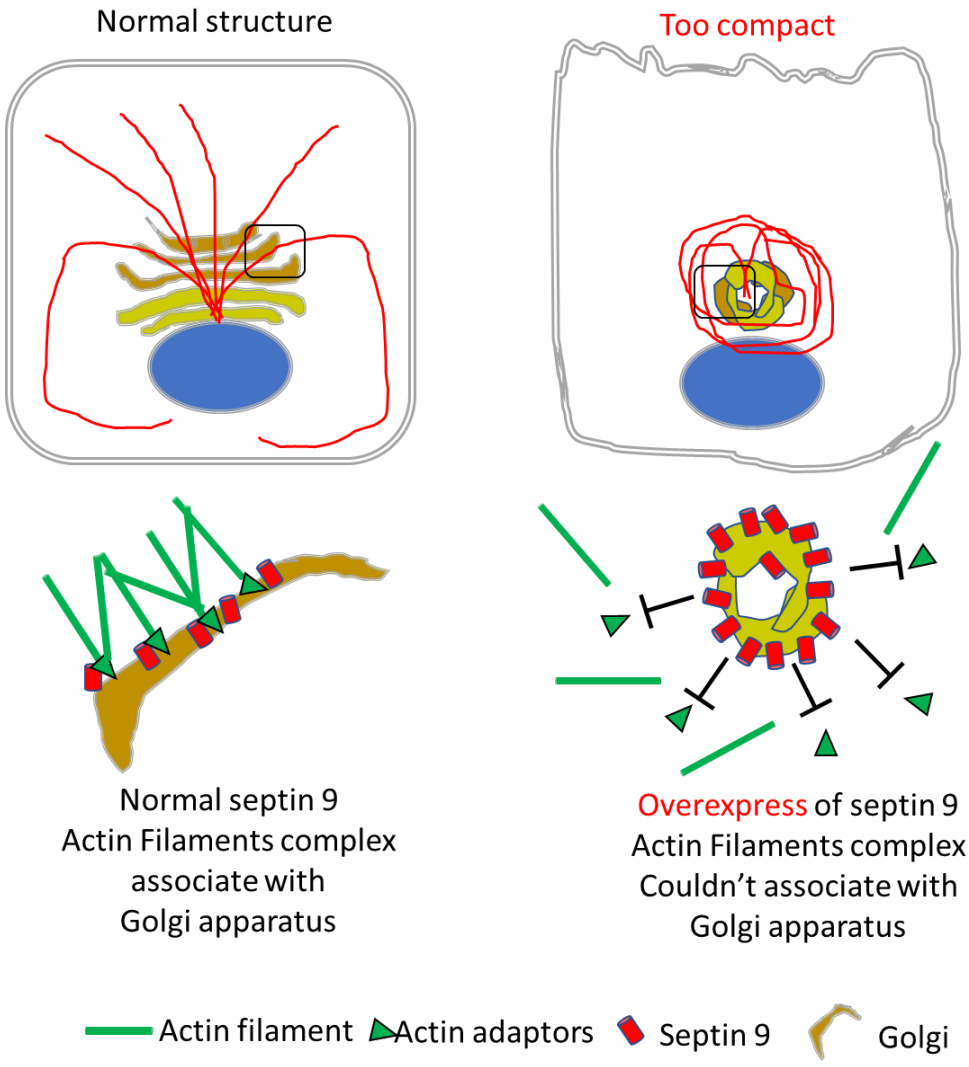


*Figure 35 A hypothesis model for Overexpression septin 9 induced Golgi dysfunctions.*
*The overexpressed septin 9 may occupy the binding site for actin adaptor protein, thus inhibiting the formation of actin filaments complex and the post-Golgi carriers (Almeida et al., 2011).*

# Septin 9 isoforms in LD and lysosome regulation

An important point that arises from this work is the analysis of septin 9_i1 isoforms. While the septin 9 gene (SEPT9) could produce up to 18 alternatively spliced mRNA variants (septin 9 V1-18) and could produce several isoforms. These septin 9 isoforms are likely to possess different binding partners, functions, and properties, and their relative levels of expression could affect cell behavior. For example, it is likely that septin 9 effects on cancer are regulated via upregulation of its specific transcripts, while mutations of its gene are rare in cancer (Angelis and Spiliotis, 2016). Upregulation of the septin 9_i1 has been reported in human cancer cell lines as well as in the corresponding tumor as observed with breast cancer (Gonzalez et al., 2007; Verdier-Pinard et al., 2017). Expression of the septin 9_i3 isoform is regulated by DNA methylation upstream of its transcription start site (Connolly et al., 2011). Overexpression of septin 9 is detected more commonly in high-grade carcinomas, which are also associated with a worse clinical prognosis (Connolly et al., 2014). The septin 9_i4 has been shown to increase the resistance to MTs-interacting drugs (Chacko et al., 2012). More recently, a study of our research laboratory showed that septins overexpression together with long-chain tubulin polyglutamylation induced significant paclitaxel resistance in several naive (taxane-sensitive) cell lines, and such resistance was coupled with a systematic re-localization of septin filaments from actin fibers to MTs. This re-localization of septin could also be promoted by acute treatment with paclitaxel of sensitive cells displaying a high basal level of septin 9_i1, not septin 9_i3 (Targa et al., 2019). Thus, it will be interesting to assess the role of the other isoforms.

Our preliminary results from Huh7 cells transfected using the specific cDNAs of the different septin 9 isoforms and stained for LAMP1 and LD, revealed that septin 9_i1 promoted the strongest effect on the clustering of LAMP1 and the increase of LD size among the five main isoforms analyzed (Figure 36). This result is in line with the fact that septin 9_i1 displayed the strongest interaction with tubulin compared to the other isoforms (Bai et al., 2013; Targa et al., 2019; Verdier-Pinard et al., 2017). However, this highest effect of septin 9_1 on LD and lysosomes may also depend on other reasons. For example, different septin 9 isoforms may have different molecular conformations due to differences in protein length, which may affect their recognition of the membrane structures. Furthermore, even in the same conformational structure, different isoforms of septin 9 may recognize specific PIs and thereby selectively bind to certain membrane structures. Therefore, revealing that the differences among septin 9 isoforms need to be investigated in various biological contexts.

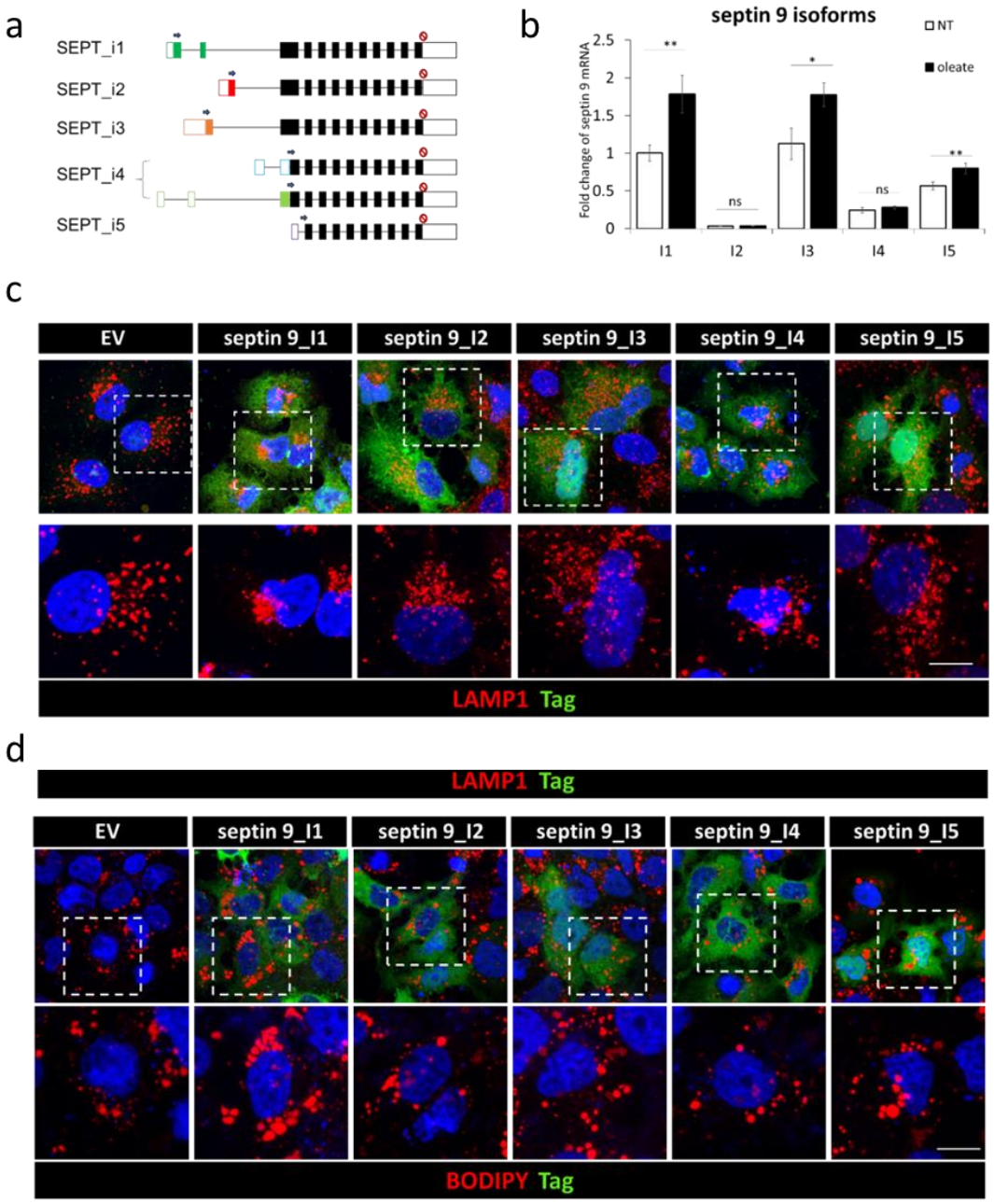


*Figure 36 Septin 9 isoforms have different effects on lysosome distribution and LD accumulation*

***a.*** *Exonic structure of SEPT9 showing known exons and splicing patterns*

***b****. Huh7 cells culture with medium supplemented with 0, 100 µM oleate for 24h. cells were analyzed for septin different variants mRNA levels by qRT-PCR. Bar graphs show results from 3 independent experiments.*

***c****.Huh7 cells were transfected with EV or septin 9_isoforms were strained for LAMP1 (red) and Tag (green). White squares indicate the zoom area shown below.*

***d****.Huh7 cells were transfected with EV or septin 9_isoforms were strained for LD (red) and Tag (green). White squares indicate the zoom area shown below.*

# Septin 9 and lysosomes in HCV infection

Chronic HCV infection is a major public health problem and the main risk factor for cirrhosis, and hepatocellular carcinoma, thus remaining the major cause of liver resection and transplantation(Yamane et al., 2013). Although major advances have been recently achieved regarding HCV infection treatment, and the combination of drugs, including protease inhibitors, represents a real breakthrough that cures almost 90% of infected patients. Understanding the key mechanisms driving HCV replication and persistence is still a charming question that will have a profound impact, beyond HCV, for the appraisal of the pathogenesis of this family of viruses.

My Ph.D. work revealed a new mechanism by which Septin 9 interplayed with PI and controls LD through affecting lysosomes in oleate-treated cells. Then, it will be interesting to study if this new mechanism is also involved in the context of HCV infection.

While what is the effect of HCV infection on lysosomes is still unclear. Although there is not much direct evidence, it seems certain that lysosomes are inhibited after HCV infection. The presence of an increased number of autophagosomes in HCV-infected cells has been reported by several groups, based on observations in either cell culture infection systems or liver samples from patients with chronic HCV infection (Ait-Goughoulte et al., 2008; Dreux et al., 2009; Rautou et al., 2011; Sir et al., 2008). By detecting the mRNA expression of lysosome-related enzymes in both cells, we found enhanced mRNA expression of multiple enzymes in Huh7-replicon cells (Figure 37), so we can propose that HCV influences lysosomes, at least in the transcriptional process. Of course, further research is needed to verify it, and what role septin 9 could play in this process also needs to be studied.

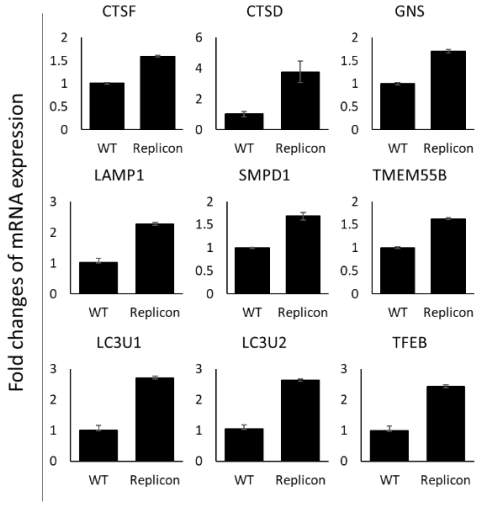


*Figure 37 HCV regulate Lysosomes*

*Huh7 WT and Huh7R were stained for lysotraker(red) and LDs (green), and analysis for Lysosomal genes.*

In addition, septin 9 may have a role in HCV infection in other ways, such as in the entry of HCV into cells. For instance, HCV entry in hepatocytes is mediated by the interaction of the viral envelope proteins with several cell surface receptors and entry cofactors including glycosaminoglycans, LDL receptor, tetraspanin CD81, scavenger receptor class B member I, tight junction proteins claudin1 and occludin, and the cholesterol uptake receptor Niemann-Pick C1-like 1(Lindenbach and Rice, 2013). HCV particles are then internalized by clathrin-mediated endocytosis (Blanchard et al., 2006), and viral-endosomal membrane fuse, in a pH-dependent manner, to release viral nucleocapsid into the cytoplasm where the uncoating occurs (Stanković et al., 2014). Septin 9, as mentioned above, plays a role in regulating the endocytosis process for several receptors and is utilized by the bacteria to invade the cells, Thus, septin 9 may also involve in the entry of HCV (Figure 38).

Furthermore, the maturation and release of HCV particles are closely linked to the very-low-density lipoprotein (VLDL) synthesis and secretion pathways(Gastaminza et al., 2008). Indeed, nascent virions associate with pre-VLDL particles to form lipoviroparticles (LVPs) containing apolipoproteins (ApoB, apoE, apoC, and apoA-I),(Catanese et al., 2013; Nielsen et al., 2006). LVPs then pass through the Golgi and are released from the cells by the secretory pathway(Scheel and Rice, 2013). And given the role of septin 9 in regulating the morphology of Golgi apparatus and Golgi-dependent secretion of proteins, we could also suggest the role of septin 9 in HCV particles maturation and release (Figure 38).

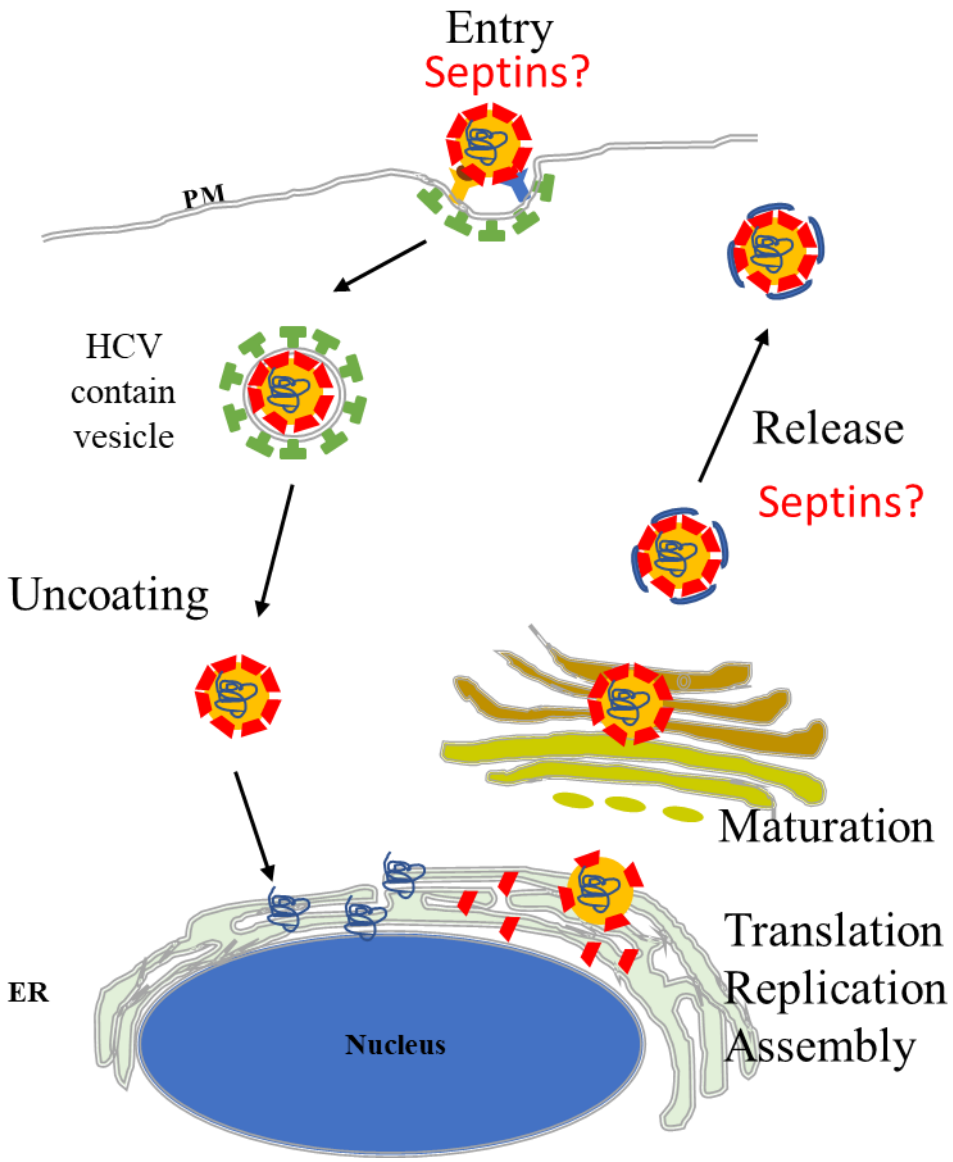


*Figure 38 The possible involvement of septin in the HCV life cycle*

*A model shows the possible role of septins in the HCV life cycle. The HCV life cycle composite multiple steps including attachment, entry, uncoating, translation, replication, assembly, maturation, and release. As described in chapter IV and what we show in this work, we propose that in addition to HCV replication, septins may also be involved in the other steps in HCV life cycle such as the entry and release of viral particles.*

# Septin 9 in liver cirrhosis and HCC

Although many studies have shown that LDs accumulation and lysosomal disorders are important inducers of steatosis and various liver injury diseases (Bessone et al., 2019; Hikita et al., 2018; Olzmann and Carvalho, 2019; Schulze and McNiven, 2019; Shyu et al., 2018; Wang et al., 2018), LDs accumulation and lysosomal dysfunction may be beneficial to maintain liver homeostasis at some stage. For example, although, treating MCD diet-fed mice with DGAT2 ASO, which inhibits the final step of TG biosynthesis, decreased hepatic steatosis, but increased hepatic free fatty acids, lipid peroxidation/oxidant stress, lobular necroinflammation and fibrosis, which is a more serious liver injury than steatosis(Yamaguchi et al., 2007). Fatty acids (FAs) are important sources of cellular energy. FAs are converted at the mitochondrial membrane into acylcarnitine (AC), which is then taken up by mitochondria and broken down via β-oxidation. However, increased FA levels can be toxic to cells. Overlord of FAs has been reported to intensify the process of β-oxidation in the mitochondria, causing mitochondrial stress, leading to excessive ROS production (Schönfeld and Wojtczak, 2008), which may lead to the occurrence of inflammation. Overlord of FAs also increased ER stress that trigger UPR (unfolded protein response) leading to inflammation in hepatocytes (Baiceanu et al., 2016). Septin 9 promotes the accumulation of LDs and sequestered FAs through LD synthesis, thereby reducing the level of FFAs in hepatocytes. This will avoid excessive FFA-initiated mitochondrial stress and thus reduce the risk of inflammation. Thus septin 9 may play a protective role in preventing the occurrence of cirrhosis.

While prolonged lysosomal inactivation will lead to the development of liver cirrhosis through other pathways. For example, the membrane protein TLR4, a liposaccharide (LPS) receptor, has been reported to play an important role in the progression of NASH (Kim et al., 2017; Płóciennikowska et al., 2015). During the progression of simple steatosis to NASH, TLR4 signaling can be activated in hepatocytes, and its downstream molecules, such as proinflammatory cytokines, are increased in NAFLD (Kim et al., 2012; Ye et al., 2012). Since the lysosomal degradation pathway is one of the major pathways for cell surface receptor degradation after ubiquitination (Yu et al., 2018), lysosome dysfunction will increase TLR4 protein expression, subsequently active its downstream molecules and produce proinflammatory cytokines. Although this effect wasn't shown in hepatocytes, in HSCs, increased TLR4 protein expression by enhanced LDLR expression and miR-33a signaling is through suppressing the endosomal-lysosomal TLR4 degradation pathway (Tomita et al., 2014). In addition to TLR4, EGFR which is overexpressed in human cirrhotic liver tissue and HCCs (Harada et al., 1999; Qiao et al., 2008), may also be driven, in part, by dysfunction of the lysosomal degradation pathway.

# Reference

Abbey, M., Hakim, C., Anand, R., Lafera, J., Schambach, A., Kispert, A., Taft, M.H., Kaever, V., Kotlyarov, A., Gaestel, M., et al. (2016). GTPase domain driven dimerization of SEPT7 is dispensable for the critical role of septins in fibroblast cytokinesis. Sci. Rep. *6*, 20007.

Abbey, M., Gaestel, M., and Menon, M.B. (2019). Septins: Active GTPases or just GTP-binding proteins? Cytoskeleton *76*, 55–62.

Abdel-Misih, S.R.Z., and Bloomston, M. (2010). Liver Anatomy. Surg. Clin. North Am. *90*, 643–653.

Ageta-Ishihara, N., Miyata, T., Ohshima, C., Watanabe, M., Sato, Y., Hamamura, Y., Higashiyama, T., Mazitschek, R., Bito, H., and Kinoshita, M. (2013). Septins promote dendrite and axon development by negatively regulating microtubule stability via HDAC6-mediated deacetylation. Nat. Commun. *4*, 2532.

Ait-Goughoulte, M., Kanda, T., Meyer, K., Ryerse, J.S., Ray, R.B., and Ray, R. (2008). Hepatitis C Virus Genotype 1a Growth and Induction of Autophagy. J. Virol. *82*, 2241–2249.

Aj, F., and F, C. (2017). Cdc42 Regulates Cdc42EP3 Function in Cancer-Associated Fibroblasts (Small GTPases).

Akhmetova, K., Balasov, M., Huijbregts, R.P.H., and Chesnokov, I. (2015). Functional insight into the role of Orc6 in septin complex filament formation in Drosophila. Mol. Biol. Cell *26*, 15–28.

Akil, A., Peng, J., Omrane, M., Gondeau, C., Desterke, C., Marin, M., Tronchère, H., Taveneau, C., Sar, S., Briolotti, P., et al. (2016a). Septin 9 induces lipid droplets growth by a phosphatidylinositol-5-phosphate and microtubule-dependent mechanism hijacked by HCV. Nat. Commun. *7*.

Akil, A., Peng, J., Omrane, M., Gondeau, C., Desterke, C., Marin, M., Tronchère, H., Taveneau, C., Sar, S., Briolotti, P., et al. (2016b). Septin 9 induces lipid droplets growth by a phosphatidylinositol-5-phosphate and microtubule-dependent mechanism hijacked by HCV. Nat. Commun. *7*, 12203.

Alexandrov, K., Horiuchi, H., Steele-Mortimer, O., Seabra, M.C., and Zerial, M. (1994). Rab escort protein-1 is a multifunctional protein that accompanies newly prenylated rab proteins to their target membranes. EMBO J. *13*, 5262–5273.

Almeida, C.G., Yamada, A., Tenza, D., Louvard, D., Raposo, G., and Coudrier, E. (2011). Myosin 1b promotes the formation of post-Golgi carriers by regulating actin assembly and membrane remodelling at the trans -Golgi network. Nat. Cell Biol. *13*, 779–789.

de Almeida Marques, I., Valadares, N.F., Garcia, W., Damalio, J.C.P., Macedo, J.N.A., de Araújo, A.P.U., Botello, C.A., Andreu, J.M., and Garratt, R.C. (2012). Septin C-terminal domain interactions: implications for filament stability and assembly. Cell Biochem. Biophys. *62*, 317–328.

Alqahtani, S.A., and Colombo, M. (2020). Viral hepatitis as a risk factor for the development of hepatocellular carcinoma. Hepatoma Res. *6*.

Andersen, J.B. (2015). Molecular pathogenesis of intrahepatic cholangiocarcinoma. J. Hepato-Biliary-Pancreat. Sci. *22*, 101–113.

Andersen, J.B., Spee, B., Blechacz, B.R., Avital, I., Komuta, M., Barbour, A., Conner, E.A., Gillen, M.C., Roskams, T., Roberts, L.R., et al. (2012). Genomic and Genetic Characterization of Cholangiocarcinoma Identifies Therapeutic Targets for Tyrosine Kinase Inhibitors. Gastroenterology *142*, 1021-1031.e15.

Angelis, D., and Spiliotis, E.T. (2016). Septin Mutations in Human Cancers. Front. Cell Dev. Biol. *4*, 122.

Anstee, Q.M., Reeves, H.L., Kotsiliti, E., Govaere, O., and Heikenwalder, M. (2019). From NASH to HCC: current concepts and future challenges. Nat. Rev. Gastroenterol. Hepatol. *16*, 411–428.

Arjonen, A., Alanko, J., Veltel, S., and Ivaska, J. (2012). Distinct recycling of active and inactive β1 integrins. Traffic Cph. Den. *13*, 610–625.

Asselah, T., Rubbia-Brandt, L., Marcellin, P., and Negro, F. (2006). Steatosis in chronic hepatitis C: why does it really matter? Gut *55*, 123–130.

Avgerinos, K.I., Spyrou, N., Mantzoros, C.S., and Dalamaga, M. (2019). Obesity and cancer risk: Emerging biological mechanisms and perspectives. Metabolism *92*, 121–135.

Bai, X., Bowen, J.R., Knox, T.K., Zhou, K., Pendziwiat, M., Kuhlenbäumer, G., Sindelar, C.V., and Spiliotis, E.T. (2013). Novel septin 9 repeat motifs altered in neuralgic amyotrophy bind and bundle microtubules. J. Cell Biol. *203*, 895–905.

Balla, T. (2013). Phosphoinositides: Tiny Lipids With Giant Impact on Cell Regulation. Physiol. Rev. *93*, 1019–1137.

Ballabio, A., and Bonifacino, J.S. (2019). Lysosomes as dynamic regulators of cell and organismal homeostasis. Nat. Rev. Mol. Cell Biol. 1–18.

Banales, J.M., Cardinale, V., Carpino, G., Marzioni, M., Andersen, J.B., Invernizzi, P., Lind, G.E., Folseraas, T., Forbes, S.J., Fouassier, L., et al. (2016). Expert consensus document: Cholangiocarcinoma: current knowledge and future perspectives consensus statement from the European Network for the Study of Cholangiocarcinoma (ENS-CCA). Nat. Rev. Gastroenterol. Hepatol. *13*, 261–280.

Banales, J.M., Huebert, R.C., Karlsen, T., Strazzabosco, M., LaRusso, N.F., and Gores, G.J. (2019). Cholangiocyte pathobiology. Nat. Rev. Gastroenterol. Hepatol. *16*, 269–281.

Banales, J.M., Marin, J.J.G., Lamarca, A., Rodrigues, P.M., Khan, S.A., Roberts, L.R., Cardinale, V., Carpino, G., Andersen, J.B., Braconi, C., et al. (2020). Cholangiocarcinoma 2020: the next horizon in mechanisms and management. Nat. Rev. Gastroenterol. Hepatol. *17*, 557–588.

Barbosa, A.D., and Siniossoglou, S. (2017). Function of lipid droplet-organelle interactions in lipid homeostasis. Biochim. Biophys. Acta BBA - Mol. Cell Res. *1864*, 1459–1468.

Barbosa, A.D., Savage, D.B., and Siniossoglou, S. (2015). Lipid droplet-organelle interactions: emerging roles in lipid metabolism. Curr. Opin. Cell Biol. *35*, 91–97.

Barneda, D., Planas-Iglesias, J., Gaspar, M.L., Mohammadyani, D., Prasannan, S., Dormann, D., Han, G.-S., Jesch, S.A., Carman, G.M., Kagan, V., et al. (2015). The brown adipocyte protein CIDEA promotes lipid droplet fusion via a phosphatidic acid-binding amphipathic helix. ELife *4*, e07485.

Barr, F.A. (2013). Review series: Rab GTPases and membrane identity: causal or inconsequential? J. Cell Biol. *202*, 191–199.

Barr, F., and Lambright, D.G. (2010). Rab GEFs and GAPs. Curr. Opin. Cell Biol. *22*, 461–470.

Bautista, D., Bermúdez-Silva, F.J., Lasarte, J.J., Rodriguez-Fonseca, F., and Baixeras, E. (2007).

Liver expression of proteins controlling interferon-mediated signalling as predictive factors in the response to therapy in patients with hepatitis C virus infection. J. Pathol. *213*, 347–355.

Beard, P.M., Griffiths, S.J., Gonzalez, O., Haga, I.R., Pechenick Jowers, T., Reynolds, D.K., Wildenhain, J., Tekotte, H., Auer, M., Tyers, M., et al. (2014). A loss of function analysis of host factors influencing Vaccinia virus replication by RNA interference. PloS One *9*, e98431.

Bechmann, L.P., Hannivoort, R.A., Gerken, G., Hotamisligil, G.S., Trauner, M., and Canbay, A. (2012). The interaction of hepatic lipid and glucose metabolism in liver diseases. J. Hepatol. *56*, 952–964.

Beck, R., Rawet, M., Ravet, M., Wieland, F.T., and Cassel, D. (2009). The COPI system: molecular mechanisms and function. FEBS Lett. *583*, 2701–2709.

Becker, J., Barysch, S.V., Karaca, S., Dittner, C., Hsiao, H.-H., Diaz, M.B., Herzig, S., Urlaub, H., and Melchior, F. (2013). Detecting endogenous SUMO targets in mammalian cells and tissues. Nat. Struct. Mol. Biol. *20*, 525–531.

Beeck, A.O.D., and Dubuisson, J. (2003). Topology of hepatitis C virus envelope glycoproteins. Rev. Med. Virol. *13*, 233–241.

Beller, M., Sztalryd, C., Southall, N., Bell, M., Jäckle, H., Auld, D.S., and Oliver, B. (2008). COPI complex is a regulator of lipid homeostasis. PLoS Biol. *6*, e292.

Ben M'barek, K., Ajjaji, D., Chorlay, A., Vanni, S., Forêt, L., and Thiam, A.R. (2017). ER Membrane Phospholipids and Surface Tension Control Cellular Lipid Droplet Formation. Dev. Cell *41*, 591-604.e7.

Benedict, M., and Zhang, X. (2017). Non-alcoholic fatty liver disease: An expanded review. World J. Hepatol. *9*, 715–732.

Bernier-Villamor, V., Sampson, D.A., Matunis, M.J., and Lima, C.D. (2002). Structural Basis for E2-Mediated SUMO Conjugation Revealed by a Complex between Ubiquitin-Conjugating Enzyme Ubc9 and RanGAP1. Cell *108*, 345–356.

Bersuker, K., and Olzmann, J.A. (2017). Establishing the lipid droplet proteome: Mechanisms of lipid droplet protein targeting and degradation. Biochim. Biophys. Acta *1862*, 1166–1177.

Bersuker, K., Peterson, C.W.H., To, M., Sahl, S.J., Savikhin, V., Grossman, E.A., Nomura, D.K., and Olzmann, J.A. (2018). A Proximity Labeling Strategy Provides Insights into the Composition and Dynamics of Lipid Droplet Proteomes. Dev. Cell *44*, 97-112.e7.

Bertin, A., McMurray, M.A., Grob, P., Park, S.-S., Garcia, G., Patanwala, I., Ng, H.-L., Alber, T., Thorner, J., and Nogales, E. (2008). Saccharomyces cerevisiae septins: supramolecular organization of heterooligomers and the mechanism of filament assembly. Proc. Natl. Acad. Sci. U. S. A. *105*, 8274–8279.

Bessone, F., Razori, M.V., and Roma, M.G. (2019). Molecular pathways of nonalcoholic fatty liver disease development and progression. Cell. Mol. Life Sci. *76*, 99–128.

Bi, J., Wang, W., Liu, Z., Huang, X., Jiang, Q., Liu, G., Wang, Y., and Huang, X. (2014). Seipin Promotes Adipose Tissue Fat Storage through the ER Ca2+-ATPase SERCA. Cell Metab. *19*, 861–871.

Blanchard, E., Belouzard, S., Goueslain, L., Wakita, T., Dubuisson, J., Wychowski, C., and Rouillé, Y. (2006). Hepatitis C Virus Entry Depends on Clathrin-Mediated Endocytosis. J. Virol. *80*, 6964–6972.

Blaner, W.S., O'Byrne, S.M., Wongsiriroj, N., Kluwe, J., D'Ambrosio, D.M., Jiang, H., Schwabe, R.F., Hillman, E.M.C., Piantedosi, R., and Libien, J. (2009). Hepatic stellate cell lipid droplets: A specialized lipid droplet for retinoid storage. Biochim. Biophys. Acta BBA - Mol. Cell Biol. Lipids *1791*, 467–473.

Blümer, J., Rey, J., Dehmelt, L., Mazel, T., Wu, Y.-W., Bastiaens, P., Goody, R.S., and Itzen, A. (2013). RabGEFs are a major determinant for specific Rab membrane targeting. J. Cell Biol. *200*, 287–300.

Boddy, K.C., Gao, A.D., Truong, D., Kim, M.S., Froese, C.D., Trimble, W.S., and Brumell, J.H. (2018). Septin- regulated actin dynamics promote Salmonella invasion of host cells. Cell. Microbiol. *20*.

Boden, G. (2006). Fatty acid—induced inflammation and insulin resistance in skeletal muscle and liver. Curr. Diab. Rep. *6*, 177–181.

Bogdan, A.R., Miyazawa, M., Hashimoto, K., and Tsuji, Y. (2016). Regulators of Iron Homeostasis: New Players in Metabolism, Cell Death, and Disease. Trends Biochem. Sci. *41*, 274–286.

Bonifacino, J.S., and Neefjes, J. (2017). Moving and positioning the endolysosomal system. Curr. Opin. Cell Biol. *47*, 1–8.

Böttcher, K., and Pinzani, M. (2017). Pathophysiology of liver fibrosis and the methodological barriers to the development of anti-fibrogenic agents. Adv. Drug Deliv. Rev. *121*, 3–8.

Boulant, S., Douglas, M.W., Moody, L., Budkowska, A., Targett-Adams, P., and McLauchlan, J. (2008). Hepatitis C virus core protein induces lipid droplet redistribution in a microtubule- and dynein-dependent manner. Traffic Cph. Den. *9*, 1268–1282.

Bowen, J.R., Hwang, D., Bai, X., Roy, D., and Spiliotis, E.T. (2011). Septin GTPases spatially guide microtubule organization and plus end dynamics in polarizing epithelia. J. Cell Biol. *194*, 187–197.

Brand, F., Schumacher, S., Kant, S., Menon, M.B., Simon, R., Turgeon, B., Britsch, S., Meloche, S., Gaestel, M., and Kotlyarov, A. (2012). The Extracellular Signal-Regulated Kinase 3 (Mitogen-Activated Protein Kinase 6 [MAPK6])–MAPK-Activated Protein Kinase 5 Signaling Complex Regulates Septin Function and Dendrite Morphology. Mol. Cell. Biol. *32*, 2467–2478.

Brasaemle, D.L., Dolios, G., Shapiro, L., and Wang, R. (2004). Proteomic Analysis of Proteins Associated with Lipid Droplets of Basal and Lipolytically Stimulated 3T3-L1 Adipocytes. J. Biol. Chem. *279*, 46835–46842.

Bridges, A.A., Jentzsch, M.S., Oakes, P.W., Occhipinti, P., and Gladfelter, A.S. (2016). Micron-scale plasma membrane curvature is recognized by the septin cytoskeleton. J. Cell Biol. *213*, 23–32.

Bucci, C., Parton, R.G., Mather, I.H., Stunnenberg, H., Simons, K., Hoflack, B., and Zerial, M. (1992). The small GTPase rab5 functions as a regulatory factor in the early endocytic pathway. Cell *70*, 715–728.

Bucci, C., Thomsen, P., Nicoziani, P., McCarthy, J., and van Deurs, B. (2000). Rab7: A Key to Lysosome Biogenesis. Mol. Biol. Cell *11*, 467–480.

Bugianesi, E., Moscatiello, S., Ciaravella, M.F., and Marchesini, G. (2010). Insulin Resistance in Nonalcoholic Fatty Liver Disease. Curr. Pharm. Des. *16*, 1941–1951.

Burkhardt, J.K., Echeverri, C.J., Nilsson, T., and Vallee, R.B. (1997). Overexpression of the dynamitin (p50) subunit of the dynactin complex disrupts dynein-dependent maintenance of membrane organelle distribution. J. Cell Biol. *139*, 469–484.

Byers, B., and Goetsch, L. (1976). A highly ordered ring of membrane-associated filaments in budding yeast. J. Cell Biol. *69*, 717–721.

Cabrera, M., Nordmann, M., Perz, A., Schmedt, D., Gerondopoulos, A., Barr, F., Piehler, J., Engelbrecht-Vandré, S., and Ungermann, C. (2014). The Mon1-Ccz1 GEF activates the Rab7 GTPase Ypt7 via a longin-fold-Rab interface and association with PI3P-positive membranes. J. Cell Sci. *127*, 1043–1051.

Cabukusta, B., and Neefjes, J. (2018). Mechanisms of lysosomal positioning and movement.

Campa, C.C., and Hirsch, E. (2017). Rab11 and phosphoinositides: A synergy of signal transducers in the control of vesicular trafficking. Adv. Biol. Regul. *63*, 132–139.

Campellone, K.G., Webb, N.J., Znameroski, E.A., and Welch, M.D. (2008). WHAMM is an Arp2/3 complex activator that binds microtubules and functions in ER to Golgi transport. Cell *134*, 148–161.

Cannon, K.S., Woods, B.L., Crutchley, J.M., and Gladfelter, A.S. (2019). An amphipathic helix enables septins to sense micrometer-scale membrane curvature. J. Cell Biol. *218*, 1128–1137.

Cao, L., Ding, X., Yu, W., Yang, X., Shen, S., and Yu, L. (2007). Phylogenetic and evolutionary analysis of the septin protein family in metazoan. FEBS Lett. *581*, 5526–5532.

Casamayor, A., and Snyder, M. (2003). Molecular dissection of a yeast septin: distinct domains are required for septin interaction, localization, and function. Mol. Cell. Biol. *23*, 2762–2777.

Castanheira, S., and García-Del Portillo, F. (2017). Salmonella Populations inside Host Cells. Front. Cell. Infect. Microbiol. *7*, 432.

Catanese, M.T., Uryu, K., Kopp, M., Edwards, T.J., Andrus, L., Rice, W.J., Silvestry, M., Kuhn, R.J., and Rice, C.M. (2013). Ultrastructural analysis of hepatitis C virus particles. Proc. Natl. Acad. Sci. *110*, 9505–9510.

Cauvin, C., Rosendale, M., Gupta-Rossi, N., Rocancourt, M., Larraufie, P., Salomon, R., Perrais, D., and Echard, A. (2016). Rab35 GTPase Triggers Switch-like Recruitment of the Lowe Syndrome Lipid Phosphatase OCRL on Newborn Endosomes. Curr. Biol. *26*, 120–128.

Celli, A., Que, F.G., Gores, G.J., and LaRusso, N.F. (1998). Glutathione depletion is associated with decreased Bcl-2 expression and increased apoptosis in cholangiocytes. Am. J. Physiol. *275*, G749-757.

Chacko, A.D., McDade, S.S., Chanduloy, S., Church, S.W., Kennedy, R., Price, J., Hall, P.A., and Russell, S.E.H. (2012). Expression of the SEPT9_i4 isoform confers resistance to microtubule-interacting drugs. Cell. Oncol. *35*, 85–93.

Chandra, M., Chin, Y.K.-Y., Mas, C., Feathers, J.R., Paul, B., Datta, S., Chen, K.-E., Jia, X., Yang, Z., Norwood, S.J., et al. (2019). Classification of the human phox homology (PX) domains based on their phosphoinositide binding specificities. Nat. Commun. *10*, 1528.

Chao, J.T., Wong, A.K.O., Tavassoli, S., Young, B.P., Chruscicki, A., Fang, N.N., Howe, L.J., Mayor, T., Foster, L.J., and Loewen, C.J.R. (2014). Polarization of the Endoplasmic Reticulum by ER-Septin Tethering. Cell *158*, 620–632.

Chauhan, N., Visram, M., Cristobal-Sarramian, A., Sarkleti, F., and Kohlwein, S.D. (2015). Morphogenesis checkpoint kinase Swe1 is the executor of lipolysis-dependent cell-cycle progression. Proc. Natl. Acad. Sci. U. S. A. *112*, E1077-1085.

Chen, Z., Xie, H., Hu, M., Huang, T., Hu, Y., Sang, N., and Zhao, Y. (2020). Recent progress in treatment of hepatocellular carcinoma. Am. J. Cancer Res. *10*, 2993–3036.

Chitraju, C., Trötzmüller, M., Hartler, J., Wolinski, H., Thallinger, G.G., Lass, A., Zechner, R., Zimmermann, R., Köfeler, H.C., and Spener, F. (2012). Lipidomic analysis of lipid droplets from murine hepatocytes reveals distinct signatures for nutritional stress. J. Lipid Res. *53*, 2141–2152.

Chorlay, A., and Thiam, A.R. (2018). An Asymmetry in Monolayer Tension Regulates Lipid Droplet Budding Direction. Biophys. J. *114*, 631–640.

Chotard, L., Mishra, A.K., Sylvain, M.-A., Tuck, S., Lambright, D.G., and Rocheleau, C.E. (2010). TBC-2 regulates RAB-5/RAB-7-mediated endosomal trafficking in Caenorhabditis elegans. Mol. Biol. Cell *21*, 2285–2296.

Choudhary, V., Ojha, N., Golden, A., and Prinz, W.A. (2015). A conserved family of proteins facilitates nascent lipid droplet budding from the ER. J. Cell Biol. *211*, 261–271.

Choudhary, V., Golani, G., Joshi, A.S., Cottier, S., Schneiter, R., Prinz, W.A., and Kozlov, M.M. (2018). Architecture of Lipid Droplets in Endoplasmic Reticulum Is Determined by Phospholipid Intrinsic Curvature. Curr. Biol. CB *28*, 915-926.e9.

Christoforidis, S., Miaczynska, M., Ashman, K., Wilm, M., Zhao, L., Yip, S.C., Waterfield, M.D., Backer, J.M., and Zerial, M. (1999). Phosphatidylinositol-3-OH kinases are Rab5 effectors. Nat. Cell Biol. *1*, 249–252.

Chu, B.-B., Liao, Y.-C., Qi, W., Xie, C., Du, X., Wang, J., Yang, H., Miao, H.-H., Li, B.-L., and Song, B.-L. (2015a). Cholesterol transport through lysosome-peroxisome membrane contacts. Cell *161*, 291–306.

Chu, K.Y., O'Reilly, L., Ramm, G., and Biden, T.J. (2015b). High-fat diet increases autophagic flux in pancreatic beta cells in vivo and ex vivo in mice. Diabetologia *58*, 2074–2078.

Clark, J.M., Brancati, F.L., and Diehl, A.M. (2002). Nonalcoholic fatty liver disease. Gastroenterology *122*, 1649–1657.

Clay, L., Caudron, F., Denoth-Lippuner, A., Boettcher, B., Buvelot Frei, S., Snapp, E.L., and Barral, Y. (2014). A sphingolipid-dependent diffusion barrier confines ER stress to the yeast mother cell. ELife *3*, e01883.

Clements, O., Eliahoo, J., Kim, J.U., Taylor-Robinson, S.D., and Khan, S.A. (2020). Risk factors for intrahepatic and extrahepatic cholangiocarcinoma: A systematic review and meta-analysis. J. Hepatol. *72*, 95–103.

Cocchiaro, J.L., Kumar, Y., Fischer, E.R., Hackstadt, T., and Valdivia, R.H. (2008). Cytoplasmic lipid droplets are translocated into the lumen of the Chlamydia trachomatis parasitophorous vacuole. Proc. Natl. Acad. Sci. *105*, 9379–9384.

Collins, K.B., Kang, H., Matsche, J., Klomp, J.E., Rehman, J., Malik, A.B., and Karginov, A.V. (2020). Septin2 mediates podosome maturation and endothelial cell invasion associated with angiogenesis. J. Cell Biol. *219*, e201903023.

Connolly, D., Yang, Z., Castaldi, M., Simmons, N., Oktay, M.H., Coniglio, S., Fazzari, M.J., Verdier-Pinard, P., and Montagna, C. (2011). Septin 9 isoform expression, localization and epigenetic changes during human and mouse breast cancer progression. Breast Cancer Res. BCR *13*, R76.

Connolly, D., Hoang, H.G., Adler, E., Tazearslan, C., Simmons, N., Bernard, V.V., Castaldi, M., Oktay, M.H., and Montagna, C. (2014). Septin 9 amplification and isoform-specific expression in peritumoral and tumor breast tissue. Biol. Chem. *395*, 157–167.

Čopič, A., Antoine-Bally, S., Giménez-Andrés, M., La Torre Garay, C., Antonny, B., Manni, M.M., Pagnotta, S., Guihot, J., and Jackson, C.L. (2018). A giant amphipathic helix from a perilipin that is adapted for coating lipid droplets. Nat. Commun. *9*, 1332.

Cuervo, A.M., and Wong, E. (2014). Chaperone-mediated autophagy: roles in disease and aging. Cell Res. *24*, 92–104.

Cusi, K. (2009). Nonalcoholic fatty liver disease in type 2 diabetes mellitus. Curr. Opin. Endocrinol. Diabetes Obes. *16*, 141–149.

Dash, S.N., Lehtonen, E., Wasik, A.A., Schepis, A., Paavola, J., Panula, P., Nelson, W.J., and Lehtonen, S. (2014). Sept7b is essential for pronephric function and development of left-right asymmetry in zebrafish embryogenesis. J. Cell Sci. *127*, 1476–1486.

De Craene, J.-O., Bertazzi, D.L., Bär, S., and Friant, S. (2017). Phosphoinositides, Major Actors in Membrane Trafficking and Lipid Signaling Pathways. Int. J. Mol. Sci. *18*.

De Matteis, M.A., Wilson, C., and D'Angelo, G. (2013). Phosphatidylinositol-4-phosphate: the Golgi and beyond. BioEssays News Rev. Mol. Cell. Dev. Biol. *35*, 612–622.

DeMay, B.S., Bai, X., Howard, L., Occhipinti, P., Meseroll, R.A., Spiliotis, E.T., Oldenbourg, R., and Gladfelter, A.S. (2011). Septin filaments exhibit a dynamic, paired organization that is conserved from yeast to mammals. J. Cell Biol. *193*, 1065–1081.

Deng, Y., Zhou, C., Mirza, A.H., Bamigbade, A.T., Zhang, S., Xu, S., and Liu, P. (2021). Rab18 binds PLIN2 and ACSL3 to mediate lipid droplet dynamics. Biochim. Biophys. Acta BBA - Mol. Cell Biol. Lipids *1866*, 158923.

Di Paolo, G., and De Camilli, P. (2006). Phosphoinositides in cell regulation and membrane dynamics. Nature *443*, 651–657.

Diesenberg, K., Beerbaum, M., Fink, U., Schmieder, P., and Krauss, M. (2015). SEPT9 negatively regulates ubiquitin-dependent downregulation of EGFR. J. Cell Sci. *128*, 397–407.

Dobbelaere, J., and Barral, Y. (2004). Spatial Coordination of Cytokinetic Events by Compartmentalization of the Cell Cortex. Science *305*, 393–396.

Dolat, L., and Spiliotis, E.T. (2016). Septins promote macropinosome maturation and traffic to the lysosome by facilitating membrane fusion. J. Cell Biol. *214*, 517–527.

Dolat, L., Hunyara, J.L., Bowen, J.R., Karasmanis, E.P., Elgawly, M., Galkin, V.E., and Spiliotis, E.T. (2014a). Septins promote stress fiber–mediated maturation of focal adhesions and renal epithelial motility. J. Cell Biol. *207*, 225–235.

Dolat, L., Hu, Q., and Spiliotis, E.T. (2014b). Septin functions in organ system physiology and pathology. Biol. Chem. *395*, 123–141.

Dong, B., Kakihara, K., Otani, T., Wada, H., and Hayashi, S. (2013). Rab9 and retromer regulate retrograde trafficking of luminal protein required for epithelial tube length control. Nat. Commun. *4*, 1358.

Douglas, L.M., Alvarez, F.J., McCreary, C., and Konopka, J.B. (2005). Septin function in yeast model systems and pathogenic fungi. Eukaryot. Cell *4*, 1503–1512.

Dreux, M., Gastaminza, P., Wieland, S.F., and Chisari, F.V. (2009). The autophagy machinery is required to initiate hepatitis C virus replication. Proc. Natl. Acad. Sci. *106*, 14046–14051.

Du, X., Zhou, L., Aw, Y.C., Mak, H.Y., Xu, Y., Rae, J., Wang, W., Zadoorian, A., Hancock, S.E., Osborne, B., et al. (2020). ORP5 localizes to ER-lipid droplet contacts and regulates the level of PI(4)P on lipid droplets. J. Cell Biol. *219*.

Dykes, S.S., Gray, A.L., Coleman, D.T., Saxena, M., Stephens, C.A., Carroll, J.L., Pruitt, K., and Cardelli, J.A. (2016). The Arf-like GTPase Arl8b is essential for three-dimensional invasive growth of prostate cancer in vitro and xenograft formation and growth in vivo. Oncotarget *7*, 31037–31052.

Encarnação, M., Espada, L., Escrevente, C., Mateus, D., Ramalho, J., Michelet, X., Santarino, I., Hsu, V.W., Brenner, M.B., Barral, D.C., et al. (2016). A Rab3a-dependent complex essential for lysosome positioning and plasma membrane repair. J. Cell Biol. *213*, 631–640.

Engidawork, E., Gulesserian, T., Fountoulakis, M., and Lubec, G. (2003). Aberrant protein expression in cerebral cortex of fetus with Down syndrome. Neuroscience *122*, 145–154.

Estey, M.P., Di Ciano-Oliveira, C., Froese, C.D., Bejide, M.T., and Trimble, W.S. (2010). Distinct roles of septins in cytokinesis: SEPT9 mediates midbody abscission. J. Cell Biol. *191*, 741–749.

Estey, M.P., Ciano-Oliveira, C.D., Froese, C.D., Fung, K.Y.Y., Steels, J.D., Litchfield, D.W., and Trimble, W.S. (2013). Mitotic Regulation of SEPT9 Protein by Cyclin-dependent Kinase 1 (Cdk1) and Pin1 Protein Is Important for the Completion of Cytokinesis *. J. Biol. Chem. *288*, 30075–30086.

Exner, T., Romero-Brey, I., Yifrach, E., Rivera-Monroy, J., Schrul, B., Zouboulis, C.C., Stremmel, W., Honsho, M., Bartenschlager, R., Zalckvar, E., et al. (2019). An alternative membrane topology permits lipid droplet localization of peroxisomal fatty acyl-CoA reductase 1. J. Cell Sci. *132*.

F, C., R, R., S, H., Aj, F., E, M., A, B., F, B., G, C., and E, S. (2015). Cdc42EP3/BORG2 and Septin Network Enables Mechano-transduction and the Emergence of Cancer-Associated Fibroblasts (Cell Rep).

Fanning, A.S., Van Itallie, C.M., and Anderson, J.M. (2012). Zonula occludens-1 and -2 regulate apical cell structure and the zonula adherens cytoskeleton in polarized epithelia. Mol. Biol. Cell *23*, 577–590.

Fei, W., Shui, G., Zhang, Y., Krahmer, N., Ferguson, C., Kapterian, T.S., Lin, R.C., Dawes, I.W., Brown, A.J., Li, P., et al. (2011). A role for phosphatidic acid in the formation of "supersized" lipid droplets. PLoS Genet. *7*, e1002201.

Ferramosca, A., and Zara, V. (2014). Modulation of hepatic steatosis by dietary fatty acids. World J. Gastroenterol. WJG *20*, 1746–1755.

Fliegauf, M., Kahle, A., Häffner, K., and Zieger, B. (2014). Distinct localization of septin proteins to ciliary sub-compartments in airway epithelial cells. Biol. Chem. *395*, 151–156.

Frampton, G., Invernizzi, P., Bernuzzi, F., Pae, H.Y., Quinn, M., Horvat, D., Galindo, C., Huang, L., McMillin, M., Cooper, B., et al. (2012). Interleukin-6-driven progranulin expression increases cholangiocarcinoma growth by an Akt-dependent mechanism. Gut *61*, 268–277.

Fujimoto, T., Ohsaki, Y., Cheng, J., Suzuki, M., and Shinohara, Y. (2008). Lipid droplets: a classic organelle with new outfits. Histochem. Cell Biol. *130*, 263–279.

Funderburk, S.F., Wang, Q.J., and Yue, Z. (2010). The Beclin 1-VPS34 complex--at the crossroads of autophagy and beyond. Trends Cell Biol. *20*, 355–362.

Fung, K.Y.Y., Dai, L., and Trimble, W.S. (2014). Chapter Seven - Cell and Molecular Biology of Septins. In International Review of Cell and Molecular Biology, K.W. Jeon, ed. (Academic Press), pp. 289–339.

G, J., Rr, P., Pj, S., M, K., M, N., T, H., and Ig, M. (2001). Borg Proteins Control Septin Organization and Are Negatively Regulated by Cdc42 (Nat Cell Biol).

Ganz, T. (2013). Systemic iron homeostasis. Physiol. Rev. *93*, 1721–1741.

Gao, M., Huang, X., Song, B.-L., and Yang, H. (2019). The biogenesis of lipid droplets: Lipids take center stage. Prog. Lipid Res. *75*, 100989.

Garcia, G., Bertin, A., Li, Z., Song, Y., McMurray, M.A., Thorner, J., and Nogales, E. (2011a). Subunit-dependent modulation of septin assembly: budding yeast septin Shs1 promotes ring and gauze formation. J. Cell Biol. *195*, 993–1004.

Garcia, G., Bertin, A., Li, Z., Song, Y., McMurray, M.A., Thorner, J., and Nogales, E. (2011b). Subunit-dependent modulation of septin assembly: budding yeast septin Shs1 promotes ring and gauze formation. J. Cell Biol. *195*, 993–1004.

García-Fernández, M., Kissel, H., Brown, S., Gorenc, T., Schile, A.J., Rafii, S., Larisch, S., and Steller, H. (2010). Sept4/ARTS is required for stem cell apoptosis and tumor suppression. Genes Dev. *24*, 2282–2293.

Garton, A.J., Campbell, D.G., Carling, D., Hardie, D.G., Colbran, R.J., and Yeaman, S.J. (1989). Phosphorylation of bovine hormone-sensitive lipase by the AMP-activated protein kinase. Eur. J. Biochem. *179*, 249–254.

Gassama-Diagne, A., Yu, W., Beest, M. ter, Martin-Belmonte, F., Kierbel, A., Engel, J., and Mostov, K. (2006). Phosphatidylinositol-3,4,5-trisphosphate regulates the formation of the basolateral plasma membrane in epithelial cells. Nat. Cell Biol. *8*, 963–970.

Gastaminza, P., Cheng, G., Wieland, S., Zhong, J., Liao, W., and Chisari, F.V. (2008). Cellular Determinants of Hepatitis C Virus Assembly, Maturation, Degradation, and Secretion. J. Virol. *82*,

2120–2129.

Gerondopoulos, A., Bastos, R.N., Yoshimura, S.-I., Anderson, R., Carpanini, S., Aligianis, I., Handley, M.T., and Barr, F.A. (2014). Rab18 and a Rab18 GEF complex are required for normal ER structure. J. Cell Biol. *205*, 707–720.

Ghossoub, R., Hu, Q., Failler, M., Rouyez, M.-C., Spitzbarth, B., Mostowy, S., Wolfrum, U., Saunier, S., Cossart, P., JamesNelson, W., et al. (2013). Septins 2, 7 and 9 and MAP4 colocalize along the axoneme in the primary cilium and control ciliary length. J. Cell Sci. *126*, 2583–2594.

Gilden, J.K., Peck, S., Chen, Y.-C.M., and Krummel, M.F. (2012). The septin cytoskeleton facilitates membrane retraction during motility and blebbing. J. Cell Biol. *196*, 103–114.

Gilleron, J., Gerdes, J.M., and Zeigerer, A. (2019). Metabolic regulation through the endosomal system. Traffic Cph. Den. *20*, 552–570.

Gillingham, A.K., Sinka, R., Torres, I.L., Lilley, K.S., and Munro, S. (2014). Toward a comprehensive map of the effectors of rab GTPases. Dev. Cell *31*, 358–373.

Giménez-Andrés, M., Čopič, A., and Antonny, B. (2018). The Many Faces of Amphipathic Helices. Biomolecules *8*, 45.

Gladfelter, A.S., Pringle, J.R., and Lew, D.J. (2001). The septin cortex at the yeast mother-bud neck. Curr. Opin. Microbiol. *4*, 681–689.

Gluchowski, N.L., Becuwe, M., Walther, T.C., and Farese, R.V. (2017). Lipid droplets and liver disease: from basic biology to clinical implications. Nat. Rev. Gastroenterol. Hepatol. *14*, 343–355.

Goginashvili, A., Zhang, Z., Erbs, E., Spiegelhalter, C., Kessler, P., Mihlan, M., Pasquier, A., Krupina, K., Schieber, N., Cinque, L., et al. (2015). Insulin granules. Insulin secretory granules control autophagy in pancreatic β cells. Science *347*, 878–882.

Gong, J., Sun, Z., Wu, L., Xu, W., Schieber, N., Xu, D., Shui, G., Yang, H., Parton, R.G., and Li, P. (2011). Fsp27 promotes lipid droplet growth by lipid exchange and transfer at lipid droplet contact sites. J. Cell Biol. *195*, 953–963.

Gonzalez, M.E., Peterson, E.A., Privette, L.M., Loffreda-Wren, J.L., Kalikin, L.M., and Petty, E.M. (2007). High SEPT9_v1 expression in human breast cancer cells is associated with oncogenic phenotypes. Cancer Res. *67*, 8554–8564.

Gonzalez, M.E., Makarova, O., Peterson, E.A., Privette, L.M., and Petty, E.M. (2009). Up-regulation of SEPT9_v1 stabilizes c-Jun-N-Terminal Kinase and contributes to its pro-proliferative activity in mammary epithelial cells. Cell. Signal. *21*, 477–487.

Goody, R.S., Rak, A., and Alexandrov, K. (2005). The structural and mechanistic basis for recycling of Rab proteins between membrane compartments. Cell. Mol. Life Sci. CMLS *62*, 1657–1670.

Gornicka, A., Fettig, J., Eguchi, A., Berk, M.P., Thapaliya, S., Dixon, L.J., and Feldstein, A.E. (2012). Adipocyte hypertrophy is associated with lysosomal permeability both in vivo and in vitro: role in adipose tissue inflammation. Am. J. Physiol. Endocrinol. Metab. *303*, E597-606.

Goud, B., Liu, S., and Storrie, B. (2018). Rab proteins as major determinants of the Golgi complex structure. Small GTPases *9*, 66–75.

Granneman, J.G., Moore, H.-P.H., Krishnamoorthy, R., and Rathod, M. (2009). Perilipin controls lipolysis by regulating the interactions of AB-hydrolase containing 5 (Abhd5) and adipose triglyceride lipase (Atgl). J. Biol. Chem. *284*, 34538–34544.

Greenberg, A.S., Egan, J.J., Wek, S.A., Garty, N.B., Blanchette-Mackie, E.J., and Londos, C. (1991). Perilipin, a major hormonally regulated adipocyte-specific phosphoprotein associated with the periphery of lipid storage droplets. J. Biol. Chem. *266*, 11341–11346.

Gronemeyer, T., Wiese, S., Grinhagens, S., Schollenberger, L., Satyagraha, A., Huber, L.A., Meyer, H.E., Warscheid, B., and Just, W.W. (2013). Localization of Rab proteins to peroxisomes: a proteomics and immunofluorescence study. FEBS Lett. *587*, 328–338.

Grumet, L., Eichmann, T.O., Taschler, U., Zierler, K.A., Leopold, C., Moustafa, T., Radovic, B., Romauch, M., Yan, C., Du, H., et al. (2016). Lysosomal Acid Lipase Hydrolyzes Retinyl Ester and Affects Retinoid Turnover. J. Biol. Chem. *291*, 17977–17987.

Guardia, C.M., Farías, G.G., Jia, R., Pu, J., and Bonifacino, J.S. (2016). BORC Functions Upstream of Kinesins 1 and 3 to Coordinate Regional Movement of Lysosomes along Different Microtubule Tracks. Cell Rep. *17*, 1950–1961.

Guo, Y., Walther, T.C., Rao, M., Stuurman, N., Goshima, G., Terayama, K., Wong, J.S., Vale, R.D., Walter, P., and Farese, R.V. (2008). Functional genomic screen reveals genes involved in lipid-droplet formation and utilization. Nature *453*, 657–661.

Gupta, G., Khadem, F., and Uzonna, J.E. (2019). Role of hepatic stellate cell (HSC)-derived cytokines in hepatic inflammation and immunity. Cytokine *124*, 154542.

Haemmerle, G., Moustafa, T., Woelkart, G., Büttner, S., Schmidt, A., van de Weijer, T., Hesselink, M., Jaeger, D., Kienesberger, P.C., Zierler, K., et al. (2011). ATGL-mediated fat catabolism regulates cardiac mitochondrial function via PPAR-α and PGC-1. Nat. Med. *17*, 1076–1085.

Hall, P.A., and Russell, S.H. (2004). The pathobiology of the septin gene family. J. Pathol. *204*, 489–505.

Hammond, G.R.V., and Balla, T. (2015). Polyphosphoinositide binding domains: key to inositol lipid biology. Biochim. Biophys. Acta *1851*, 746–758.

Hammond, G.R.V., and Burke, J.E. (2020). Novel roles of phosphoinositides in signaling, lipid transport, and disease. Curr. Opin. Cell Biol. *63*, 57–67.

Hanai, N., Nagata, K., Kawajiri, A., Shiromizu, T., Saitoh, N., Hasegawa, Y., Murakami, S., and Inagaki, M. (2004). Biochemical and cell biological characterization of a mammalian septin, Sept11. FEBS Lett. *568*, 83–88.

Harada, A., Takei, Y., Kanai, Y., Tanaka, Y., Nonaka, S., and Hirokawa, N. (1998). Golgi vesiculation and lysosome dispersion in cells lacking cytoplasmic dynein. J. Cell Biol. *141*, 51–59.

Harada, K., Shiota, G., and Kawasaki, H. (1999). Transforming growth factor-alpha and epidermal growth factor receptor in chronic liver disease and hepatocellular carcinoma. Liver *19*, 318–325.

Hasegawa, J., Strunk, B.S., and Weisman, L.S. (2017). PI5P and PI(3,5)P2: Minor, but Essential Phosphoinositides. Cell Struct. Funct. *42*, 49–60.

Hau, A.M., Gupta, S., Leivo, M.Z., Nakashima, K., Macias, J., Zhou, W., Hodge, A., Wulfkuhle, J.,

Conkright, B., Bhuvaneshwar, K., et al. (2019). Dynamic Regulation of Caveolin-1 Phosphorylation and Caveolae Formation by Mammalian Target of Rapamycin Complex 2 in Bladder Cancer Cells. Am. J. Pathol. *189*, 1846–1862.

Havugimana, P.C., Hart, G.T., Nepusz, T., Yang, H., Turinsky, A.L., Li, Z., Wang, P.I., Boutz, D.R., Fong, V., Phanse, S., et al. (2012). A census of human soluble protein complexes. Cell *150*, 1068–1081.

He, C., and Klionsky, D.J. (2009). Regulation mechanisms and signaling pathways of autophagy. Annu. Rev. Genet. *43*, 67–93.

He, H., Li, J., Xu, M., Kan, Z., Gao, Y., and Yuan, C. (2019). Expression of septin 2 and association with clinicopathological parameters in colorectal cancer. Oncol. Lett. *18*, 2376–2383.

Hendriks, I.A., and Vertegaal, A.C.O. (2016). A comprehensive compilation of SUMO proteomics. Nat. Rev. Mol. Cell Biol. *17*, 581–595.

Hendriks, I.A., Lyon, D., Young, C., Jensen, L.J., Vertegaal, A.C.O., and Nielsen, M.L. (2017). Site-specific mapping of the human SUMO proteome reveals co-modification with phosphorylation. Nat. Struct. Mol. Biol. *24*, 325–336.

Henzi, T., Lannes, N., and Filgueira, L. (2021). Septins in Infections: Focus on Viruses. Pathogens *10*.

Herms, A., Bosch, M., Reddy, B.J.N., Schieber, N.L., Fajardo, A., Rupérez, C., Fernández-Vidal, A., Ferguson, C., Rentero, C., Tebar, F., et al. (2015). AMPK activation promotes lipid droplet dispersion on detyrosinated microtubules to increase mitochondrial fatty acid oxidation. Nat. Commun. *6*, 1–14.

Hernández-Rodríguez, Y., and Momany, M. (2012a). Posttranslational modifications and assembly of septin heteropolymers and higher-order structures. Curr. Opin. Microbiol. *15*, 660–668.

Hernández-Rodríguez, Y., and Momany, M. (2012b). Posttranslational modifications and assembly of septin heteropolymers and higher-order structures. Curr. Opin. Microbiol. *15*, 660–668.

Heuser, J. (1989). Changes in lysosome shape and distribution correlated with changes in cytoplasmic pH. J. Cell Biol. *108*, 855–864.

Higuchi, Y., Kawakami, S., Yamashita, F., and Hashida, M. (2007). The potential role of fucosylated cationic liposome/NFκB decoy complexes in the treatment of cytokine-related liver disease. Biomaterials *28*, 532–539.

Hikita, H., Sakane, S., and Takehara, T. (2018). Mechanisms of the autophagosome-lysosome fusion step and its relation to non-alcoholic fatty liver disease. Liver Res. *2*, 120–124.

Hino, K., Hara, Y., and Nishina, S. (2014). Mitochondrial reactive oxygen species as a mystery voice in hepatitis C. Hepatol. Res. Off. J. Jpn. Soc. Hepatol. *44*, 123–132.

Hoefer, J., Schäfer, G., Klocker, H., Erb, H.H.H., Mills, I.G., Hengst, L., Puhr, M., and Culig, Z. (2012). PIAS1 is increased in human prostate cancer and enhances proliferation through inhibition of p21. Am. J. Pathol. *180*, 2097–2107.

Homma, Y., Hiragi, S., and Fukuda, M. (2021). Rab family of small GTPases: an updated view on their regulation and functions. FEBS J. *288*, 36–55.

Hu, Q., and Nelson, W.J. (2011). Ciliary diffusion barrier: the gatekeeper for the primary cilium compartment. Cytoskelet. Hoboken NJ *68*, 313–324.

Hu, G.-Q., Song, P.-X., Chen, W., Qi, S., Yu, S.-X., Du, C.-T., Deng, X.-M., Ouyang, H.-S., and Yang, Y.-J. (2017). Cirtical role for Salmonella effector SopB in regulating inflammasome activation. Mol. Immunol. *90*, 280–286.

Hu, Q., Milenkovic, L., Jin, H., Scott, M.P., Nachury, M.V., Spiliotis, E.T., and Nelson, W.J. (2010). A septin diffusion barrier at the base of the primary cilium maintains ciliary membrane protein distribution. Science *329*, 436–439.

Huijbregts, R.P.H., Svitin, A., Stinnett, M.W., Renfrow, M.B., and Chesnokov, I. (2009). Drosophila Orc6 facilitates GTPase activity and filament formation of the septin complex. Mol. Biol. Cell *20*, 270–281.

Huotari, J., and Helenius, A. (2011). Endosome maturation. EMBO J. *30*, 3481–3500.

Huynh, K.K., Eskelinen, E.-L., Scott, C.C., Malevanets, A., Saftig, P., and Grinstein, S. (2007). LAMP proteins are required for fusion of lysosomes with phagosomes. EMBO J. *26*, 313–324.

Ihara, M., Tomimoto, H., Kitayama, H., Morioka, Y., Akiguchi, I., Shibasaki, H., Noda, M., and Kinoshita, M. (2003). Association of the cytoskeletal GTP-binding protein Sept4/H5 with cytoplasmic inclusions found in Parkinson's disease and other synucleinopathies. J. Biol. Chem. *278*, 24095–24102.

Inami, Y., Yamashina, S., Izumi, K., Ueno, T., Tanida, I., Ikejima, K., and Watanabe, S. (2011). Hepatic steatosis inhibits autophagic proteolysis via impairment of autophagosomal acidification and cathepsin expression. Biochem. Biophys. Res. Commun. *412*, 618–625.

Iwase, M., Luo, J., Nagaraj, S., Longtine, M., Kim, H.B., Haarer, B.K., Caruso, C., Tong, Z., Pringle, J.R., and Bi, E. (2006). Role of a Cdc42p effector pathway in recruitment of the yeast septins to the presumptive bud site. Mol. Biol. Cell *17*, 1110–1125.

Jacome-Sosa, M.M., and Parks, E.J. (2014). Fatty acid sources and their fluxes as they contribute to plasma triglyceride concentrations and fatty liver in humans. Curr. Opin. Lipidol. *25*, 213–220.

Jaishy, B., and Abel, E.D. (2016). Lipids, lysosomes, and autophagy. J. Lipid Res. *57*, 1619–1635.

Jean, S., and Kiger, A.A. (2012). Coordination between RAB GTPase and phosphoinositide regulation and functions. Nat. Rev. Mol. Cell Biol. *13*, 463–470.

Jiang, H., Hua, D., Zhang, J., Lan, Q., Huang, Q., Yoon, J.-G., Han, X., Li, L., Foltz, G., Zheng, S., et al. (2014). MicroRNA-127-3p promotes glioblastoma cell migration and invasion by targeting the tumor-suppressor gene SEPT7. Oncol. Rep. *31*, 2261–2269.

Jin, Y., Ren, Z., Tan, Y., Zhao, P., and Wu, J. (2021). Motility Plays an Important Role in the Lifetime of Mammalian Lipid Droplets. Int. J. Mol. Sci. *22*.

Jing, J., and Prekeris, R. (2009). Polarized endocytic transport: the roles of Rab11 and Rab11-FIPs in regulating cell polarity. Histol. Histopathol. *24*, 1171–1180.

Johansson, M., Lehto, M., Tanhuanpää, K., Cover, T.L., and Olkkonen, V.M. (2005). The oxysterol-binding protein homologue ORP1L interacts with Rab7 and alters functional properties of late endocytic compartments. Mol. Biol. Cell *16*, 5480–5492.

Johansson, M., Rocha, N., Zwart, W., Jordens, I., Janssen, L., Kuijl, C., Olkkonen, V.M., and Neefjes, J. (2007). J. Cell Biol. *176*, 459–471.

John, C.M., Hite, R.K., Weirich, C.S., Fitzgerald, D.J., Jawhari, H., Faty, M., Schläpfer, D., Kroschewski, R., Winkler, F.K., Walz, T., et al. (2007). The Caenorhabditis elegans septin complex is nonpolar. EMBO J. *26*, 3296–3307.

Johnson, E.S., and Blobel, G. (1999a). Cell Cycle–Regulated Attachment of the Ubiquitin-Related Protein Sumo to the Yeast Septins. J. Cell Biol. *147*, 981–994.

Johnson, E.S., and Blobel, G. (1999b). Cell cycle-regulated attachment of the ubiquitin-related protein SUMO to the yeast septins. J. Cell Biol. *147*, 981–994.

Johnson, E.S., and Gupta, A.A. (2001). An E3-like Factor that Promotes SUMO Conjugation to the Yeast Septins. Cell *106*, 735–744.

Jongsma, M.L.M., Berlin, I., Wijdeven, R.H.M., Janssen, L., Janssen, G.M.C., Garstka, M.A., Janssen, H., Mensink, M., van Veelen, P.A., Spaapen, R.M., et al. (2016a). An ER-Associated Pathway Defines Endosomal Architecture for Controlled Cargo Transport. Cell *166*, 152–166.

Jongsma, M.L.M., Berlin, I., Wijdeven, R.H.M., Janssen, L., Janssen, G.M.C., Garstka, M.A., Janssen, H., Mensink, M., van Veelen, P.A., Spaapen, R.M., et al. (2016b). An ER-Associated Pathway Defines Endosomal Architecture for Controlled Cargo Transport. Cell *166*, 152–166.

Joo, E., Tsang, C.W., and Trimble, W.S. (2005). Septins: traffic control at the cytokinesis intersection. Traffic Cph. Den. *6*, 626–634.

Joo, E., Surka, M.C., and Trimble, W.S. (2007). Mammalian SEPT2 Is Required for Scaffolding Nonmuscle Myosin II and Its Kinases. Dev. Cell *13*, 677–690.

Jr, B., D, H., X, B., D, R., and Et, S. (2011). Septin GTPases Spatially Guide Microtubule Organization and Plus End Dynamics in Polarizing Epithelia (J Cell Biol).

Kalikin, L.M., Sims, H.L., and Petty, E.M. (2000). Genomic and Expression Analyses of Alternatively Spliced Transcripts of the MLL Septin-like Fusion Gene (MSF) That Map to a 17q25 Region of Loss in Breast and Ovarian Tumors. Genomics *63*, 165–172.

Karasmanis, E.P., Phan, C.-T., Angelis, D., Kesisova, I.A., Hoogenraad, C.C., McKenney, R.J., and Spiliotis, E.T. (2018). Polarity of Neuronal Membrane Traffic Requires Sorting of Kinesin Motor Cargo during Entry into Dendrites by a Microtubule-Associated Septin. Dev. Cell *46*, 518–524.

Kassan, A., Herms, A., Fernández-Vidal, A., Bosch, M., Schieber, N.L., Reddy, B.J.N., Fajardo, A., Gelabert-Baldrich, M., Tebar, F., Enrich, C., et al. (2013). Acyl-CoA synthetase 3 promotes lipid droplet biogenesis in ER microdomains. J. Cell Biol. *203*, 985–1001.

Kato, N. (2000). Genome of Human Hepatitis C Virus (HCV): Gene Organization, Sequence Diversity, and Variation. Microb. Comp. Genomics *5*, 129–151.

Katz, Z.B., Zhang, C., Quintana, A., Lillemeier, B.F., and Hogan, P.G. (2019). Septins organize endoplasmic reticulum-plasma membrane junctions for STIM1-ORAI1 calcium signalling. Sci. Rep. *9*.

Kaushik, S., and Cuervo, A.M. (2015). Degradation of lipid droplet-associated proteins by chaperone-mediated autophagy facilitates lipolysis. Nat. Cell Biol. *17*, 759–770.

Kesisova, I.A., Robinson, B.P., and Spiliotis, E.T. (2020). A septin GTPase scaffold of dynein-dynactin motors triggers retrograde lysosome transport. BioRxiv 2020.06.01.128488.

Khomich, O., Ivanov, A.V., and Bartosch, B. (2020). Metabolic Hallmarks of Hepatic Stellate Cells in Liver Fibrosis. Cells *9*, 24.

Kim, C.S., Seol, S.K., Song, O.-K., Park, J.H., and Jang, S.K. (2007). An RNA-binding protein, hnRNP A1, and a scaffold protein, septin 6, facilitate hepatitis C virus replication. J. Virol. *81*, 3852–3865.

Kim, K.-A., Gu, W., Lee, I.-A., Joh, E.-H., and Kim, D.-H. (2012). High fat diet-induced gut microbiota exacerbates inflammation and obesity in mice via the TLR4 signaling pathway. PloS One *7*, e47713.

Kim, M.S., Froese, C.D., Estey, M.P., and Trimble, W.S. (2011). SEPT9 occupies the terminal positions in septin octamers and mediates polymerization-dependent functions in abscission. J. Cell Biol. *195*, 815–826.

Kim, S.K., Shindo, A., Park, T.J., Oh, E.C., Ghosh, S., Gray, R.S., Lewis, R.A., Johnson, C.A., Attie-Bittach, T., Katsanis, N., et al. (2010). Planar cell polarity acts through septins to control collective cell movement and ciliogenesis. Science *329*, 1337–1340.

Kim, S.Y., Jeong, J.-M., Kim, S.J., Seo, W., Kim, M.-H., Choi, W.-M., Yoo, W., Lee, J.-H., Shim, Y.-R., Yi, H.-S., et al. (2017). Pro-inflammatory hepatic macrophages generate ROS through NADPH oxidase 2 via endocytosis of monomeric TLR4-MD2 complex. Nat. Commun. *8*, 2247.

Kinoshita, M. (2003). The septins. Genome Biol. *4*, 236.

Kinoshita, M., and Noda, M. (2001). Roles of septins in the mammalian cytokinesis machinery. Cell Struct. Funct. *26*, 667–670.

Kinoshita, A., Kinoshita, M., Akiyama, H., Tomimoto, H., Akiguchi, I., Kumar, S., Noda, M., and Kimura, J. (1998). Identification of Septins in Neurofibrillary Tangles in Alzheimer's Disease. Am. J. Pathol. *153*, 1551–1560.

Kinoshita, M., Kumar, S., Mizoguchi, A., Ide, C., Kinoshita, A., Haraguchi, T., Hiraoka, Y., and Noda, M. (1997). Nedd5, a mammalian septin, is a novel cytoskeletal component interacting with actin-based structures. Genes Dev. *11*, 1535–1547.

Kinoshita, M., Field, C.M., Coughlin, M.L., Straight, A.F., and Mitchison, T.J. (2002). Self- and Actin-Templated Assembly of Mammalian Septins. Dev. Cell *3*, 791–802.

Kirkbride, K.C., Hong, N.H., French, C.L., Clark, E.S., Jerome, W.G., and Weaver, A.M. (2012). Regulation of late endosomal/lysosomal maturation and trafficking by cortactin affects Golgi morphology. Cytoskelet. Hoboken NJ *69*, 625–643.

Klinkert, K., and Echard, A. (2016). Rab35 GTPase: A Central Regulator of Phosphoinositides and F-actin in Endocytic Recycling and Beyond. Traffic *17*, 1063–1077.

Koch, S., Acebron, S.P., Herbst, J., Hatiboglu, G., and Niehrs, C. (2015). Post-transcriptional Wnt Signaling Governs Epididymal Sperm Maturation. Cell *163*, 1225–1236.

Koike, K. (2009). Steatosis, liver injury, and hepatocarcinogenesis in hepatitis C viral infection. J. Gastroenterol. *44 Suppl 19*, 82–88.

Komori, J., Marusawa, H., Machimoto, T., Endo, Y., Kinoshita, K., Kou, T., Haga, H., Ikai, I., Uemoto, S., and Chiba, T. (2008). Activation-induced cytidine deaminase links bile duct inflammation to human cholangiocarcinoma. Hepatology *47*, 888–896.

Koo, S.-H. (2013). Nonalcoholic fatty liver disease: molecular mechanisms for the hepatic steatosis. Clin. Mol. Hepatol. *19*, 210–215.

Korolchuk, V.I., Saiki, S., Lichtenberg, M., Siddiqi, F.H., Roberts, E.A., Imarisio, S., Jahreiss, L., Sarkar, S., Futter, M., Menzies, F.M., et al. (2011). Lysosomal positioning coordinates cellular nutrient responses. Nat. Cell Biol. *13*, 453–460.

Kory, N., Thiam, A.-R., Farese, R.V., and Walther, T.C. (2015). Protein Crowding Is a Determinant of Lipid Droplet Protein Composition. Dev. Cell *34*, 351–363.

Kory, N., Farese, R.V., and Walther, T.C. (2016). Targeting Fat: Mechanisms of Protein Localization to Lipid Droplets. Trends Cell Biol. *26*, 535–546.

Krahmer, N., Guo, Y., Wilfling, F., Hilger, M., Lingrell, S., Heger, K., Newman, H.W., Schmidt-Supprian, M., Vance, D.E., Mann, M., et al. (2011). Phosphatidylcholine Synthesis for Lipid Droplet Expansion Is Mediated by Localized Activation of CTP:Phosphocholine Cytidylyltransferase. Cell Metab. *14*, 504–515.

Krahmer, N., Hilger, M., Kory, N., Wilfling, F., Stoehr, G., Mann, M., Farese, R.V., and Walther, T.C. (2013a). Protein Correlation Profiles Identify Lipid Droplet Proteins with High Confidence. Mol. Cell. Proteomics *12*, 1115–1126.

Krahmer, N., Hilger, M., Kory, N., Wilfling, F., Stoehr, G., Mann, M., Farese, R.V., and Walther, T.C. (2013b). Protein correlation profiles identify lipid droplet proteins with high confidence. Mol. Cell. Proteomics MCP *12*, 1115–1126.

Kremer, B.E., Haystead, T., and Macara, I.G. (2005). Mammalian septins regulate microtubule stability through interaction with the microtubule-binding protein MAP4. Mol. Biol. Cell *16*, 4648–4659.

Kremer, B.E., Adang, L.A., and Macara, I.G. (2007). Septins regulate actin organization and cell-cycle arrest through nuclear accumulation of NCK mediated by SOCS7. Cell *130*, 837–850.

Krintel, C., Osmark, P., Larsen, M.R., Resjö, S., Logan, D.T., and Holm, C. (2008). Ser649 and Ser650 Are the Major Determinants of Protein Kinase A-Mediated Activation of Human Hormone-Sensitive Lipase against Lipid Substrates. PLoS ONE *3*.

Krishna, M. (2013). Microscopic anatomy of the liver. Clin. Liver Dis. *2*, S4–S7.

Krokowski, S., Lobato-Márquez, D., Chastanet, A., Pereira, P.M., Angelis, D., Galea, D., Larrouy-Maumus, G., Henriques, R., Spiliotis, E.T., Carballido-López, R., et al. (2018). Septins Recognize and Entrap Dividing Bacterial Cells for Delivery to Lysosomes. Cell Host Microbe *24*, 866-874.e4.

Krzewski, K., Gil-Krzewska, A., Nguyen, V., Peruzzi, G., and Coligan, J.E. (2013). LAMP1/CD107a is required for efficient perforin delivery to lytic granules and NK-cell cytotoxicity. Blood *121*, 4672–4683.

Kumar, S., Duan, Q., Wu, R., Harris, E.N., and Su, Q. (2021). Pathophysiological communication between hepatocytes and non-parenchymal cells in liver injury from NAFLD to liver fibrosis. Adv. Drug Deliv. Rev. 113869.

Kuo, Y.-C., Lin, Y.-H., Chen, H.-I., Wang, Y.-Y., Chiou, Y.-W., Lin, H.-H., Pan, H.-A., Wu, C.-M., Su, S.-M., Hsu, C.-C., et al. (2012). SEPT12 mutations cause male infertility with defective sperm annulus. Hum. Mutat. *33*, 710–719.

Kurat, C.F., Wolinski, H., Petschnigg, J., Kaluarachchi, S., Andrews, B., Natter, K., and Kohlwein, S.D. (2009). Cdk1/Cdc28-dependent activation of the major triacylglycerol lipase Tgl4 in yeast links lipolysis to cell-cycle progression. Mol. Cell *33*, 53–63.

Kwanten, W.J., Martinet, W., Michielsen, P.P., and Francque, S.M. (2014). Role of autophagy in the pathophysiology of nonalcoholic fatty liver disease: a controversial issue. World J. Gastroenterol. *20*, 7325–7338.

Labib, P.L., Goodchild, G., and Pereira, S.P. (2019). Molecular Pathogenesis of Cholangiocarcinoma. BMC Cancer *19*, 185.

Lamber, E.P., Siedenburg, A.-C., and Barr, F.A. (2019). Rab regulation by GEFs and GAPs during membrane traffic. Curr. Opin. Cell Biol. *59*, 34–39.

Lambert, J.E., Ramos–Roman, M.A., Browning, J.D., and Parks, E.J. (2014). Increased De Novo Lipogenesis Is a Distinct Characteristic of Individuals With Nonalcoholic Fatty Liver Disease. Gastroenterology *146*, 726–735.

Lass, A., Zimmermann, R., Oberer, M., and Zechner, R. (2011). Lipolysis - a highly regulated multi-enzyme complex mediates the catabolism of cellular fat stores. Prog. Lipid Res. *50*, 14–27.

Lázaro-Diéguez, F., Jiménez, N., Barth, H., Koster, A.J., Renau-Piqueras, J., Llopis, J.L., Burger, K.N.J., and Egea, G. (2006). Actin filaments are involved in the maintenance of Golgi cisternae morphology and intra-Golgi pH. Cell Motil. Cytoskeleton *63*, 778–791.

Leandro, G., Mangia, A., Hui, J., Fabris, P., Rubbia-Brandt, L., Colloredo, G., Adinolfi, L.E., Asselah, T., Jonsson, J.R., Smedile, A., et al. (2006). Relationship between steatosis, inflammation, and fibrosis in chronic hepatitis C: a meta-analysis of individual patient data. Gastroenterology *130*, 1636–1642.

Lee, P.P., Lobato-Márquez, D., Pramanik, N., Sirianni, A., Daza-Cajigal, V., Rivers, E., Cavazza, A., Bouma, G., Moulding, D., Hultenby, K., et al. (2017). Wiskott-Aldrich syndrome protein regulates autophagy and inflammasome activity in innate immune cells. Nat. Commun. *8*, 1576.

Leipe, D.D., Wolf, Y.I., Koonin, E.V., and Aravind, L. (2002). Classification and evolution of P-loop GTPases and related ATPases. J. Mol. Biol. *317*, 41–72.

Leite, F., and Way, M. (2015). The role of signalling and the cytoskeleton during Vaccinia Virus egress. Virus Res. *209*, 87–99.

Leung, K.F., Baron, R., and Seabra, M.C. (2006). Thematic review series: lipid posttranslational modifications. geranylgeranylation of Rab GTPases. J. Lipid Res. *47*, 467–475.

Li, W., Zou, W., Zhao, D., Yan, J., Zhu, Z., Lu, J., and Wang, X. (2009). C. elegans Rab GTPase activating protein TBC-2 promotes cell corpse degradation by regulating the small GTPase RAB-5. Dev. Camb. Engl. *136*, 2445–2455.

Li, X., Rydzewski, N., Hider, A., Zhang, X., Yang, J., Wang, W., Gao, Q., Cheng, X., and Xu, H. (2016). A molecular mechanism to regulate lysosome motility for lysosome positioning and tubulation. Nat. Cell Biol. *18*, 404–417.

Lindenbach, B.D., and Rice, C.M. (2013). The ins and outs of hepatitis C virus entry and assembly. Nat. Rev. Microbiol. *11*, 688–700.

Liu, B., and Shuai, K. (2008). Targeting the PIAS1 SUMO ligase pathway to control inflammation. Trends Pharmacol. Sci. *29*, 505–509.

Liu, S., and Storrie, B. (2012). Are Rab Proteins the Link Between Golgi Organization and Membrane Trafficking? Cell. Mol. Life Sci. CMLS *69*, 4093–4106.

Liu, K., Xing, R., Jian, Y., Gao, Z., Ma, X., Sun, X., Li, Y., Xu, M., Wang, X., Jing, Y., et al. (2017). WDR91 is a Rab7 effector required for neuronal development. J. Cell Biol. *216*, 3307–3321.

Liu, M., Shen, S., Chen, F., Yu, W., and Yu, L. (2010). Linking the septin expression with carcinogenesis. Mol. Biol. Rep. *37*, 3601–3608.

Lizaso, A., Tan, K.-T., and Lee, Y.-H. (2013). β-adrenergic receptor-stimulated lipolysis requires the RAB7-mediated autolysosomal lipid degradation. Autophagy *9*, 1228–1243.

Longtine, M.S., and Bi, E. (2003). Regulation of septin organization and function in yeast. Trends Cell Biol. *13*, 403–409.

Luedde, T., Kaplowitz, N., and Schwabe, R.F. (2014). Cell Death and Cell Death Responses in Liver Disease: Mechanisms and Clinical Relevance. Gastroenterology *147*, 765-783.e4.

Luedeke, C., Frei, S.B., Sbalzarini, I., Schwarz, H., Spang, A., and Barral, Y. (2005). Septin-dependent compartmentalization of the endoplasmic reticulum during yeast polarized growth. J. Cell Biol. *169*, 897–908.

M, F., A, K., K, H., and B, Z. (2014a). Distinct Localization of Septin Proteins to Ciliary Sub-Compartments in Airway Epithelial Cells (Biol Chem).

M, M., Y, A.-G., Fc, T., J, A., A, B., F, I., A, K., S, B., Gh, K., and T, L. (2014b). Septins Promote F-actin Ring Formation by Crosslinking Actin Filaments Into Curved Bundles (Nat Cell Biol).

Macara, I.G., Baldarelli, R., Field, C.M., Glotzer, M., Hayashi, Y., Hsu, S.-C., Kennedy, M.B., Kinoshita, M., Longtine, M., Low, C., et al. (2002). Mammalian Septins Nomenclature. Mol. Biol. Cell *13*, 4111–4113.

Macedo, J.N.A., Valadares, N.F., Marques, I.A., Ferreira, F.M., Damalio, J.C.P., Pereira, H.M., Garratt, R.C., and Araujo, A.P.U. (2013). The structure and properties of septin 3: a possible missing link in septin filament formation. Biochem. J. *450*, 95–105.

Maimaitiyiming, M., Kobayashi, Y., Kumanogoh, H., Nakamura, S., Morita, M., and Maekawa, S. (2013). Identification of dynamin as a septin-binding protein. Neurosci. Lett. *534*, 322–326.

Marat, A.L., and Haucke, V. (2016). Phosphatidylinositol 3-phosphates-at the interface between cell signalling and membrane traffic. EMBO J. *35*, 561–579.

Marcinkiewicz, A., Gauthier, D., Garcia, A., and Brasaemle, D.L. (2006). The Phosphorylation of Serine 492 of Perilipin A Directs Lipid Droplet Fragmentation and Dispersion. J. Biol. Chem. *281*, 11901–11909.

Marcus, E.A., Tokhtaeva, E., Turdikulova, S., Capri, J., Whitelegge, J.P., Scott, D.R., Sachs, G., Berditchevski, F., and Vagin, O. (2016). Septin oligomerization regulates persistent expression of

ErbB2/HER2 in gastric cancer cells. Biochem. J. *473*, 1703–1718.

Marcus, J., Bejerano-Sagie, M., Patterson, N., Bagchi, S., Verkhusha, V.V., Connolly, D., Goldberg, G.L., Golden, A., Sharma, V.P., Condeelis, J., et al. (2019). Septin 9 isoforms promote tumorigenesis in mammary epithelial cells by increasing migration and ECM degradation through metalloproteinase secretion at focal adhesions. Oncogene *38*, 5839–5859.

Martin, S., Driessen, K., Nixon, S.J., Zerial, M., and Parton, R.G. (2005). Regulated localization of Rab18 to lipid droplets: effects of lipolytic stimulation and inhibition of lipid droplet catabolism. J. Biol. Chem. *280*, 42325–42335.

Mas, V.R., Maluf, D.G., Archer, K.J., Yanek, K., Kong, X., Kulik, L., Freise, C.E., Olthoff, K.M., Ghobrial, R.M., McIver, P., et al. (2009). Genes involved in viral carcinogenesis and tumor initiation in hepatitis C virus-induced hepatocellular carcinoma. Mol. Med. Camb. Mass *15*, 85–94.

Matsushita, M., Tanaka, S., Nakamura, N., Inoue, H., and Kanazawa, H. (2004). A novel kinesin-like protein, KIF1Bbeta3 is involved in the movement of lysosomes to the cell periphery in non-neuronal cells. Traffic Cph. Den. *5*, 140–151.

McCaffrey, M.W., Lindsay, A.J., and Kitainda, V. (2021). G-proteins | Rab Family☆. In Encyclopedia of Biological Chemistry III (Third Edition), J. Jez, ed. (Oxford: Elsevier), pp. 462–468.

McFie, P.J., Stone, S.L., Banman, S.L., and Stone, S.J. (2010). Topological orientation of acyl-CoA:diacylglycerol acyltransferase-1 (DGAT1) and identification of a putative active site histidine and the role of the n terminus in dimer/tetramer formation. J. Biol. Chem. *285*, 37377–37387.

McIntosh, A.L., Storey, S.M., and Atshaves, B.P. (2010). Intracellular lipid droplets contain dynamic pools of sphingomyelin: ADRP binds phospholipids with high affinity. Lipids *45*, 465–477.

McMahon, H.T., and Boucrot, E. (2015). Membrane curvature at a glance. J. Cell Sci. *128*, 1065–1070.

McMurray, M. (2014). Lean forward: Genetic analysis of temperature-sensitive mutants unfolds the secrets of oligomeric protein complex assembly. BioEssays News Rev. Mol. Cell. Dev. Biol. *36*, 836–846.

McMurray, M.A. (2019). The long and short of membrane curvature sensing by septins. J. Cell Biol. *218*, 1083–1085.

Mège, R.M., and Ishiyama, N. (2017). Integration of Cadherin Adhesion and Cytoskeleton at Adherens Junctions. Cold Spring Harb. Perspect. Biol. *9*, a028738.

Menon, M.B., Sawada, A., Chaturvedi, A., Mishra, P., Schuster-Gossler, K., Galla, M., Schambach, A., Gossler, A., Förster, R., Heuser, M., et al. (2014). Genetic deletion of SEPT7 reveals a cell type-specific role of septins in microtubule destabilization for the completion of cytokinesis. PLoS Genet. *10*, e1004558.

Meseroll, R.A., Howard, L., and Gladfelter, A.S. (2012). Septin ring size scaling and dynamics require the coiled-coil region of Shs1p. Mol. Biol. Cell *23*, 3391–3406.

Meseroll, R.A., Occhipinti, P., and Gladfelter, A.S. (2013). Septin Phosphorylation and Coiled-Coil Domains Function in Cell and Septin Ring Morphology in the Filamentous Fungus Ashbya

gossypii. Eukaryot. Cell *12*, 182–193.

Mészáros, G., Pasquier, A., Vivot, K., Goginashvili, A., and Ricci, R. (2018). Lysosomes in nutrient signalling: A focus on pancreatic β-cells. Diabetes Obes. Metab. *20 Suppl 2*, 104–115.

Michelotti, G.A., Machado, M.V., and Diehl, A.M. (2013). NAFLD, NASH and liver cancer. Nat. Rev. Gastroenterol. Hepatol. *10*, 656–665.

Mihm, S., Fayyazi, A., Hartmann, H., and Ramadori, G. (1997). Analysis of histopathological manifestations of chronic hepatitis C virus infection with respect to virus genotype. Hepatol. Baltim. Md *25*, 735–739.

Mijaljica, D., Prescott, M., and Devenish, R.J. (2011). Microautophagy in mammalian cells: revisiting a 40-year-old conundrum. Autophagy *7*, 673–682.

Mitchell, L., Lau, A., Lambert, J.-P., Zhou, H., Fong, Y., Couture, J.-F., Figeys, D., and Baetz, K. (2011). Regulation of Septin Dynamics by the Saccharomyces cerevisiae Lysine Acetyltransferase NuA4. PLOS ONE *6*, e25336.

Miyagawa, K., Oe, S., Honma, Y., Izumi, H., Baba, R., and Harada, M. (2016). Lipid-Induced Endoplasmic Reticulum Stress Impairs Selective Autophagy at the Step of Autophagosome-Lysosome Fusion in Hepatocytes. Am. J. Pathol. *186*, 1861–1873.

Miyanari, Y., Atsuzawa, K., Usuda, N., Watashi, K., Hishiki, T., Zayas, M., Bartenschlager, R., Wakita, T., Hijikata, M., and Shimotohno, K. (2007). The lipid droplet is an important organelle for hepatitis C virus production. Nat. Cell Biol. *9*, 1089–1097.

Miyoshi, H., Perfield, J.W., Souza, S.C., Shen, W.-J., Zhang, H.-H., Stancheva, Z.S., Kraemer, F.B., Obin, M.S., and Greenberg, A.S. (2007). Control of adipose triglyceride lipase action by serine 517 of perilipin A globally regulates protein kinase A-stimulated lipolysis in adipocytes. J. Biol. Chem. *282*, 996–1002.

Mizuno-Yamasaki, E., Rivera-Molina, F., and Novick, P. (2012). GTPase networks in membrane traffic. Annu. Rev. Biochem. *81*, 637–659.

Mizushima, N., Levine, B., Cuervo, A.M., and Klionsky, D.J. (2008). Autophagy fights disease through cellular self-digestion. Nature *451*, 1069–1075.

Møller, A.M.J., Füchtbauer, E.-M., Brüel, A., Andersen, T.L., Borggaard, X.G., Pavlos, N.J., Thomsen, J.S., Pedersen, F.S., Delaisse, J.-M., and Søe, K. (2018). Septins are critical regulators of osteoclastic bone resorption. Sci. Rep. *8*, 13016.

Montagna, C., Sagie, M., and Zechmeister, J. (2015). Mammalian septins in health and disease. Res. Rep. Biochem. 59.

Moreno-Castellanos, N., Rodríguez, A., Rabanal-Ruiz, Y., Fernández-Vega, A., López-Miranda, J., Vázquez-Martínez, R., Frühbeck, G., and Malagón, M.M. (2017). The cytoskeletal protein septin 11 is associated with human obesity and is involved in adipocyte lipid storage and metabolism. Diabetologia *60*, 324–335.

Morozko, E.L., Smith-Geater, C., Monteys, A.M., Pradhan, S., Lim, R.G., Langfelder, P., Kachemov, M., Hill, A., Stocksdale, J.T., Cullis, P.R., et al. (2021). PIAS1 modulates striatal transcription, DNA damage repair, and SUMOylation with relevance to Huntington's disease. Proc. Natl. Acad. Sci. U. S. A. *118*, e2021836118.

Mostowy, S., and Cossart, P. (2012). Septins: the fourth component of the cytoskeleton. Nat. Rev. Mol. Cell Biol. *13*, 183–194.

Mostowy, S., Danckaert, A., Tham, T.N., Machu, C., Guadagnini, S., Pizarro-Cerdá, J., and Cossart, P. (2009a). Septin 11 Restricts InlB-mediated Invasion by Listeria. J. Biol. Chem. *284*, 11613–11621.

Mostowy, S., Nam Tham, T., Danckaert, A., Guadagnini, S., Boisson-Dupuis, S., Pizarro-Cerdá, J., and Cossart, P. (2009b). Septins regulate bacterial entry into host cells. PloS One *4*, e4196.

Mostowy, S., Bonazzi, M., Hamon, M.A., Tham, T.N., Mallet, A., Lelek, M., Gouin, E., Demangel, C., Brosch, R., Zimmer, C., et al. (2010). Entrapment of Intracytosolic Bacteria by Septin Cage-like Structures. Cell Host Microbe *8*, 433–444.

Mostowy, S., Janel, S., Forestier, C., Roduit, C., Kasas, S., Pizarro-Cerdá, J., Cossart, P., and Lafont, F. (2011). A role for septins in the interaction between the Listeria monocytogenes INVASION PROTEIN InlB and the Met receptor. Biophys. J. *100*, 1949–1959.

Murray, J.T., Panaretou, C., Stenmark, H., Miaczynska, M., and Backer, J.M. (2002). Role of Rab5 in the recruitment of hVps34/p150 to the early endosome. Traffic Cph. Den. *3*, 416–427.

Nagayama, M., Uchida, T., and Gohara, K. (2007). Temporal and spatial variations of lipid droplets during adipocyte division and differentiation. J. Lipid Res. *48*, 9–18.

Nakada-Tsukui, K., Watanabe, N., Maehama, T., and Nozaki, T. (2019). Phosphatidylinositol Kinases and Phosphatases in Entamoeba histolytica. Front. Cell. Infect. Microbiol. *9*, 150.

Nakahira, M., Macedo, J.N.A., Seraphim, T.V., Cavalcante, N., Souza, T.A.C.B., Damalio, J.C.P., Reyes, L.F., Assmann, E.M., Alborghetti, M.R., Garratt, R.C., et al. (2010). A draft of the human septin interactome. PloS One *5*, e13799.

Nakata, T., and Hirokawa, N. (1995). Point mutation of adenosine triphosphate-binding motif generated rigor kinesin that selectively blocks anterograde lysosome membrane transport. J. Cell Biol. *131*, 1039–1053.

Neefjes, J., Jongsma, M.M.L., and Berlin, I. (2017). Stop or Go? Endosome Positioning in the Establishment of Compartment Architecture, Dynamics, and Function. Trends Cell Biol. *27*, 580–594.

Neubauer, K., and Zieger, B. (2017). The Mammalian Septin Interactome. Front. Cell Dev. Biol. *5*.

Ng, M.M., Dippold, H.C., Buschman, M.D., Noakes, C.J., and Field, S.J. (2013). GOLPH3L antagonizes GOLPH3 to determine Golgi morphology. Mol. Biol. Cell *24*, 796–808.

Nielsen, S.U., Bassendine, M.F., Burt, A.D., Martin, C., Pumeechockchai, W., and Toms, G.L. (2006). Association between Hepatitis C Virus and Very-Low-Density Lipoprotein (VLDL)/LDL Analyzed in Iodixanol Density Gradients. J. Virol. *80*, 2418–2428.

Nishida, N., Yada, N., Hagiwara, S., Sakurai, T., Kitano, M., and Kudo, M. (2016). Unique features associated with hepatic oxidative DNA damage and DNA methylation in non-alcoholic fatty liver disease. J. Gastroenterol. Hepatol. *31*, 1646–1653.

Nishihama, R., Onishi, M., and Pringle, J.R. (2011). New insights into the phylogenetic distribution and evolutionary origins of the septins. Biol. Chem. *392*, 681–687.

Noor, M.T., and Manoria, P. (2017). Immune Dysfunction in Cirrhosis. J. Clin. Transl. Hepatol. *5*, 50–58.

Nordmann, M., Cabrera, M., Perz, A., Bröcker, C., Ostrowicz, C., Engelbrecht-Vandré, S., and Ungermann, C. (2010). The Mon1-Ccz1 complex is the GEF of the late endosomal Rab7 homolog Ypt7. Curr. Biol. CB *20*, 1654–1659.

Olzmann, J.A., and Carvalho, P. (2019). Dynamics and functions of lipid droplets. Nat. Rev. Mol. Cell Biol. *20*, 137–155.

Omrane, M., Camara, A.S., Taveneau, C., Benzoubir, N., Tubiana, T., Yu, J., Guérois, R., Samuel, D., Goud, B., Poüs, C., et al. (2019). Septin 9 has Two Polybasic Domains Critical to Septin Filament Assembly and Golgi Integrity. IScience *13*, 138–153.

Orabi, D., Berger, N.A., and Brown, J.M. (2021). Abnormal Metabolism in the Progression of Nonalcoholic Fatty Liver Disease to Hepatocellular Carcinoma: Mechanistic Insights to Chemoprevention. Cancers *13*, 3473.

Osaka, M., Rowley, J.D., and Zeleznik-Le, N.J. (1999). MSF (MLL septin-like fusion), a fusion partner gene of MLL, in a therapy-related acute myeloid leukemia with a t(11;17)(q23;q25). Proc. Natl. Acad. Sci. *96*, 6428–6433.

Ozeki, S., Cheng, J., Tauchi-Sato, K., Hatano, N., Taniguchi, H., and Fujimoto, T. (2005). Rab18 localizes to lipid droplets and induces their close apposition to the endoplasmic reticulum-derived membrane. J. Cell Sci. *118*, 2601–2611.

Pagliuso, A., Tham, T.N., Stevens, J.K., Lagache, T., Persson, R., Salles, A., Olivo-Marin, J.-C., Oddos, S., Spang, A., Cossart, P., et al. (2016). A role for septin 2 in Drp1-mediated mitochondrial fission. EMBO Rep. *17*, 858–873.

Pan, F., Malmberg, R.L., and Momany, M. (2007). Analysis of septins across kingdoms reveals orthology and new motifs. BMC Evol. Biol. *7*, 103.

Pankiv, S., Alemu, E.A., Brech, A., Bruun, J.-A., Lamark, T., Overvatn, A., Bjørkøy, G., and Johansen, T. (2010). Gerondopoulos et al., 2014mediate microtubule plus end-directed vesicle transport. J. Cell Biol. *188*, 253–269.

Pastore, N., Vainshtein, A., Klisch, T.J., Armani, A., Huynh, T., Herz, N.J., Polishchuk, E.V., Sandri, M., and Ballabio, A. (2017). TFE3 regulates whole-body energy metabolism in cooperation with TFEB. EMBO Mol. Med. *9*, 605–621.

Paul, D., Madan, V., and Bartenschlager, R. (2014). Hepatitis C virus RNA replication and assembly: living on the fat of the land. Cell Host Microbe *16*, 569–579.

Payrastre, B., Missy, K., Giuriato, S., Bodin, S., Plantavid, M., and Gratacap, M. (2001). Phosphoinositides: key players in cell signalling, in time and space. Cell. Signal. *13*, 377–387.

Pellett, P.A., Dietrich, F., Bewersdorf, J., Rothman, J.E., and Lavieu, G. (2013). Inter-Golgi transport mediated by COPI-containing vesicles carrying small cargoes. ELife *2*, e01296.

Pemberton, J.G., and Balla, T. (2019). Polyphosphoinositide-Binding Domains: Insights from Peripheral Membrane and Lipid-Transfer Proteins. Adv. Exp. Med. Biol. *1111*, 77–137.

Pennington, K., Beasley, C.L., Dicker, P., Fagan, A., English, J., Pariante, C.M., Wait, R., Dunn,

M.J., and Cotter, D.R. (2008). Prominent synaptic and metabolic abnormalities revealed by proteomic analysis of the dorsolateral prefrontal cortex in schizophrenia and bipolar disorder. Mol. Psychiatry *13*, 1102–1117.

Penno, A., Hackenbroich, G., and Thiele, C. (2013). Phospholipids and lipid droplets. Biochim. Biophys. Acta *1831*, 589–594.

Pereira-Leal, J.B., Hume, A.N., and Seabra, M.C. (2001). Prenylation of Rab GTPases: molecular mechanisms and involvement in genetic disease. FEBS Lett. *498*, 197–200.

Perera, R.M., and Zoncu, R. (2016). The Lysosome as a Regulatory Hub. Annu. Rev. Cell Dev. Biol. *32*, 223–253.

Pfanzelter, J., Mostowy, S., and Way, M. (2018). Septins suppress the release of vaccinia virus from infected cells. J. Cell Biol. *217*, 2911–2929.

Pinzani, M. (2015). Pathophysiology of Liver Fibrosis. Dig. Dis. *33*, 492–497.

Pizarro-Cerdá, J., Jonquières, R., Gouin, E., Vandekerckhove, J., Garin, J., and Cossart, P. (2002). Distinct protein patterns associated with Listeria monocytogenes InlA- or InlB-phagosomes. Cell. Microbiol. *4*, 101–115.

Płóciennikowska, A., Hromada-Judycka, A., Borzęcka, K., and Kwiatkowska, K. (2015). Co-operation of TLR4 and raft proteins in LPS-induced pro-inflammatory signaling. Cell. Mol. Life Sci. CMLS *72*, 557–581.

Poisson, J., Lemoinne, S., Boulanger, C., Durand, F., Moreau, R., Valla, D., and Rautou, P.-E. (2017). Liver sinusoidal endothelial cells: Physiology and role in liver diseases. J. Hepatol. *66*, 212–227.

Poli, A., Billi, A.M., Mongiorgi, S., Ratti, S., McCubrey, J.A., Suh, P.-G., Cocco, L., and Ramazzotti, G. (2016). Nuclear Phosphatidylinositol Signaling: Focus on Phosphatidylinositol Phosphate Kinases and Phospholipases C. J. Cell. Physiol. *231*, 1645–1655.

Postic, C., and Girard, J. (2008). Contribution of de novo fatty acid synthesis to hepatic steatosis and insulin resistance: lessons from genetically engineered mice (American Society for Clinical Investigation).

Poteryaev, D., Datta, S., Ackema, K., Zerial, M., and Spang, A. (2010). Identification of the switch in early-to-late endosome transition. Cell *141*, 497–508.

Prévost, C., Sharp, M.E., Kory, N., Lin, Q., Voth, G.A., Farese, R.V., and Walther, T.C. (2018). Mechanism and Determinants of Amphipathic Helix-Containing Protein Targeting to Lipid Droplets. Dev. Cell *44*, 73-86.e4.

Pu, J., Schindler, C., Jia, R., Jarnik, M., Backlund, P., and Bonifacino, J.S. (2015). BORC, a Multisubunit Complex that Regulates Lysosome Positioning. Dev. Cell *33*, 176–188.

Pu, J., Guardia, C.M., Keren-Kaplan, T., and Bonifacino, J.S. (2016). Mechanisms and functions of lysosome positioning. J. Cell Sci. *129*, 4329–4339.

Puche, J.E., Saiman, Y., and Friedman, S.L. (2013). Hepatic Stellate Cells and Liver Fibrosis. In Comprehensive Physiology, (American Cancer Society), pp. 1473–1492.

Pulido, M.R., Diaz-Ruiz, A., Jiménez-Gómez, Y., Garcia-Navarro, S., Gracia-Navarro, F.,

Tinahones, F., López-Miranda, J., Frühbeck, G., Vázquez-Martínez, R., and Malagón, M.M. (2011). Rab18 dynamics in adipocytes in relation to lipogenesis, lipolysis and obesity. PloS One *6*, e22931.

Qayyum, A., Nystrom, M., Noworolski, S.M., Chu, P., Mohanty, A., and Merriman, R. (2012). MRI steatosis grading: development and initial validation of a color mapping system. AJR Am. J. Roentgenol. *198*, 582–588.

Qiao, Q., Zhang, J., Wang, W., and Li, Q. (2008). Over expression of transforming growth factor-alpha and epidermal growth factor receptor in human hepatic cirrhosis tissues. Hepatogastroenterology. *55*, 169–172.

Qt, P., Dk, E., S, M., H, P., P, C., and Sg, F. (2013). Role of Endothelial Cell Septin 7 in the Endocytosis of Candida Albicans (mBio).

Raiborg, C., Wenzel, E.M., Pedersen, N.M., Olsvik, H., Schink, K.O., Schultz, S.W., Vietri, M., Nisi, V., Bucci, C., Brech, A., et al. (2015). Repeated ER-endosome contacts promote endosome translocation and neurite outgrowth. Nature *520*, 234–238.

Rambold, A.S., Cohen, S., and Lippincott-Schwartz, J. (2015). Fatty acid trafficking in starved cells: regulation by lipid droplet lipolysis, autophagy, and mitochondrial fusion dynamics. Dev. Cell *32*, 678–692.

Ramos, A.R., Ghosh, S., Suhel, T., Chevalier, C., Obeng, E.O., Fafilek, B., Krejci, P., Beck, B., and Erneux, C. (2020). Phosphoinositide 5-phosphatases SKIP and SHIP2 in ruffles, the endoplasmic reticulum and the nucleus: An update. Adv. Biol. Regul. *75*, 100660.

Rautou, P.-E., Cazals-Hatem, D., Feldmann, G., Mansouri, A., Grodet, A., Barge, S., Martinot-Peignoux, M., Duces, A., Bièche, I., Lebrec, D., et al. (2011). Changes in Autophagic Response in Patients with Chronic Hepatitis C Virus Infection. Am. J. Pathol. *178*, 2708–2715.

Razumilava, N., and Gores, G.J. (2013). Classification, Diagnosis, and Management of Cholangiocarcinoma. Clin. Gastroenterol. Hepatol. Off. Clin. Pract. J. Am. Gastroenterol. Assoc. *11*, 13-e4.

Ren, J., Pei-Chen Lin, C., Pathak, M.C., Temple, B.R.S., Nile, A.H., Mousley, C.J., Duncan, M.C., Eckert, D.M., Leiker, T.J., Ivanova, P.T., et al. (2014). A phosphatidylinositol transfer protein integrates phosphoinositide signaling with lipid droplet metabolism to regulate a developmental program of nutrient stress–induced membrane biogenesis. Mol. Biol. Cell *25*, 712–727.

Reungoat, E., Grigorov, B., Zoulim, F., and Pécheur, E.-I. (2021). Molecular Crosstalk between the Hepatitis C Virus and the Extracellular Matrix in Liver Fibrogenesis and Early Carcinogenesis. Cancers *13*, 2270.

Ribet, D., Boscaini, S., Cauvin, C., Siguier, M., Mostowy, S., Echard, A., and Cossart, P. (2017a). SUMOylation of human septins is critical for septin filament bundling and cytokinesis. J. Cell Biol. *216*, 4041–4052.

Ribet, D., Boscaini, S., Cauvin, C., Siguier, M., Mostowy, S., Echard, A., and Cossart, P. (2017b). SUMOylation of human septins is critical for septin filament bundling and cytokinesis. J Cell Biol *216*, 4041–4052.

Rink, J., Ghigo, E., Kalaidzidis, Y., and Zerial, M. (2005). Rab Conversion as a Mechanism of Progression from Early to Late Endosomes. Cell *122*, 735–749.

Roberts, M.A., and Olzmann, J.A. (2020). Protein Quality Control and Lipid Droplet Metabolism. Annu. Rev. Cell Dev. Biol. *36*, 115–139.

Rocha, N., Kuijl, C., van der Kant, R., Janssen, L., Houben, D., Janssen, H., Zwart, W., and Neefjes, J. (2009). Cholesterol sensor ORP1L contacts the ER protein VAP to control Rab7-RILP-p150 Glued and late endosome positioning. J. Cell Biol. *185*, 1209–1225.

Rodriguez-Boulan, E., and Macara, I.G. (2014). Organization and execution of the epithelial polarity programme. Nat. Rev. Mol. Cell Biol. *15*, 225–242.

Rosa-Ferreira, C., and Munro, S. (2011). Arl8 and SKIP Act Together to Link Lysosomes to Kinesin-1. Dev. Cell *21*, 1171–1178.

Rose, K., Rudge, S.A., Frohman, M.A., Morris, A.J., and Engebrecht, J. (1995). Phospholipase D signaling is essential for meiosis. Proc. Natl. Acad. Sci. *92*, 12151–12155.

Rothman, J.E. (2002). The machinery and principles of vesicle transport in the cell. Nat. Med. *8*, 1059–1062.

Rowe, E.R., Mimmack, M.L., Barbosa, A.D., Haider, A., Isaac, I., Ouberai, M.M., Thiam, A.R., Patel, S., Saudek, V., Siniossoglou, S., et al. (2016). Conserved Amphipathic Helices Mediate Lipid Droplet Targeting of Perilipins 1–3 *. J. Biol. Chem. *291*, 6664–6678.

Rubbia-Brandt, L., Quadri, R., Abid, K., Giostra, E., Malé, P.J., Mentha, G., Spahr, L., Zarski, J.P., Borisch, B., Hadengue, A., et al. (2000). Hepatocyte steatosis is a cytopathic effect of hepatitis C virus genotype 3. J. Hepatol. *33*, 106–115.

Russell, S.E.H., and Hall, P.A. (2011). Septin genomics: a road less travelled. Biol. Chem. *392*, 763–767.

Rytinki, M.M., Kaikkonen, S., Pehkonen, P., Jääskeläinen, T., and Palvimo, J.J. (2009). PIAS proteins: pleiotropic interactors associated with SUMO. Cell. Mol. Life Sci. CMLS *66*, 3029–3041.

S, M., and P, C. (2011). Septins as Key Regulators of Actin Based Processes in Bacterial Infection (Biol Chem).

S, T., C, S., T, W., P, P.-G., J, S., G, R., and B, H. (2014). Septin6 and Septin7 GTP Binding Proteins Regulate AP-3- And ESCRT-dependent Multivesicular Body Biogenesis (PLoS One).

Saad, Y., Shaker, O., Nassar, Y., Ahmad, L., Said, M., and Esmat, G. (2014). A polymorphism in the microsomal triglyceride transfer protein can predict the response to antiviral therapy in Egyptian patients with chronic hepatitis C virus genotype 4 infection. Gut Liver *8*, 655–661.

Saftig, P., and Klumperman, J. (2009). Lysosome biogenesis and lysosomal membrane proteins: trafficking meets function. Nat. Rev. Mol. Cell Biol. *10*, 623–635.

Sahu, R., Kaushik, S., Clement, C.C., Cannizzo, E.S., Scharf, B., Follenzi, A., Potolicchio, I., Nieves, E., Cuervo, A.M., and Santambrogio, L. (2011). Microautophagy of cytosolic proteins by late endosomes. Dev. Cell *20*, 131–139.

Sanders, S.L., and Field, C.M. (1994). Cell division. Septins in common? Curr. Biol. CB *4*, 907–910.

Sandrock, K., Bartsch, I., Bläser, S., Busse, A., Busse, E., and Zieger, B. (2011). Characterization of human septin interactions. Biol. Chem. *392*, 751–761.

Sasaki, T., Takasuga, S., Sasaki, J., Kofuji, S., Eguchi, S., Yamazaki, M., and Suzuki, A. (2009). Mammalian phosphoinositide kinases and phosphatases. Prog. Lipid Res. *48*, 307–343.

Sathyanarayan, A., Mashek, M.T., and Mashek, D.G. (2017). ATGL Promotes Autophagy/Lipophagy via SIRT1 to Control Hepatic Lipid Droplet Catabolism. Cell Rep. *19*, 1–9.

Scheel, T.K.H., and Rice, C.M. (2013). Understanding the hepatitis C virus life cycle paves the way for highly effective therapies. Nat. Med. *19*, 837–849.

Schink, K.O., Tan, K.-W., and Stenmark, H. (2016). Phosphoinositides in Control of Membrane Dynamics. Annu. Rev. Cell Dev. Biol. *32*, 143–171.

Schott, M.B., Weller, S.G., Schulze, R.J., Krueger, E.W., Drizyte-Miller, K., Casey, C.A., and McNiven, M.A. (2019). Lipid droplet size directs lipolysis and lipophagy catabolism in hepatocytes. J. Cell Biol. *218*, 3320–3335.

Schroeder, B., Schulze, R.J., Weller, S.G., Sletten, A.C., Casey, C.A., and McNiven, M.A. (2015). The small GTPase Rab7 as a central regulator of hepatocellular lipophagy. Hepatol. Baltim. Md *61*, 1896–1907.

Schuldiner, M., and Bohnert, M. (2017). A different kind of love - lipid droplet contact sites. Biochim. Biophys. Acta Mol. Cell Biol. Lipids *1862*, 1188–1196.

Schulze, R.J., and McNiven, M.A. (2019). Lipid Droplet Formation and Lipophagy in Fatty Liver Disease. Semin. Liver Dis. *39*, 283–290.

Schulze, R.J., Rasineni, K., Weller, S.G., Schott, M.B., Schroeder, B., Casey, C.A., and McNiven, M.A. (2017). Ethanol exposure inhibits hepatocyte lipophagy by inactivating the small guanosine triphosphatase Rab7. Hepatol. Commun. *1*, 140–152.

Schulze, R.J., Schott, M.B., Casey, C.A., Tuma, P.L., and McNiven, M.A. (2019). The cell biology of the hepatocyte: A membrane trafficking machine. J. Cell Biol. *218*, 2096–2112.

Schulze, R.J., Krueger, E.W., Weller, S.G., Johnson, K.M., Casey, C.A., Schott, M.B., and McNiven, M.A. (2020). Direct lysosome-based autophagy of lipid droplets in hepatocytes. Proc. Natl. Acad. Sci. *117*, 32443–32452.

Sellin, M.E., Sandblad, L., Stenmark, S., and Gullberg, M. (2011). Deciphering the rules governing assembly order of mammalian septin complexes. Mol. Biol. Cell *22*, 3152–3164.

Settembre, C., Fraldi, A., Medina, D.L., and Ballabio, A. (2013). Signals from the lysosome: a control centre for cellular clearance and energy metabolism. Nat. Rev. Mol. Cell Biol. *14*, 283–296.

Shah, Z.H., Jones, D.R., Sommer, L., Foulger, R., Bultsma, Y., D'Santos, C., and Divecha, N. (2013). Nuclear phosphoinositides and their impact on nuclear functions. FEBS J. 6295–6310.

Sheffield, P.J., Oliver, C.J., Kremer, B.E., Sheng, S., Shao, Z., and Macara, I.G. (2003). Borg/septin interactions and the assembly of mammalian septin heterodimers, trimers, and filaments. J. Biol. Chem. *278*, 3483–3488.

Shehadeh, L., Mitsi, G., Adi, N., Bishopric, N., and Papapetropoulos, S. (2009). Expression of Lewy body protein septin 4 in postmortem brain of Parkinson's disease and control subjects. Mov. Disord. Off. J. Mov. Disord. Soc. *24*, 204–210.

Shen, S., Liu, M., Wu, Y., Saiyin, H., Liu, G., and Yu, L. (2012). Involvement of SEPT4_i1 in

hepatocellular carcinoma: SEPT4_i1 regulates susceptibility to apoptosis in hepatocellular carcinoma cells. Mol. Biol. Rep. *39*, 4519–4526.

Sheriff, S., Du, H., and Grabowski, G.A. (1995). Characterization of lysosomal acid lipase by site-directed mutagenesis and heterologous expression. J. Biol. Chem. *270*, 27766–27772.

Shin, K., and Margolis, B. (2006). ZOning out Tight Junctions. Cell *126*, 647–649.

Shinde, S.R., and Maddika, S. (2016). PTEN modulates EGFR late endocytic trafficking and degradation by dephosphorylating Rab7. Nat. Commun. *7*, 10689.

Shinde, S.R., and Maddika, S. (2017). Post translational modifications of Rab GTPases. Small GTPases *9*, 49–56.

Shindo, A., Audrey, A., Takagishi, M., Takahashi, M., Wallingford, J.B., and Kinoshita, M. (2018). Septin-dependent remodeling of cortical microtubule drives cell reshaping during epithelial wound healing. J. Cell Sci. *131*, jcs212647.

Shiryaev, A., Kostenko, S., Dumitriu, G., and Moens, U. (2012). Septin 8 is an interaction partner and in vitro substrate of MK5. World J. Biol. Chem. *3*, 98–109.

Shuai, K. (2006). Regulation of cytokine signaling pathways by PIAS proteins. Cell Res. *16*, 196–202.

Shyu, P., Wong, X.F.A., Crasta, K., and Thibault, G. (2018). Dropping in on lipid droplets: insights into cellular stress and cancer. Biosci. Rep. *38*, BSR20180764.

Sibulesky, L. (2013). Normal liver anatomy. Clin. Liver Dis. *2*, S1–S3.

Singh, R., and Cuervo, A.M. (2012). Lipophagy: connecting autophagy and lipid metabolism. Int. J. Cell Biol. *2012*, 282041.

Singh, N., Reyes-Ordoñez, A., Compagnone, M.A., Moreno, J.F., Leslie, B.J., Ha, T., and Chen, J. (2021). Redefining the specificity of phosphoinositide-binding by human PH domain-containing proteins. Nat. Commun. *12*, 4339.

Singh, R., Kaushik, S., Wang, Y., Xiang, Y., Novak, I., Komatsu, M., Tanaka, K., Cuervo, A.M., and Czaja, M.J. (2009). Autophagy regulates lipid metabolism. Nature *458*, 1131–1135.

Sir, D., Chen, W., Choi, J., Wakita, T., Yen, T.S.B., and Ou, J.J. (2008). Induction of incomplete autophagic response by hepatitis C virus via the unfolded protein response. Hepatology *48*, 1054–1061.

Sirajuddin, M., Farkasovsky, M., Hauer, F., Kühlmann, D., Macara, I.G., Weyand, M., Stark, H., and Wittinghofer, A. (2007a). Structural insight into filament formation by mammalian septins. Nature *449*, 311–315.

Sirajuddin, M., Farkasovsky, M., Hauer, F., Kühlmann, D., Macara, I.G., Weyand, M., Stark, H., and Wittinghofer, A. (2007b). Structural insight into filament formation by mammalian septins. Nature *449*, 311–315.

Sirajuddin, M., Farkasovsky, M., Zent, E., and Wittinghofer, A. (2009). GTP-induced conformational changes in septins and implications for function. Proc. Natl. Acad. Sci. *106*, 16592–16597.

Sirianni, A., Krokowski, S., Lobato-Márquez, D., Buranyi, S., Pfanzelter, J., Galea, D., Willis, A., Culley, S., Henriques, R., Larrouy-Maumus, G., et al. (2016). Mitochondria mediate septin cage assembly to promote autophagy of Shigella. EMBO Rep. *17*, 1029–1043.

Sivan, G., Martin, S.E., Myers, T.G., Buehler, E., Szymczyk, K.H., Ormanoglu, P., and Moss, B. (2013). Human genome-wide RNAi screen reveals a role for nuclear pore proteins in poxvirus morphogenesis. Proc. Natl. Acad. Sci. U. S. A. *110*, 3519–3524.

Smith, C., Dolat, L., Angelis, D., Forgacs, E., Spiliotis, E.T., and Galkin, V.E. (2015). Septin 9 Exhibits Polymorphic Binding to F-Actin and Inhibits Myosin and Cofilin Activity. J. Mol. Biol. *427*, 3273–3284.

Song, K., Russo, G., and Krauss, M. (2016). Septins As Modulators of Endo-Lysosomal Membrane Traffic. Front. Cell Dev. Biol. *4*, 124.

Song, K., Gras, C., Capin, G., Gimber, N., Lehmann, M., Mohd, S., Puchkov, D., Rödiger, M., Wilhelmi, I., Daumke, O., et al. (2019). A SEPT1-based scaffold is required for Golgi integrity and function. J. Cell Sci. *132*, jcs225557.

Soni, K.G., Mardones, G.A., Sougrat, R., Smirnova, E., Jackson, C.L., and Bonifacino, J.S. (2009). Coatomer-dependent protein delivery to lipid droplets. J. Cell Sci. *122*, 1834–1841.

Søreng, K., Neufeld, T.P., and Simonsen, A. (2018). Chapter One - Membrane Trafficking in Autophagy. In International Review of Cell and Molecular Biology, L. Galluzzi, ed. (Academic Press), pp. 1–92.

Sørensen, A.B., Lund, A.H., Ethelberg, S., Copeland, N.G., Jenkins, N.A., and Pedersen, F.S. (2000). Sint1, a Common Integration Site in SL3-3-Induced T-Cell Lymphomas, Harbors a Putative Proto-Oncogene with Homology to the Septin Gene Family. J. Virol. *74*, 2161–2168.

Soto-Avellaneda, A., and Morrison, B.E. (2020). Signaling and other functions of lipids in autophagy: a review. Lipids Health Dis. *19*, 214.

Stanković, M.N., Mladenović, D.R., Duričić, I., Šobajić, S.S., Timić, J., Jorgačević, B., Aleksić, V., Vučević, D.B., Ješić-Vukićević, R., and Radosavljević, T.S. (2014). Time-dependent changes and association between liver free fatty acids, serum lipid profile and histological features in mice model of nonalcoholic fatty liver disease. Arch. Med. Res. *45*, 116–124.

Starling, G.P., Yip, Y.Y., Sanger, A., Morton, P.E., Eden, E.R., and Dodding, M.P. (2016). Folliculin directs the formation of a Rab34-RILP complex to control the nutrient-dependent dynamic distribution of lysosomes. EMBO Rep. *17*, 823–841.

Stone, S.J., Levin, M.C., and Farese, R.V. (2006). Membrane topology and identification of key functional amino acid residues of murine acyl-CoA:diacylglycerol acyltransferase-2. J. Biol. Chem. *281*, 40273–40282.

Stone, T.W., McPherson, M., and Gail Darlington, L. (2018). Obesity and Cancer: Existing and New Hypotheses for a Causal Connection. EBioMedicine *30*, 14–28.

Sui, X., Arlt, H., Brock, K.P., Lai, Z.W., DiMaio, F., Marks, D.S., Liao, M., Farese, R.V., and Walther, T.C. (2018). Cryo-electron microscopy structure of the lipid droplet-formation protein seipin. J. Cell Biol. *217*, 4080–4091.

Sun, Z., Gong, J., Wu, H., Xu, W., Wu, L., Xu, D., Gao, J., Wu, J., Yang, H., Yang, M., et al.

(2013). Perilipin1 promotes unilocular lipid droplet formation through the activation of Fsp27 in adipocytes. Nat. Commun. *4*, 1594.

Sung, H., Ferlay, J., Siegel, R.L., Laversanne, M., Soerjomataram, I., Jemal, A., and Bray, F. (2021). Global Cancer Statistics 2020: GLOBOCAN Estimates of Incidence and Mortality Worldwide for 36 Cancers in 185 Countries. CA. Cancer J. Clin. *71*, 209–249.

Sunman, J.A., Hawke, R.L., LeCluyse, E.L., and Kashuba, A.D.M. (2004). Kupffer Cell-Mediated Il-2 Suppression of Cyp3a Activity in Human Hepatocytes. Drug Metab. Dispos. *32*, 359–363.

Surka, M.C., Tsang, C.W., and Trimble, W.S. (2002). The Mammalian Septin MSF Localizes with Microtubules and Is Required for Completion of Cytokinesis. Mol. Biol. Cell *13*, 3532–3545.

Sutti, S., and Albano, E. (2020). Adaptive immunity: an emerging player in the progression of NAFLD. Nat. Rev. Gastroenterol. Hepatol. *17*, 81–92.

T, B., M, A., C, C., I, P., L, B., C, T., E, K., and B, H. (2008). Protein Networks Supporting AP-3 Function in Targeting Lysosomal Membrane Proteins (Mol Biol Cell).

T, N., C, S., F, L., K, Ø., O, P., and K, A. (2016). Septins Guide Microtubule Protrusions Induced by Actin-Depolymerizing Toxins Like Clostridium Difficile Transferase (CDT) (Proc Natl Acad Sci U S A).

Tabibian, J.H., Masyuk, A.I., Masyuk, T.V., O'Hara, S.P., and LaRusso, N.F. (2013). Physiology of Cholangiocytes. Compr. Physiol. *3*.

Tada, T., Simonetta, A., Batterton, M., Kinoshita, M., Edbauer, D., and Sheng, M. (2007). Role of Septin cytoskeleton in spine morphogenesis and dendrite development in neurons. Curr. Biol. CB *17*, 1752–1758.

Takahashi, Y. (2003). Comparative Analysis of Yeast PIAS-Type SUMO Ligases In Vivo and In Vitro. J. Biochem. (Tokyo) *133*, 415–422.

Takahashi, Y., Iwase, M., Konishi, M., Tanaka, M., Toh-e, A., and Kikuchi, Y. (1999a). Smt3, a SUMO-1 Homolog, Is Conjugated to Cdc3, a Component of Septin Rings at the Mother-Bud Neck in Budding Yeast. Biochem. Biophys. Res. Commun. *259*, 582–587.

Takahashi, Y., Iwase, M., Konishi, M., Tanaka, M., Toh-e, A., and Kikuchi, Y. (1999b). Smt3, a SUMO-1 homolog, is conjugated to Cdc3, a component of septin rings at the mother-bud neck in budding yeast. Biochem. Biophys. Res. Commun. *259*, 582–587.

Takizawa, P.A., DeRisi, J.L., Wilhelm, J.E., and Vale, R.D. (2000). Plasma membrane compartmentalization in yeast by messenger RNA transport and a septin diffusion barrier. Science *290*, 341–344.

Tan, S.C., Scherer, J., and Vallee, R.B. (2011). Recruitment of dynein to late endosomes and lysosomes through light intermediate chains. Mol. Biol. Cell *22*, 467–477.

Tanaka, M., Tanaka, T., Kijima, H., Itoh, J., Matsuda, T., Hori, S., and Yamamoto, M. (2001). Characterization of Tissue- and Cell-Type-Specific Expression of a Novel Human Septin Family Gene, Bradeion. Biochem. Biophys. Res. Commun. *286*, 547–553.

Tanaka-Takiguchi, Y., Kinoshita, M., and Takiguchi, K. (2009). Septin-Mediated Uniform Bracing of Phospholipid Membranes. Curr. Biol. *19*, 140–145.

Tang, T., Abbott, M.J., Ahmadian, M., Lopes, A.B., Wang, Y., and Sul, H.S. (2013). Desnutrin/ATGL activates PPARδ to promote mitochondrial function for insulin secretion in islet β cells. Cell Metab. *18*, 883–895.

Tao, Y., Qiu, T., Yao, X., Jiang, L., Wang, N., Jiang, J., Jia, X., Wei, S., Zhang, J., Zhu, Y., et al. (2021). IRE1α/NOX4 signaling pathway mediates ROS-dependent activation of hepatic stellate cells in NaAsO2 -induced liver fibrosis. J. Cell. Physiol. *236*, 1469–1480.

Tapia, D., Jiménez, T., Zamora, C., Espinoza, J., Rizzo, R., González-Cárdenas, A., Fuentes, D., Hernández, S., Cavieres, V.A., Soza, A., et al. (2019). KDEL receptor regulates secretion by lysosome relocation- and autophagy-dependent modulation of lipid-droplet turnover. Nat. Commun. *10*, 735.

Targa, B., Klipfel, L., Cantaloube, I., Salameh, J., Benoit, B., Poüs, C., and Baillet, A. (2019). Septin filament coalignment with microtubules depends on SEPT9_i1 and tubulin polyglutamylation, and is an early feature of acquired cell resistance to paclitaxel. Cell Death Dis. *10*, 54.

Tauchi-Sato, K., Ozeki, S., Houjou, T., Taguchi, R., and Fujimoto, T. (2002). The Surface of Lipid Droplets Is a Phospholipid Monolayer with a Unique Fatty Acid Composition *. J. Biol. Chem. *277*, 44507–44512.

Thiam, A.R., and Beller, M. (2017). The why, when and how of lipid droplet diversity. J. Cell Sci. *130*, 315–324.

Thiam, A.R., and Dugail, I. (2019). Lipid droplet–membrane contact sites – from protein binding to function. J. Cell Sci. *132*.

Thiam, A.R., and Forêt, L. (2016). The physics of lipid droplet nucleation, growth and budding. Biochim. Biophys. Acta *1861*, 715–722.

Thiam, A.R., Farese Jr, R.V., and Walther, T.C. (2013a). The biophysics and cell biology of lipid droplets. Nat. Rev. Mol. Cell Biol. *14*, 775–786.

Thiam, A.R., Antonny, B., Wang, J., Delacotte, J., Wilfling, F., Walther, T.C., Beck, R., Rothman, J.E., and Pincet, F. (2013b). COPI buds 60-nm lipid droplets from reconstituted water-phospholipid-triacylglyceride interfaces, suggesting a tension clamp function. Proc. Natl. Acad. Sci. U. S. A. *110*, 13244–13249.

Toledo, D.A.M., D'Avila, H., and Melo, R.C.N. (2016). Host Lipid Bodies as Platforms for Intracellular Survival of Protozoan Parasites. Front. Immunol. *7*.

Tomita, K., Teratani, T., Suzuki, T., Shimizu, M., Sato, H., Narimatsu, K., Okada, Y., Kurihara, C., Irie, R., Yokoyama, H., et al. (2014). Free cholesterol accumulation in hepatic stellate cells: Mechanism of liver fibrosis aggravation in nonalcoholic steatohepatitis in mice. Hepatology *59*, 154–169.

Tooley, A.J., Gilden, J., Jacobelli, J., Beemiller, P., Trimble, W.S., Kinoshita, M., and Krummel, M.F. (2009). Amoeboid T lymphocytes require the septin cytoskeleton for cortical integrity and persistent motility. Nat. Cell Biol. *11*, 17–26.

Trefts, E., Gannon, M., and Wasserman, D.H. (2017). The liver. Curr. Biol. CB *27*, R1147–R1151.

Tsuji, T., Fujimoto, M., Tatematsu, T., Cheng, J., Orii, M., Takatori, S., and Fujimoto, T. (2017).

Niemann-Pick type C proteins promote microautophagy by expanding raft-like membrane domains in the yeast vacuole. ELife *6*, e25960.

Tummala, K.S., Gomes, A.L., Yilmaz, M., Graña, O., Bakiri, L., Ruppen, I., Ximénez-Embún, P., Sheshappanavar, V., Rodriguez-Justo, M., Pisano, D.G., et al. (2014). Inhibition of De Novo NAD+ Synthesis by Oncogenic URI Causes Liver Tumorigenesis through DNA Damage. Cancer Cell *26*, 826–839.

Tyson, G.L., and El-Serag, H.B. (2011). Risk factors for cholangiocarcinoma. Hepatology *54*, 173–184.

Vanlandingham, P.A., and Ceresa, B.P. (2009). Rab7 regulates late endocytic trafficking downstream of multivesicular body biogenesis and cargo sequestration. J. Biol. Chem. *284*, 12110–12124.

Várnai, P., Gulyás, G., Tóth, D.J., Sohn, M., Sengupta, N., and Balla, T. (2017). Quantifying lipid changes in various membrane compartments using lipid binding protein domains. Cell Calcium *64*, 72–82.

Vekemans, K., and Braet, F. (2005). Structural and functional aspects of the liver and liver sinusoidal cells in relation to colon carcinoma metastasis. World J. Gastroenterol. WJG *11*, 5095–5102.

Verdier-Pinard, P., Salaun, D., Bouguenina, H., Shimada, S., Pophillat, M., Audebert, S., Agavnian, E., Coslet, S., Charafe-Jauffret, E., Tachibana, T., et al. (2017). Septin 9_i2 is downregulated in tumors, impairs cancer cell migration and alters subnuclear actin filaments. Sci. Rep. *7*, 44976.

Versele, M., and Thorner, J. (2005). Some assembly required: yeast septins provide the instruction manual. Trends Cell Biol. *15*, 414–424.

Volceanov, L., Herbst, K., Biniossek, M., Schilling, O., Haller, D., Nölke, T., Subbarayal, P., Rudel, T., Zieger, B., and Häcker, G. Septins Arrange F-Actin-Containing Fibers on the Chlamydia trachomatis Inclusion and Are Required for Normal Release of the Inclusion by Extrusion. MBio *5*, e01802-14.

Walikonis, R.S., Jensen, O.N., Mann, M., Provance, D.W., Mercer, J.A., and Kennedy, M.B. (2000). Identification of proteins in the postsynaptic density fraction by mass spectrometry. J. Neurosci. Off. J. Soc. Neurosci. *20*, 4069–4080.

Wallroth, A., and Haucke, V. (2018). Phosphoinositide conversion in endocytosis and the endolysosomal system. J. Biol. Chem. *293*, 1526–1535.

Walsh, S.R., and Dolin, R. (2011). Vaccinia viruses: vaccines against smallpox and vectors against infectious diseases and tumors. Expert Rev. Vaccines *10*, 1221–1240.

Walther, T.C., and Farese, R.V. (2012). Lipid droplets and cellular lipid metabolism. Annu. Rev. Biochem. *81*, 687–714.

Wandinger-Ness, A., and Zerial, M. (2014). Rab Proteins and the Compartmentalization of the Endosomal System. Cold Spring Harb. Perspect. Biol. *6*, a022616.

Wang, C.-W. (2016). Lipid droplets, lipophagy, and beyond. Biochim. Biophys. Acta *1861*, 793–805.

Wang, T., and Hong, W. (2002). Interorganellar Regulation of Lysosome Positioning by the Golgi Apparatus through Rab34 Interaction with Rab-interacting Lysosomal Protein. Mol. Biol. Cell *13*, 4317–4332.

Wang, H., Becuwe, M., Housden, B.E., Chitraju, C., Porras, A.J., Graham, M.M., Liu, X.N., Thiam, A.R., Savage, D.B., Agarwal, A.K., et al. (2016). Seipin is required for converting nascent to mature lipid droplets. ELife *5*, e16582.

Wang, H., Lo, W.-T., and Haucke, V. (2019). Phosphoinositide switches in endocytosis and in the endolysosomal system. Curr. Opin. Cell Biol. *59*, 50–57.

Wang, X., Zhang, X., Chu, E.S.H., Chen, X., Kang, W., Wu, F., To, K.-F., Wong, V.W.S., Chan, H.L.Y., Chan, M.T.V., et al. (2018). Defective lysosomal clearance of autophagosomes and its clinical implications in nonalcoholic steatohepatitis. FASEB J. *32*, 37–51.

Warner, T.G., Dambach, L.M., Shin, J.H., and O'Brien, J.S. (1981). Purification of the lysosomal acid lipase from human liver and its role in lysosomal lipid hydrolysis. J. Biol. Chem. *256*, 2952–2957.

Weirich, C.S., Erzberger, J.P., and Barral, Y. (2008). The septin family of GTPases: architecture and dynamics. Nat. Rev. Mol. Cell Biol. *9*, 478–489.

Welch, M.D., and Way, M. (2013). Arp2/3-mediated actin-based motility: a tail of pathogen abuse. Cell Host Microbe *14*, 242–255.

Welte, M.A. (2009). Fat on the move: intracellular motion of lipid droplets. Biochem. Soc. Trans. *37*, 991–996.

Welte, M.A., and Gould, A.P. (2017). Lipid droplet functions beyond energy storage. Biochim. Biophys. Acta BBA - Mol. Cell Biol. Lipids *1862*, 1260–1272.

Wilfling, F., Wang, H., Haas, J.T., Krahmer, N., Gould, T.J., Uchida, A., Cheng, J.-X., Graham, M., Christiano, R., Fröhlich, F., et al. (2013). Triacylglycerol synthesis enzymes mediate lipid droplet growth by relocalizing from the ER to lipid droplets. Dev. Cell *24*, 384–399.

Wilfling, F., Haas, J.T., Walther, T.C., and Farese, R.V. (2014a). Lipid droplet biogenesis. Curr. Opin. Cell Biol. *29*, 39–45.

Wilfling, F., Thiam, A.R., Olarte, M.-J., Wang, J., Beck, R., Gould, T.J., Allgeyer, E.S., Pincet, F., Bewersdorf, J., Farese, R.V., et al. (2014b). Arf1/COPI machinery acts directly on lipid droplets and enables their connection to the ER for protein targeting. ELife *3*, e01607.

Willett, R., Martina, J.A., Zewe, J.P., Wills, R., Hammond, G.R.V., and Puertollano, R. (2017). TFEB regulates lysosomal positioning by modulating TMEM55B expression and JIP4 recruitment to lysosomes. Nat. Commun. *8*, 1–17.

Wolins, N.E., Quaynor, B.K., Skinner, J.R., Schoenfish, M.J., Tzekov, A., and Bickel, P.E. (2005). S3-12, Adipophilin, and TIP47 Package Lipid in Adipocytes. J. Biol. Chem. *280*, 19146–19155.

Wolins, N.E., Brasaemle, D.L., and Bickel, P.E. (2006). A proposed model of fat packaging by exchangeable lipid droplet proteins. FEBS Lett. *580*, 5484–5491.

Wu, P.-S., Chang, T.-S., Lu, S.-N., Su, H.-J., Chang, S.-Z., Hsu, C.-W., and Chen, M.-Y. (2019). An Investigation of the Side Effects, Patient Feedback, and Physiological Changes Associated with

Direct-Acting Antiviral Therapy for Hepatitis C. Int. J. Environ. Res. Public. Health *16*, 4981.

Wu, R., Cui, X., Dong, W., Zhou, M., Simms, H.H., and Wang, P. (2006). Suppression of hepatocyte CYP1A2 expression by Kupffer cells via AhR pathway: The central role of proinflammatory cytokines. Int. J. Mol. Med. *18*, 339–346.

Xu, D., Li, Y., Wu, L., Li, Y., Zhao, D., Yu, J., Huang, T., Ferguson, C., Parton, R.G., Yang, H., et al. (2018a). Rab18 promotes lipid droplet (LD) growth by tethering the ER to LDs through SNARE and NRZ interactions. J. Cell Biol. *217*, 975–995.

Xu, D., Liu, A., Wang, X., Chen, Y., Shen, Y., Tan, Z., and Qiu, M. (2018b). Repression of Septin9 and Septin2 suppresses tumor growth of human glioblastoma cells. Cell Death Dis. *9*, 514.

Y, M., H, I., I, I., R, M., H, K., M, S., and K, N. (2013). Possible Role of a Septin, SEPT1, in Spreading in Squamous Cell Carcinoma DJM-1 Cells (Biol Chem).

Yamaguchi, K., Yang, L., McCall, S., Huang, J., Yu, X.X., Pandey, S.K., Bhanot, S., Monia, B.P., Li, Y.-X., and Diehl, A.M. (2007). Inhibiting triglyceride synthesis improves hepatic steatosis but exacerbates liver damage and fibrosis in obese mice with nonalcoholic steatohepatitis. Hepatology *45*, 1366–1374.

Yamamoto, E., Domański, J., Naughton, F.B., Best, R.B., Kalli, A.C., Stansfeld, P.J., and Sansom, M.S.P. (2020). Multiple lipid binding sites determine the affinity of PH domains for phosphoinositide-containing membranes. Sci. Adv. *6*, eaay5736.

Yamane, D., McGivern, D.R., Masaki, T., and Lemon, S.M. (2013). Liver injury and disease pathogenesis in chronic hepatitis C. Curr. Top. Microbiol. Immunol. *369*, 263–288.

Yan, R., Qian, H., Lukmantara, I., Gao, M., Du, X., Yan, N., and Yang, H. (2018). Human SEIPIN Binds Anionic Phospholipids. Dev. Cell *47*, 248-256.e4.

Yang, Y., and Klionsky, D.J. (2020). Autophagy and disease: unanswered questions. Cell Death Differ. *27*, 858–871.

Yang, Z., and Klionsky, D.J. (2010). Mammalian autophagy: core molecular machinery and signaling regulation. Curr. Opin. Cell Biol. *22*, 124–131.

Yarwood, R., Hellicar, J., Woodman, P.G., and Lowe, M. (2020). Membrane trafficking in health and disease. Dis. Model. Mech. *13*.

Ye, K., and Ahn, J.-Y. (2008). Nuclear phosphoinositide signaling. Front. Biosci. J. Virtual Libr. *13*, 540–548.

Ye, D., Li, F.Y.L., Lam, K.S.L., Li, H., Jia, W., Wang, Y., Man, K., Lo, C.M., Li, X., and Xu, A. (2012). Toll-like receptor-4 mediates obesity-induced non-alcoholic steatohepatitis through activation of X-box binding protein-1 in mice. Gut *61*, 1058–1067.

Yu, L., Chen, Y., and Tooze, S.A. (2018). Autophagy pathway: Cellular and molecular mechanisms. Autophagy *14*, 207–215.

Yw, H., M, Y., Rf, C., Je, D., S, G., and Ws, T. (2008). Mammalian Septins Are Required for Phagosome Formation (Mol Biol Cell).

Zabron, A., Edwards, R.J., and Khan, S.A. (2013). The challenge of cholangiocarcinoma: dissecting the molecular mechanisms of an insidious cancer. Dis. Model. Mech. *6*, 281–292.

Zanghellini, J., Wodlei, F., and von Grünberg, H.H. (2010). Phospholipid demixing and the birth of a lipid droplet. J. Theor. Biol. *264*, 952–961.

Zeng, Y., Cao, Y., Liu, L., Zhao, J., Zhang, T., Xiao, L., Jia, M., Tian, Q., Yu, H., Chen, S., et al. (2019). SEPT9_i1 regulates human breast cancer cell motility through cytoskeletal and RhoA/FAK signaling pathway regulation. Cell Death Dis. *10*.

Zent, E., and Wittinghofer, A. (2014). Human septin isoforms and the GDP-GTP cycle. Biol. Chem. *395*, 169–180.

Zeraik, A.E., Pereira, H.M., Santos, Y.V., Brandão-Neto, J., Spoerner, M., Santos, M.S., Colnago, L.A., Garratt, R.C., Araújo, A.P.U., and DeMarco, R. (2014). Crystal structure of a Schistosoma mansoni septin reveals the phenomenon of strand slippage in septins dependent on the nature of the bound nucleotide. J. Biol. Chem. *289*, 7799–7811.

Zhang, J., Kong, C., Xie, H., McPherson, P.S., Grinstein, S., and Trimble, W.S. (1999a). Phosphatidylinositol polyphosphate binding to the mammalian septin H5 is modulated by GTP. Curr. Biol. *9*, 1458–1467.

Zhang, J., Kong, C., Xie, H., McPherson, P.S., Grinstein, S., and Trimble, W.S. (1999b). Phosphatidylinositol polyphosphate binding to the mammalian septin H5 is modulated by GTP. Curr. Biol. *9*, 1458–1467.

Zhang, N., Liu, L., Fan, N., Zhang, Q., Wang, W., Zheng, M., Ma, L., Li, Y., and Shi, L. (2016a). The requirement of SEPT2 and SEPT7 for migration and invasion in human breast cancer via MEK/ERK activation. Oncotarget *7*, 61587–61600.

Zhang, N., Liu, L., Fan, N., Zhang, Q., Wang, W., Zheng, M., Ma, L., Li, Y., and Shi, L. (2016b). The requirement of SEPT2 and SEPT7 for migration and invasion in human breast cancer via MEK/ERK activation. Oncotarget *7*, 61587–61600.

Zhang, S., Wang, Y., Cui, L., Deng, Y., Xu, S., Yu, J., Cichello, S., Serrero, G., Ying, Y., and Liu, P. (2016c). Morphologically and Functionally Distinct Lipid Droplet Subpopulations. Sci. Rep. *6*.

Zhen, Y., and Stenmark, H. (2015). Cellular functions of Rab GTPases at a glance. J. Cell Sci. *128*, 3171–3176.

Zhu, M., Wang, F., Yan, F., Yao, P., Du, J., Gao, X., Wang, X., Wu, Q., Ward, T., Li, J., et al. (2008). Septin 7 Interacts with Centromere-associated Protein E and Is Required for Its Kinetochore Localization. J. Biol. Chem. *283*, 18916–18925.

Zlatanou, A., and Stewart, G.S. (2010). A PIAS-ed view of DNA double strand break repair focuses on SUMO. DNA Repair *9*, 588–592.

université PARIS-SACLAY | ÉCOLE DOCTORALE Cancérologie : biologie - médecine - santé (CBMS)

**Titre :** Le rôle de la septine 9 dans l'accumulation des gouttelettes lipidiques et la pathogenèse du foie par la régulation du trafic intracellulaire.

**Mots clés :** Gouttelette lipidique, septine 9, Lysosome, Appareil de Golgi, Phosphoinositides.

**Résumé :** Les septines appartiennent à la famille des protéines GTPases qui peuvent former des structures hétéro-oligomériques et sont capables de se lier à l'actine et aux microtubules. Les septines s'associent également aux membranes cellulaires et recrutent ainsi des protéines cytosoliques et d'autres éléments du cytosquelette pour contrôler de nombreuses fonctions cellulaires. Dans notre équipe, nous avons montré que la septine 9 est détournée par le virus de l'hépatite C (VHC) pour induire l'accumulation périnucléaire des gouttelettes lipidiques (GLs). En effet, l'accumulation de GLs est souvent associée à un dysfonctionnement des lysosomes, nous avons donc émis l'hypothèse que la septine 9 pourrait être impliquée dans l'accumulation des GLs en affectant la fonction des lysosomes. Nous montrons dans ce travail que le contenu cellulaire et la distribution des GLs sont corrélés à ceux du lysosome et régulés par l'ajout d'oléate sur les cellules et par la septine 9. Une expression élevée de la septine 9 favorise le regroupement périnucléaire des lysosomes qui se co-localisent avec le Golgi et non avec les GLs qui les entourent. Inversement, l'inhibition de l'expression de la septine 9 par des siRNAs entraine une dispersion des deux organites qui se colocalisent à la périphérie de la cellule. Ces résultats ont également été validés par l'analyse de Rab7. De même l'addition du PtdIns5P exogène sur les cellules qui se lie à la septine 9 ou la transfection de MTMR3 qui produit du PtdIns5P à partir du PtdIns(3,5)P2 produisent des effets similaires à ceux de la septine 9 sur le lysosome et les GLs. En revanche, la PtdIns(3,5)P2 favorise la co-localisation des GLs avec les lysosomes. Ainsi, nos données dans leur ensemble révèlent un mécanisme d'accumulation intracellulaire des GLs dépendant du rôle du complexe PtdIns5P /septine 9 sur les lysosomes.

**Title :** The role of septin 9 in lipid droplet accumulation and liver pathogenesis through intracellular trafficking regulation

**Keywords :** Lipid droplet, septin 9, Lysosome, Golgi apparatus, Phosphoinositides

**Abstract :** Septins belong to the family of protein GTPases that can form hetero-oligomeric structures and are capable of binding to actin and microtubules. Septins also associate with cell membranes and thus recruit cytosolic proteins and other cytoskeletal elements to control many cellular functions. In our team, we have shown that septin 9 is hijacked by the hepatitis C virus (HCV) to induce the perinuclear accumulation of lipid droplets (LDs). Indeed, LDs accumulation is often associated with lysosome dysfunction, so we hypothesized that septin 9 could be involved in LDs accumulation by affecting lysosome function. In this work, we show that the cellular content and distribution of LDs are correlated with those of the lysosome and regulated by the addition of oleate to cells and by septin 9. High expression of septin 9 promotes perinuclear clustering of lysosomes that co-localize with the Golgi and not with the surrounding LDs. Conversely, inhibition of septin 9 expression by siRNAs results in dispersion of both organelles which co-localize at the cell periphery. These results were also validated by Rab7 analysis. Similarly the addition of exogenous PtdIns5P to cells that binds to septin 9 or transfection of MTMR3 that produces PtdIns5P from PtdIns(3,5)P2 produce similar effects to septin 9 on the lysosome and LDs. In contrast, PtdIns(3,5)P2 promotes GL co-localization with lysosomes. Thus, our data reveal a mechanism of intracellular LDs accumulation dependent on the role of the PtdIns5P /septin 9 complex on lysosomes.